Coordination Chemistry Reviews, 139 (1995) 17–243

From mononuclear to polynuclear macrocyclic or macroacyclic complexes

P. Guerriero, S. Tamburini and P.A. Vigato

Istituto di Chimica e Tecnologie Inorganiche e dei Materiali Avanzati, CNR Corso Stati Uniti 4, 35100 Padova, Italy

(Received 6 January 1993; revised 28 October 1993)

CONTENTS

ABSTRACT

The design and synthesis of polydentate Schiff bases and their properties and potential in the selective coordination of metal ions is reviewed. The self-condensation reaction of appropriate formyl or keto precursors with suitable polyamines can give rise to well-defined planar or tridimensional macrocyclic or macroacyclic Schiff bases, but different reaction pathways can also occur. Illustrative examples of [1 + 1], [2 + 2], [2 + 3] condensation products and of unexpected compounds are included.

Moreover, the role of metal ions as templating agents and the capability of several Schiff base complexes to undergo transmetallation reactions are reported. Ring expansion and ring contraction processes of the macrocyclic cavity of Schiff bases occur and the experimental conditions for the obtainment or the stabilization of one isomer with respect to the others, in the presence or in the absence of suitable metal ions, are discussed.

The preparation of functionalized ligands, containing pendant arms, capable of promoting dynamic complexation–decomplexation processes and their use in selective metal ion transportation and separation are also evaluated.

Correspondence to: P.A. Vigato, Istituto di Chimica e Tecnologie Inorganiche e dei Materiali Avanzati, CNR Corso Stati Uniti 4, 35100 Padova, Italy.

0010-8545/95/$29.00

SSDI 0010-8545(93)01105-7

The formation of polydentate, particularly macrocyclic, Schiff base complexes, followed by reductive demetallation with $NaBH_4$ is also discussed especially for the obtention of more stable, flexible and versatile ligands useful in metal transfer studies.

The synthetic strategies for the preparation of macrocyclic and/or macroacyclic mononuclear and polynuclear complexes from these Schiff bases are outlined. For mononuclear and dinuclear complexes only the most recent and significant examples are considered, while particular attention is devoted to the preparation of ligands capable of organizing more than two metal centres into a predetermined arrangement.

Different synthetic strategies for the assembly of polynuclear molecular arrays are studied and the synthesis of trinuclear, tetranuclear, hexanuclear, dodecanuclear etc. complexes together with their properties (especially the structural and magnetic aspects) are discussed in detail. In particular the enlargement of the macrocyclic cavity, the introduction of suitable bridging groups or the use of "spacers" between dinuclear entities to obtain polynuclear complexes with predetermined properties are considered in detail.

Finally some related systems, such as polyaza macrocycles, compartmental ligands etc., also capable of forming polynuclear systems, are briefly discussed.

1. INTRODUCTION

The preparation and characterization of metal complexes with macrocyclic or macroacyclic ligands was the goal of much research in recent years [1–9]. Starting from simple linear or cyclic compounds, well-defined classes of synthetic compounds such as macro-bi or macro-polycyclic systems are currently available [10–17]. This has produced an area of growing interest in basic and applied chemistry.

Bioinorganic chemistry, material science, catalysis, separation and encapsulation processes, hydrometallurgy, formation of compounds with unusual properties, metal–metal interactions, transport and activation of small molecules have received considerable stimulus from the employment of such ligands. For example, the selective transport of metal ions across lipid membranes is a fundamental process in biology. Biological membranes, such as those surrounding cells, are composed of lipids and proteins exhibiting a partially structured arrangement. Neutral cyclic antibiotics of the valinomycin, enniatin B and monactin classes are well-studied ionophores which aid the selective transport of an alkali metal cation such as potassium across both natural and artificial membranes. A property of these species is that, on metal complex formation, the inside of the molecule is hydrophilic while the outside is hydrophobic. This arrangement is important since the lipid components of biological membranes tend to be oriented such that their polar groups face the membrane surfaces with the non-polar hydrocarbon portions occupying the interior of the membrane. The resulting hydrophobic nature of the central region of the membrane will thus tend to inhibit the passage of charged ions in the absence of an ionophore.

Many ligands have been designed and synthesized not only to mimic the functions of natural carriers in transporting metal ions but also for the development of new methodologies in separation science. Most of the work has been concerned with alkaline and alkaline earth cations, and transport studies have been made in parallel with the development of multidentate carriers containing oxygen donor atoms, in particular crown ethers and cryptands [18–26]. In contrast, much less attention has been devoted to transport processes involving d or f metal ions.

Macrocyclic and macroacyclic ligands have been synthesized to verify the influence of the donor atoms and their relative position, the number and size of the chelate ring formed, the flexibility and the shape of the coordinating moiety, their planar or tridimensional architecture etc. on the metal ion binding and selectivity [18].

For the macrocyclic systems, the hole size is an additional parameter which may influence greatly the ability to discriminate among metal ions [18]. These ligands have primarily been designed to form 1:1 complexes. Parallel studies have focused on the formation of dinuclear complexes in order to study the mutual influence of the two metal centres on the physicochemical properties or on the catalytic activity of these systems [1–17].

Recently, attention has been devoted to the synthesis and characterization of polynuclear species, closely related to the dinuclear analogues, which can extend, magnify and in some cases considerably modify the unusual properties of dinuclear complexes.

Pendant arm macrocycles and their metal complexes have also attracted attention [27–30]. Arms bearing additional potential ligating groups have been introduced at both carbon and nitrogen atoms of macrocycles which have generally been based on polyaza or polyoxa donor sets. One potential of this area derives from the concept that the presence of two pendant arms, bearing ligating groups attached at appropriate positions on a macrocyclic framework, would result in an "opened" cryptand thus leading to modified complexation properties relative to the corresponding clathrochelates or simple macrocyclic precursors (Fig. 1) [31,32].

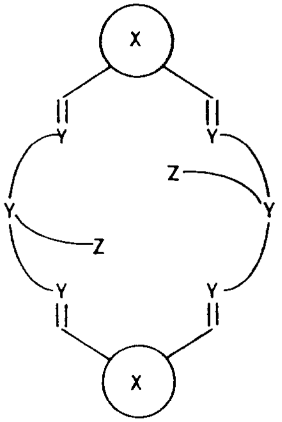

Fig. 1. Schematic representation of open cryptands (X ≡ pyridine, furan, thiophene, pyrrole, phenol; Y ≡ N; Z ≡ pyridine, carboxylic acid, amines etc.).

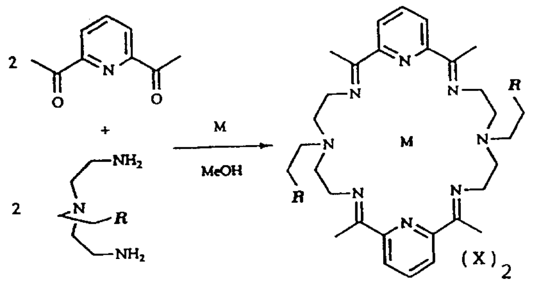

$R = OCH_3;\ NHC_6H_5;\ C_5H_4N;\ NH_2$

$M = Ba^{2+}\ \ Ag_2^{2+};\ Cu_2^{2+};\ Cu_2^{4+}$

$X = ClO_4^-;\ BF_4^-$

Scheme 1. The synthesis of flexible dinculeating macrocyclic ligands capable of generating clefts.

The incorporation of functionalized pendant arms into Schiff base macrocycles has given rise to a series of compounds which provide molecular clefts for metal ion complexation (Scheme 1) [33].

These have a similarity to the clefts which exist in proteins and enzymes and so give opportunity for biomimetic studies. An example is the [2 + 2] tetramine system derived from 2,6-diacetylpyridine and tris(2-ethylamino)amine. Further functionalization of the disilver complex with salicylaldehyde leads to the corresponding hexaimine species. This complex on transmetallation with Cu^{2+} gives the homotrinuclear copper(II) complex with the Schiff base reported in Scheme 2, the structure of which [34] shows that the triangle of copper atoms present bears a remarkable resemblance to the *triangulo*-Cu_3 site found to be present in the enzyme ascorbate oxidase [35].

Attempts to construct in vitro systems that mimic the catalytic activity of enzymes have produced increasing attention to compounds that contain cavities of sufficient diameter and depth to form host–guest complexes, such complexes constituting the first intermediate in enzyme model processes.

A wide variety of different compounds (i.e. cavitands, calixarenes, polyporphyrins, polydentate Schiff bases, polyaza, polyoxamacropolycycles) have been designed to throw light on these problems. Starting from simple 1 : 1 host : guest aggregation, synthetic efforts have progressively been directed toward quite sophisticated systems capable of contemporary multirecognition processes.

It is thus impossible to include a comprehensive, although short, report on these systems in a single review. Of the concepts mentioned above only those using Schiff base and related systems will be illustrated in detail, while we present some explanatory examples of the other synthetic macrocycles. They may illustrate the remarkable efforts directed towards the synthesis of progressively larger systems, capable of securing into their coordination moiety one or more metal ions in order to determine the variation in the physical and chemical properties on going from mononuclear to polynuclear complexes.

Cavitands [36,37] and calixarenes [38,44] represent two examples of macrocyclic systems with an enhanced capability to form stable inclusion complexes with

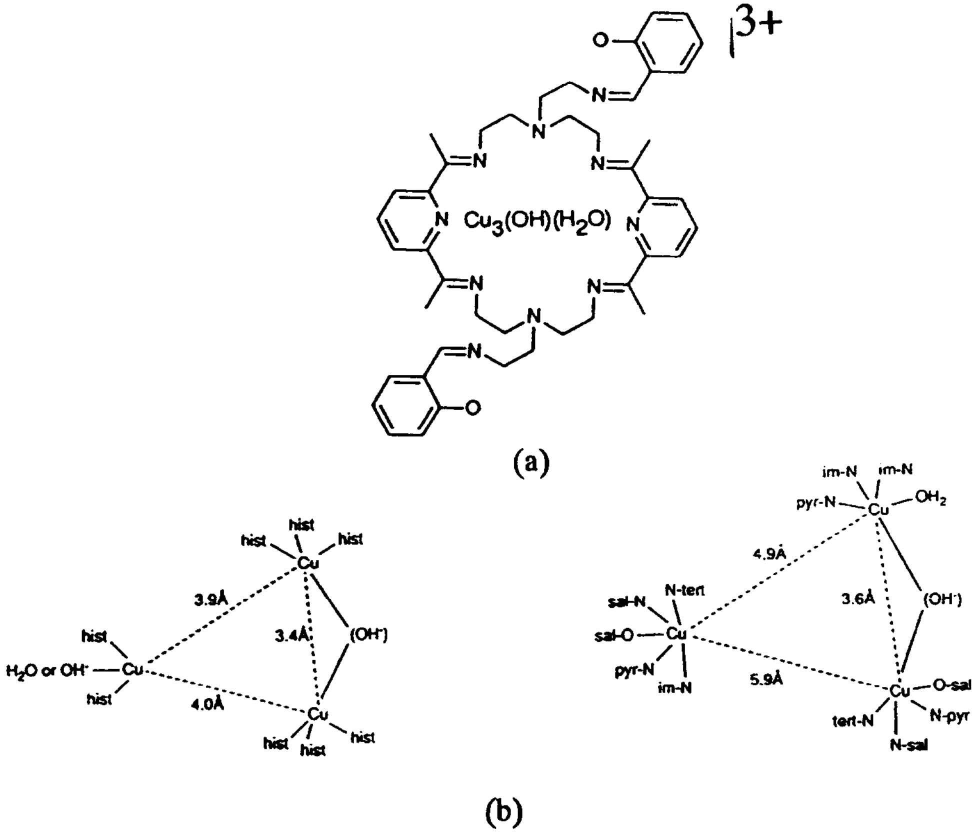

Scheme 2. (a) The trinuclear copper complex with a functionalized hexaimine Schiff base and (b) structure resemblance between this trinuclear copper and the *triangulo*-Cu_3 site in ascorbate oxidase.

both charged and neutral molecules and to act, after suitable functionalization, as selective catalysts. They have been widely used since the clarification of the phenol–formaldehyde condensation reaction involved in their systems.

Cavitands [33] contain cavities large enough to accommodate single molecules or ions. **1** is a specific type of cavitand [34]. Unlike the crowns or cryptands, they contain rigid cavities formed during their syntheses rather than during their complexation. The spherands's preorganization resulted in a very high binding and selectivity for the alkali metal ions [35]. More sophisticated and rigid cavitands (**3**–**7**) have been prepared from the conformationally mobile resorcinol–acetaldehyde condensation product cyclophene **2**, through suitable reaction [33–37]. Compound **7** is particularly attractive, owing to the presence of a solvation-temperature-driven equilibrium between an extended form (**7a**) and vessel-like form (**7b**) [33] which presents a large lipophilic cavity. This equilibrium can be tuned [37]. The diazanaphthalene groups can adopt either axial or equatorial positions. In the all-axial conformer the molecule is shaped with a C_{4v} symmetry cavity; in the all-equatorial conformer, the molecule is elongated in one direction and it has C_{2v} symmetry. In solution, the C_{2v} conformer is more stable at low temperatures, while the C_{4v} conformer is more stable at higher temperatures. This behaviour is rationalized in terms of differential solvation and strain of the two forms [37].

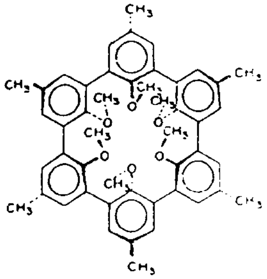

1

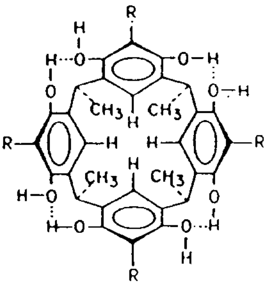

2 R=H
3 R=Br

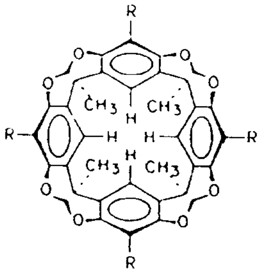

4 R=H
5 R=Br
6 R=CO_2CH_3

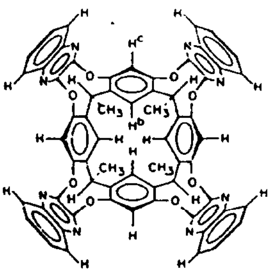

7a

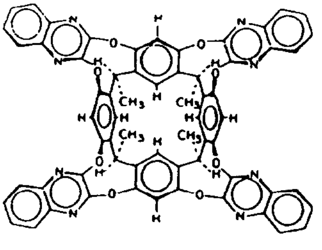

7b

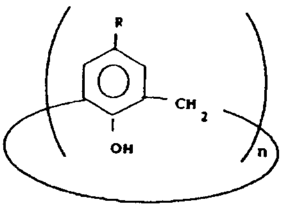

8

The X-ray structure of 7, crystallized from acetone, shows an average 7.2 Å wide and 8.3 Å deep cavity [37]. One molecule of acetone is located inside the cavity with the carbonyl double bond oriented parallel to the axis of the cavity and the two methyl groups pointing toward two quinoxaline rings (Fig. 2) and thus interacting with the p electrons of the quinoxalines. The second guest molecule of acetone lies into the intramolecular void created by the four aliphatic chains on the bottom part of the molecule. The third acetone molecule perches on top of the cavity, so that its arrangement seems determined, at least in part, by the voids created in the crystal lattice, rather than by the still available cavity space.

Cavitand 7 selectively binds aromatic compounds in organic solvents and in the gas phase. In acetone 1:1 cavitands precipitate when the guest concentration

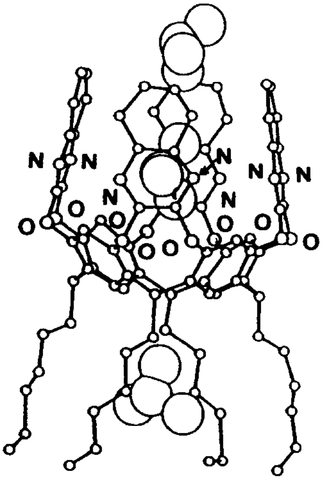

Fig. 2. Structure of 7 · 3acetone.

reaches a value of about three times the host concentration. Among the aromatic compounds tested so far, complexation with benzene, toluene, chlorobenzene, fluorobenzene and benzonitrile was found while no cavitands were detected with benzaldehyde, anisole, benzoic acid and phenol.

Among the calixarenes **8** [38–42], *p-tert*-butyl-calix[4]arene (**9**) is particularly interesting since it is able to form 1:1 [39] or 2:1 [42] inclusion complexes with aromatic guest molecules which occupy intramolecular cavities, whereas other calix[4]arenes give clathrates with the guest held in intermolecular voids or channels of the crystal lattice [41–43]. The X-ray structure of cyclo{quater[(5-*tert*-butyl-2-hydroxy-1,3-phenylene)methylene]}toluene 1:1 clathrate **9** [39] (Fig. 3) shows the inclusion of a toluene molecule into the tetramer.

The conformation of the tetramer, which has a fourfold symmetry, is calix shaped and is mainly determined by the four intramolecular hydrogen bonds. The dihedral angle formed by the phenyl rings with the molecular fourfold axis is 123°. The interactions between the host molecule and the cavity are mainly due to the *tert*-butyl groups.

Calixarenes can be chemically modified in various ways. The *tert*-butyl group in the readily available *tert*-butylcalixarenes may be replaced by different substituents such as SO_3H [45], NO_2 [46], $N{=}N{-}C_6H_4{-}R$ [47], $CH_2CH_2NH_2$ [48] and CH_2CH_2COOH [49]. Reactions at the phenolic hydroxy groups lead to esters [50], ketones [51] and amides [52]. Macrobicyclic derivatives such as calixcrowns [53] or calixspherands [54] also deserve mention. The methylene groups may also be converted into keto groups by oxidation.

After this functionalization they can act as complexing agents selective for particular metal ions. Conformationally immobile calix[4]arene derivatives with

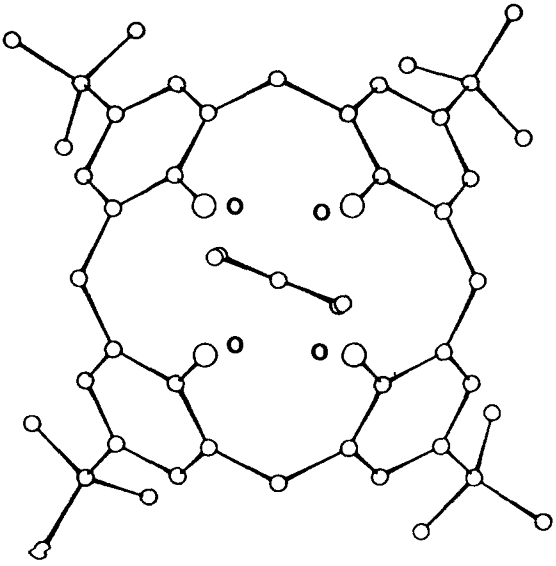

Fig. 3. Structure of **9** · toluene.

fixed "cone" structures and convergent binding chains have been synthesized. By reaction of *p*-*tert*-butylcalix[4]arene with α-chloro-*N*,*N*-diethyl acetamide or *tert*-butylbromacetate, the related tetraamide **10** or tetraester **11** have been obtained and their fixed cone structure established both in solution and in the solid state [54,55].

The X-ray structure of the tetraamide ligand (Fig. 4) exhibits a slightly distorted cone conformation with the four amide groups on one side and the *tert*-butyl groups

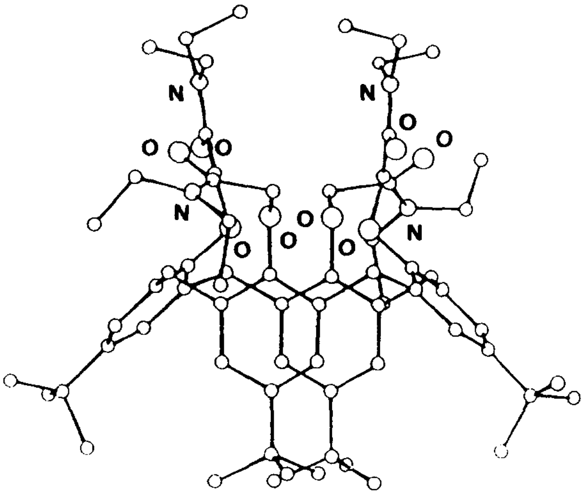

Fig. 4. Structure of **10**.

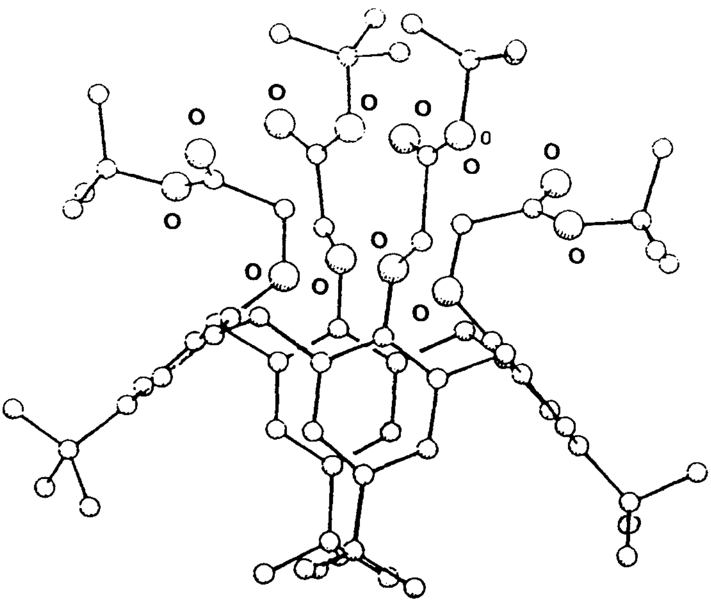

Fig. 5. Structure of **11**.

on the other side of the plane containing the bridging methylene groups of the macrocycle. The molecular conformation is similar to that reported for the tetraester **11** (Fig. 5) [54,55] which has a slightly distorted cone structure having two distinct regions with respect to an ideal plane containing the bridging methylene groups: a top hydrophilic region created by the ether oxygen atoms and that of the four ester groups which are all on the same side and a second hydrophobic cavity on the bottom created by the aromatic and *tert*-butyl groups.

The ester chains attached to the two aromatic rings, which are almost parallel to each other and perpendicular to the molecular plane, have the hydrogen atoms of the methylene groups pointing outside and the alkyl part of the ester moieties inside the hydrophilic cavity, whereas the other two ester chains of the units have the CH_2 inside and the $COOBu^t$ groups directed toward the exterior of the macrocycle. ^1H and ^{13}C nuclear magnetic resonance (NMR) spectra show that the dome structure is maintained in solution.

The tetraester and tetramide ligands exhibit very high efficiency and good selectivity toward sodium cation: the $[Na^+]/[Li^+]$ (about 10^4 for **11** and about 5×10^2 for **10**) and $[Na^+]/[K^+]$ (about 2×10^3 for **11** and 4×10^2 for **10**) selectivity makes calix[4]arene esters and amides attractive for sodium-selective electrodes or other sensors.

These substituted calixarenes completely encapsulate the complexed cation and efficiently deshield it from the counterion and from the solvent as observed in the structure of the potassium sulphocyanide complex with **10** (Fig. 6) where the cation

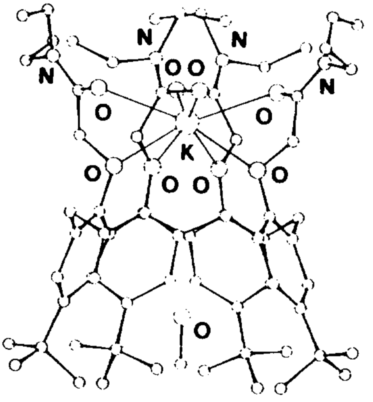

Fig. 6. Structure of K(**10**)·SCN·MeOH.

is coordinated by eight oxygen atoms which form an antiprism. The hydrophobic pocket of the macrocycle contains a methanol molecule for which there is no evidence of a short contact with the host molecule. The ether and amide oxygen atoms lie on two distinct parallel planes.

Analogously, lanthanide(III) ions (Eu^{3+}, Gd^{3+}, Tb^{3+}) have been encapsulated into the tetraamide moiety of **10** [56].

The selective bridging of two opposite OH groups in *p*-*tert*-butylcalix[4]arene allowed the synthesis of a new class of cation receptors, the calixcrowns. Some of them have ionizable phenolic or carboxylic groups and have been used in the active transport of monovalent and divalent cations across liquid membranes. Thus the macrobicyclic compound crowned-*p*-*tert*-butylcalix[4]arene **12**, obtained by bridging two opposite phenolic OH groups of the *p*-*tert*-butylcalix[4]arene with a polyethereal chain, possesses a hydrophilic cavity suitable for complexing cations and a lipophilic one for the inclusion of neutral molecules.

The X-ray structure of the pyridine 1:1 complex (Fig. 7) reveals a distorted cone conformation which defines an intramolecular apolar cavity. A molecule of pyridine is included in this cavity whereas the intermolecular cavities of the host lattice remain empty [57].

The development of these studies cleared the way to design and synthesize larger polydentate systems capable of securing into their coordination moiety more than one metal ion. This was to link the possibility offered by the series of new coordinating systems with the uncommon properties arising from the simultaneous presence of equal or different metal centres at a suitable distance. Thus many efforts were directed towards the preparation and the study of polynuclear complexes with macrocyclic or macroacyclic ligands. One of the first successful approaches was to obtain dinuclear systems and to understand in detail their physicochemical properties and chemical behaviour. This has allowed a better understanding of some biological

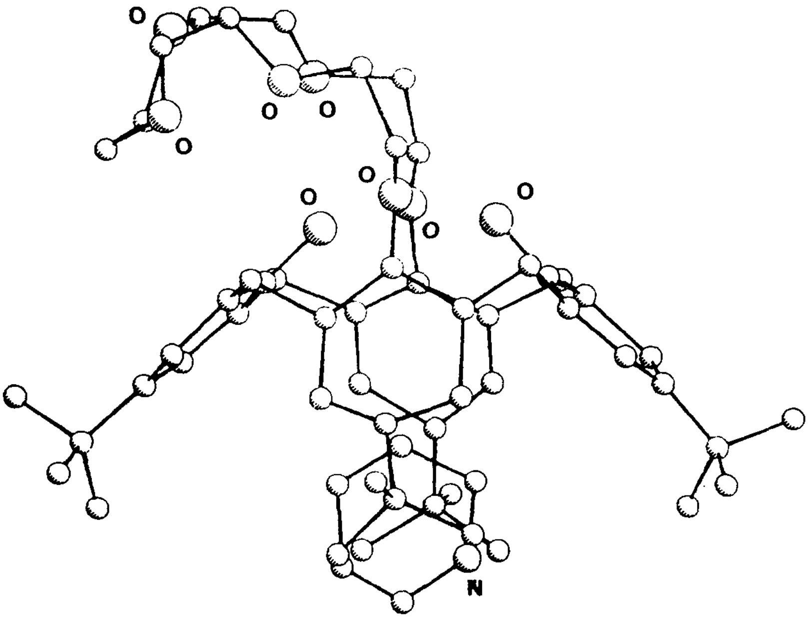

Fig. 7. Perspective view of **12** · pyridine.

processes which need the presence of such a molecular complexity to occur and of the magnetic and/or optical interactions between the metal centres.

The condensation of *p*-substituted phenols with formaldehyde forms cyclic oligomers, the above-mentioned calixarenes, whose distribution depends on the conditions of the condensation.

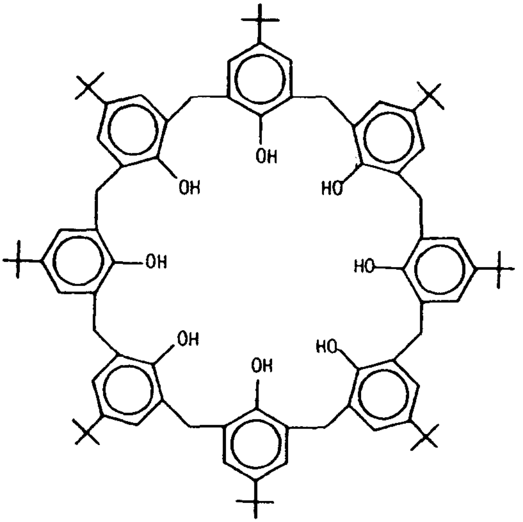

13

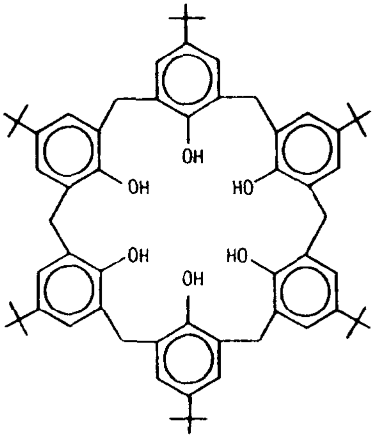

13'

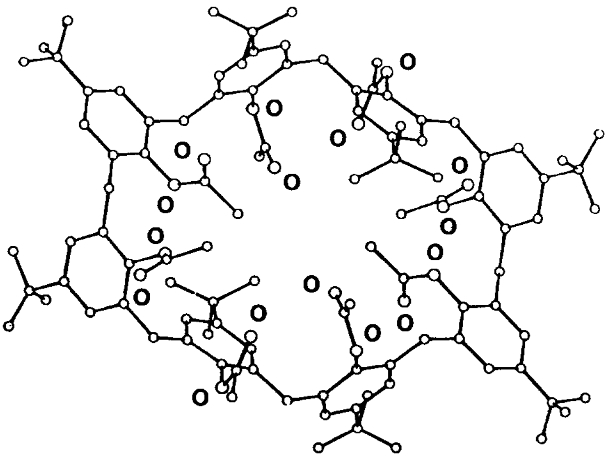

Fig. 8. Structure of the tetraacetyl derivative of **13**.

From a one-step process involving *p-tert*-butylphenol, paraformaldehyde, and a trace of base in refluxing xylene, the cyclic octamer *p-tert*-butylcalix[8]arene (**13**) can be isolated in high yields. With a larger amount of base, a cyclic hexamer *p-tert*-butylcalix[6]arene (**13′**), becomes a major product, isolable in high yield when rubidium hydroxide is used [58].

The X-ray structure of the octamer **13** [59], where acetyl groups replace hydroxyl groups, demonstrates such an enlargement of the cavity (Fig. 8). The molecule lies on a centre of symmetry and possesses an ellipsoid shape with the polar acetyl groups oriented within the cavity and the hydrophobic *tert*-butyl groups outside. The four methylene bridging carbon atoms of the asymmetric unit roughly lie on a plane. In this crystal the internal cavity is not occupied and has an approximate size of 1.51 × 3.73 × 4.56 Å.

Under carefully controlled conditions, **13** affords a 1:1 complex with europium(III). The calixarene binds in a bidentate mode to give $[Eu(\mathbf{13}\text{-}2H)(NO_3)dmf_4]\cdot 3dmf$ (Fig. 9(a)).

Addition of $[Eu(dmf)_8](ClO_4)_3$ to a dimethylformamide solution of **13** containing triethylamine forms yellow crystals of the neutral complex $[Eu_2(\mathbf{13}\text{-}6H)(dmf)_5]\cdot 4dmf$ [60], whose structure has shown (Fig. 9(b)) the ligand to adopt a pinched conformation with near-twofold rotational symmetry, both europium atoms being coordinated by the ligand in essentially identical environments. The europium atoms are bridged by two phenoxide donor atoms of the macrocyclic ligand and by a dmf molecule. Each is also independently bound to two dmf molecules and three phenolic groups giving a bicapped trigonal prismatic eight coordination. One of the capping groups on each europium atom is believed to be a phenolic donor of the calixarene.

The related complexes $[Ln_2(\mathbf{13}\text{-}6H)(dmso)_5]$ (Ln ≡ La, Eu, Tm, and Lu) have

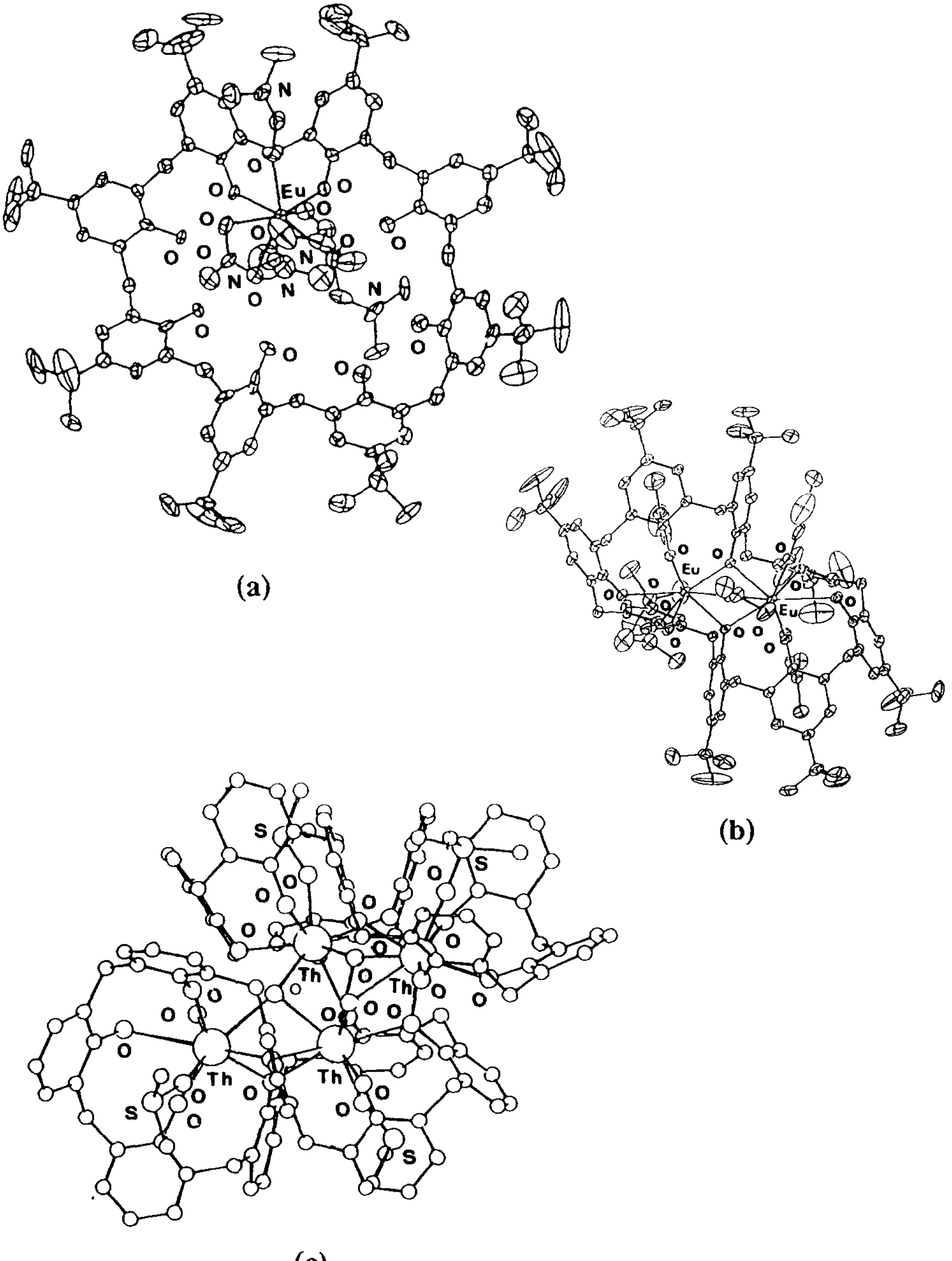

Fig. 9. Structures of (a) Eu(**13**-2*H*)(NO_3)dmf$_4$, (b) [Eu$_2$(**13**-6*H*)(dmf)$_5$] and (c) [Th$_4$(**13**-7*H*)(**13**-6*H*)(dmso)$_4$(OH)$_3$(OH)$_2$].

also been isolated and are isomorphous, containing eight-coordinate lanthanide ions bound to both dmso and the calixarene [60].

A chemical and photophysical study of homo- and heterodinuclear complexes $[(Ln^1_xLn^2_{2-x})(\mathbf{13}\text{-}6H)(dmf)_5](dmf)_4$ (Ln ≡ Nd, Gu, Tb, Gd, Mo, Yb) was carried out, aimed at probing the structure and luminescent properties of lanthanide(III) ions held at short distance (about 3.7 Å) in a macrocyclic ligand [60]. Luminescence measurements at 77 K suggest that the two lanthanide(III) ions encompassed by the ligand are in very similar environments with pseudo C_{3h} symmetry.

The presence of a low-lying metal-to-ligand charge transfer state in the Eu-containing complexes at ca. 20 000 cm^{-1} induces unusual spectroscopic properties. Very large absorption probabilities (about 10^{-6}) have been determined for the Eu(III) transitions and the Judd–Ofelt theory for f–f transitions fail to explain the very large value of the Ω_2 parameter (448×10^{-20} cm^2). In dmf solution, an efficient energy transfer from the ligand to Tb(III) occurs and makes the Tb(III) calixarene complex an interesting luminescence label [60].

Compound **13** reacts with $Th(ClO_4)_4 \cdot 12dmso$ to form the tetranuclear complex $[Th_4(\mathbf{13}\text{-}7H)(\mathbf{13}\text{-}6H)(dmso)_4(OH)_3(OH)_2] \cdot dmso \cdot 2H_2O$ [60] (Fig. 9(c)). Each calixarene unit is coordinated to two thorium atoms, the environment of each thorium comprising five ligand phenolic oxygen atoms, three monodentate and two bridging. A monodentate O-bonded dmso group enters through each cup of each ligand. The hydroxide groups variously bridge to the other thorium atoms within the same ligand, binding the two Th_2(calixarene) systems together [60].

Reaction of europium(III) salts with *p-tert*-butylcalix[4]arene (**9**) under the same conditions as used for reactions with the larger calixarene **13** yields the yellow crystalline complex $[Eu_2(\mathbf{9}\text{-}3H)_2(dmf)_4] \cdot 7dmf$ [61]. The complex is binuclear and centrosymmetric with the europium atoms bridged by one phenoxide group from each calixarene ligand and each europium atom being bound to two unidentate dmf ligands as well as the three other phenolic oxygen atoms of a calixarene ligand. The calixarene ligands adopt a distorted cone conformation in which a dmf molecule not coordinated to europium is included (Fig. 10(a)).

A similar dimeric europium(III) structure was also observed for the complex $[Eu_2(\mathbf{9}'\text{-}3H)(dmso)_2] \cdot 2acetone$ with the expanded calix[4]arene bis(homoxa)-*p-tert*-butylcalix[4]arene (**9′**) [61].

There are, however, several significant differences. Most obvious is the fact that, seemingly as a result of the increase in the size of the ligand and a strong coordinative interaction with the ether oxygen donor atom, the metal ion is drawn further into the ligand cup of **9′**, thereby leaving no room for any unincluded solvent binding as found with the Eu complex with **9**. Seven coordination of the metal ion is retained by O coordination of a dmso molecule which also has its methyl groups positioned close to the *tert*-butyl rim of calixarene and which therefore can be considered coordinatively included [61].

An understanding of the importance of distance, orientation and number of

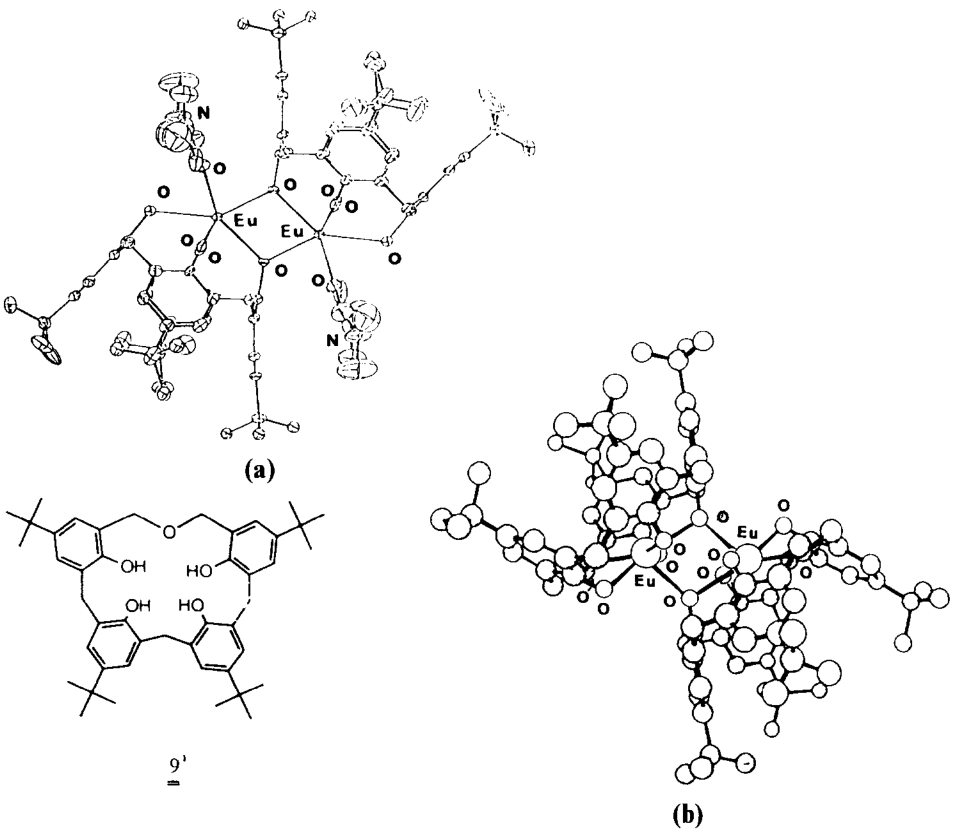

Fig. 10. Structures of (a) $Eu_2(\mathbf{9}\text{-}3H)_2(dmf)_4$ and (b) $[Eu_2(\mathbf{9'}\text{-}3H)(dmso)_2]\cdot 2acetone$.

donor atoms inside the macrocyclic components of the ligands is crucial for obtaining polynuclear complexes with unusual properties. To this end, the synthesis of polyporphyrins has been carried out with the preparation steps from mononuclear to hexanuclear derivatives [62–65].

The diamine porphyrin **14** [62,63] represents the starting material for ordered aggregates of tetrapyrroles. The synthetic route employs a linear, stepwise sequence with the diaminoporphyrin **14** in the two outer ring positions. The porphyrin **14** has D_{2h} symmetry and thus avoids the problems of diastereoisomerism encountered in this approach when porphyrins of C_{2h} symmetry are used. In addition, the aza seven-membered rings ensure relatively close and rigid connections to a second porphyrin.

High dilution coupling of the diamine **14** and the appropriate functionalized porphyrin gives dimeric **15**, trimeric **16**, tetrameric **17**, or hexameric **18** porphyrins [64,65]. Controlled metallation of these polyporphyrins (i.e. with $Zn(OAc)_2$) provides the bis-, tris-, tetra-, and hexametal derivatives [65].

Many excellent papers have been published during the last two decades on the

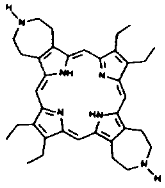

14

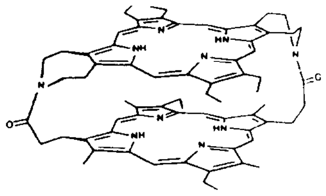

15

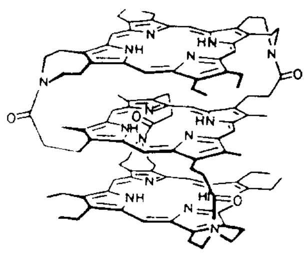

16

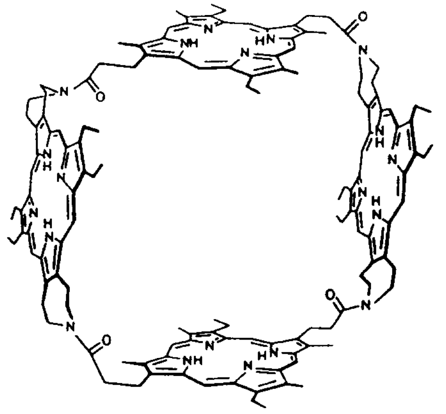

17

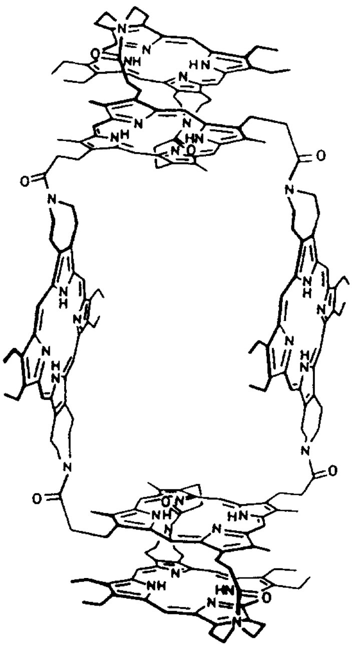

18

preparation and properties of dinuclear complexes and the most relevant results have also been reviewed [11,12]. In particular, attention was devoted to their correlation with the active site of metallo enzymes and metallo proteins containing dinuclear metallo entities in order to elucidate the factors that determine the reversible binding and activation of O_2 in various natural oxygen transport systems and mono- and dioxygenases and to mimic their activity [1,12,66,67].

Macrocyclic and macroacyclic ligands have also been used for the generation of compounds with specific spectroscopic and magnetic properties. It was found that complexes containing magnetic metal centres exhibit magnetic properties which are not simply the sum of those of the individual ions surrounded by their nearest-neighbour ligands. These properties result from both the nature and the magnitude of the interactions between the metal ions within the molecular unit.

Binucleating ligands containing two identical or different metal binding sites have also been designed with the aim of complexation to one of the sites will transform the second metal binding. This introduces the idea of positive cooperativity in the binding of two metal ions and new concepts of host organization. Podands having two β-diketones at both terminals of polyethylene glycol and related copper(II) and zinc(II) complexes have been prepared (Scheme 3) [68].

1:1 metal complexes with two metal ions coordinated by two β-ketoenolate groups have been used for the extraction of alkali metal picrates from H_2O into $CHCl_3$. The results indicate that [Cu(**19**)] was selective in the extraction of sodium ion, as was [Cu(**20**)] for potassium, exhibiting selectivity for ionic diameters based on cavity size similar to that observed in macrocyclic antibiotics or crown ethers. In these complexes, especially copper(II) compounds, contributions from two anionic oxygen atoms each from two β-ketoenolate units and three or four neutral oxygen atoms in the polyether linkage afford the most appropriate and selective binding site to alkali metal ions as shown in Scheme 3. The partition coefficients of Na^+ and K^+ picrates were negligibly small when H_2-**19** and H_2-**20** were used in their free or K^+ salt forms. Therefore, the cooperativity is absolute in the sense that the extraction of metal picrates takes place only with the assistance of another metal binding.

The use of dissociated anionic ligands is crucial for the successful observation of positive cooperativity since they coordinate strongly to the first transition metal ion and compensate its positive charge to allow the acceptance of the second positive metal ion into the organized molecular arrangement which is constructed through the structure-forming capacity of the first metal ion. This provides an interesting method of molecular organization in place of preorganization which has long been a dominant principle in crown ether chemistry. The metal-assisted organization after chemical synthesis may be an interesting alternative because the ligand synthesized could be subjected further to a reversible organization to construct or destroy the structure as required. Therefore, the method is expected to lead to a new strategy for design in supramolecular chemistry.

Using compartmental ligands, binuclear complexes can be synthesized, where the two metal centres, if paramagnetic, can interact with each other through the bridging donor atoms of the ligands in a ferromagnetic or antiferromagnetic way.

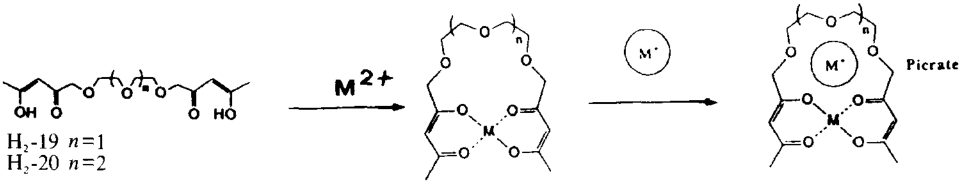

Scheme 3.

By changing the type of the ligand, the distance between the two chambers and/or the paramagnetic centres, it is possible to vary considerably the magnetic interaction and, with particular complexes, ferromagnetic interactions have been observed. Thus these complexes may be good building blocks for the fabrication of a molecular ferromagnet.

Complexes in which a single ligand organizes more than two metal centres into some predetermined arrangement may exhibit unique behaviour. In particular the preparation of complexes which contain two transition metal ions separated by distances of 3.5–6 Å is of considerable interest. At these distances, no direct interaction between the metal ions is expected, yet a substrate could interact simultaneously with both ions, and it has been shown that pairs of metal ions at suitable distance and/or with an appropriate structure can mediate certain chemical reactions either better than, or in different manner to, isolated centres [11].

In this article we present a review of the progress made in the development of synthetic procedures for the preparation of mono-, di- and polynuclear Schiff base complexes together with some examples of closely related systems. A short account on the same topics has already been published [5].

2. SCHIFF BASES

2.1. *Metal-free condensation reactions*

Simple di-, ter-, tetra-, and pentadentate Schiff bases **21–26** have been used for metal complexation and many complexes have been characterized also by X-ray diffraction. More recently, acyclic and macrocyclic ligands (including dinucleating and/or compartmental ligands) have been synthesized and their interaction with metal-ions studied [12,69].

For the synthesis of macrocycles, the dicarbonyl precursors of Scheme 4 and a wide range of diamines have been used. The condensation products are thus of the type reported in Scheme 5, with the formation of [1 + 1] and [2 + 2] macrocycles.

The use of particular precursors in condensation reactions or easy modification of the synthetic procedures has produced the desired macrocyclic or macroacyclic ligand.

When equimolar quantities of thiophene-2,5-dicarbaldehyde and an α,ω-primary diamine are allowed to react in methanol or ethanol, white or pale yellow powders or crystals of [2 + 2] macrocycles are obtained [70].

The structure of the macrocycle derived by condensation of 2,5-diformylthiophene and 1,5-diamino-3-oxapentene **27** confirms the discrete [2 + 2] nature of these compounds (Fig. 11). The free macrocycle possesses approximate C_5 symmetry through the two sulphur atoms and perpendicular to the thiophene rings; the latter are each planar and, although not parallel, are aligned and approximately eclipsed with minimum separations of 3.49 Å.

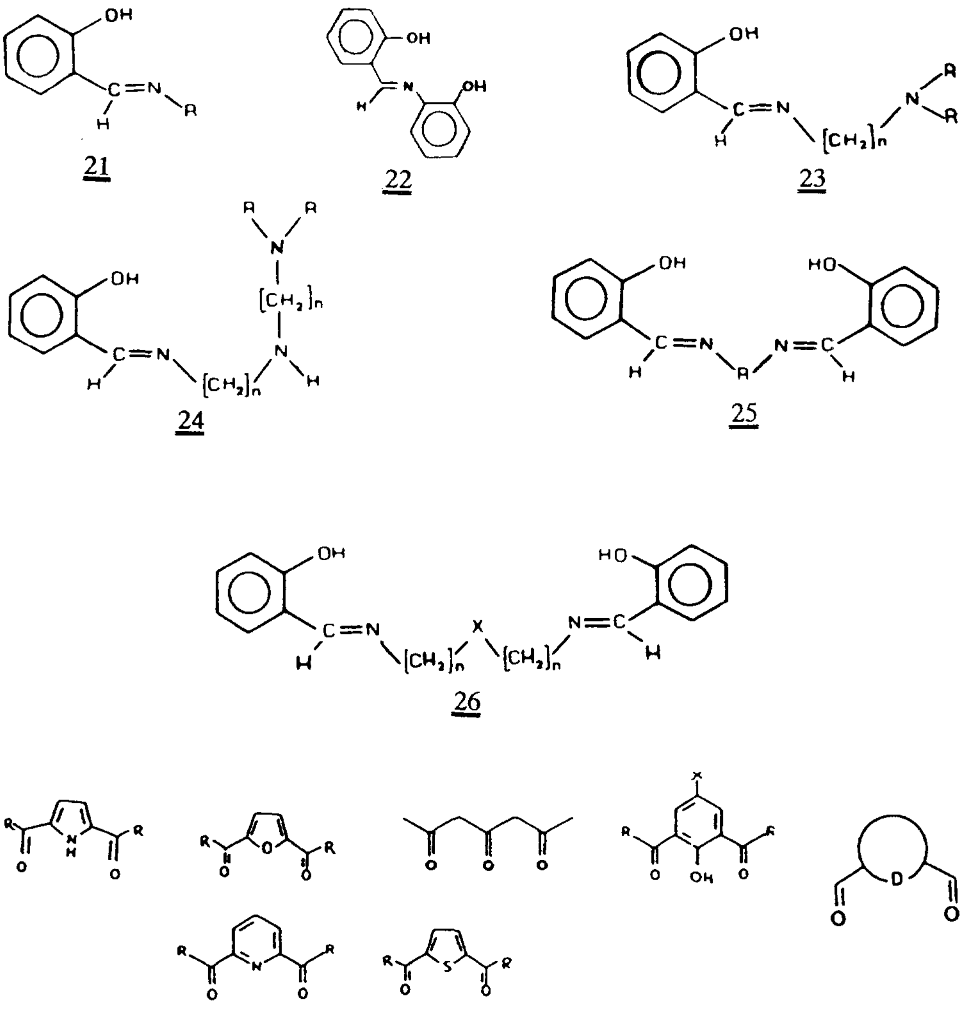

Scheme 4.

The presence of metal ions with the appropriate ionic radius has also allowed the synthesis, via the template effect, of larger coordinating systems. The structure of the dinuclear silver complex of the [2+2] macrocycle, derived from 2,5-diformylthiophene and 3,6-dioxaoctane-1,8-diamine, confirms the dinucleating ability of these ligands (Fig. 12).

The structure of this disilver complex cation has a twisted-loop configuration for the macrocycle. The two symmetry-related silver ions are accommodated at opposite ends of the macrocycle, each being coordinated most strongly by a pair of imine nitrogen atoms and by an H_2O molecule. Longer contacts to one of the ether oxygen atoms and to the two symmetry-related sulphur atoms of the thiophene fragments give rise to a coordination number between 3 and 6: the remaining ether

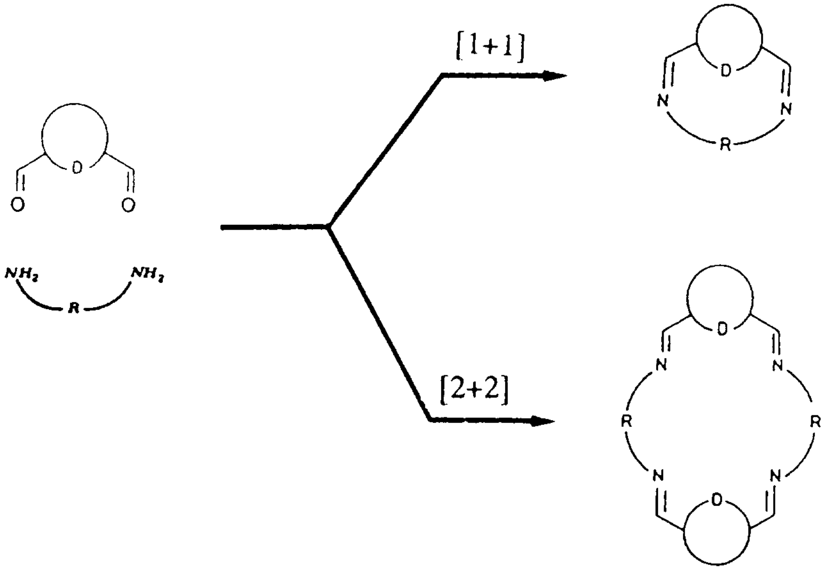

Scheme 5. Schematic representation of the [1 + 1] and [2 + 2] Schiff base macrocycles.

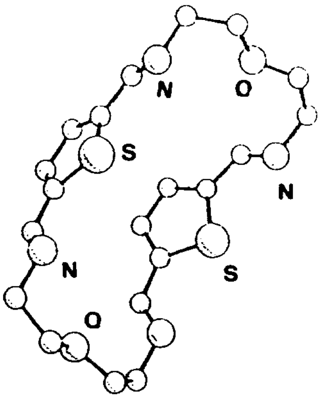

Fig. 11. Structure of **27**.

oxygen atom is distant and pointing away from the metal. The coordinated water molecule forms hydrogen bonds to two perchlorate anions; the thiophene fragment is planar [70].

The reaction of 2,6-diformyl-4Z-phenol ($Z \equiv Cl, CH_3$) with 1,2-diaminobenzene in alcoholic solution forms the corresponding [2 + 2] macrocycles which, on the basis of their IR and NMR spectra and X-ray structural analysis, have been formulated as the partially reduced compounds where two C=N groups have been reduced to CH_2–NH– groups [71].

Compound **29** (Fig. 13) has crystallographically imposed $\bar{1}$ molecular symmetry

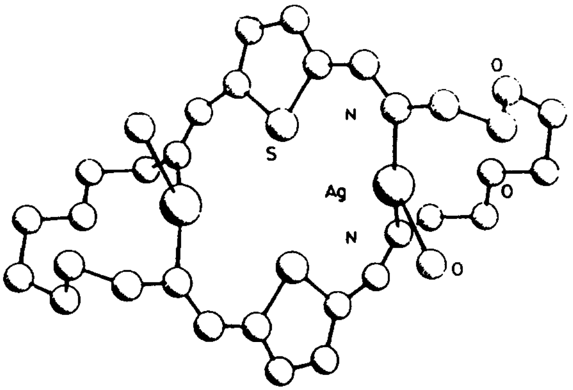

Fig. 12. Structure of $[Ag(\mathbf{27'})(H_2O)]^{2+}$.

	Z
28	Cl
29	CH_3

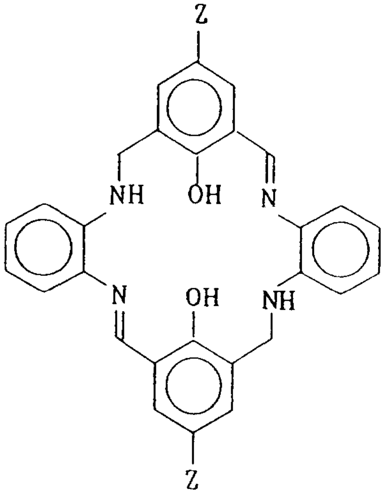

and the four nitrogen atoms are necessarily coplanar while the bounded aromatic rings are approximately so. The molecules, considered overall, adopt a two-step-like conformation. Significantly the two nitrogen atoms of each molecule present different characteristics, one iminic and the other aminic. The bond and torsion angles indicate the presence of sp^3 hybridization for the carbon atoms bonded to the aminic nitrogen atoms and sp^2 hybridization for the carbon atoms bonded to the iminic nitrogen atoms, confirming that a partial reduction has occurred during the synthesis.

The evolution of these Schiff bases has produced macrobicyclic ligands obtained in one-step multiple condensation reactions [72]. Thus the cyclic [2 + 3] Schiff base condensation represents the extension of the [2 + 2] macrocyclic coordination system into the third dimension. In addition to the uses in the field of molecular recognition, catalysis and transport, these cage molecules show particular promise in the stabilization of particular species. The nature and disposition of donor atoms in the rigid

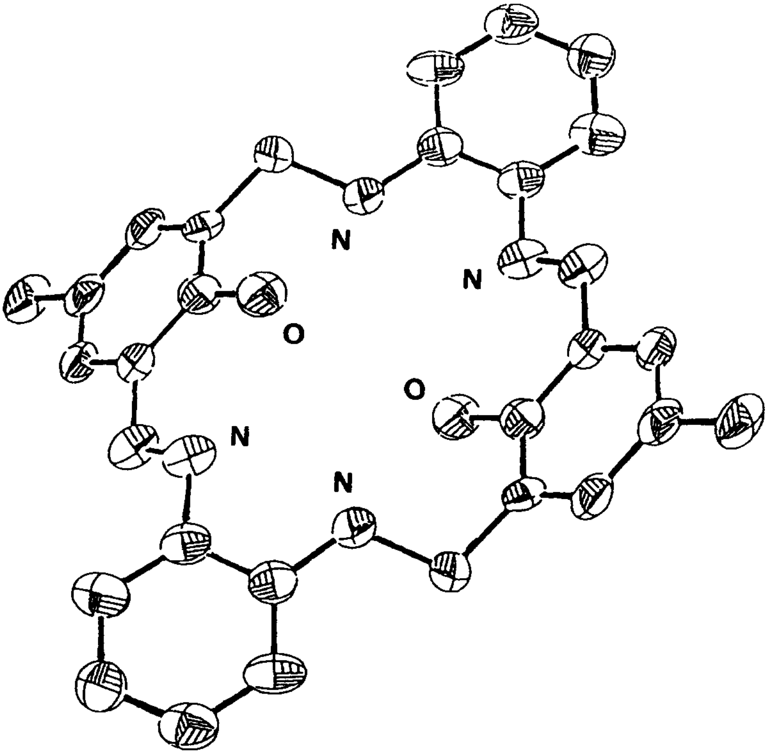

Fig. 13. Structure of **29**.

cage may enhance the stability of unusual oxidation states in the coordinated transition metal ion [73], while encapsulation may protect normally labile substrate species. It is hoped that this combination of characteristics will eventually permit moisture-sensitive chemistry to be carried out in the protected cavity under room temperature and atmospheric pressure [72–76].

Treatment of the tripod amine tris(2-aminoethyl)amine in refluxing alcohol with 4,4-diformyldiphenylmethane, isophthaldehyde, 2,6-diformylpyridine or 2,5-diformylfuran in stoichiometric ratio 2:3 results in the isolation of **30** or **31** as white crystals [72,73].

The solvent employed and its purity in the condensation reaction are of primary importance and can considerably influence the Schiff base formation. A representative example is the condensation reaction of 2,6-diformylpyridine with 1,2-bis(1-aminophenoxy)ethane which produces, in "dry" or "wet" benzene, the usual [2+2] macrocyclic or the macrobicyclic aminal compound **32** according to Scheme 6 [77] as confirmed by its X-ray structure (Fig. 14).

The condensation of 1,2-diaminobenzene with 2,6-diacetylpyridine was originally supposed to form **34a**.

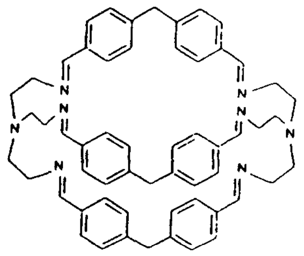

30

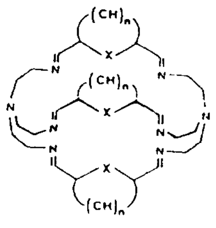

31

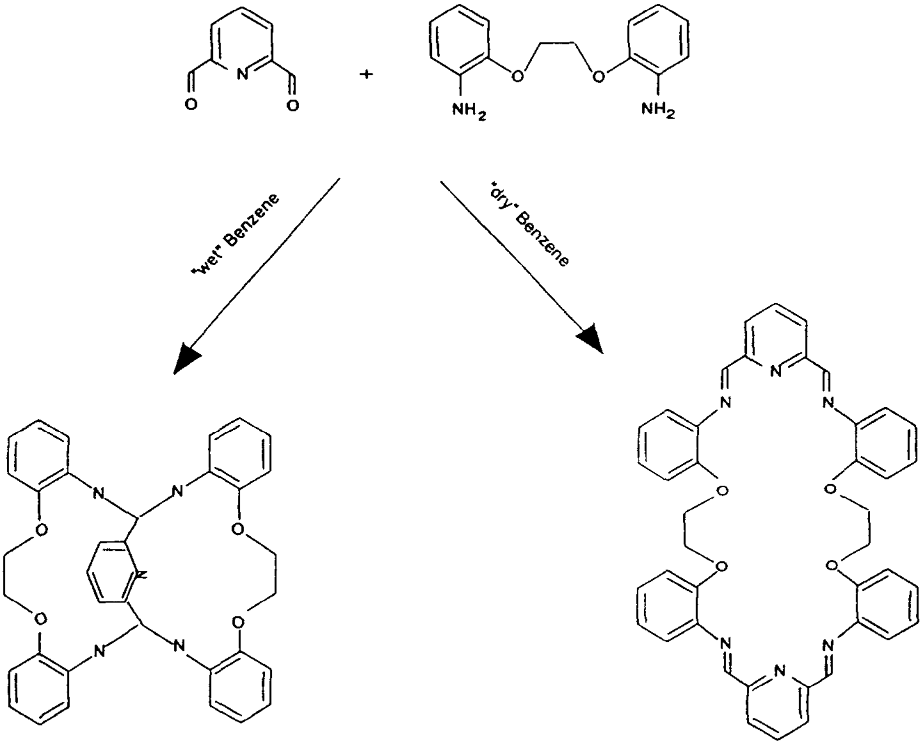

Macrobicyclic
aminal **32**

[2+2]

Scheme 6.

A subsequent reinvestigation [78] demonstrated that the reaction product contains one 12-membered and two 7-membered inner rings and not a single 18-membered inner ring (Fig. 15).

The adoption of structure **33** rather than **34a** can be understood in terms of

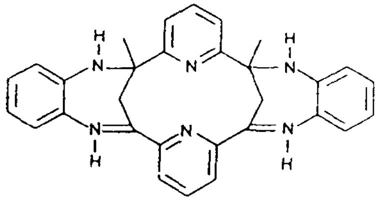

33

	R
34a	CH$_3$
34b	H

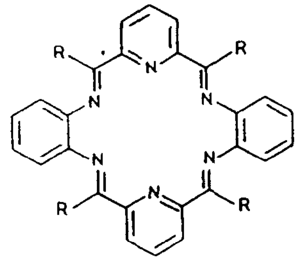

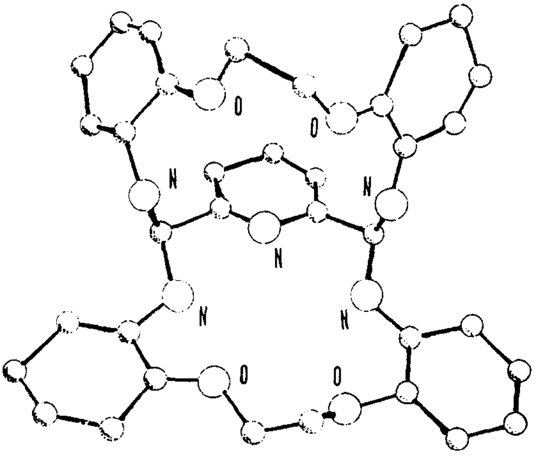

Fig. 14. Structure of **32**.

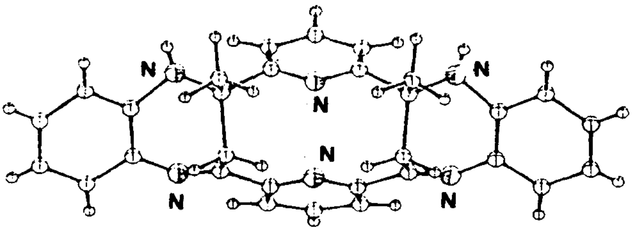

Fig. 15. Structure of **33**.

the steric hindrance which would exist in the latter between the methyl groups and the *ortho*-hydrogen atoms of the phenyl rings. A possible mechanism for its formation is indicated in Scheme 7. Structure (1) may be taken to represent a segment of an intermediate in the formation of **33**. The steric interaction inherent in (1) would favour a tautomeric shift to the enamine form (2). Free rotation about the single C–N bond so formed now allows nucleophilic attack by the electron-rich C=CH$_2$

function at the imino carbon atom of a neighbouring azomethine linkage in (3) to give (4) containing the 7-membered ring.

The structure of **33** also satisfactorily accounts for the failure to form stable metal complexes with a range of metal ions. Molecular models show that the molecule cannot act as other than a monodentate ligand to one metal ion. Not only is the central 12-membered ring too small to accommodate a metal ion, the positions and orientations of the two pyridine nitrogen lone pairs are such that they cannot chelate to a metal ion sitting outside the ring [78].

Treatment of **33** with an excess of $Cu(ClO_4)_2 \cdot 6H_2O$ in refluxing MeOH in the presence of air afforded dark green crystals [Cu(**35**)(H_2O)]$(ClO_4)_2 \cdot H_2O$ whose structure contains discrete [Cu(**35**)(H_2O)]$^{2+}$ cations, disordered ClO_4^- anions and a lattice water molecule [79]. Compound **33** has rearranged from a structure containing a (7 + 12 + 7) inner ring system to one containing a (15 + 6 + 3) inner ring system with loss of two hydrogen atoms. The Cu(II) ion is contained within the 15-membered ring being bonded to the imino nitrogen atoms and sitting 0.37 Å above the N_4 plane in the direction of an apical water molecule; the coordination geometry is thus a distorted square pyramid. The macrocycle is folded (Fig. 16).

Two important features of the **33** to **35** rearrangement may be noted. One is the reversal of the $C{=}CH_2$ to C=N addition described in Scheme 7 and the second is the aziridine ring formation via dehydrogenation at nitrogen and carbon atoms. The observation of a rather positive reversible one-electron reduction for [Cu(**35**)(H_2O)]$(ClO_4)_2 \cdot H_2O$ would be consistent with a Cu(II)→Cu(I)→Cu(II) redox cycle in the oxidative dehydrogenation. It was proposed that the driving force

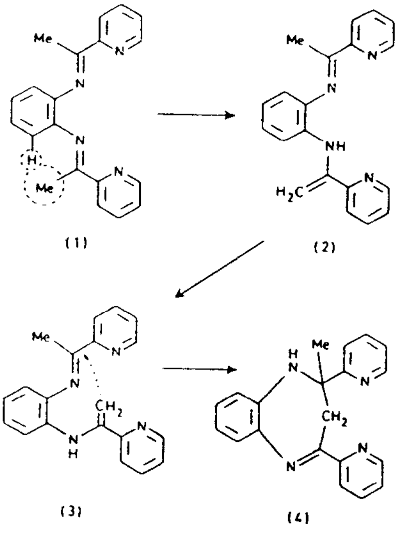

Scheme 7.

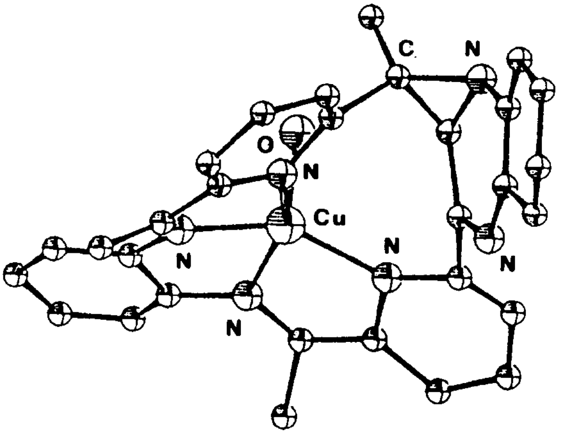

Fig. 16. Structure of $[Cu(\mathbf{35})(H_2O)]^{2+}$.

for the rearrangement is the stability gained by providing a suitably sized macrocycle cavity for the metal ion.

The necessity of dioxygen in the liquid rearrangement is confirmed by the following observation: when the reaction was carried out in the absence of dioxygen, the product was the brown microcrystalline complex $Cu(\mathbf{36})(ClO_4)_2 \cdot H_2O$, where **36** is the product of addition of two molecules of MeOH across the two azomethine bonds of **33** as confirmed by IR data [79]. The complex has a square pyramidal coordination geometry.

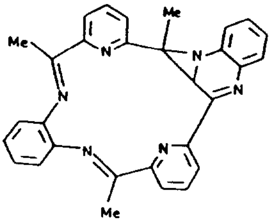

35

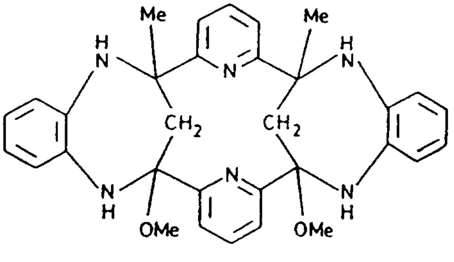

36

Unlike **33**, the dimethanol adduct **36** has sufficient flexibility to fold so as to bring the four secondary amine groups into a square planar arrangement with the lone pairs directed inwards towards a centrally coordinated metal ion leaving one axial site available for the attachment of a fifth ligand (H_2O or ClO_4^-). In agreement with the predictions of the IR spectra, this conformation (C_{2v}) of **36** does not permit coordination of the pyridine groups, these being disposed roughly parallel to each other. Significantly, recrystallization of Cu(**36**)$(ClO_4)_2 \cdot H_2O$ from O_2-free MeCN led to recovery of the free **33** macrocycle.

The easy recovery of **33** during attempts to obtain metal complexes of **34a** by template procedures led to the conclusion that steric crowding inhibited the formation of **34a**. This could arise via interaction of the methyl groups with proximal aromatic hydrogen atoms.

The condensation of 2,6-diacetylpyridine and 1,2-diaminobenzene in the presence of the nitrate of lanthanum(III), praseodymium(III) or neodymium(III) yielded the metal-free tricyclic compound **33** and a metal-free "half-cycle". However, minute yields of metal-containing compounds having the general formula $[M(NO_3)_3($**34a**$)] \cdot nH_2O$ ($n = 0.5$–3.0) could be obtained from the mother liquid after the removal of **33** and of the half-cycle.

The structure of [Pr(**34a**)$(NO_3)_2 \cdot (MeOH)](ClO_4) \cdot 0.5MeOH \cdot 0.5H_2O$ reveals with certainty the formation of macrocyclic complexes of **34a** [80] (Fig. 17). The tetraimine macrocycle **34a** coordinates with its six nitrogen atoms to the central metal ion, which is 11 coordinated, being bound also in two bidentate nitrate ions and to the oxygen atom of a methanol molecule. The presence of one nitrate and one methanol group, both coordinated on the same side, causes an asymmetric bonding mode of this nitrate group. The chelate on the opposite site is not influenced by steric factors and the two Pr–O distances are almost equal. The macrocyclic ring is not planar but strongly bent, in a way reminiscent of the shape of the free ligand, although this exists in the tricyclic conformation [80].

In contrast, the related template condensation of 1,2-diaminobenzene with

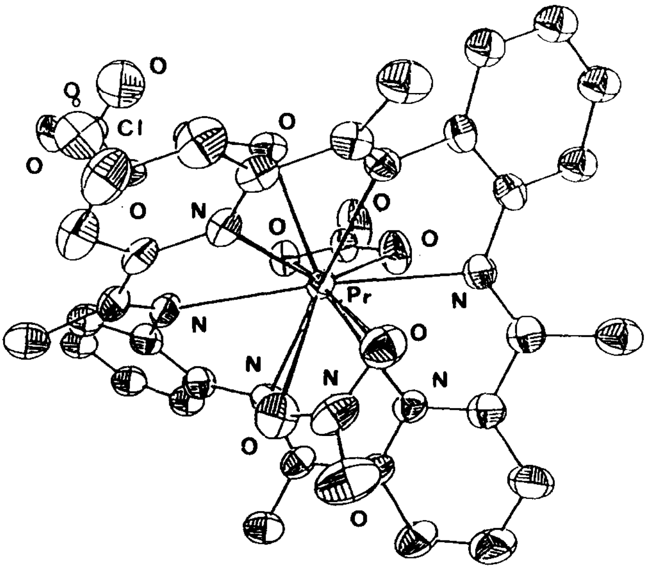

Fig. 17. Structure of [Pr(**34a**)$(NO_3)_2(MeOH)] \cdot ClO_4$.

2,6-diformylpyridine in the presence of Ca(II), Sr(II), Ba(II) and Pb(II) readily gives complexes of the hexaazamacrocycle **34b** [81], bearing out the predictions made for the [18]annulene analogue via theoretical calculations [82].

Although a pattern appears to be emerging for non-template formation of macrocycles (high dilution reactions in non-protic solvents and access to ring-contracted forms), it is too early to state that any general behavioural principle has been established.

2.2. *The template effect*

Ideally, a macrocyclic complex is formed by adding the required metal ion to a preformed ligand. However, the synthesis of the required macrocycle often results in a low yield of the desired product with side reactions such as polymerization predominating. In order to circumvent this problem, the ring-closure step in the synthesis may be carried out under conditions of "high diffusion", or "rigid groups" may be introduced to restrict rotation and internal entropy losses in the open-chain precursor and so facilitate cyclization. One effective method for the synthesis of macrocyclic complexes involves an in situ approach wherein the presence of a metal ion in the cyclization reaction markedly increases the yield of the cyclic product. The metal ion plays an important role in directing the steric course of the reaction; this has been termed the metal template effect [83].

The size of the cation used as a template has proved to be of importance in directing the synthetic pathway in the Schiff base systems (Scheme 8). Of the alkaline earth cations only magnesium generates the pentadentate [1 + 1] macrocycle but it is ineffective in generating the hexadentate [1 + 1] macrocycle which is readily synthesized in the presence of the larger cations calcium, strontium, barium and lead(II). These cations, however, generate the [2 + 2] macrocycle derived from the components giving the [1 + 1] macrocycle with magnesium [84].

The similarity in ionic radii between the alkaline earth metal cations and the lanthanide(III) cations suggested that the latter should also be efficient templating devices, and this has proven to be the case.

The actinides, with their high ionic radii and/or unusual coordination geometry, can produce and stabilize expanded macrocyclic ligands as in the preparation of "superphthalocyanines" [85]. With certain precursors (i.e. 2,6-diacetylpyridine and 1,3-diamino-2-hydroxypropane), [3 + 3] and [4 + 4] macrocyclic complexes have been synthesized. For the [2 + 2] ligands, the head and the lateral units can be varied with the consequent formation of macrocycles with different donor atoms and/or different cavity sizes.

2.3. *Transmetallation reactions*

Because of the synthetic difficulty and instability of the macrocyclic Schiff base ligands in the uncomplexed state, it seems that the synthesis of metal macrocyclic

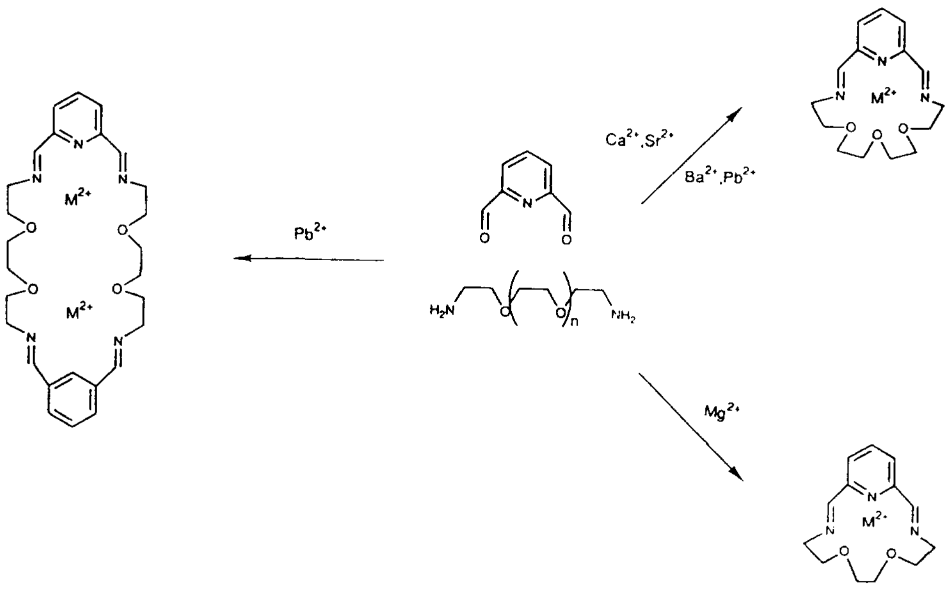

Scheme 8. Schiff base macrocycle synthesis in the presence of non-transition-metal templates.

complexes is often restricted to those metals which are effective as templates. In spite of that, it has been found that this class of complexes are usually kinetically labile and that the complexed template ion could be exchanged in many cases with other metal ions present in solution. Since that observation, attention has been focused on the synthesis of macrocyclic complexes by transmetallation reactions to obtain complexes of metal ions which were not effective if fused in the direct template route. Furthermore, when some metal ions were used in the transmetallation reactions, new types of macrocyclic ligands arising from ring expansions or contractions were obtained. This was dependent on the demands and the size of the transmetalling ion.

For the larger Schiff base macrocycles, it has been generally found that the transition metal cations are ineffective as templates. Consequently the kinetic lability of the metals present in the generation of macrocyclic complexes derived from the use of alkaline earth, lanthanides and main group templating agents has enabled the generation of the corresponding transition metal complexes through transmetallation reactions (Scheme 9) [84,86–88]. This approach has been particularly successful when applied to the generation of dinuclear copper complexes of tetraimine Schiff base macrocycles especially starting from barium(II) analogues.

This reaction has recently been extended to a series of similar bibracchial [2+2] macrocyclic Schiff base complexes derived from functionalized triamines. While copper(II) ions did not act as templates for the [2+2] cyclocondensation of *N*,*N*-bis(2-aminoethyl)-2-methoxyethylamine and 2,6-diacetylpyridine, the larger and less stereochemically demanding barium(II) ion was found to be successful. This

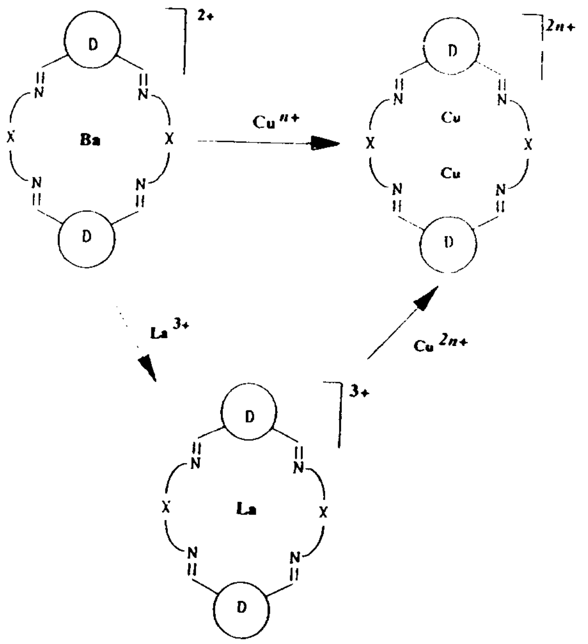

Scheme 9. Schematic representation of mononuclear lanthanide(III) and binuclear copper formation via transmetallation reaction from the analogous mononuclear barium macrocyclic complex.

reaction resulted in the formation of the mononuclear complex of the 24-membered macrocycle **37** (Scheme 10) [89].

Vapour diffusion of diethylether into a solution of [Ba(**37**)]$(ClO_4)_2$ in acetonitrile resulted in the formation of crystals suitable for an X-ray crystallographic study. The molecular structure of the cation is shown in Fig. 18.

The asymmetric unit consists of two crystallographically almost identical independent molecules of the barium macrocyclic complex and four perchlorate anions. The macrocycle adopts a conformation with approximate C_2 symmetry, defining a molecular cleft between the pyridine diimine units. The chiral nature of the cleft arises from the different enantiomorphic configurations of the 5-membered chelate rings formed by the pendant arms which results in the presence of both the $\Lambda(\delta\delta)$ and $\Delta(\lambda\lambda)$ stereoisomers (Fig. 19) within the unit cell.

All ten donor atoms of the ligand interact with the barium ion. The pyridyl fragments are planar and the angle between the rings is 24°. The imine bonds are twisted out of the planes of pyridyl rings presumably to accommodate the interaction of the imino nitrogens with the metal ion. The space-filling diagram of the cation (Fig. 20) clearly shows the cleft-like structure of the molecule and the extent to which the barium ion is encapsulated within the macrocyclic ligand [89].

The ^1H NMR spectrum of [Ba(**37**)]$(ClO_4)_2$ indicates that the macrocyclic ligand **37** is maintained in a conformationally rigid state in solution. Rotation about

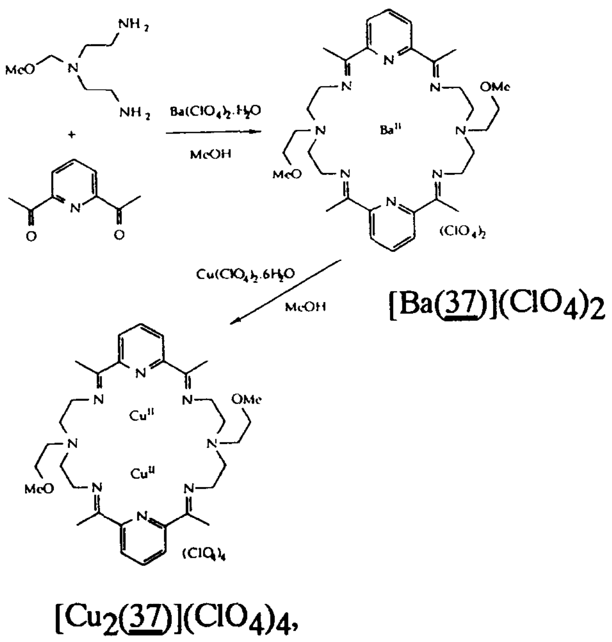

Scheme 10.

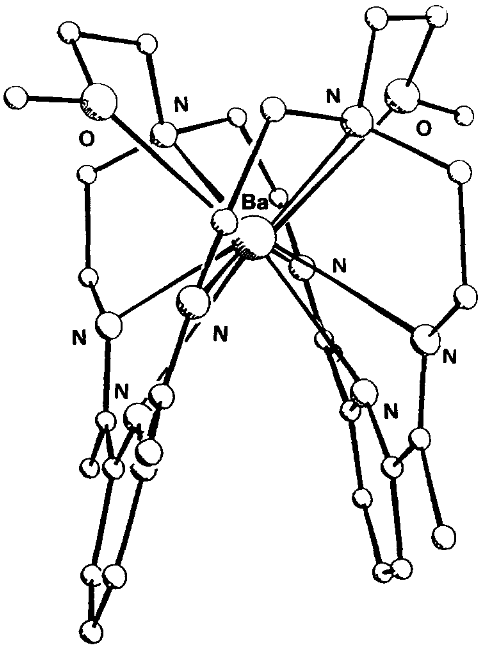

Fig. 18. Structure of $[Ba(\mathbf{37})]^{2+}$.

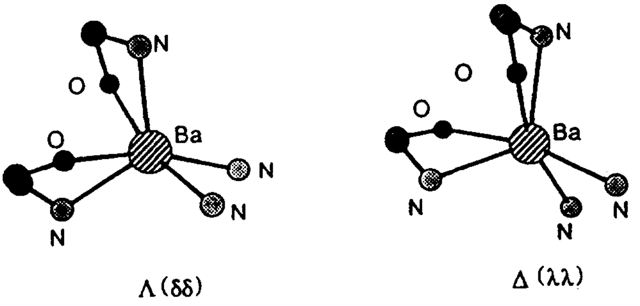

Fig. 19. Representation of two enantiomeric forms of $[Ba(37)]^{2+}$.

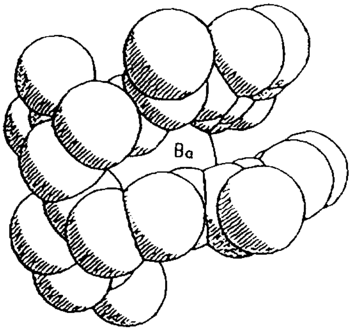

Fig. 20. Space-filling diagram of the $[Ba(37)]^{2+}$ cation.

the ring CH_2CH_2 groups is restricted and no inversion occurs at the tertiary amine nitrogen atoms. As a result, the two hydrogen atoms constituting each macrocyclic methylene group are magnetically inequivalent [89].

The dinucleating capability of the 24-membered bibracchial macrocycle **37** was readily demonstrated by transmetallation of the mononuclear barium complex with copper(II). A refluxing methanolic solution of the complex was treated with copper(II) perchlorate hexahydrate affording $[Cu_2(\mathbf{37})](ClO_4)_4$, a blue powder (Scheme 10). Crystals suitable for an X-ray structure determination were obtained by vapour diffusion of diethyl ether into a solution of $Cu_2(\mathbf{37})(ClO_4)_4$ in acetonitrile. In the crystalline state, the bibracchial macrocycle **37** of the dicopper(II) complex adopts an open conformation (Fig. 21) in contrast to the folded cleft-like structure found in the barium(II) complex. The two copper(II) ions are bound within the pyridine diimine head units of the macrocycle, in identical environments related by a crystallographic inversion centre. The metal ions are separated by a Cu–Cu distance of 5.56 Å with the donor atoms constituting two isolated coordination sites. In accordance with this observation, the effective magnetic moment of $[Cu_2(\mathbf{37})](ClO_4)_4$ at room temperature is $1.73\mu_B$ per copper atom, indicating the absence of any spin interaction within the copper(II) pair.

The coordination geometry around each copper(II) ion may be described as

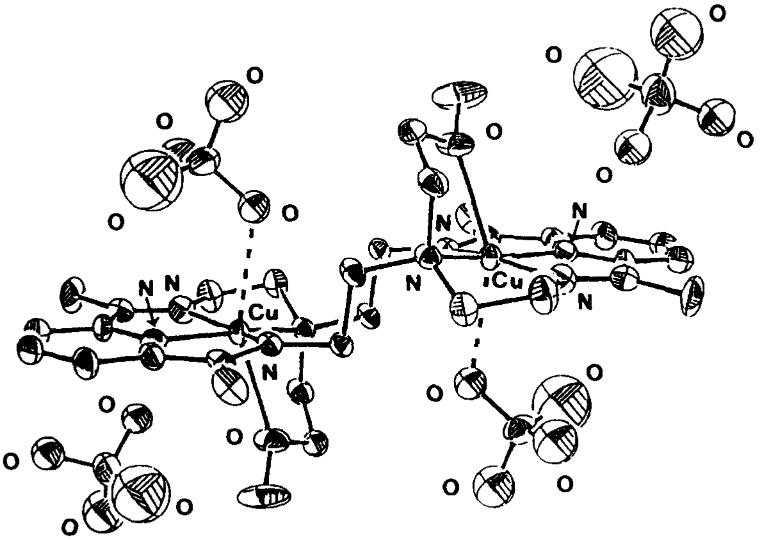

Fig. 21. Structure of $[Cu_2(37)](ClO_4)_4$.

severely distorted square-based pyramidal. The four basal donors are provided by the nitrogen atoms of the macrocyclic ring. The apical site is filled by a longer interaction with the ethereal oxygen donor of the pendant arm. The steric restrictions placed on the donor atoms by the ligand constitution account for the significant deviations that occur from the ideal square-based pyramidal geometry. It is apparent from Fig. 21 that the tertiary amino nitrogen atom is distorted from the basal plane in accordance with the desire of the pendant arm ethereal oxygen to attain an orthogonal, apical coordination mode. In addition to the interactions of each copper(II) ion with the macrocyclic ligand **37**, there is a long-range, electrostatic interaction with an oxygen atom of a perchlorate ion [89].

Precisely why the macrocycle in $[Cu_2(\mathbf{37})](ClO_4)_4$ opens out destroying the molecular cleft is unclear particularly as the cleft is retained in related disilver(I) complexes; the process is, however, not unprecedented. It is possible that the higher ionic potential of the copper(II) ions leads to an enhanced electrostatic repulsion between the encapsulated metal cations and that this, together with the favoured coordination opportunity offered by the planar "head" units, provides the stimulus for the observed conformational change. In view of the electrochemically stable nature of the barium(II) ions used in the template synthesis of **37**, the possibility of introducing copper(I) ions via a transmetallation reaction was investigated. Employing acetonitrile as a solvent under anaerobic and moisture-free conditions, a colourless solution of $[Cu(MeCN)]_4(BF_4)$ was added to a colourless solution of $[Ba(\mathbf{37})](ClO_4)_2$ resulting in the immediate appearance of an intense brown–orange colour. A similar feature has been observed with a number of copper(I) complexes of ligands containing pyridine diimine units, indicating that transmetallation had been achieved. After cooling to 238 K, dioxygen was bubbled through the solution for 15 min without any discernible changes occurring. However, as the solution was allowed to warm to room temperature a dark green colour developed. This could not be removed either by application of vacuum or by purging the solution with nitrogen, thus demonstrating that the copper(I) species had been irreversibly oxidized. Addition of diethyl ether resulted in the precipitation of a dark green solid which could not be characterized satisfactorily. The conformational flexibility of the macrocyclic ligand leading to the loss of the molecular cleft on transmetallation has been demonstrated in the above crystal structures. Given the open nature of the dicopper complex, it is likely that any dicopper(II) peroxo species formed within the macrocyclic cavity would not be prevented from undergoing intermolecular autoxidation reactions. Thus it appears that a prospective room temperature synthetic dicopper dioxygen carrier requires the incorporation into its ligand architecture of a more rigidly defined cleft or cavity to protect sterically the binding site [89].

A transmetallation reaction was also successfully carried out for the preparation, in high yield, of macrocyclic hexamine complexes of lanthanide ions [90,91]. The complex [Ba(**38**)$(ClO_4)_2$], suspended in an excess of aqueous lanthanide nitrate, slowly dissolved and crystals of the hexamine complex of the lanthanide were deposited. Two types of complex were formed: [M$(NO_3)_2$(**38**)(H_2O)]$NO_3 \cdot H_2O$ (M ≡ La, Ce, or Pr) and [{M(NO_3)(**38**)$(H_2O)_2$}$_2$]$(NO_3)[ClO_4]_3 \cdot 4H_2O$ (M ≡ Nd, Sm, Eu, Gd, Tb, Dy, Ho, or Er) [90,91]. The complexes [Ln(**34b**)$(NO_3)_3$] have been conveniently prepared by reaction of [Ba(**34b**)$_2$]$(ClO_4)_2$ with the appropriate lanthanide(III) nitrate hexahydrate in a methanol–water solution [91].

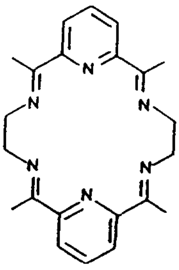

38

Similarly to the barium complexes, the analogous lanthanide(III)(**38**) complexes, undergo a transmetallation reaction with the consequent formation of the macrocyclic dicopper(II) complexes when reacted with $Cu(ClO_4)_2$ [92,93]. The lanthanide(III) complexes are therefore sufficiently kinetically labile for the transmetallation reaction to occur with copper(II) and produce essentially the same complexes as have been found using the corresponding barium(II) complexes (Scheme 9).

The [2 + 3] condensation of the tripod amine tris(2-ethylamino) amine with glyoxal, using group 2 metal ion templates, results in the formation of hexamino macrobicyclic complexes according to Scheme 11.

The template ion may be easily removed by transmetallation to produce mononuclear or dinuclear complexes. The X-ray structure of [Co(**39**)]$(ClO_4)_2$ [94] shows that the cobalt atom and the two bridgehead nitrogen atoms lie on a crystallographic 3-fold axis. The metal is coordinated to all six imino donors (only two of which are crystallographically independent) and has D_3 symmetry (Fig. 22).

Similarly, the condensation of a tris(3-aminopropyl)amine with benzene-1,3-dicarbaldehyde in the presence of $AgNO_3$ produces the dinuclear silver(I) complex of the octaazahexa Schiff base macrocyclic ligand **40** which is converted to a unique dinuclear copper(I) hexa Schiff base cryptate complex by transmetallation [95]. In the cation $[Cu_2(\mathbf{40})]^{2+}$, the two copper atoms are enclosed within the ligand, separated by 4.41 Å. Each copper atom is four coordinated by

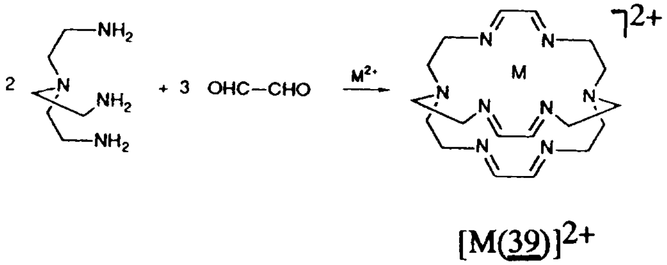

Scheme 11.

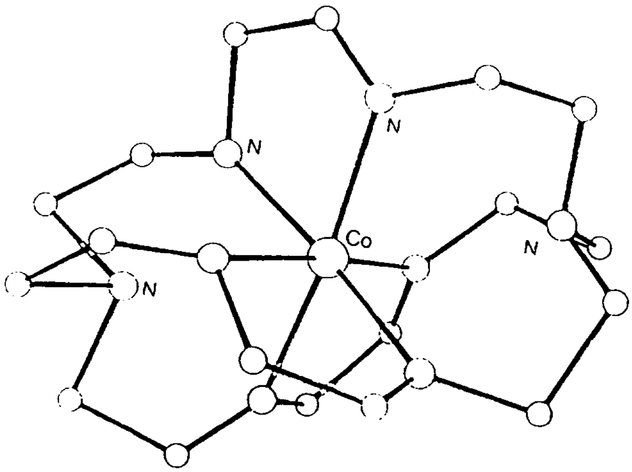

Fig. 22. Structures of $[Co(\mathbf{39})]^{2+}$.

three nitrogen atoms from the weakly basic imine-*m*-xylene moiety and one more basic tertiary bridgehead nitrogen from the tris(3-aminopropyl) moiety. The coordination around each copper atom has been considered essentially trigonal planar (Fig. 23).

Transmetallation of $[M(\mathbf{39})]^{2+}$ with an excess of $[Cu(CH_3CN)_4]ClO_4$ forms $[Cu_2(\mathbf{39})](ClO_4)_2$ while, with an excess of copper(II) salts, $Cu_2(H\text{-}\mathbf{39})X_4$ ($X \equiv ClO_4^-$, $CH_3SO_3^-$) is obtained. By adjustment of the pH in the preparation of the perchlorate salt, the mixed-valence complex $[Cu_2(\mathbf{39})](ClO_4)_3$ has been obtained [94,96]. The X-ray structure of $[Cu_2(\mathbf{39})](ClO_4)_2$ (Fig. 24) reveals a very short (2.448 Å) copper–copper separation. These copper ions are pulled slightly (0.182 Å) out of the trigonal plane toward each other, an observation which has been considered consistent with the existence of bonding interaction between copper ions [96].

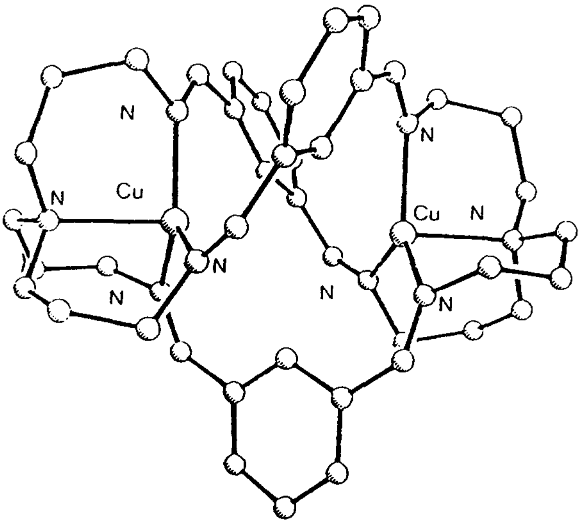

Fig. 23. Structure of $[Cu_2(\mathbf{40})]^{2+}$.

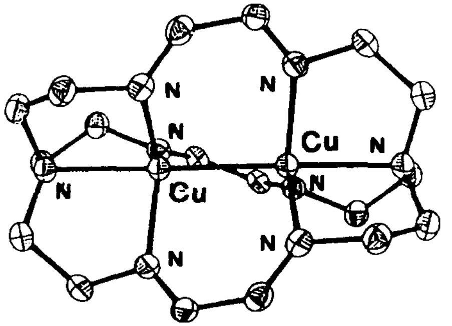

Fig. 24. Structure of $[Cu_2(\mathbf{39})]^{2+}$.

Magnetic and spectroscopic properties of Cu_2(H-**39**)X_4 support the presence of mixed-valence copper(I)–copper(II) species [96].

When complexes derived from compartmental ligands are employed, the transmetallation reaction can take place also with a change in the coordination chamber for the incoming ion. As an example, the reaction of the $Ba(ClO_4)_2$ complexes with uranyl(VI) diacetate in refluxing methanol forms the mononuclear uranyl(VI) complexes according to Scheme 12.

NMR, IR and mass spectra indicate that the uranyl(VI) cation occupies the Schiff base cavity as confirmed by the X-ray structure of uranyl(VI) complex UO_2(**42**-2*H*)(urea) [97], while the analogous starting barium(II) complexes are in the polyether coordination chamber.

The structure of Ba(**40**)$(ClO_4)_2$, which appeared to contain a molecule of MeOH, and the structure of Ba(**41**)$(CF_3SO_3)_2$ were determined by X-ray crystallography (Fig. 25). In Ba(**40**)$(ClO_4)_2$·(MeOH), the macrocycle is folded around the barium ion in order to achieve coordination of the cation by all eight oxygen atoms of the host. A perchlorate anion and a methanol oxygen atom complete the coordination. In Ba(**41**)$(CF_3SO_3)_2$, which has a shorter polyether bridge, all macrocyclic oxygens again coordinate the barium cation, but here the six hetero atoms form an almost planar arrangement. Triflate anions above and below this plane complete the ninefold coordination of the cation (Fig. 25(b)).

In the uranyl(VI) complex UO_2(**42**-2*H*)(urea), urea is coordinated within the

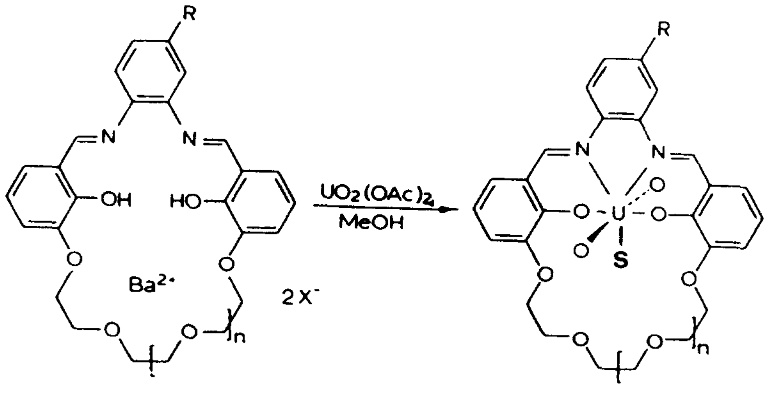

Ba(40)X_2 (X=ClO_4^-; n=3)
Ba(41)X_2 (X=$CF_3SO_3^-$; n=1)
UO_2(42-2H)(S) (S=urea; n=5)

Scheme 12.

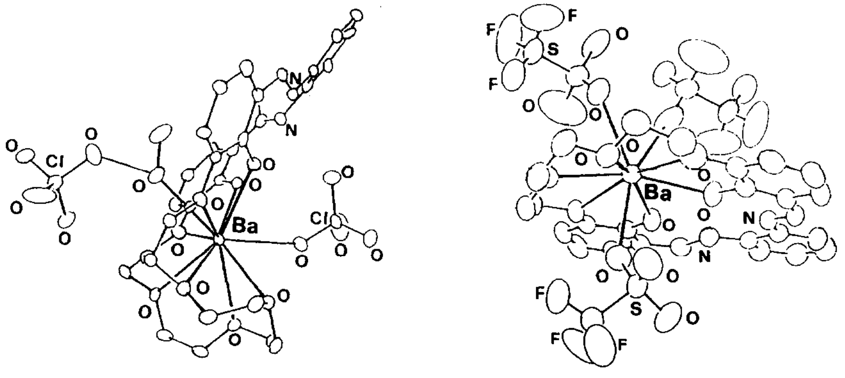

(a) (b)

Fig. 25. Structures of (a) $Ba(\mathbf{40})(ClO_4)_2 \cdot MeOH$ and (b) $Ba(\mathbf{41})(CF_3SO_3)_2$.

macrocyclic cavity (Fig. 26(a)). The uranyl cation, owing to its size, opens up the Schiff base moiety allowing the approach of the urea carbonyl oxygen atom which results in a pentagonal planar coordination of the cation. Urea is also coordinated to one of the phenolate oxygens and to five oxygen atoms of the polyether chain via hydrogen bonds donated by the NH_2 groups. The result is a highly structured complex with a large number of host–guest interactions.

The structure of the urea–uranyl complex $UO_2(\mathbf{40}\text{-}2H)$(urea) also confirms that it is possible to complex a neutral molecule within a macrocyclic ligand that possesses an immobilized electrophilic cation provided that the geometry of the coordination of the cation is in agreement with the geometry necessary for the complexation of the neutral guest.

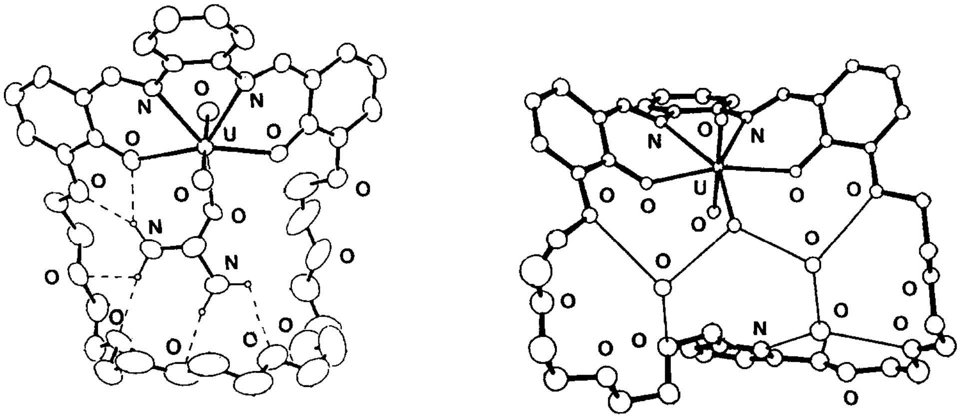

(a) (b)

Fig. 26. Structures of Schiff base uranyl(VI) complexes containing crown ether moieties.

The decomplexation of $Ba(ClO_4)_2$ during the complexation of UO_2^{2+} is probably due to the large size of the UO_2^{2+} cation. It must be noted that Ba^{2+} forces the uranyl(VI) ion to coordinate to the Schiff base compartment. The electrostatic repulsion that results from the complexation of UO_2^{2+} causes the decomplexation of barium while UO_2^{2+} remains in the Schiff base coordination chamber [97].

This is a general reaction, and a synthetic strategy for the preparation of uranyl(VI) complexes containing additional groups (i.e., pyridine, furan, xylene) into the crown ether cavity has been reported [97]. The general synthetic route is reported in Scheme 13.

The intermediate barium(II) complexes (**I** of Scheme 13) can be reacted with $UO_2(CH_3COO)_2$ without prior isolation and purification. Again the X-ray structure of the uranyl(VI) complex **IIb**$(H_2O)\cdot 3H_2O$ shows that the uranyl cation is complexed in the salophene moiety (Fig. 26(b)). The cavity is filled with four water molecules, one of which is coordinated at the fifth position of the uranyl ion. The water molecules are hydrogen bonded to each other and with several of the heteroatoms of the crown ether moiety of the metallo macrocycle, including the pyridine nitrogen atom. The encapsulation of water molecules into the cavity of the uranyl(VI) compound demonstrates the potential to complex guest molecules.

It was found that uranyl(VI) Schiff base complexes **III** of Scheme 13, where amido groups have been introduced to the coordination moiety, can act as efficient receptors also for anions [97].

The complexes obtained by reaction of the corresponding aldehydes and *cis*-1,2-cyclohexanediamine in the presence of uranyl(VI) diacetate exhibit high association constants for anion complexation as dihydrogen phosphate (**A**). Moreover, the combination of a Lewis and uranyl centre and the presence of amide NH groups which can form a favourable H bond with a coordinated anion guest in a preorganized receptor can lead to highly specific anion recognition [97].

2.4. *Ring contraction and ring expansion*

A ring contraction of the macrocyclic cavity of Schiff bases, often leading to a stabilization of metal-free ligands, has been observed when there is a functional group (=NH or –OH) available for addition to the imine bond and/or there is a metal ion too small for the macrocyclic cavity. In this second case, the ring contraction causes a smaller, more accommodating cavity for the available metal.

The cyclization reaction of Scheme 14(a) which readily occurs when equimolar amounts of the precursors are reacted in methanol is confirmed by IR (ν(C=N) at 1625–1640 cm^{-1} and no bands attributable to free C=O or NH_2), ^1H NMR (a singlet at 8.3 ppm due to HC=N and one singlet at 7.2 ppm due to the thiophene protons) and mass spectra (the highest peak at the appropriate *m/z* value) of the [2 + 2] condensation macrocycles [70]. The NMR spectra of the macrocycles with $R \equiv -(CH_2)_2-NH-(CH_2)_2-$ and $-(CH_2)_3-NH-(CH_2)_3-$ which, in addition to the

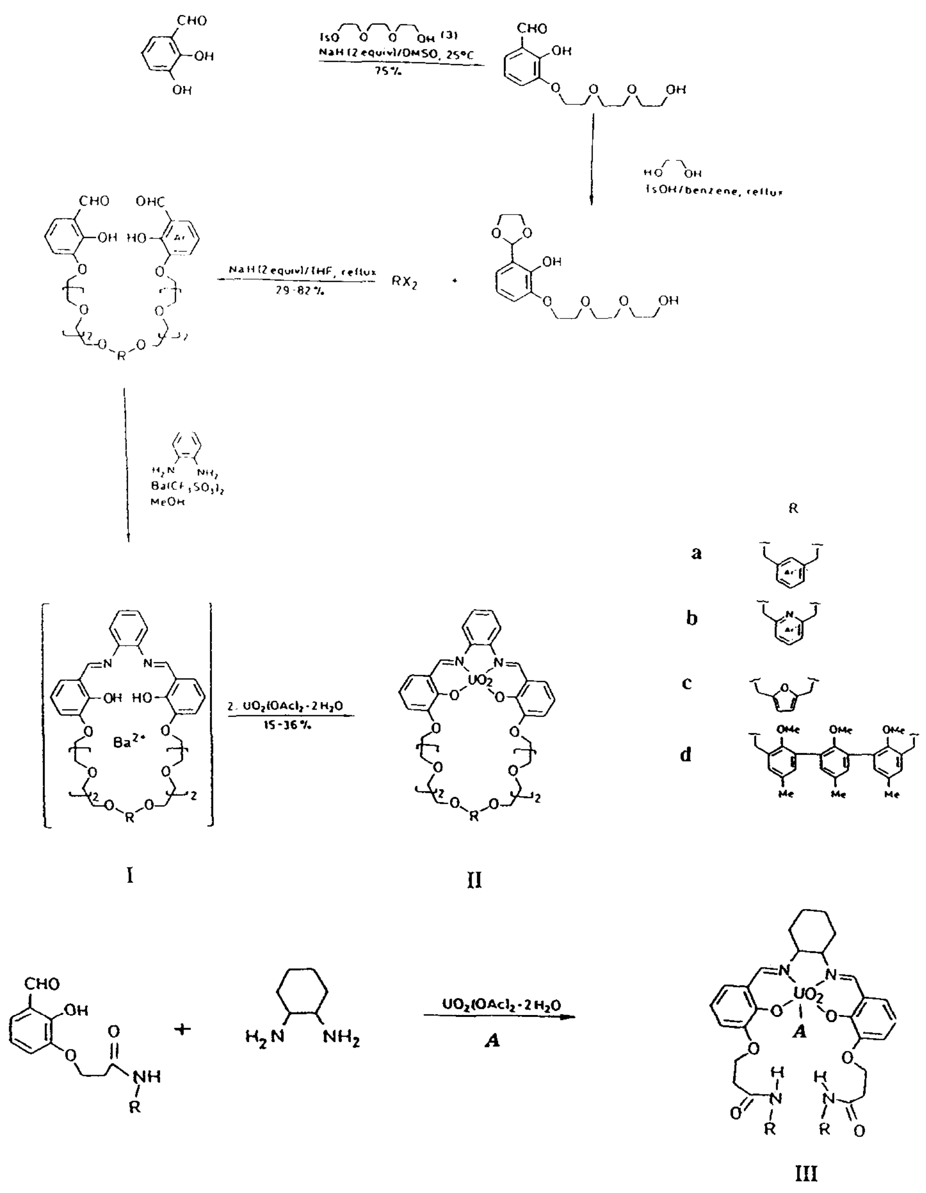

Scheme 13.

signals due to the tetraimine macrocycles, contain a further set corresponding to macrocycles in which a ring contraction has occurred indicate the presence of more than one solution species (Scheme 14(b)).

The direct [2 + 2] condensation of isophthalaldehyde with diethylenetriamine produces a {24} → {18} ring closure; in the solid state the macrocycle contains an

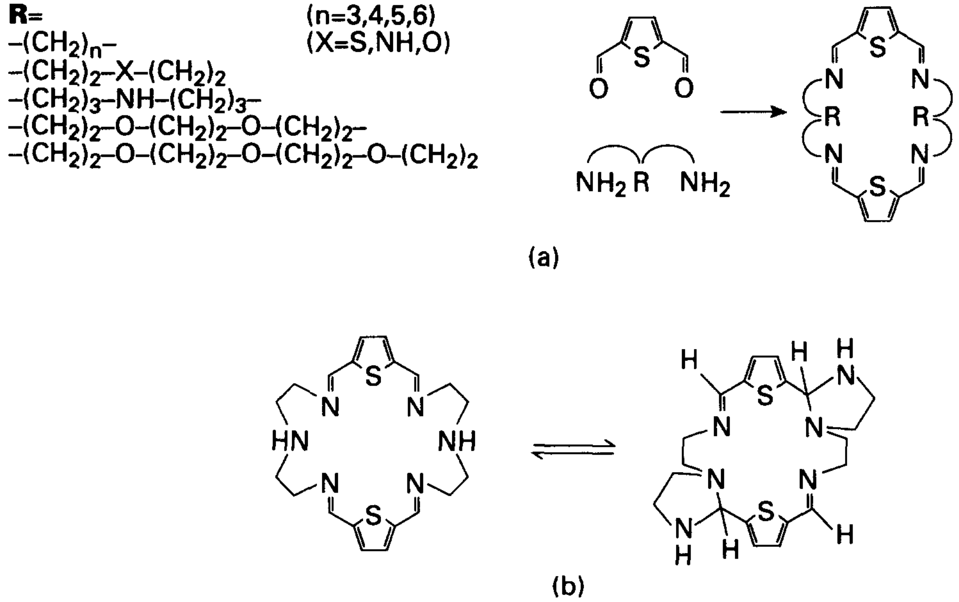

Scheme 14.

18-membered inner ring, two imine bands and two 5-membered imidazoline outer rings (Fig. 27) [67]. In solution, a series of isomers according to Scheme 15 was observed [67].

Reaction of 2,6-diacetylpyridine with diethylenetriamine in the presence of Ba^{2+}, Sr^{2+} or Ca^{2+} in refluxing methanol forms complexes of the macrocyclic ligand **43**, while Mg^{2+} is ineffective [95,98].

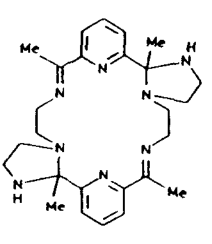

43

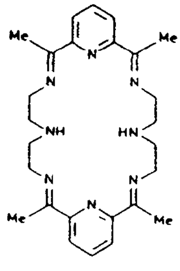

44

In the barium perchlorate complex, the metal ion is positioned on a centre of symmetry being bonded to six nitrogen atoms of the macrocycle and to four oxygen atoms of two perchlorate groups [98]. The BaN_6 moiety is approximately planar. The macrocycle has a structure containing an 18-membered inner ring rather than

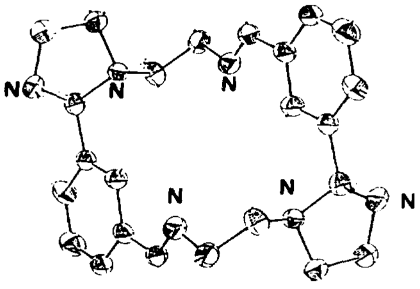

Fig. 27. Structural view of the macrocycle derived from condensation of diethylenetriamine with isophthalaldehyde.

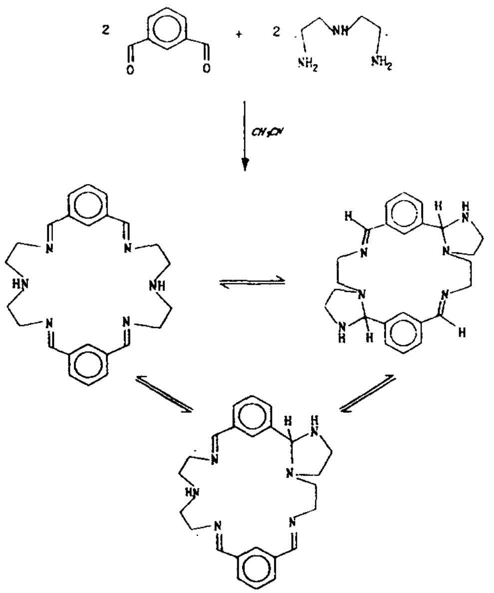

Scheme 15.

the expected 24-membered larger ring. A mechanism of ring contraction formation has been postulated [98] (Fig. 28).

Mg^{2+} is too small for the macrocycle even in its contracted form; thus the preparation of the macrocyclic complex failed.

The extended macrocycle **44** is not well suited to the encapsulation of a single metal ion; however, the same restrictions do not apply to the accommodation of two metal ions. A ring expansion of the coordinated macrocycle occurs on treatment of $[Sr(\mathbf{43})](ClO_4)_2$ with $AgClO_4$. The binuclear $[Ag_2(\mathbf{44})](ClO_4)_2$ has been obtained. This **43** → **44** ring expansion on exchange of a coordinated alkaline earth metal ion by two silver(I) ions was found to be reversible. Treatment of $[Ag_2(\mathbf{44})](ClO_4)_2$ with

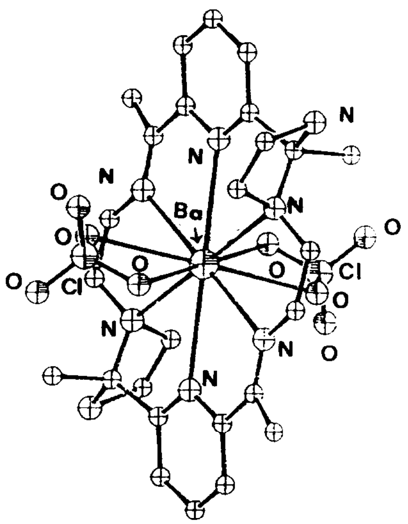

Fig. 28. Structure of $[Ba(\mathbf{43})]^{2+}$ cation.

$BaCl_2$ in methanol gave AgCl together with the complex $[Ba(\mathbf{43})](ClO_4)_2$, identical in properties to an authentic sample prepared via the template method [98].

The same behaviour was also found for the [2 + 2] condensation reaction of 2,6-diformyl-4-chlorophenol and 1,5-diamino-3-azapentane (Scheme 16). For this macrocycle, an NMR investigation confirms the presence of the different isomers in solution while a fast atom bombardment mass reveals fragmentation patterns arising from the various isomers [71,99]. This condensation reaction, carried out in the presence of lanthanide(III) salts (i.e. $Eu(NO_3)_3$ or $Tb(NO_3)_3$), revealed that the metal ions are directly bonded to four oxygen atoms of two bidentate nitrate ions while the third nitrate is ionic. Two oxygen and three nitrogen atoms of the ligand complete the coordination polyhedron (Fig. 29(a)) [100]. The metal ion is coordinated to only one chamber of the macrocycle which is in the Schiff base form. The other chamber, not engaged in coordination, undergoes a ring closure. This ring contraction allows a diminution of the macrocyclic cavity and a reduction in ligand denticity [100] with the formation of the isomer **B** of Scheme 16.

In analogous complexes obtained from 1,5-diamino-3-thiapentene, the ligand cannot undergo further reaction and coordinates intact as a pentadentate ligand to the lanthanide ions as confirmed by the X-ray structure of the uranyl(VI) complex (Fig. 29(b)). Five donor atoms of the ligand, including sulphur, are equatorially bonded to the O–U–O group to form discrete monomeric molecules with the seven-coordinated metal ion in the usual distorted pentagonal bipyramidal coordination geometry. The cyclic ligand includes a second compartment which could act as a second coordination set.

Variable temperature proton and carbon NMR spectra of the La(III) and

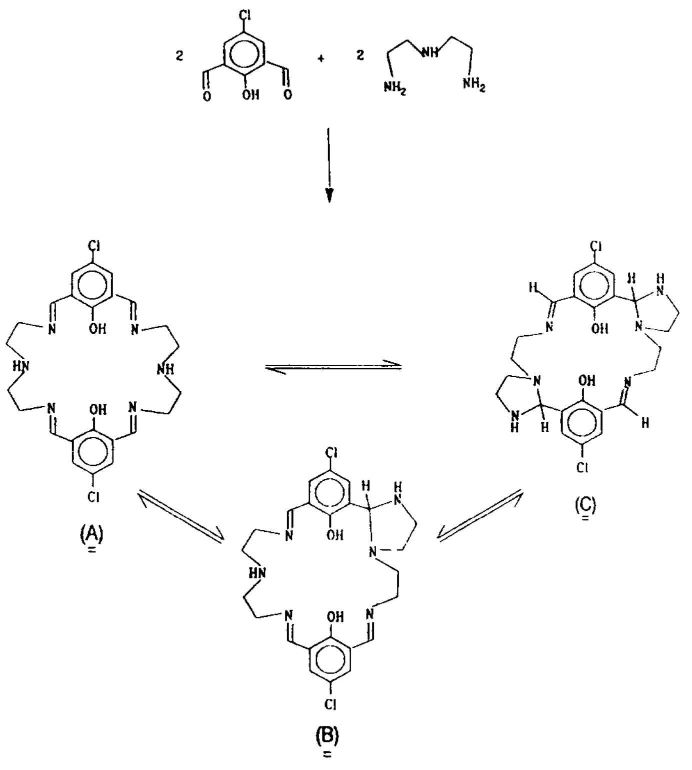

Scheme 16.

Lu(III) complexes reported in Fig. 29(a) provide evidence for a chemical exchange process consisting in the reversible formation and breaking of an imidazoline ring formed by the intramolecular nucleophilic attack of a secondary amino group at the imino carbon atom of a neighbouring azo methine group (Scheme 17) [101]. In agreement with the X-ray structures, 24 different resonances are detected in the ^{13}C NMR spectra of these lanthanide(III) complexes at −10°C in pyridine-d_5.

As the temperature is increased all the resonances broaden, collapse and merge into a set of two-by-two averaged signals. Only the average signal corresponding to a pair of carbon atoms has not yet merged in the spectrum recorded at 90°C. The reduction from 24 to 12 resonances in the high temperature limiting spectrum clearly suggests that a dynamic process is occurring in this temperature range. The observed exchange pathways is indicative of an equilibration process of the kind depicted in Scheme 17 which involves a reversible ring contraction.

From the coalescence temperature of each pair of exchanging resonances in both the proton and carbon spectra of the lanthanum(III) complex, an average activation energy of 57.0 kJ mol^{-1} for this dynamic process was determined. A further proof that the dynamic behaviour corresponds to reversible cleavage and

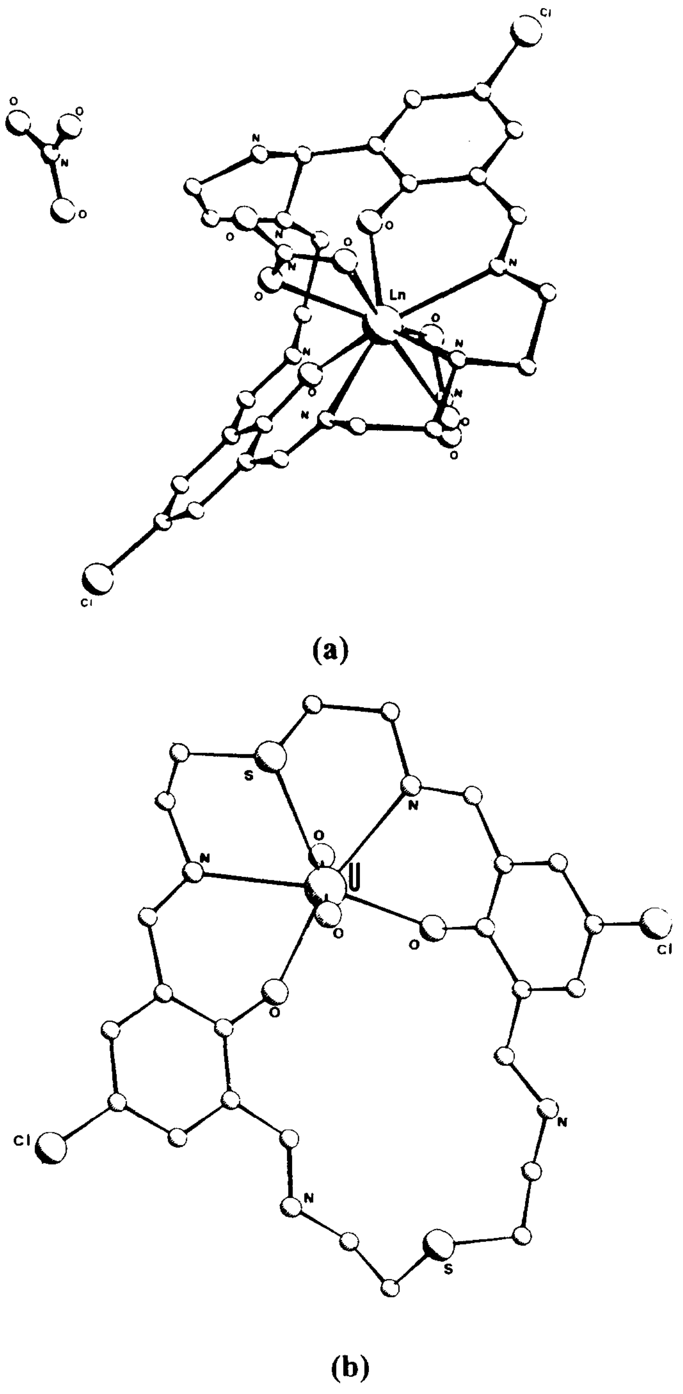

Fig. 29. Structures of the macrocyclic complexes obtained by condensation of 2,6-diformyl-4-chlorophenol with (a) 1,5-diamino-3-azapentene in the presence of $Ln(NO_3)_3$ (Ln ≡ Eu, Tb) and (b) 1,5-diamino-3-thiapentene in the presence of uranyl(VI) ion.

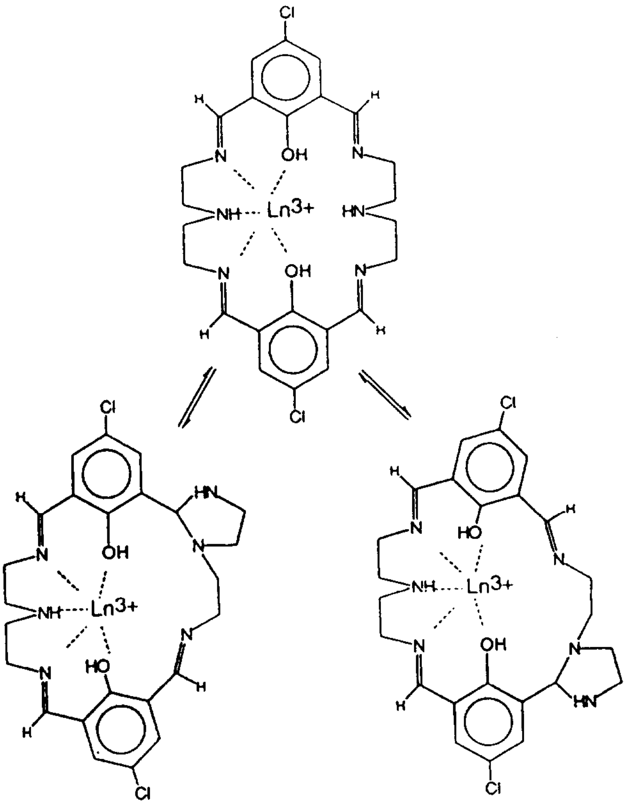

Scheme 17.

formation of the imidazoline group was gained by substituting 1,5-diamino-3-azapentane with 1,5-diamino-3-methylazapentane in the template synthesis of the macrocyclic La(III) complex. The methyl substitution at the secondary amino groups prevents the formation of the imidazoline ring. In this complex, the ligand is then in a type **A** conformation (Scheme 16) as shown by the 14 resonances of its ^{13}C NMR spectrum. The complex is stereochemically rigid in spite of the availability of two identical coordination chambers.

The reaction of 2,6-diacetylpyridine with 1,3-diamino-2-hydroxypropane in methanol in the presence of $Ba(NCS)_2$ or $Ba(ClO_4)_2$ leads readily to the corresponding mononuclear barium complex of the [2 + 2] 20-membered ring macrocycle **45**. Transmetallation reactions in the presence of $Pb(NCS)_2$ or $Pb(ClO_4)_2$ resulted in isolation of the corresponding lead complex of the ring-contracted macrocycle 18-membered ring **46** [102].

In the X-ray structure of [Pb(**46**)(NCS)](NCS)·MeOH, the lead is bonded to six sites within the macrocycle, two pyridyl and two imino nitrogen atoms and two oxygen atoms which were originally substituent hydroxy groups. These hydroxy groups became incorporated into two hinged oxazolidine rings formed by the addi-

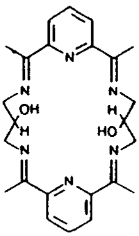

45

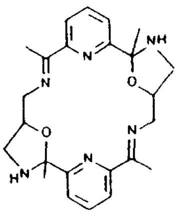

46

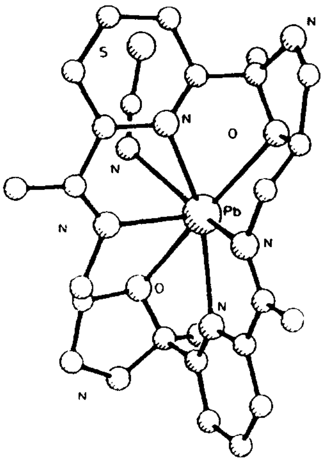

Fig. 30. Structure of [Pb(**46**)(NCS)]$^+$.

tion of the endogenous hydroxy group across the adjacent C=N double bond with consequent proton transfer to the nitrogen (Fig. 30).

No evidence was obtained from ^{1}H NMR for the existence of an equilibrium in solution between the open and contracted isomers. Again the ring contraction, from an octadentate, 20-membered ring unit to a hexadentate, 18-membered ring unit, is believed to be facilitated by the use of the smaller Pb^{2+} cation ($r = 1.21$; cf. $r = 1.35$ Å for Ba^{2+}) and its requirement for the smaller ring cavity [102].

Transmetallation reaction in methanol of $[Ba(\mathbf{45})(H_2O)_2](ClO_4)_2$ by VCl_3 in methanol affords brown crystals of $[V_2(\mathbf{45}\text{-}2H)(H_2O)_4]\cdot(ClO_4)_2\cdot 2H_2O$ stable in air and in water [103]. The ligand **45** presumably has a stabilizing effect for vanadium(III) originating from either donor group or geometric characteristics since such reaction conditions would normally be expected to yield oxovanadium(IV) products. It is interesting to note that deprotonation of **45** has occurred in the absence of added base. The crystal structure of this complex shows a highly symmetrical cation, displayed in Fig. 31, which has a centre of inversion in the middle of the molecule and which is surrounded by four ClO_4^- ions. The coordinated macrocycle is remarkably flat. Each V^{III} has a pentagonal bipyramidal coordination geometry

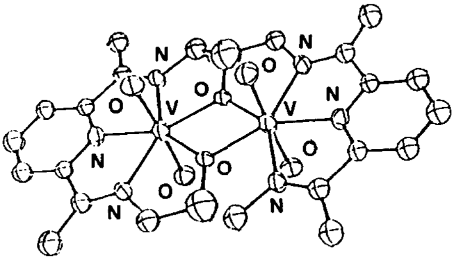

Fig. 31. Structure of $[V_2(\mathbf{45}\text{-}2H)(H_2O)_4]^{2+}$.

made up of two H_2O molecules in the apical positions and atoms O, N of **45**-2*H* in the pentagonal plane.

The room temperature magnetic moment of $[V(\mathbf{45}\text{-}2H)(H_2O)_4](ClO_4)_2 \cdot 2H_2O$ ($1.97\mu_B$) shows the two vanadium(III) ions are strongly antiferromagnetically coupled [103].

The template synthesis, via large metal ions such as alkaline earth (Ca^{2+}, Sr^{2+}, Ba^{2+}) or Pb^{2+}, of the conjugated, hexadentate macrocyclic Schiff base derived from the condensation of two molecules of 2,6-diformylpyridine with two molecules of *o*-phenylenediamine in methanol or acetonitrile has been reported [104]. The X-ray analysis of $[Pb(\mathbf{34b})(H_2O)](ClO_4)_2 \cdot 2H_2O$ (Fig. 32) shows that the metal ion is bonded to all six nitrogen atoms of the macrocycle and to the oxygen atom of a water molecule in one axial position. The macrocycle is not quite planar; the four imino nitrogens form a plane with the two pyridine nitrogen displaced to one side and the metal atom to the other. Thus the structure is best described as a distorted hexagonal pyramid [104].

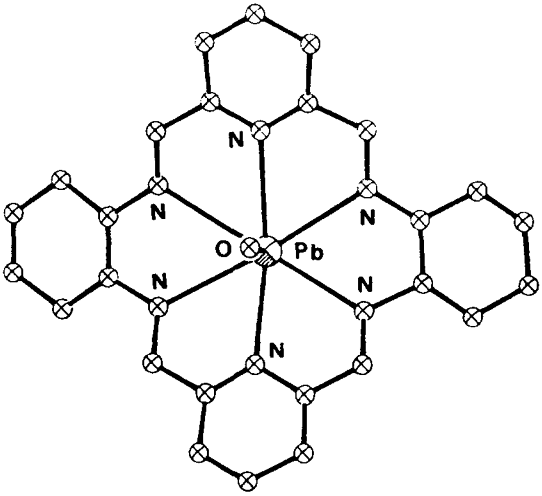

Fig. 32. Structure of $[Pb(\mathbf{34b})(H_2O)]^{2+}$.

No macrocyclic products have been isolated from reactions carried out in the presence of Mg^{2+} and Cd^{2+} or the transition metal ions $Mn^{2+} \rightarrow Zn^{2+}$ [104]. However the reaction of $[Ba(\mathbf{34b})_2](ClO_4)_2$ with Cd^{2+} in MeOH forms $[Cd(\mathbf{34b})(H_2O)](ClO_4)_2$: the structure of this complex is similar to that of $[Pb(\mathbf{34b})(H_2O)](ClO_4)_2$ [104].

Treatment of the barium macrocyclic complex with an excess of a salt of Mn^{2+}, Fe^{2+}, Co^{2+} or Zn^{2+} in refluxing methanol yields complexes considered to have closely related structure [105]. The structure of the cobalt(II) complex (Fig. 33) showed that the large inner ring, present in the barium complex, has contracted (Scheme 18) from an 18- to a 15-membered ring with formation of a 5-membered imidazoline ring.

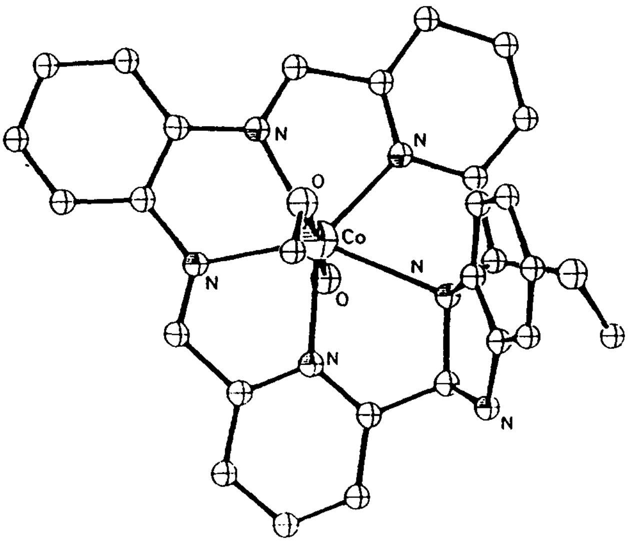

Fig. 33. Structure of $[Co(\mathbf{34b'})(H_2O)(CH_3OH)]^{2+}$.

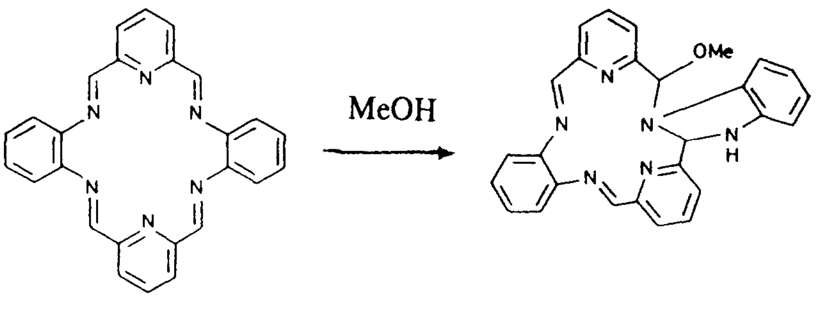

34b **34b'**

Scheme 18.

The ring contraction has left the Co^{2+} atom in a pentagonal bipyramidal environment with the five nitrogen atoms of the 15-membered inner large ring making up the equatorial girdle. The ion is also bonded to a water and a methanol molecule [105].

From the results, it appears that Mn^{2+}, Fe^{2+}, Co^{2+} and Zn^{2+} ions are too small to be effectively bonded to all six nitrogen atoms of the planar macrocycle; this is the reason for the rearrangement of the 18-membered ring to a 15-membered ring. Thus the smaller Zn^{2+} effects the ring contraction while the Cd^{2+} ion does not.

2.5. *Functionalized ligands*

The development of specific macrocyclic and macroacyclic ligands soluble in organic solvents has opened new possibilities of their applications in the field of selective metal ion recognition, transport and separation. Separation techniques, especially those connected with the use of liquid membranes, offer the possibility for many of these ligands to be used in processes of industrial relevance. A serious problem connected with these investigations comes from the low solubility of the complexes in the organic solvents of industrial use. With the separation technique mentioned above high solubility in non-coordinating solvents (xylene, aliphatic hydrocarbons etc.) is needed. The addition of lateral chains to Schiff bases considerably enhances the solubility of the related complexes in aromatic or aliphatic solvents. Accordingly the macrocyclic and macroacyclic Schiff bases soluble in organic solvents (including hydrocarbons), have been prepared in one step by condensation of 2,6-diformyl-4-substituted phenol and 4-*N*-dodecyldiethylenetriamine (H_2-**47** to H_2-**49**) or with the step-by-step reactions (H_2-**51**) (Scheme 19) [106,107].

The ketoprecursors 2,6-diformyl-4-Z-phenols ($Z \equiv Cl$, CH_3–, $(CH_3)_3C$–), by reaction with 4-*N*-dodecyldiethylenetriamine in chloroform or in methanol in a 1 : 1 molar ratio, produce yellow oils or sticky solids formulated, according to the physicochemical data, as the macrocycles H_2-**47** to H_2-**49** reported in Scheme 19(a). The same 2,6-diformyl-4-Z-phenols give, with the facultative diamines 1,5-diamino-3-azapentane or 1,5-diaminothiapentane, the acyclic, potentially pentadentate ligands H_2-**50** which contain C=O groups that can be involved in further condensation reactions with primary amines. Using NH_2–$(CH_2)_{17}$–CH_3, the macroacyclic ligands H_2-**51** of Scheme 19(b) have been obtained. Both macrocyclic and macroacyclic ligands are capable of forming complexes soluble in hydrocarbons.

Electron impact mass spectrometry evidences the parent peak $[M^+]$ at the appropriate value for H_2-**47** and H_2-**49** while it does not lead to the molecular ion for H_2-**47**, although some fragmentation ions can be related to the Cl compound structure. Fast atom bombardment mass spectrometry revealed a well-detectable molecular peak at the appropriate *m*/*z* value for all three macrocycles H_2-**47** to H_2-**49** which perfectly matches with the theoretical one for $[M–H]^+$. It originates through a proton extraction which leads to a singly charged molecular cation. Symmetric

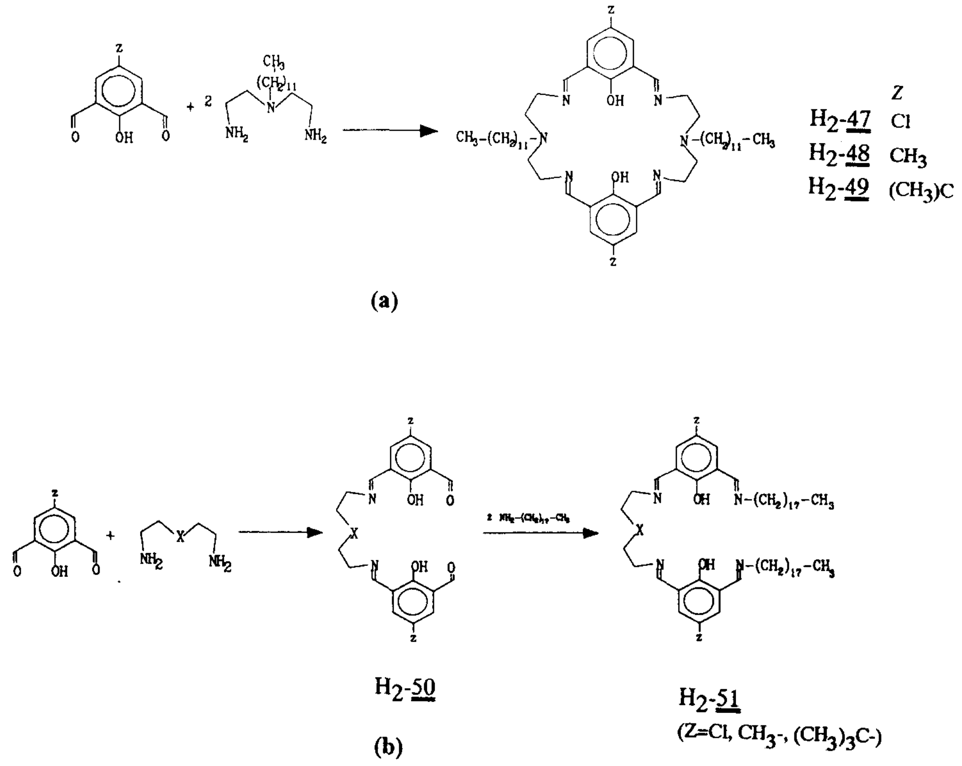

(a)

(b)

Scheme 19.

cleavages, leading to $[M/2]^{+\cdot}$ ions, are present in the electron impact spectra of the compounds as observed in macrocyclic polyetherester compounds.

The species $[M/2\text{–}H]^{+\cdot}$, common in crown ether mass spectrometry, are absent in electron impact but are clearly detectable in fast atom bombardment spectra of all three compounds.

In addition, a series of functionalized polyamines and related open cryptands have been prepared. The polyamine 7-(2′-pyridyl)-3,6-diazaheptylamine (**52**) was obtained according to Scheme 20 and its reactivity toward 2,6-diformylphenol and/or metal ions was studied [108].

The X-ray structure of $[Cu(\mathbf{52})(ClO_4)_2]$, obtained by reaction of **52** with $Cu(ClO_4)_2$, shows that the quadridentate ligand is equatorially coordinated to the metal ion through the nitrogen donor atoms. The metal ion makes two relatively long axial Cu $\cdots$ O contacts with oxygen atoms from the two ClO_4^- anions [108] (Fig. 34).

Crystals of $[Ba(\mathbf{53})(SCN)_2]$, synthesized by template condensation of 2,6-diformyl-4-chlorophenol and **52** in the presence of barium(II) dithiocyanate, show that the macrocyclic neutral ligand **53** behaves as sexadentate; two SCN^- ions,

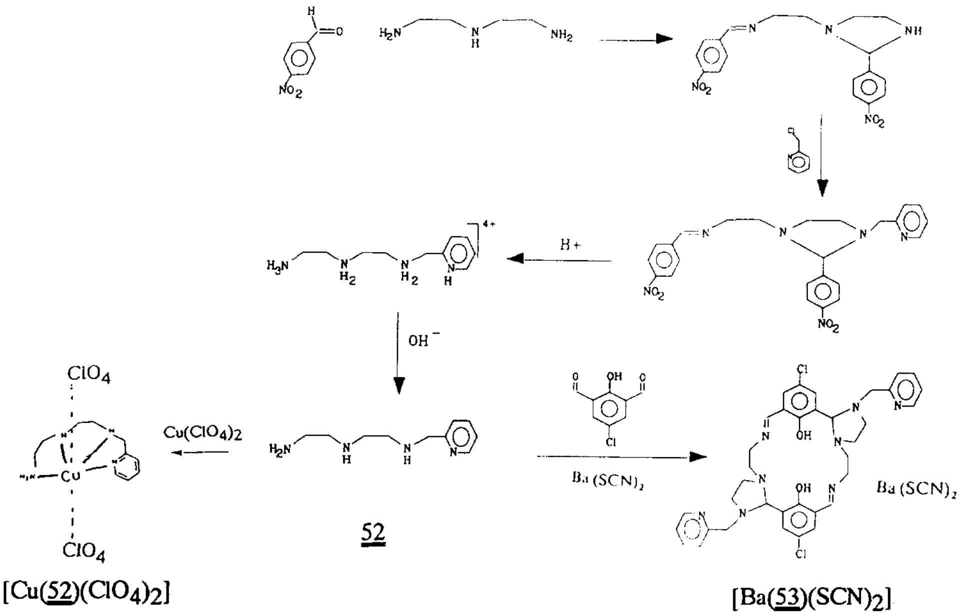

Scheme 20. Preparation of the polyamine **52** and related [Cu(**52**)(ClO_4)$_2$] and [Ba(**53**)(SCN)$_2$] complexes.

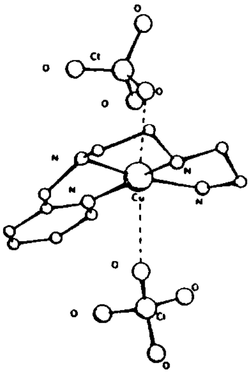

Fig. 34. Structure of [Cu(**52**)(ClO_4)$_2$].

N bonded to Ba^{2+}, complete the coordinate polyhedron around the metal which can approximately be described as a distorted square antiprism [108] (Fig. 35).

[2 + 2] tetraimine Schiff base macrocycles are readily prepared by the template cyclocondensation of heterocyclic dicarbonyl derivatives and 1,*n*-diaminoalkanes. Extension of this approach to include functionalized triamines bearing 2-pyridylmethyl-2-methoxyethyl and 2-methoxybenzyl substituents leads to the synthesis of *N,N′*-bibracchial macrocyclic (**54** to **57**) complexes of the templating cation. Mono- and binuclear complexes are recovered in the presence of barium and silver(I) templates respectively. The crystal structures of a mononuclear barium complex of **54** and of four homobinuclear silver(I) complexes, one from each macrocyclic ligand **54–57**, have been reported [109].

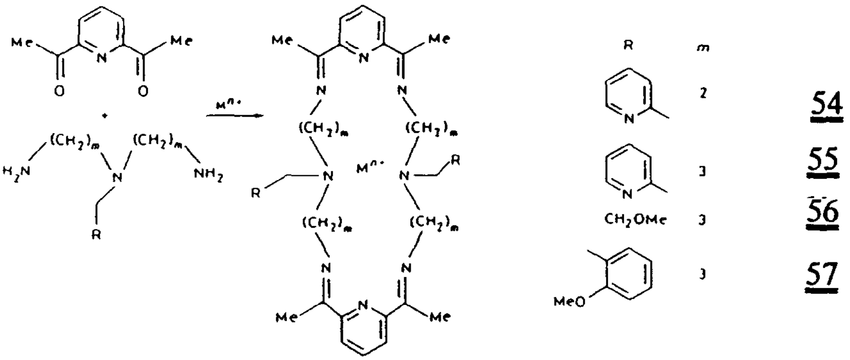

The macrocycle in $[Ba(\mathbf{54})](ClO_4)_2$ is folded back upon itself to provide a "molecular cleft" in which the pyridyl fragments at opposite ends lie approximately parallel, although not "face to face" with the barium "sandwiched", although displaced towards the more open part of the macrocycle. All ten nitrogen atoms from the ligand are close enough to interact with the central barium ion [109] (Fig. 36).

In the complex $[Ag_2(\mathbf{54})](ClO_4)_2$ the macrocycle retains its cleft-like appearance and coordinates to two silver atoms which are closely spaced (Ag $\cdots$ Ag, 3.068 Å). Each silver atom is coordinated to two pyridyl nitrogen atoms (one in the macrocyclic and one in the pendant picoline fragment), to a tertiary amino nitrogen and to both imino nitrogen atoms lying adjacent to the coordinating macrocycle pyridyl. One silver atom is also close to a third imino nitrogen atom which is

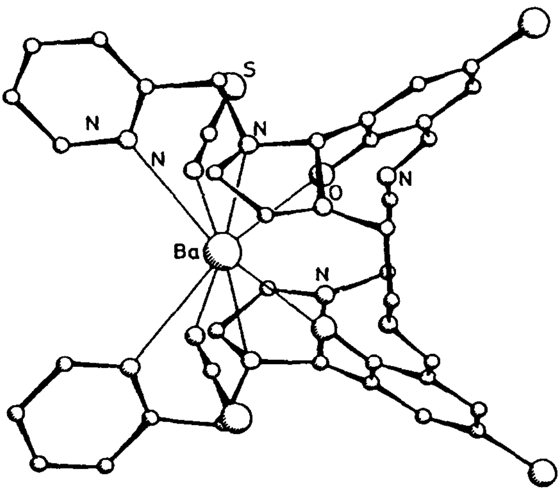

Fig. 35. Structure of $[Ba(\mathbf{53})(SCN)_2]$.

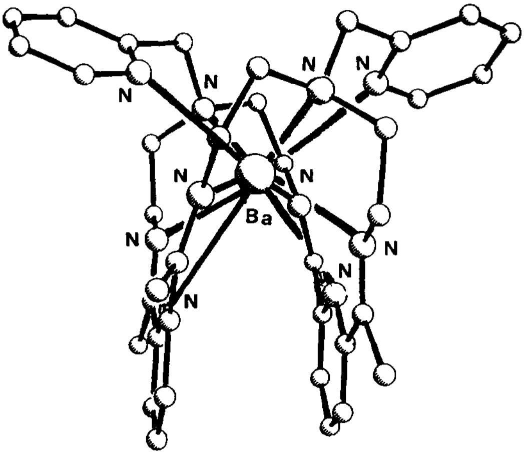

Fig. 36. Structure of $[Ba(\mathbf{54})]^{2+}$.

therefore symmetrically bridging the two silver atoms; the diametrically opposite imino nitrogen atom is much further from the second silver atom. The coordination geometries of the silver atoms are not closely related to regular polyhedra (Fig. 37(a)).

In the structure of the dication $[Ag_2(\mathbf{55})]^{2+}$ in which the macrocyclic ring size has been expanded from 24 to 28 membered, the macrocycle again coordinates to two silver atoms which are in very similar and widely separated environments (Ag · · · Ag, 6.824 Å).

Again each silver atom is coordinated to two pyridyl nitrogen atoms, to a tertiary amino nitrogen atom and to the imino nitrogen atom lying between the coordinating macrocyclic pyridyl and tertiary amine nitrogen atoms; there is a longer bond to the other imino nitrogen atom which is adjacent to the coordinating macrocyclic pyridyl. The five coordinate geometry is not closely related to either trigonal bipyramidal or square-based pyramidal. Again, the pendant group is fully incorporated in the silver coordination sphere [109] (Fig. 37(b)).

In the structure of the $[Ag_2(\mathbf{56})]^{2+}$ dication, the macrocycle coordinates to two silver atoms which are asymmetrically bridged by a pair of imino groups and the silver–silver distance is remarkably short (2.907 Å). The macrocycle adopts a conformation which closely resembles that of $[Ag(\mathbf{54})]^{2+}$ where the smaller 24-membered macrocycle carries pendant pyridyl substituents of a greater donor capacity, rather than that of $[Ag_2(\mathbf{55})]^{2+}$ where the 28-membered macrocycle also carries pendant pyridyl groups [109] (Fig. 37(c).

In the cation $[Ag_2(\mathbf{57})]^{2+}$, the macrocycle coordinates to two silver atoms which are in very similar and well separated environments (Ag · · · Ag, 5.828 Å). Each silver atom is linked to a pyridyl nitrogen atom, to the two adjacent imino nitrogen atoms, and to a tertiary amino nitrogen atom. Each set of four nitrogen atoms is approximately coplanar. The cleft in the molecule between the planes of the pyridyl

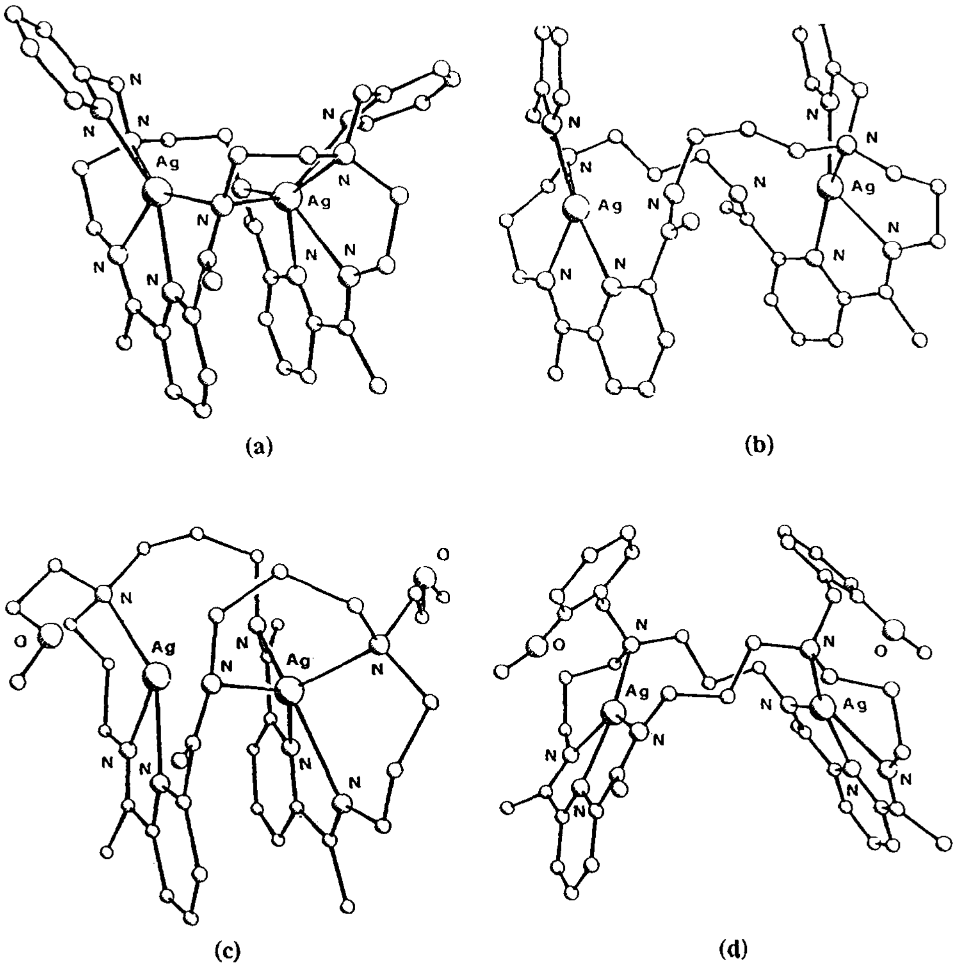

(a) (b)

(c) (d)

Fig. 37. Structures of (a) $[Ag_2(\mathbf{54})]^{2+}$, (b) $[Ag_2(\mathbf{55})]^{2+}$, (c) $[Ag_2(\mathbf{56})]^{2+}$ and (d) $[Ag_2(\mathbf{57})]^{2+}$.

rings is "hinged" open such that the angle between their planes is 44°. This may be compared with the complex dications $[Ag_2(\mathbf{55})]^{2+}$ and $[Ag_2(\mathbf{56})]^{2+}$ where, for the same macrocyclic framework, the pyridyl groups are approximately parallel. In the latter they give a narrow cleft with a short silver–silver distance whereas, in the former, the macrocycles had undergone a "concertina" expansion. Presumably, this is attributable to the greater donor capacity of the methyl aryl ether as compared with its alkyl counterpart, thus permitting the silver to achieve full coordination without recourse to imine bridging and a consequently shorter silver–silver distance [109] (Fig. 37(d)).

The use of two imino residues as bridging or semibridging groups and the consequent silver–silver distances that ensue seem likely to be related to the donor capacity of the pendant groups and the need to achieve adequate coordination of the silver ions.

On forming the binuclear silver(I) complexes the cleft-like appearance of the macrocyclic ligand is retained, but the Ag ··· Ag separation and the configuration of the ligand change with both ring expansion and the introduction of pendant groups of varying donor strength. The Ag ··· Ag separation ranges from 2.91 to 6.82 Å [109].

Similar bibracchial tetraimine Schiff base macrocycles have been achieved by metal-templated cyclocondensation of functionalized diamines such as *N*,*N*-bis(2-aminoethyl)-2-methylthioethylamine and *N*,*N*-bis(2-aminoethyl)-2-phenylethylamine with 2,5-diformylthiophen. The macrocycles are isolated as their dinuclear metal complexes while adopting a molecular cleft, as has been the case in related systems where 2,6-diacetylpyridine is the header unit. Macrocyclic products were isolated when silver(I) and lead(II) were used as templating agents but not for copper(I). The dinuclear copper(I) macrocycles are, however, accessible by transmetallation of the dilead(II) macrocycles under anhydrous and anaerobic conditions [109].

3. NEW POLYDENTATE LIGAND MACROCYCLES, VIA SCHIFF BASE FORMATION AND REDUCTION

As reported above it is possible to obtain cyclic Schiff bases by reaction of the appropriate precursors if the condensation product is stable to hydrolysis. Thus 2,6-bis(2-formylphenoxymethyl)pyridine and bis(2-aminoethyl)ether undergo a cyclocondensation reaction in methanol in the absence of templating agents (Scheme 21(a)) to give a [1 + 1] Schiff base macrocyclic product (**59**), whose crystal structure [110] (Fig. 38) includes a methanol of solvation hydrogen bonded to an imine nitrogen atom.

The IR spectrum of **59** gave a strong band at 1640 cm^{-1} assignable to ν(CN), and the fast atom bombardment mass spectrum gave a peak at 416 amu corresponding to $[\mathbf{59} + 1]^+$ together with a higher molecular weight species corresponding to the dimer **59′** at 831 amu.

The ^{1}H NMR spectrum run in $(CD_3)_2SO$ reveals a single set of signals, but when the spectrum is run in $CDCl_3$ each set of signals is doubled and there are at least three signals for the imino protons indicating that the behaviour of **59** in solution is not obvious.

The use of Pb(II) as the metal template was found to be unsuccessful leading only to the bis(acetal) derivative (**58′**). In contrast, application of Ba(II) as the template yielded the complex $[Ba(\mathbf{59})](NCS)_2$ of which the IR spectrum gave a strong band at 1650 cm^{-1} assignable to ν(CN). The fast atom bombardment mass spectrum gave a higher molecular weight peak corresponding to $[Ba(\mathbf{59})(NCS)]^+$ with no evidence for higher molecular weight species derived from dimeric or oligomeric forms of the ligand such as **59′**.

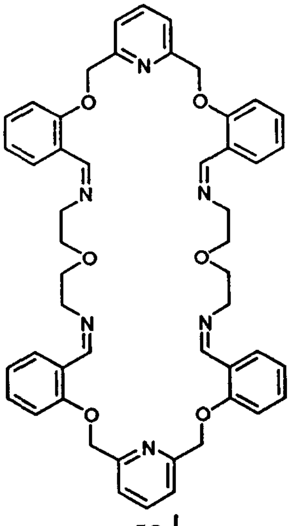

59'

It would appear that the presence of Ba(II) directs the pathway towards the exclusive isolation of the [1 + 1] macrocycle **59** as its metal complex, whereas in the absence of the metal there is a strong possibility that the [2 + 2] macrocycle **59'** is also formed [110].

Generally the condensation of the appropriate dialdehyde and diamine in the presence of suitable metal ions (i.e. Mn(II) or Pb(II)) results in isolation of the corresponding complexes of the diimine ligands **60a** and **60b** (Scheme 21(b)) containing 15 to 19 members in the inner rings.

The routes to the macrocyclic compounds of Scheme 21(b) involve the template action of either Mn(II) or Pb(II); Mn(II) dominates route (A) while Pb(II) dominates route (B). Lead(II) tends to be an effective template ion, not only for the larger 18-membered rings but also when X and Y contain additional ligating groups; thus the radius of the metal ion as well as its coordination preferences both appear to influence template behaviour although the relative importance of these factors is difficult to define for specific complexes [111]. The corresponding reduced macrocycles **60c** and **60d** (Scheme 21(b)) were obtained by reduction of their complexed diimine precursors using sodium tetrahydroborate. Although initially the intermediate complexes were isolated, it was also found possible to obtain the metal-free reduced macrocycles in one step by preforming the reduction in situ.

The easy formation of a wide variety of new macrocyclic ligands involves therefore (i) template cyclocondensation and (ii) reductive demetallation.

Physicochemical measurements indicate that many of these oxoaza macrocycles form 1:1 complexes although compounds with a 1:2 metal:ligand ratio have also been obtained. The metal ion is generally retained in the macrocyclic moiety, but

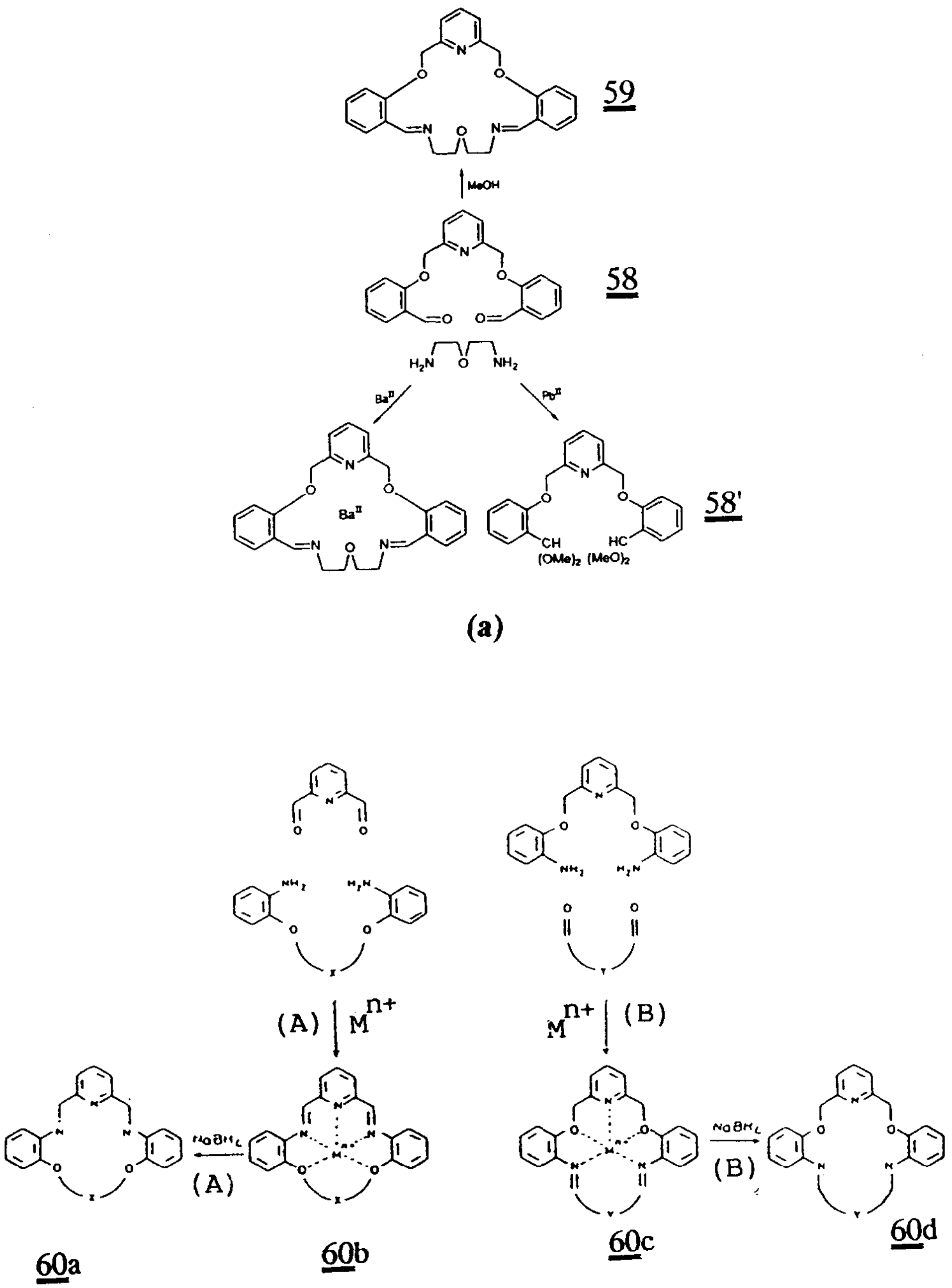
59
MeOH
58
H_2N
O
NH_2
Ba^{II}
Pb^{II}
Ba^{II}
CH
HC
$(OMe)_2$ $(MeO)_2$
58'
(a)
(A) M^{n+}
M^{n+} (B)
$NaBH_4$ (A)
$NaBH_4$ (B)
60a
60b
60c
60d
(b)

Scheme 21.

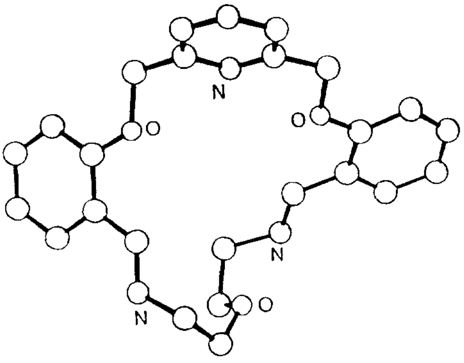

Fig. 38. Structure of **59**.

variation of the anion can induce the metal ion to be coordinated exocyclically to the macrocycle via the two secondary amine nitrogen atoms.

The stabilities of selected complexes have been determined using the potentiometric (pH) titration technique. In all cases much greater stability for the complexes of Cu(II) relative to those of Co(II) or Ni(II) was observed. The structural origin of this selectivity has been investigated by X-ray diffraction studies. The nickel(II), [Ni(**60d**)$(NO_3)_2$]·$0.5H_2O$, and copper(II), [Cu(**60d**)(NO_3)]NO_3·0.33MeOH·-$0.17H_2O$ ($Y \equiv CH_2CH_2$) complexes have markedly different structures. In the nickel(II) species the geometry is distorted octahedral with the macrocycle occupying four coordination positions with one ether oxygen atom not coordinated. The remaining (*cis*) coordination positions are filled by nitrate ions. In the copper(II) complexes the macrocycle folds in such a way that an unsymmetric but apparently favourable cavity is formed and all five donor atoms coordinate to the metal. A sixth coordination position is filled by a nitrate ion [112]. In the zinc(II) complex [Zn(**60d**)$(H_2O)(NO_3)$](NO_3), the metal ion is seven coordinated with the macrocycle binding to this ion via its five donor groups in an approximately pentagonal-planar fashion. The axial sites are occupied by a nitrate ion and a water molecule.

The larger macrocyclic homologues **61a** and **61b**, which also contain the N_3O_2 donor set, have been prepared and the X-ray structure of **61a** has been reported (Fig. 39(a)).

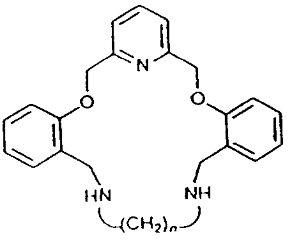

n=2 **61a**
n=3 **61b**

Spectroscopic studies on the interaction of Cu^{2+}, Ni^{2+}, Zn^{2+}, Cd^{2+} and Hg^{2+} reveal the formation of 1 : 1 and 1 : 2 species [110,111].

The metal in $[Cu(\mathbf{61a})(H_2O)][ClO_4]_2$ is six coordinated and lies within the folded macrocyclic cavity. The donor set comprises the five macrocyclic donor atoms and a water molecule. Overall, the coordination sphere corresponds to a restricted tetragonal rhombic arrangement [111]. The complex $[Ni(\mathbf{61a})(I)]\cdot MeOH$ also has

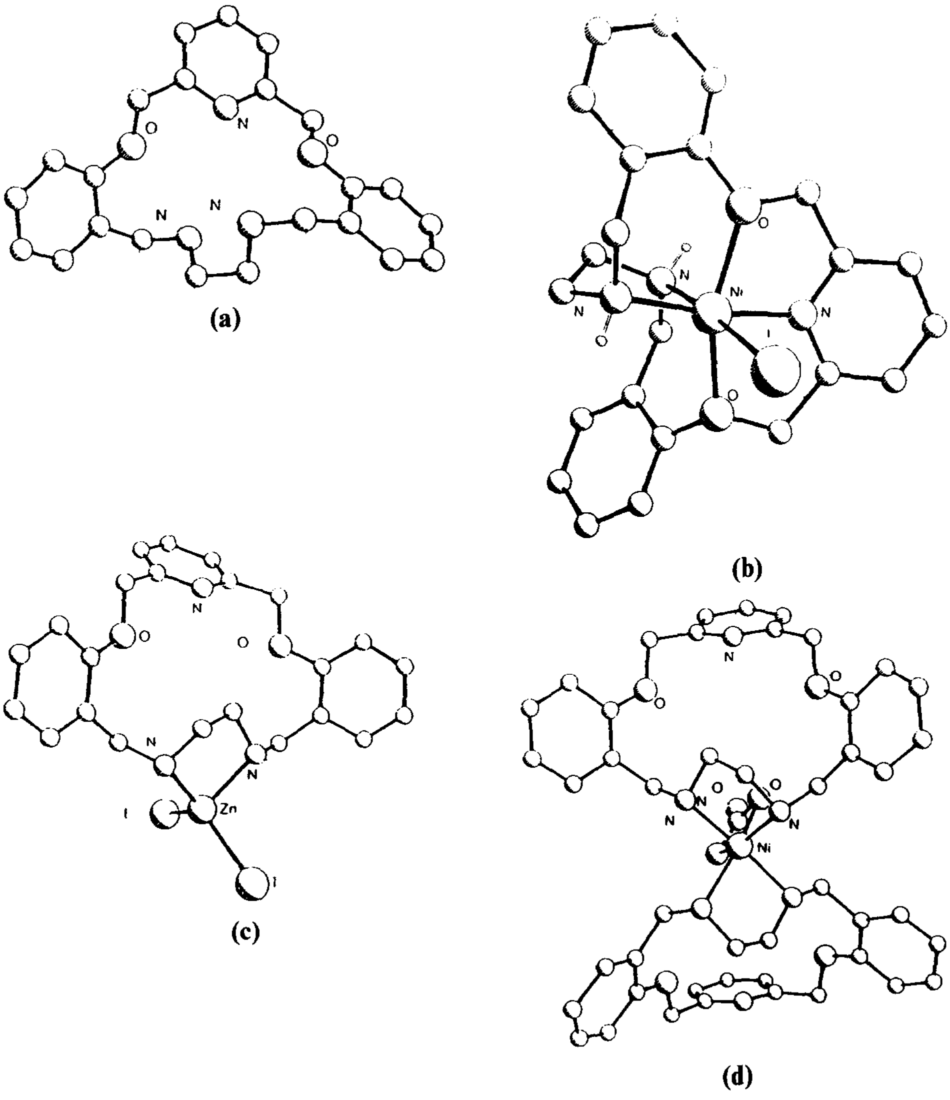

Fig. 39. Structures of (a) **61a**, (b) $[Ni(\mathbf{61a})(I)]^+$ as an example of 1 : 1 complex with the metal inside the macrocycle, (c) $[Zn(\mathbf{61a})(I)_2]$ as an example of 1 : 1 complex with the metal ion coordinated exocyclically and of (d) the complex $[Ni(\mathbf{61a})_2(NO_3)]\cdot(NO_3)$ with the metal ion coordinated exocyclically.

all donors of the macrocycle coordinated with an iodide anion occupying the sixth site to yield a distorted-octahedral geometry (Fig. 39(b)).

The metal atoms in [Zn(**61a**)(I)$_2$] · H_2O and [Hg(**61a**)I_2] are four coordinated in a tetrahedral geometry and lie outside the macrocyclic cavity. The donor set in each molecule comprises the two secondary amine nitrogen atoms from the macrocycle and the two iodide anions. Thus the coordination of iodide favours zinc(II) mercury(II) with a tetrahedral geometry at the metal (Fig. 39(c)) [111].

The complex [Zn(**61a**)(NO_3)]NO_3 has all donors of the macrocycle coordinated with one oxygen atom from a nitrate anion occupying the sixth site to yield an approximately trigonal-prismatic geometry. The structure of [Cd(**61a**)(NO_3)(MeOH)]NO_3 shows that the metal is seven coordinated in an approximately pentagonal-bipyramidal environment consisting of the full donor set of the macrocycle together with one oxygen atom each from a nitrate anion and a methanol of solvation [111].

The structure of [Cd(**61b**)(ClO_4)(MeCN)]ClO_4 shows that the metal has a coordination environment consisting of the full donor set of the macrocycle together with an oxygen atom from a perchlorate anion and a nitrogen atom from acetonitrile of solvation [111].

The structure of the 1:2 nickel(II) dinitrate complex [Ni(**61a**)$_2$(NO_3)]NO_3 · 2MeOH shows that the metal is 6 coordinated to the aliphatic nitrogen atoms from the macrocycle, one pair from each ring, and a bidentate nitrate anion. The nickel(II) is therefore complexed in an exomacrocyclic manner (Fig. 39(d)).

Ligands of this type represent a series of compounds of intermediate rigidity. The selective complexation and transport of metal ions may be facilitated by macrocyclic ligands of intermediate rigidity (that is, sufficient rigidity to present a donor set with a defined geometry to a metal ion but flexible enough to encourage favourable kinetics of metal ion incorporation and release). In some cases, the stability constants of such complexes have been shown to correlate with the goodness of fit of the metal ion for the donor cavity although other mechanisms for discrimination may also operate. Nevertheless, when metal ions are discriminated against by a poor fit for the cavity the possibility exists that the favoured mode of interaction will involve exomacrocyclic complexation using only part of the macrocyclic donor set.

Extraction experiments (water–chloroform) and related transport experiments (water–chloroform–water) were successfully carried out using **61a** and **61b** in the chloroform phases which also contained hexadecanoic acid as a counterion to inhibit bleeding into the aqueous phase of charged species such as the protonated macrocycle and/or the corresponding metal complexes.

For the transport runs, the pH gradient across the cell served to "drive" the transfer of the metals from the source to the receiving phase.

In all single-metal extraction and transport studies, Cu(II) was favoured over Ni(II). The results from these transport and extraction studies parallel each other.

In particular the transport results follow the corresponding log *K* values for the individual complexes although it is noted that this need not necessarily be the case. The results from the competitive extraction and transport experiments also follow the above trends and confirm the potential of systems such as these for the discrimination of metals of the present type. Stability constant studies reveal a stronger complexation to cadmium than to zinc.

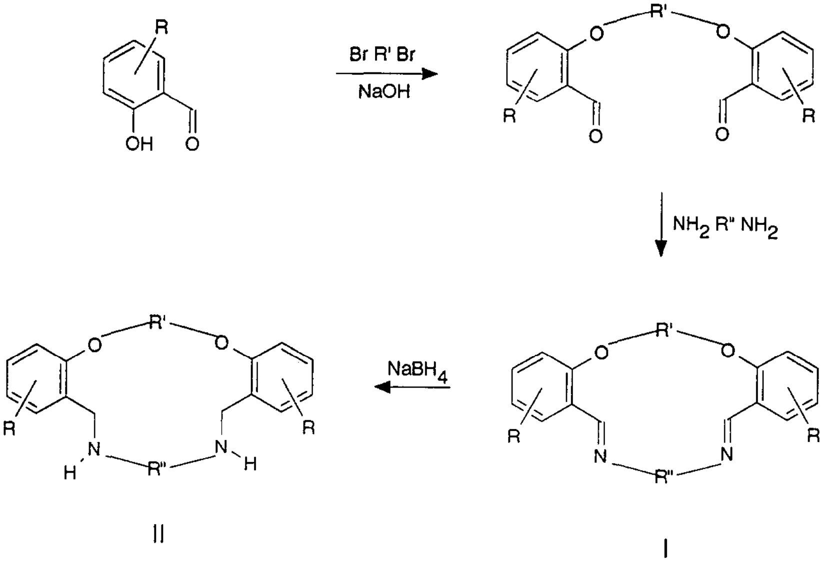

Scheme 22.

A range of (14–19)-membered macrocyclic Schiff bases incorporating O_2N_2, O_2N_3 and O_3N_2 donor sets (**1** of Scheme 22) has been obtained through a reaction pathway of the type reported in Scheme 22.

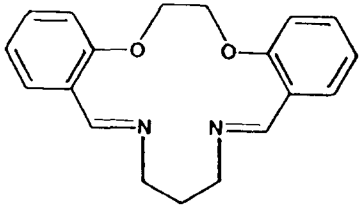

62

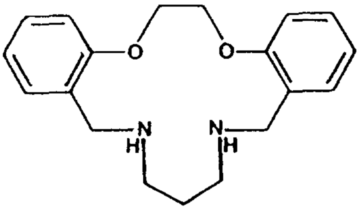

62a

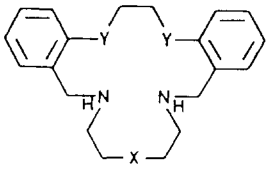

Y = O, X = NH	62b
Y = O, X = O	62c
Y = NH, X = S	62d
Y = S, X = NH	62e
Y = S, X = O	62f

The dihaldehydes, synthesized by Williamson condensation of substituted salicylaldehyde and the appropriate dibromoalkanes, undergo Schiff base cyclization reactions when allowed to react with diamine [112]. These macrocycles form 1:1 cobalt(II), copper(II), nickel(II), zinc(II) and 1:2 cadium(II) complexes [112]. The X-ray structure of the cobalt(II) dithiocyanate complex with the macrocycle **62** [113] shows that the metal is six coordinated being bonded to the nitrogen atoms of the thiocyanate anions and to the imine nitrogen and ether oxygen atoms of the macrocycle. The macrocycle ligand does not present a planar N_2O_2 donor set to the cobalt atom but is folded giving a β-cis configuration. The polyhedron about the cobalt atom is a markedly distorted octahedron (Fig. 40(a)).

The related macrocycles **II** have been prepared by reduction with $NaBH_4$ of the corresponding diimine precursors **I** of Scheme 22 [112] to evaluate the effect of ligand changes on metal ion complexation and recognition [113]. The reduced

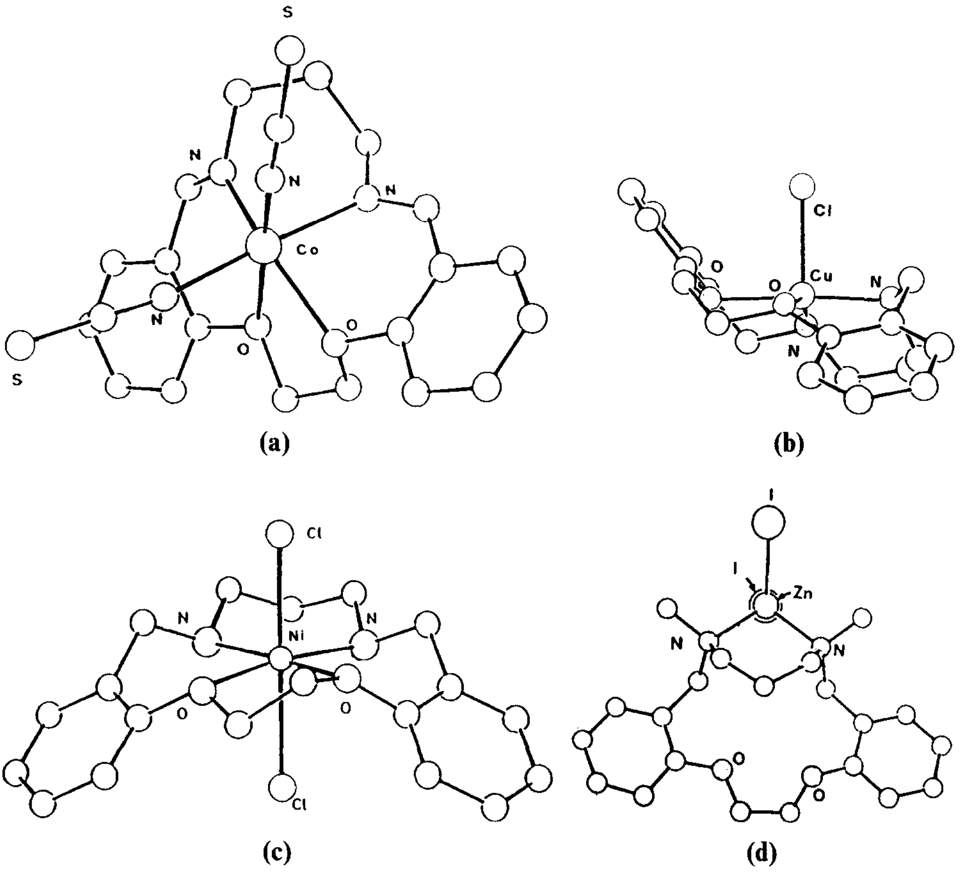

(a) (b)

(c) (d)

Fig. 40. Structures of (a) $Co(\mathbf{62})(NCS)_2$, (b) $[Cu(\mathbf{62a})(Cl)]^+$, (c) $Ni(\mathbf{62a})(Cl_2)$ and (d) $[Zn(\mathbf{62a})(I_2)]$.

ligands are not susceptible to the metal ion promoted imine hydrolysis found for their precursors [112,113].

Complexes of the type M(**62a**)X_2, where M ≡ Cu, Ni, Co, Zn, Cd and X ≡ Cl^-, Br^-, I^-, NCS^-, ClO_4^- have been synthesized from a range of (14–17)-membered macrocycles and the X-ray structures of them solved [113,114].

The structure of the copper complex with the macrocycle containing the 15-membered macrocycle [Cu(**62a**)(Cl)](ClO_4) shows that the coordination sphere of the copper consists of the four donor atoms of the macrocycle together with a chloride ion. The copper ion sits above the hole of the macrocycle which is coordinated in a bent conformation [114] (Fig. 40(b)).

The nickel(II) dichloride or dibromide complexes with **62a** and the homologous larger 16-membered macrocycle have a trans six-coordinate structure with the nickel ion contained in the hole of the ligand [114] (Fig. 40(c)).

The zinc diiodide complex with the 15-membered macrocycle indicates that the two nitrogen donors of the macrocycle, together with two iodide ions, coordinate to the zinc atom in an approximately tetrahedral arrangement such that the zinc lies outside the cavity of the macrocycle. The ether oxygen atoms of the macrocycle do not coordinate [114] (Fig. 40(d)).

The kinetics of dissociation in acid of a range of nickel(II), copper(II) and zinc(II) complexes of the above (14–17)-membered macrocycles show that, for the unsubstituted macrocycles, the kinetic labilities follow the ring size sequence $14 > 15 > 16 < 17$. In accord with the sequence, hole size considerations suggest that the 16-membered macrocycle provides the ring of the best fit for nickel in this series of ligands [112,113]. In contrast to the nickel complexes which exhibit a peak in both the kinetic and the thermodynamic stabilities at the 16-membered ring complex, the copper complexes exhibit no definite ring-size discrimination effects; this different behaviour has been discussed in terms of the structures of these two sets of complexes. Also, for zinc complexes, no well-defined correlation between macrocyclic size and thermodynamic stability was observed [112,113].

The interaction of a range of (17–19)-membered macrocycles incorporating N_3O_2 and O_3N_2 donor sets with nickel(II), copper(II), cobalt(II), zinc(II) and cadium(II) has also been studied [113,114]. The X-ray structure of the 17-membered O_3N_2 macrocycle **62b** indicates that the macrocyclic hole size is too large to enable simultaneous coordination of all donor atoms to the copper(II), nickel(II) or zinc(II) (Fig. 41(a)).

The X-ray structure of the copper(II) diperchlorate monohydrate complex with the same macrocycle [Cu(**62b**)(H_2O)][ClO_4]$_2$ · H_2O indicates that this complex has a pseudo-square-planar coordination geometry with the coordination sphere consisting of the three nitrogen atoms of the macrocycle together with an oxygen atom from water. The ether oxygen donors of the macrocycle do not coordinate (Fig. 41(b)).

In [Zn(**68b**)(NO_3)$_2$], the macrocyclic ligand clearly adopts an arrangement

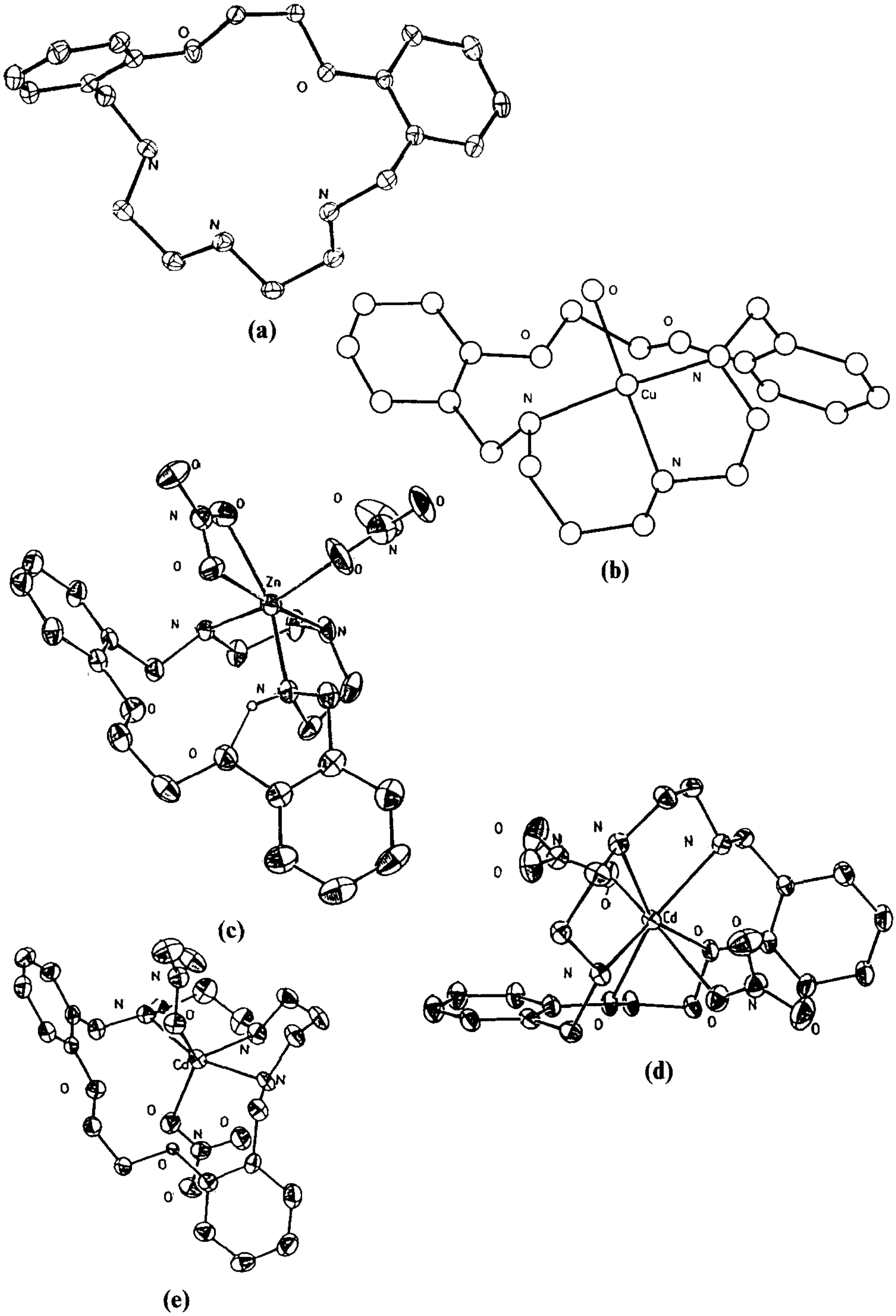

Fig. 41. Structures of (a) **62b**, (b) $[Cu(\mathbf{62b})(H_2O)]^{2+}$, (c) $[Zn(\mathbf{62b})(NO_3)_2]$, (d) $Cd(\mathbf{62b})(NO_3)_2$ and (e) $Cd(\mathbf{62c})(NO_3)_2$.

that removes the ether donors from the coordination sphere. The three nitrogen donors of the macrocycle occupy an approximately facial arrangement around the zinc with its overall coordination number being 6; the remaining coordination positions are filled by a monodentate and bidentate nitrate ligand (Fig. 41(c)). The X-ray structure of [Cd(**62b**)(NO_3)$_2$] shows that this complex has a very distorted pentagonal-bipyramidal coordination geometry in the solid state with the Cd(II) ion lying in the cavity of the five "equatorial" donor atoms of the 17-membered macrocycle (Fig. 41(d)); nitrate groups occupy the axial sites and are best described as monodentate.

In the corresponding 19-membered ring cadmium complex [Cd(**62c**)(NO_3)$_2$] (Fig. 41(e)), the other donors are also outside bonding distance to the metal. The complex contains an approximately planar CdN_3 unit with a ruffled O_2N_3 arrangement. Overall, the coordination number is 5 with two monodentate nitrate groups completing the coordination shell.

The interaction of different metal ions with a series of O_2N_3 donor macrocycles gives rise to new examples of dislocation behaviour in the coordination patterns of the resulting complexes. Dislocations occur when a gradual change in properties along the ligand series induces a sudden change in coordination behaviour for adjacent complexes in the series. The presence of such dislocations may form a basis for metal ion recognition [113,114].

For the nickel complexes in the solid state and in solution, the results are consistent with the presence of either octahedral or pseudo-octahedral coordination geometries. In solution, the unsubstituted 17- and 18-membered O_2N_3 rings appear to adopt a configuration about nickel in which two oxygen and two nitrogen atoms occupy equatorial positions while the remaining nitrogen atom coordinates at an axial site. The remaining axial position is occupied by a halide ion. In contrast, each of the 19-membered ring complexes are found to adopt a structure different from that of the above complexes. A similar structural dislocation has been induced by introduction of two methyl substituents onto the N_3-containing backbone of the unsubstituted 17-membered ring complex. The effects of such structural dislocations are most readily apparent in the stability constants that are 10^3–10^5 lower than those of the remaining complexes. A comparison of the stability constants for the nickel complexes with those for the corresponding cobalt(II) complexes indicates that both series have similar dislocation patterns. In contrast, the complexes of copper(II) (for which the evidence suggests non-coordination of one or both ether oxygen atoms in some complexes) exhibit a different stability pattern [113,114].

When Zn(II) and Cd(II) react with unsubstituted 17-, 18-, and 19-membered macrocycles, the trends in the stabilities for each ion parallel each other for the first two ligands (with the stability constants falling in the order Cd(II) > Zn(II)). However, for the 19-membered ring ligand, a dislocation of the trend is in evidence for the Cd(II) complex but not for the Zn(II): the stability of the Cd(II) complex is considerably lower than expected (the stability order is now Zn(II) > Cd(II)). The origin of the observed dislocation along the Cd(II) series appears to have crossed from coordination of the ether groups in the 17- and 18-membered ring systems to their non-coordination in the 19-membered ring system. For corresponding substituted ligands derivatives, a similar dislocation pattern is observed and hence the dislocation appears to be primarily a function of ring size for these systems.

These studies serve to illustrate the manner in which minor changes in macrocyclic ligand structure may be reflected by major changes within the coordination spheres of particular complexes and hence can be used to control alternate modes of ligand coordination, a process that can contribute to metal ion recognition by organic substrates [113,114].

As a continuation of these investigations, a study of the interaction of cobalt(II), nickel(II) and copper(II) with a much extended series of these ligands, including also sulphur-containing species where systematic variations in donor atom pattern and ring size are more clearly designed, has recently been reported [115].

The X-ray structures of one ligand **62d** with an N_4S donor set, of the related [Cu(**62d**)(H_2O)](ClO_4)$_2$ and of [Cu(**62e**)](ClO_4)$_2$, [Ni(**62e**)(H_2O)](ClO_4)$_2$, and Ag(**62e**)(ClO_4) with the similar N_3S_2 macrocycle and of Ni(**62f**)(H_2O)(NO_3)$_2$ with the macrocycle **62f** containing an ON_2S_2 donor set reveal that all the donor atoms are coordinated to the central metal ions.

In [Cu(**62d**)(H_2O)]$^{2+}$, the ligand adopts a configuration different from that in **62d** (Fig. 42). In the complex the macrocycle occupies a square pyramidal arrangement around Cu^{II}, which also has a water molecule weakly bound in the sixth position. The overall coordination geometry is distorted tetragonal and contains the copper slightly displaced from the N_4 equatorial plane towards the axial sulphur donor [115].

In [Cu(**62**)](ClO_4)$_2$, the coordination about the copper(II) ion is square

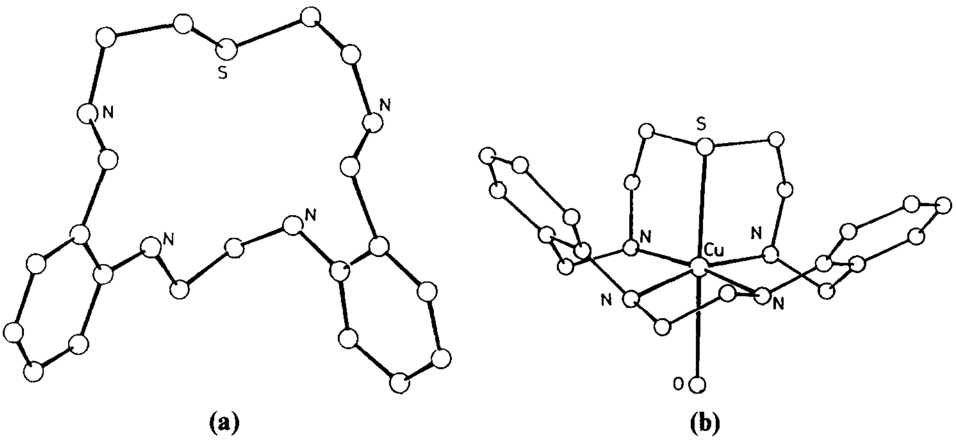

Fig. 42. Structures of (a) **62d** and (b) [Cu(**62d**)(H_2O)]$^{2+}$.

pyramidal with the sulphur atom in the axial site (Fig. 43(a)) [115]. The similar $[Ni(\mathbf{62e})(H_2O)](ClO_4)_2$ displays an octahedral coordination, a water molecule being bound to the central metal ion (Fig. 43(b)) [115].

The silver(I) analogue, $[Ag(\mathbf{62e})](ClO_4)_2$, exhibits a distorted pentagonal bipyramidal coordination (Fig. 43(c)) [105].

In $[Cu(\mathbf{62e})]^{2+}$, the 1,4,7-triazaheptane fragment of **62e** is meridionally coordinated, but facially coordinated in $[Ni(\mathbf{62e})(H_2O)]^{2+}$ and intermediate in $[Ag(\mathbf{62e})]^+$ [115].

In $Ni(\mathbf{62f})(H_2O)](NO_3)_2$ the nickel ion is six coordinated with the complex cation exhibiting a distorted-octahedral geometry defined by all five donor atoms of the ON_2S_2 macrocycle and a water molecule; the macrocyclic backbone incorporating the N–O–N donor fragment is arranged meridionally (Fig. 44) [115].

Studies in solution demonstrate for all these complexes the formation of 1:1 complexes and extremely large stability differentials (up to 10^{10} for copper(II)) that may be achieved through structural variation within the ligand framework employed for this study. The contribution of the donor atom types to overall complex stability was found to follow the expected order of NH(aliphatic) > NH(anilino) > S > O [115].

Metal complexes of the macrocycles H-**63** were prepared and characterized.

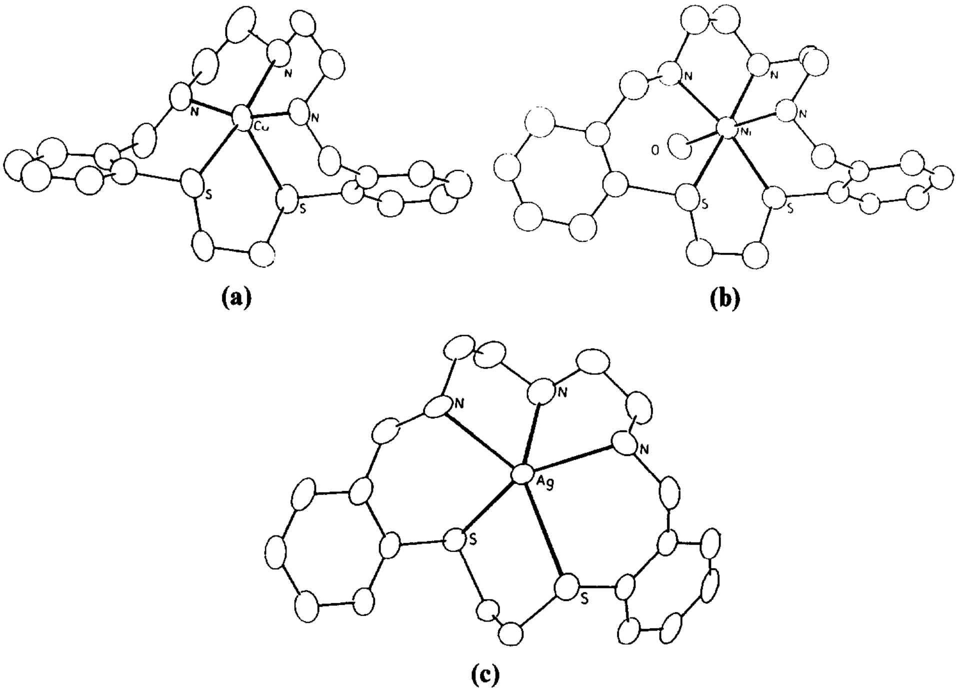

(a)

(b)

(c)

Fig. 43. Structures of (a) $[Cu(\mathbf{62e})]^{2+}$, (b) $[Ni(\mathbf{62e})(H_2O)]^{2+}$ and (c) $[Ag(\mathbf{62e})]^+$.

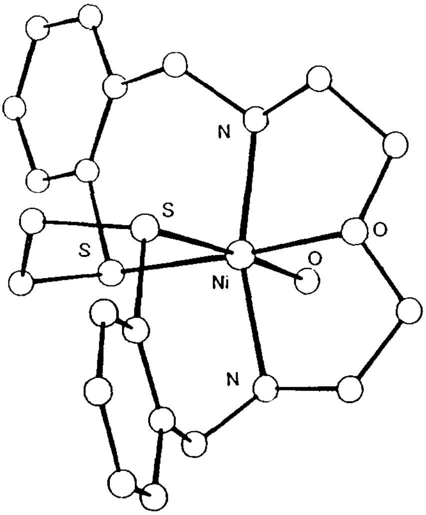

Fig. 44. Structure of $[Ni(\mathbf{62f})(H_2O)]^{2+}$.

Mononuclear complexes, $M(H\text{-}\mathbf{63})X_2$, were recovered for $M \equiv Co(I)$, Ni(II), Zn(II), Cd(II), or Hg(II) and $X \equiv Cl$ or Br and homodinuclear complexes, $Cu_2(\mathbf{63})(Cl)_2(OH) \cdot nH_2O$, for $CuCl_2$. The salts $M(ClO_4)_2$ and $M(NO_3)_2$ ($M \equiv Co(II)$, Ni(II), Cu(II), Zn(II), or Cd(II)) gave complexes $[M(\mathbf{63})X]$ and fast atom bombardment mass spectrometry provided evidence for oligomer formation [116].

The homodinuclear copper(II) complexes are proposed as having the structure shown in Fig. 45(a). Attempts to grow crystals of these species were unsuccessful; however, the complex $[Cu_2(\mathbf{63})(Cl)_2(OH)]$ (where $R \equiv CH_2CH_2$) was recovered from benzyl alcohol and the structure solved. This not only confirmed the exocyclic homodinuclear nature of the complex but also showed that the exogenous hydroxyl group had been replaced by a benzoate anion present in the solvent [116].

The structure of $[\{Cu_2(\mathbf{63})(\mu\text{-}O_2CPh)(H_2O)(Cl)_2\}_2] \cdot 2PhCH_2OH$ comprises a centrosymmetric tetranuclear complex in which each of two pairs of copper atoms is coordinated exocyclically by a macrocyclic ligand via two amine nitrogen atoms (one to each copper), and by an oxygen atom of a deprotonated pendant hydroxyl group which bridges the two copper atoms; the pair of copper atoms is also bridged by a benzoate anion. The coordination sphere of the "outer" copper atom of each pair is completed by a terminal chlorine atom and, more remotely, by a water ligand. The "inner" two centrosymmetrically related copper atoms (one from each pair) are asymmetrically bridged by a pair of chlorine ligands. The Cu · · · Cu distances are 3.489 and 3.391 Å, the latter being between symmetry-related, dichloride-bridged copper atoms. Each of the independent copper atoms has a five-coordinated geometry [116] (Fig. 45(b)).

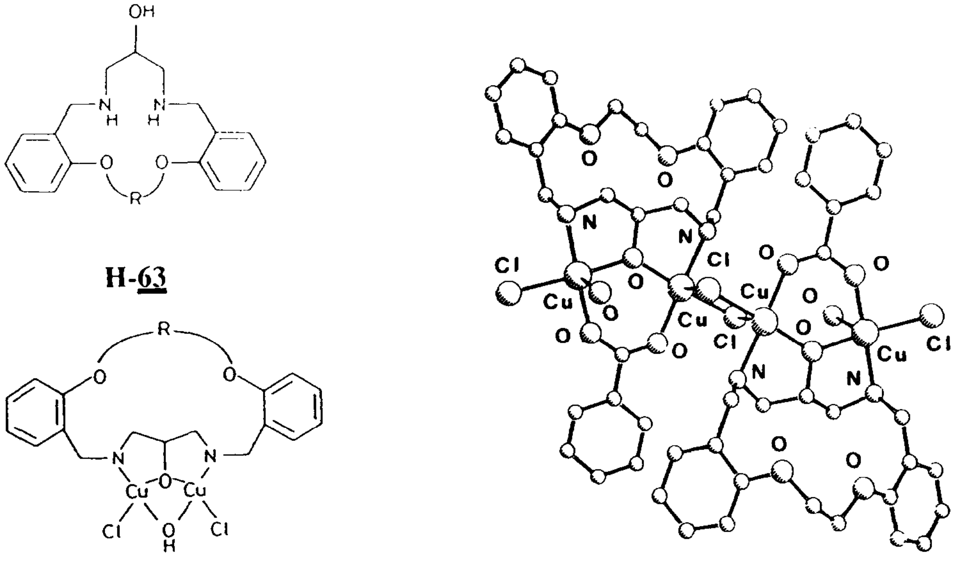

(a) (b)

Fig. 45. (a) The proposed structure of the homodinuclear complex $Cu_2(\mathbf{63})(Cl)_2(OH)$. (b) The molecular structure of the tetranuclear complex $[\{Cu_2(\mathbf{63})(\mu\text{-}O_2CPh)(H_2O)(Cl)_2\}_2]\cdot 2PhCH_2OH$.

[1 + 1] macrocyclic Schiff bases containing N_4 donor atoms have been prepared by reaction of the appropriate diformyldianilino and polyamine precursors (Scheme 23(a)) in very high yield (76%–84%) under a variety of experimental conditions [117]. The formation of these diimino macrocycles is strongly facilitated by the stabilization of the imine bond by intramolecular hydrogen bonding. From the reaction of the related dihaldehyde, which has no anilino hydrogen atom, with 1,2-diaminoethane, 1,2-diaminobenzene, and 1,3-diaminopropane, the 1 : 2 linear condensation products [117] were obtained instead of the macrocyclic diimines. These macroacyclic Schiff bases adopt an extended configuration which minimizes nitrogen lone pair–lone pair repulsion.

Structural determination of the macrocyclic Schiff base systems shows that the presence of anilino hydrogen atoms allows intramolecular hydrogen bonding which reduces such lone-pair interactions in the centres of the rings. Almost planar hydrogen-bonded units are observed in the X-ray structures of several of these macrocycles [117]. The overall configurations of the macrocycles differ considerably, probably to preserve the planarities of the hydrogen-bonded units and to minimize contact between the anilino protons in the two halves of the molecules [117].

The N_4 macrocycles containing two *o*-iminoanilino units can give neutral magnesium complexes on reaction with 2 mol of ethylmagnesium bromide [117] but undergo stereoselective C alkylation on treatment with an excess of the Grignard reagent [117]. The subsequent hydrolysis affords the *meso*-diethyl-substituted tetra-

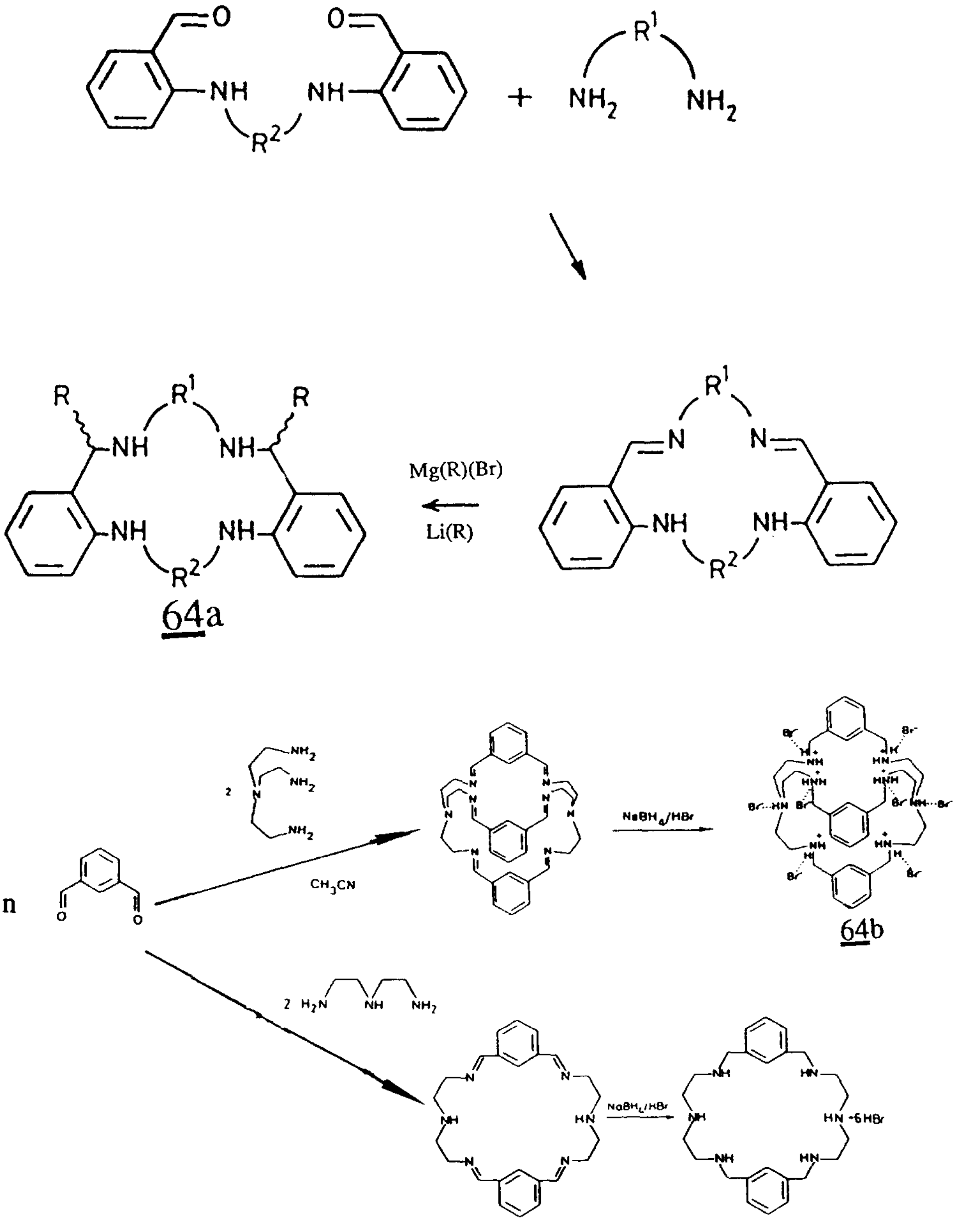

Scheme 23.

amines **64** of Scheme 23(a) [117]. The tetraaza ($R \equiv H$) macrocycles have been prepared by reduction with an excess of $NaBH_4$ of the corresponding diimine precursors [117]. The reductive C alkylation was also achieved using methyllithium or *n*-butyllithium (Scheme 23(a)) [117].

The structure of the macrocycles **64a** where $R^1 \equiv (CH_2)_3$ and $R^2 \equiv C(CH_2)_2$ and $R \equiv C_3H_7$ or C_2H_5 [117] shows them to be the *meso* isomer. Both R groups and the benzylamino N–H bonds are displaced to the same side of the mean plane of the four nitrogen atoms (Fig. 46(a) and 46(b)).

The dimethyl substitute macrocycle ($R \equiv CH_3$; $R' \equiv C_6H_4$; $R'' \equiv (CH_2)_3$), which was obtained from the reaction with the lithium reagent, is also a *meso* isomer as revealed by the structure determination of the copper(II) complex [Cu(**64a**)(dmf)]$(ClO_4)_2 \cdot$dmf. In this complex, the ligand more nearly approaches mirror plane symmetry (Fig. 46(c)). The copper ion is penta coordinated with a pyramidal square environment [117].

The interaction of Zn(II) and Cd(II) with an extensive series of dibenzo-substituted macrocycles **64a** and related open-chain tetraamines has been investigated [117].

The complex [Zn(**64a**)$(NO_3)(H_2O)]^+$ ($R \equiv H$, $R' \equiv (CH_2)_3$, $R'' \equiv (CH_2)_2$) has a six-coordinated structure with the metal atom lying fairly close to the best plane through the four nitrogen donors and with a monodentate nitrate and a water molecule defining apical sites in an approximately octahedral geometry [117] (Fig. 46(d)). In contrast, the cadmium complexes [Cd(**64a**)$(NO_3)]^+$ with the same ligand and [Cd(**64a**)$(NO_3)]^+$ ($R \equiv n$-Bu, $R' \equiv (CH_2)_3$ and $R'' \equiv (CH_2)_2$) have only one ligand in addition to the macrocycle in the coordination sphere and have the metal much further displaced from the N_4 planes towards the coordination nitrate ions. The nitrate groups adopt an unsymmetrical bidentate mode of coordination [117] (Figs. 46(e) and 46(f)).

The structure of [Zn(**64a**)(I)$]^+$ ($R \equiv H$, $R' \equiv (CH_2)_3$ and $R' \equiv (CH_2)_2$) confirms a square pyramidal coordination geometry for the Zn(II) in which the metal is bound by the four nitrogen atoms of the macrocycle and has one axial iodine ligand (Fig. 46(g)).

In all these complexes, the ligands adopt a folded conformation [117]. All N_4 macrocyclic **63a** ligands form 1:1 (metal–ligand) complexes in solution with the metal ions mentioned above; the thermodynamic stabilities of the complexes in 95% methanol ($I = 0.1$ mol dm^{-3}, NEt_4ClO_4) have been determined. Along one series of 14- to 16-membered macrocyclic systems a dislocation in the stability pattern occurs for Zn(II) at the 16-membered ring complex while, for Cd(II), the dislocation corresponded to the 15-membered ring species. As a consequence, there is an enhanced stability difference (Zn(II) > Cd(II)) between the complexes of the latter ring. The observed discrimination shown by the 15-membered ring is largely maintained when bulk alkyl substituents are appended to carbon atoms adjacent to two of the secondary amine donors; however, the absolute magnitudes of the stabilities are decreased because of steric effects. In an extension of this study, it has been found that open-chain analogues exhibit no unusual discrimination between Zn(II) and Cd(II). Other macrocyclic and open-chain ligands containing only anilino nitrogen

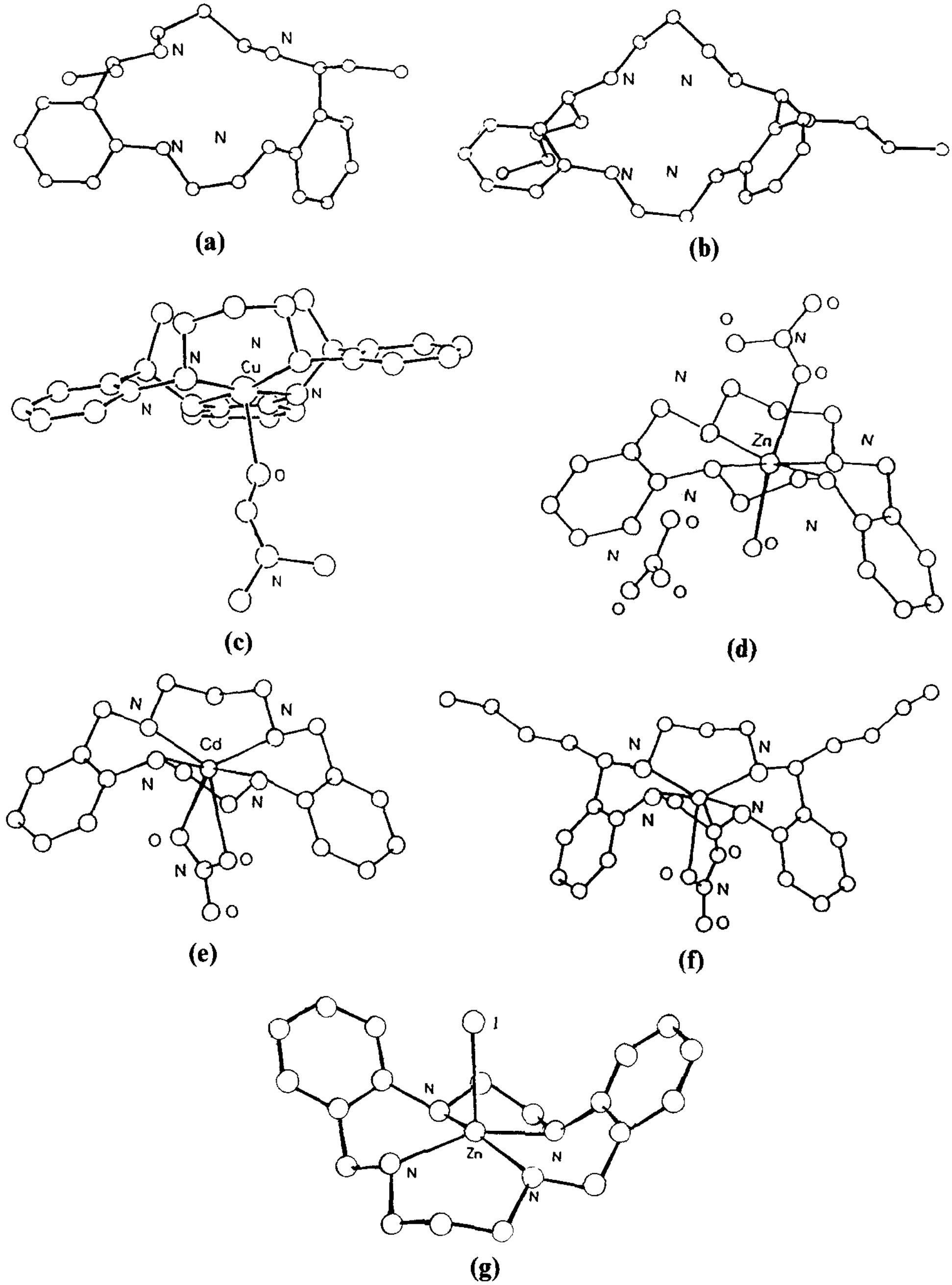

Fig. 46. Structures of (a) and (b) macrocycles **64a** with two different pendant arms, of (c) [Cu(**64a**)(dmf)]$^{2+}$, (d) [Zn(**64a**)(NO_3)(H_2O)]$^+$, (e) and (f) [Cd(**64a**)(NO_3)]$^+$ with two different pendant arms and (g) [Zn(**64a**)(I)]$^+$.

donors have been shown to form only very weak complexes with Zn(II) and Cd(II) [117].

The synthesis of the saturated binucleating macrocycle and its analogous macrobicycle via efficient and facile direct condensation of benzene-1,3-dicarboxaldehyde with diethylenetriamine [118] or with tris(2-aminoethyl)-amine [117], followed by hydrogenation with $NaBH_4$, represents a valuable route to pairs of analogous macrocyclic and macrobicyclic ligands [72,119] (Scheme 23(b)).

The X-ray structure of the [3 + 2] macrobicycle **64b** (Fig. 47) [118] shows that the cryptand is associated with three of the bromide anions, which are situated on the cryptand periphery between two of the three bridges but outside the cavity of the cryptand. The structure therefore could be described as $[3Br^-,(\mathbf{64})(H^+)_8](Br^-)_5 \cdot 6H_2O$. The octaprotonated cryptand has a "Y" shape with the three legs being the planes of the phenyl rings (Fig. 47). The length of the macrobicyclic cage (distance between the bridgehead nitrogen atoms) is 7.60(1) Å. The internal central cavity of the cryptand can be described as a sphere of diameter 7.4–7.6 Å. The protons located at the bridgehead nitrogen atoms point toward the outside of the spherical internal cavity. This cavity is empty and does not contain a solvent molecule. The protonated macrobicycle exhibits bromide anion binding, but none of the three bromide anions is located inside the internal cavity.

In view of the importance of macrocyclic and macrobicyclic ligands in the fields of molecular recognition, catalysis, and transport, the study of the effect of adding a bridge to a given macrocycle on the chemistry of the resulting cryptand should generate insights about the importance of the encapsulation of pairs of metal ions in the crypt, compared with coordinating them to the more flexible macrocyclic ligands. It is hoped that determination of crystal structures of corresponding pairs of ligands and their complexes will contribute to the understanding on the molecular level of the importance of rigidity in the stabilization of the dinuclear structures and the binding of secondary bridging bifunctional donor groups.

Similarly, by tetrahydroborate reduction of the [2 + 3] condensation product

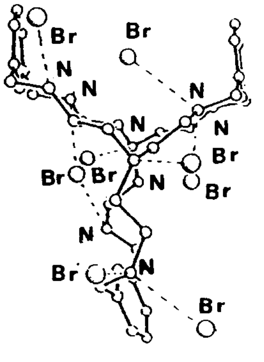

Fig. 47. Structure of **64b**.

of tris(2-ethylamino)amine with terephthalaldehyde **31**, or of the disilver or dilead complexes of **31**, a complete reduction of all six imino functions was obtained and the structure of the resulting octamino cryptand was determined by X-ray diffractometry [120]. This octamino cryptand acts as a host for pairs of protons or first series transition metal cations. Pairs of transition metal cations coordinated to the amino N donors accommodate mono- and triatomic briding ligands, such as OH^- or imidazolate, generating weak to moderate antiferromagnetic interaction. For the dicopper(II) μ-azido complexes a triplet ground state was suggested, possibly derived from a near-linear alignment of the M–NNN–M assembly [120].

Also, the complexes Ba(**65**)$(Cl)_2$ obtained by a template procedure (Scheme 24) can be reduced with $NaBH_4$ to form the corresponding 18-membered macrocyclic ligand **65′** containing saturated amine and pyridine heterocyclic units. The same behaviour has been obtained with the analogous complex containing furan as the head unit instead of pyridine [121].

4. MONONUCLEAR COMPLEXES

Although the formation of mononuclear macrocyclic complexes via template procedures has been achieved with transition or alkaline earth metal cations, the early work concerning the use of lanthanide templates in the synthesis of [2+2] tetraimine Schiff base macrocycles suggested that the potential application was limited [122]. Nevertheless, the formation of mononuclear macrocyclic complexes in the presence of lanthanide(III) ions has been widely studied and the progress made reviewed [12]. [2+2] macrocyclic complexes have been prepared by the template condensation of the appropriate amine and formyl or keto precursors in the presence of lanthanide(III) salts or by transmetallation reaction from the barium complex as reported above in Scheme 9.

Almost the whole series of lanthanide nitrate and lanthanum perchlorate complexes have been prepared with the macrocycle **38** [90,123].

The heavier lanthanides (Tb → Lu) were effective as templating agents also in the synthesis of the smaller 14-membered macrocycle obtained by condensation of 2,6-diacetylpyridine and hydrazine [124]; use of the lighter lanthanides as templates gave complexes of the acyclic ligands derived from the condensation of two 2,6-diacetylpyridine with one hydrazine. On reaction with water, the macrocyclic species ring opened to give the acyclic complexes [124].

The X-ray crystal structure of [La(**38**)$(NO_3)_3$] [90,122] shows that the lanthanum ion is 12 coordinated by six macrocyclic nitrogen atoms of the approximately planar macrocycle and one bidentate nitrate above and the other two, also bidentate, below the plane (Fig. 48).

The complex [Ce$(NO_3)_2$(**38**)(H_2O)]$(NO_3)\cdot H_2O$ has an 11-coordinated cerium ion. The metal ion is coordinated to the six ring nitrogen atoms, to one

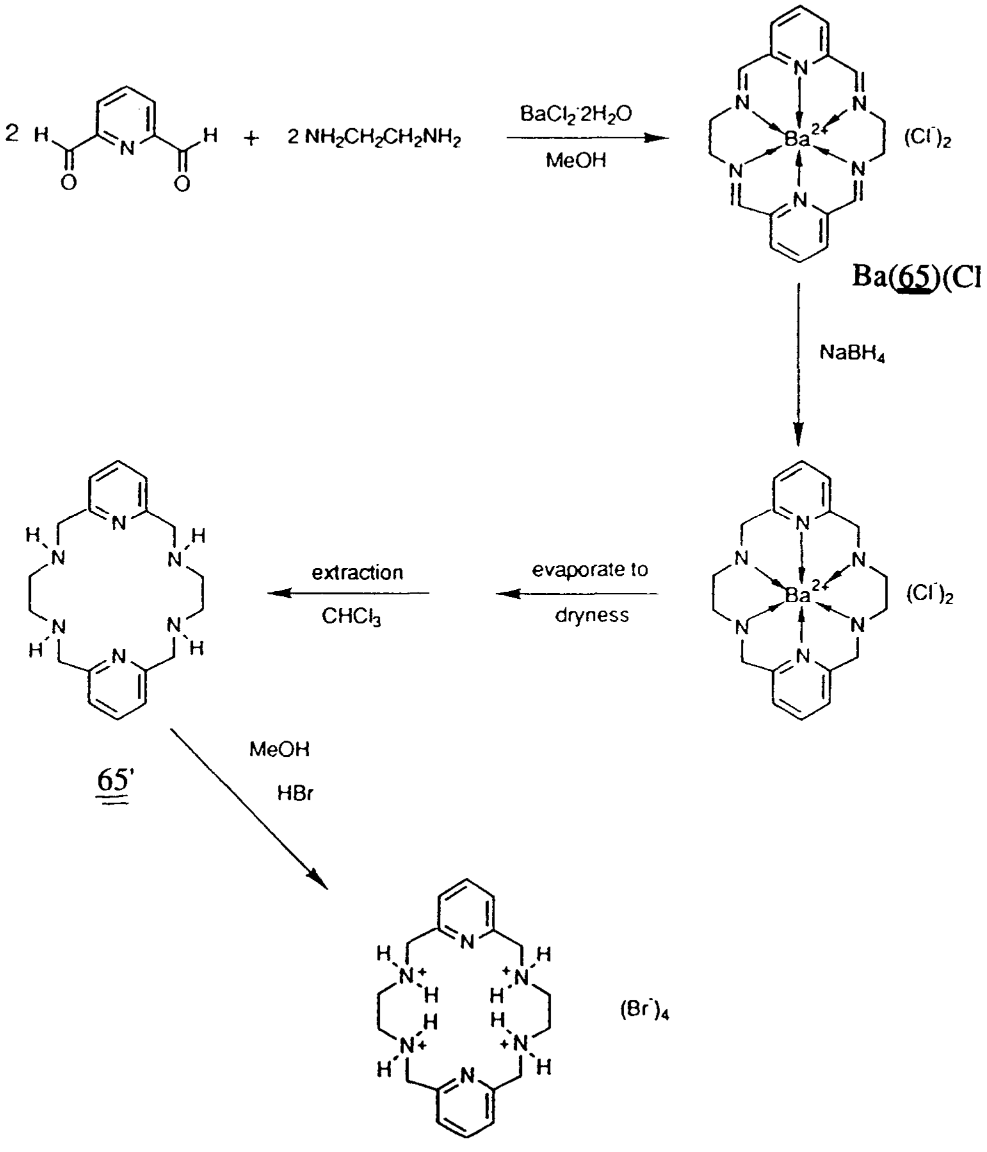

Scheme 24.

bidentate nitrate ion on one side of the macrocycle and to the remaining nitrate ion and the water molecule on the other (Fig. 49) [122].

The complex $[\{Nd(NO_3)(\mathbf{38})(H_2O)_2\}_2](NO_3)(ClO_4)_3 \cdot 4H_2O$ has 10-coordinated Nd, the metal being coordinated to the six ring nitrogen atoms and to one bidentate nitrate ion on one side of the macrocycle and to the two water molecules on the other (Fig. 50) [122].

In addition to the three compounds whose structures were fully determined,

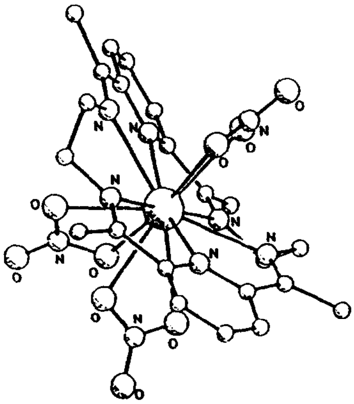

Fig. 48. Structure of [La(**38**)(NO_3)$_3$].

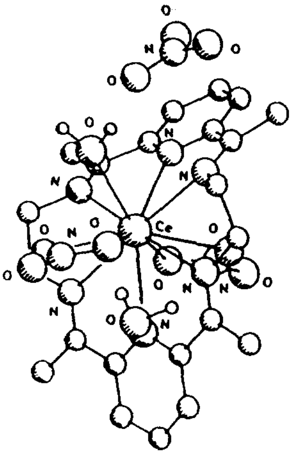

Fig. 49. Structure of [Ce(NO_3)$_2$(**38**)(H_2O)]NO_3 · H_2O.

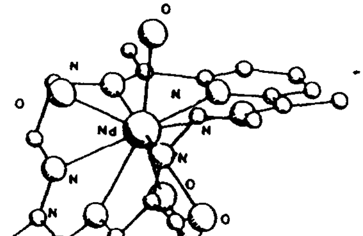

Fig. 50. Structure of [Nd(NO_3)(**38**)(H_2O)$_2$]$^{2+}$.

the other complexes of similar stoichiometries were also examined. The 12-coordinate structure which is adopted by La was confirmed by single-crystal cell dimension determinations to be adopted by Ce also. The 11-coordinate structure adopted by Ce was shown by similar means to be adopted also by La and Pr. Crystals of the Tb complex were similarly found to be isostructural with those of the 10-coordinate Nd complex, and although twinning was present in some other cases, giving difficulty with cell dimension determination, the same structure was proposed for the series Nd, Sm, Eu, Gd, Tb, Dy and Ho. However, single-crystal cell dimension determination shows that the last member of this third group, Er, adopts a different crystal structure, as yet undetermined [122].

These three structures adopted by the metals La–Ho exhibit decreasing coordination numbers, namely 12, 11 and 10. The smallest lanthanides have ionic radii too small to coordinate predominantly with the macrocyclic ligand in competition with barium and, furthermore, they do not form a suitably sized template for condensation of the components of the macrocycle. These two circumstances, which are shown by the failure of both the ligand replacement and the template synthetic methods, are clearly interrelated. The early lanthanides seem to be on the 12 to 11 coordination borderline in these complexes and accept compact bidentate nitrate ligands in non-aqueous solution, to give a coordination number of 12, while in aqueous solution, the overall effect is to substitute a coordinated bidentate nitrate ion by a monodentate water molecule. A further noticeable effect is the non-coplanarity of the macrocycle which increases in the sequence $12 \rightarrow 11 \rightarrow 10$ coordination and thus seems to be a result of the ligand buckling in order to retain hexadentate contact with the smaller ions rather than being the result of different steric requirements of the ligands of either side of the macrocycle. These steric requirements are in no case too dissimilar but are at their most dissimilar in $[La(\mathbf{38})(NO_3)_3]$ which has the smallest interplanar angle. However, these unbalanced steric requirements do determine the direction, although not the extent, of the folding [122].

The time frame of metal exchange and ligand exchange kinetics becomes a major consideration when lanthanide complexes are to be used as probes for biological systems. In the dilute aqueous or aqueous–organic solutions required for these systems, which often involve potentially competing ligands, even a highly stable complex, if labile, may not give reliable results. Therefore, a systematic investigation of the conditions leading to the lanthanide macrocyclic synthesis has been undertaken.

2,6-diformylpyridine and α,ω-diamines in the presence of $Ln(NO_3)_3$ form complexes of the macrocycles **65** to **67** for all the lanthanides save promethium [92]. IR and NMR spectra show that for heavier lanthanide (Nd → Lu, except Eu) complexes with **65**, addition of a water molecule across the imine double bond leading to the formation of **68**, had occurred. The lighter lanthanide (La → Pr) complexes have the Schiff base in the tetraiminic form **65**.

During the course of recrystallization, there was a reversion of the macrocycle to the tetraimine form as confirmed by the X-ray structure of $[Sm(\mathbf{65})(NO_3)(OH)(H_2O)]NO_3 \cdot 2MeOH$ [125]. The X-ray crystal structure consists of discrete complex $[Sm(\mathbf{65})(NO_3)(OH)(H_2O)]^+$ cations, NO_3^- anions, and clathrate MeOH molecules. The Sm^{3+} ion is ten coordinated, being directly bonded to the heteroatoms of the sexidentate ligand, to one chelating nitrate group, to the oxygen atoms of the OH^- ion and of one H_2O molecule. The coordination polyhedron can be described as an irregular antiprism capped on its "square" faces by the nitrogen atoms of the pyridine groups [125] (Fig. 51).

	R
65	$-CH_2CH_2-$
66	$-CH_2CH(CH_3)-$
67	$-CH_2CH_2CH_2-$

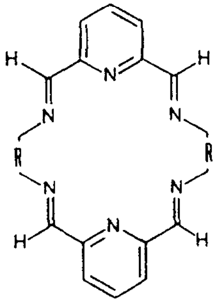

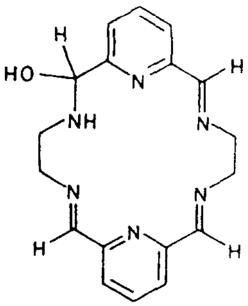

68

Tetraimine Schiff bases derived from 2,6-diformylpyridine and 1,2-diaminopropane (**66**) and from 2,6-diformylpyridine and 1,3-diaminopropane (**67**) have been isolated for the lanthanides (except promethium). With the latter complexes, no evidence for carbinolamine intermediates was found [92].

In order to assess how a decrease in the ionic radius of the lanthanide(III)

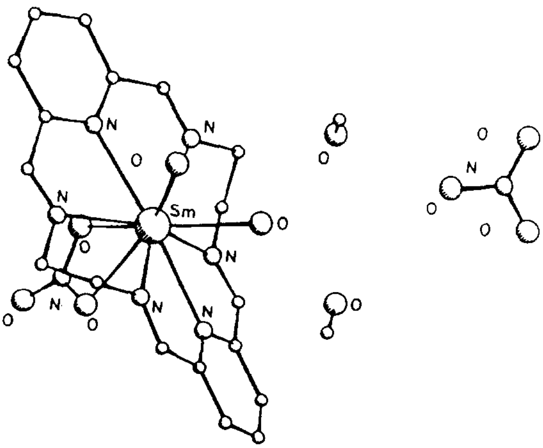

Fig. 51. Structure of $[Sm(\mathbf{65})(NO_3)(OH)(H_2O)]NO_3 \cdot 2MeOH$.

ions influence the structural feature and special arrangement of the macrocyclic entity itself, a series of lanthanide(III) complexes with the macrocycle **38** and different counteranions have been prepared. The Schiff base condensation of 2,6-diacetylpyridine and ethylenediamine in the presence of lutetium(III) acetate followed by precipitation with ClO_4^-, yields $[Lu(\mathbf{38})(CH_3COO)(OH)](ClO_4)(CH_3OH)(H_2O)_n$ depending on the treatment of the sample [80].

A noteworthy feature of the structure of this complex is that the crystal consists of the two species shown in Fig. 52, present in a 1:1 ratio.

The structure of the complex is ionic with the cation consisting of 9-coordinated lutetium(III) linked to the six N donor atoms of the macrocycle, to a bidentate chelating acetate and to either a water or a methanol molecule. Non-coordinated OH^- and ClO_4^- balance the residual cationic charges; clathrated methanol is also present.

The Lu–macrocyclic moiety has a "folded butterfly" arrangement whereas, for the La and Sm complexes, there was only a minor displacement from planarity. The hinging of the macrocycle at the flexible ethylenic side chains is suggested to relieve strain in the cycle and to minimize repulsion between the hetero ligands to allow optimum coordination at the metal. As there are non-coordinated but potentially strong O donor ligands present it is also suggested that 9 is the limit for Lu coordination in such species. There remains the question of whether the folding of the macrocycle is indeed governed by the ionic size of the metal or by the steric requirement of the ligand.

The complexes of the general formula $Ln(\mathbf{38})(CH_3COO)_2Cl \cdot nH_2O$ ($n = 3$–6) have also been obtained by the template procedure. The X-ray structure of a series of these complexes, $[Ln(\mathbf{38})(CH_3COO)_2] \cdot Cl \cdot 4H_2O$ (Ln ≡ Nd(III), Eu(III),

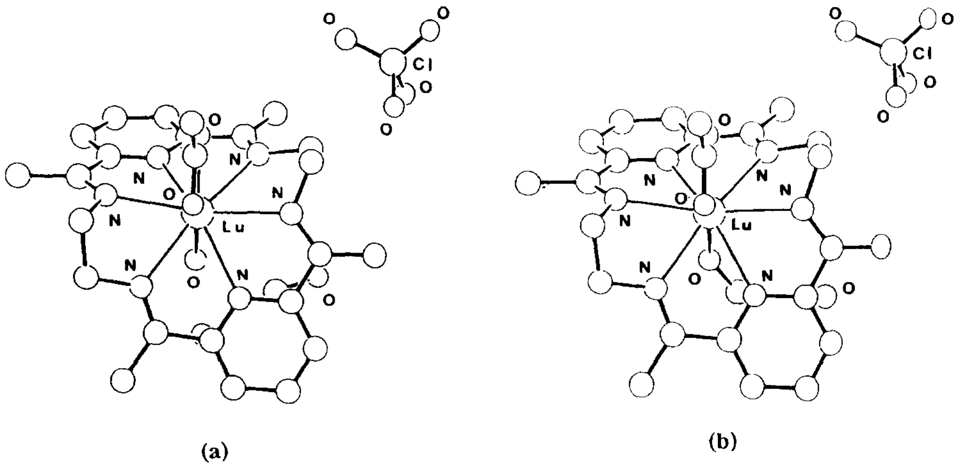

Fig. 52. Perspective views of (a) $[Lu(\mathbf{38})(CH_3COO)(H_2O)](CH_3OH)(OH)(ClO_4)$ and (b) $[Lu(\mathbf{38})(CH_3COO)(CH_3OH)](OH)(ClO_4)$.

Gd(III)) shows that the complex cations consist of a 10-coordinated metal centre linked to the six nitrogen donor atoms of the macrocycle which has a folded butterfly configuration. An ionic chloride balances the residual metal charge. The paramagnetic-shifted NMR spectra of the complexes were measured in various solvents and confirm that the metal–macrocycle moieties remain undissociated. Also, the spectra depend on the counterions showing that, on average, at least one of the labile acetate ligands is bound to the metal ion even in aqueous solution [126,127] (Fig. 53).

By the reaction of $[\mathrm{Ln}(\mathbf{38})(\mathrm{CH_3COO})_2]\mathrm{Cl}\cdot n\mathrm{H_2O}$ (Ln ≡ Y(III), Eu(III)) with an excess of NaNCS, the trisisothiocyanate complexes of the general formula $[\mathrm{Ln}(\mathbf{38})(\mathrm{NCS})_3]$ have been synthesized and characterized. The two complexes are isostructural [128] and are composed of two distinct asymmetric units both formed by $[\mathrm{Ln}(\mathbf{38})(\mathrm{NCS})_3]$ having almost the same ligand conformation. The lanthanide(III) ion is nonacoordinated by six nitrogen atoms of the macrocycle and by the three nitrogen atoms of the thiocyanate groups which behave as monodentates. The macrocycle ligand is bent in the direction of the singly coordinated ligand (Fig. 54).

The interaction of uncharged N donor ligands with the complex $[\mathrm{Eu}(\mathbf{38})(\mathrm{CH_3COO})_2]\mathrm{Cl}\cdot 4\mathrm{H_2O}$ was investigated in solution by NMR spectroscopy and luminescence titration. Both experiments indicated little or no interaction of the N donor ligands with the metal centre of the macrocyclic complex. Attempts to isolate a 1,10-phenanthroline complex of the europium macrocycle produced instead $\{[\mathrm{Eu}(\mathbf{38})(\mathrm{CH_3COO})]_2(\mu\text{-}\mathrm{CO_3})\}(\mathrm{OH})_2\cdot 7\mathrm{H_2O}$, which incorporated atmospheric carbon dixoide. The X-ray crystal structure reveals a bis-chelating carbonate group linking two europium macrocycles, each of which was folded in a butterfly configuration towards the external bidentate chelating acetates. Ionic hydroxides and clathrate water molecules completed the structure [127].

These results show that the considerable contraction in ionic radius that occurs

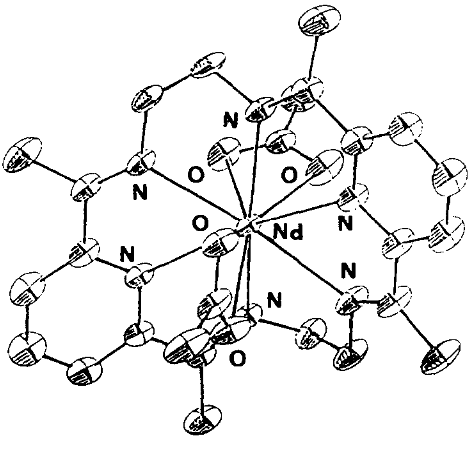

Fig. 53. A view of $[\mathrm{Nd}(\mathbf{38})(\mathrm{CH_3COO})_2]^+$.

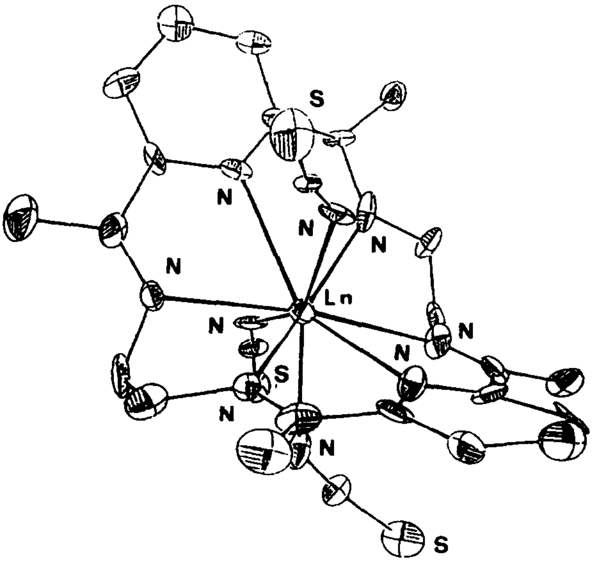

Fig. 54. Structure of [Ln(**38**)$(NCS)_3$] (Ln ≡ Y(III), Eu(III)).

along the 4f series does not appreciably affect the ability of the lanthanide(III) ions to act as templating agents for the formation of the 18-atom macrocycle. The ease and the yield of the metal template macrocyclic synthesis appear to depend more on the counterion present than on the metal ion; good O donor anionic ligands, such as acetate, favour the reaction much more effectively than do chloride and perchlorate [80,129].

The hexaaza macrocyclic complexes undergo reversible dehydration in the crystalline state and anion loss through hydrolysis, but the macrocyclic entity is stable to 240°C, an unusually high temperature for lanthanide-bound N donor organic ligands. In solutions, the macrocycle remains intact in the presence of H_2O and dmso; this is evidenced by the NMR spectra recorded in these solvents. Typical precipitating agents such as F^-, OH^- or $C_2O_4^=$ do not remove the lanthanide cation from the macrocycle [129].

NMR spectra show that all six N donor atoms of the macrocyclic cavity remain coordinated to the metal ion not only for La(III) but also for the smaller Lu(III) ion [129]. Because of this unique inertness and because of their solubility in both water and organic solvents, the complexes of the paramagnetic lanthanides should prove to be useful and versatile NMR shift reagents [129].

The template reactions of 2,5-furandicarbaldehyde and α,ω primary diamines in the presence of the lighter lanthanide nitrate produce Ln(**69**)$(NO_3)_3 \cdot nH_2O$ (n = 0–2) (Ln ≡ La–Eu except Pm), Ln(**70**)$(NO_3)_3 \cdot nH_2O$ (n = 0–2) (Ln ≡ La, Ce, Pr) and Ln(**71**)$(NO_3)_3 \cdot nH_2O$ (n = 0, 1) (Ln ≡ La, Ce, Pr) [93]. IR, NMR and mass spectra (a peak corresponding to the macrocycle, with no peaks at higher mass number, is present) agree with a [2 + 2] condensation.

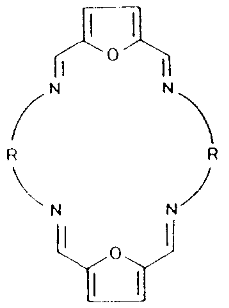

	R
69	$-CH_2CH_2-$
70	$-CH_2CH(Me)-$
71	$-CH_2CH_2CH_2$

In the absence of metal ions only viscous, probably polymeric, oils were recovered, clearly indicating the role of the lanthanides in promoting the macrocyclic synthesis.

The template reactions of 2,5-furandicarbaldehyde with 1,2-diaminoethane in the presence of the heavier lanthanide nitrates (Gd–Lu), however, gave compounds whose analyses suggest a three metal cation to two macrocyclic unit ratio $[Ln_3(\mathbf{69})_2(NO_3)_9]\cdot 4H_2O$.

For the heavier lanthanide cations, a sandwich structure, in which groups of donors are shared, seems to be preferred.

In the template reactions using the diaminopropanes with the heavier lanthanides (Nd–Lu, except Pm) intractable materials were obtained. Dissolution of these lanthanide complexes in water leads to decomposition.

The weakly donating furan head unit should help in labilizing the system. The ^1H NMR of $[La(\mathbf{69})](NO_3)_3$ in dmso-d_6 gave two sets of signals when run immediately after dissolution. After ca. 1 h only one set remained; it was proposed that this was due to the free macrocycle. Attempts to isolate the free macrocycle were unsuccessful; presumably the macrocycle breaks down during the isolation procedure owing to hydrolysis of the strained imine bonds [93].

These examples clearly reveal the ability of the lanthanide(III) and yttrium(III) ions to act as templates for the [2 + 2] Schiff base condensation of 1,2-diaminoethane with 2,6-diacetylpyridine.

These complexes are unique among the compounds of the lanthanides in that the metal–macrocyclic entity is extremely inert with respect to release of the metal ion, whereas the exocyclic ligands (anions or solvent molecules) are labile and easily exchangeable. The inertness of the metal–**38** entity must arise from an especially favourable combination of metal ionic radius, cavity size of the 18-membered macrocyclic ligand **38**, and bonding ability of the six nitrogen donor atoms. This suggestion is supported by the observation that the imine macrocycles similar to **38** but having furan instead of pyridine head units, are labile and decompose rapidly when dissolved in water. Also, a lanthanum(III) complex of the **69** macrocycle was found to undergo transmetallation with copper(II), while complexes of the smaller lanthanides (Tb–Lu) with the **69** macrocycle are readily hydrolysed to complexes of an open-cycle diketone. The flexibility of the $-CH_2-CH_2-$ diimine side chains of the **38** macrocycle must also represent a favourable factor in the stabilization of its lanthanide complexes, as the derivatives of the **34a** macrocycle are both more difficult to synthesize and less inert to metal release or rearrangement.

When 2,6-diacetylpyridine and facultative polyamines containing additional donor atoms in the R chain are reacted in the presence of lanthanide(III) ions, [1 + 1] macrocycles are obtained [12,122].

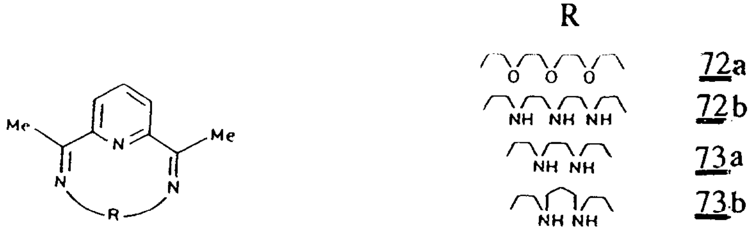

$[La(m/c)](NO_3)_3 \cdot nH_2O$ have been recovered for m/c ≡ **72a** and **72b**; with macrocycles m/c ≡ **73a** and **73b**, $[La(m/c)](NO_3)_2OH \cdot nH_2O$ are obtained [121,122].

When $La(SCN)_3$ is used as the template, mixed OH–SCN complexes are obtained throughout, $La(m/c)(SCN)(OH)_2$ (m/c ≡ **73a**, **73b**) and $La(m/c)(SCN)_2(OH)$ (m/c = **72a**, **72b**). The presence of the macrocycle is supported by IR and ^1H NMR studies, and, for La(**72a**)$(NO_3)_3$, an X-ray structure is available to confirm the assignment. The lanthanum is centred in the macrocyclic ring, 12 coordinated by the six heteroatoms and the three bidentate nitrate anions, one on one side of the macrocycle and two on the other side [131] (Fig. 55). There appears to be consistency in the 12 coordination of lanthanum in the presence of 18-membered rings bearing 6 donor atoms, and three potentially bidentate anions. In [Ln(**72a**)]$(NO_3)_3$, the macrocycle is quite bent, folding away from the hemisphere containing the two nitrate anions and towards that containing the lone nitrate.

The lanthanide complexes are considerably less stable in water than the analogous complexes of the hexaimine; they are more similar in behaviour to the complexes of **70** and of cyclic polyethers. Metal hydroxide is readily precipitated on dissolution in H_2O; it is probable that this is begun by initial breaking of the three adjacent ether–lanthanum bonds. The ^1H NMR of the complexes [La(**72a**)]$(NO_3)_3$ recovered in acetonitrile solution indicates the integrity of the macrocycle in that medium [122].

Lanthanide(III) and uranyl(VI) complexes with the functionalized macrocyclic and macroacyclic ligands of Scheme 25 have been obtained by reaction of the

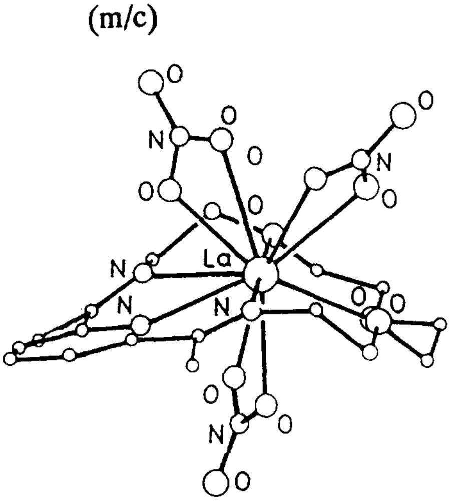

Fig. 55. Structure of [La(**72a**)]$(NO_3)_3$.

preformed ligands with the appropriate metal ion or by template procedure [106,107,132].

The Schiff bases behave as neutral pentadentate ligands in the lanthanide complexes and as pentadentate dinegative ligands in the dioxouranium(VI) analogues.

These functionalized ligands, owing to their solubility and that of related f-containing complexes in organic solvents, can be used for separation of f ions. The solubility of the mononuclear complexes depends on the substituent Z and follows the order $-Cl < -CH_3 < -C(CH_3)_3$.

Macrocyclic ligands H_2-**48** and H_2-**49** offer the advantage of a single-step preparation and, owing to their cyclic nature, selectivity towards lanthanides. They are good extractants for some trivalent lanthanides (Dy–La) from a nitrate medium.

Competitive extractions were carried out to verify whether selectivity could be achieved from aqueous solution containing equimolecular amounts of two lanthanide nitrate or chloride salts: Dy–La, Dy–Eu, La–Eu. These extraction experiments have been carried out with the two ligands H-**48** and H_2-**49** and several aqueous phases which differ from one another in the nature of the counteranion (Cl^- or NO_3^-) and in the presence (or not) of an excess of a monovalent cation such as Li^+ or NH_4^+ (ionic radii: Li^+, 0.68 Å; NH_4^+, 1.43 Å; $r(Li^+) < r(Ln^{3+})$; $r(NH_4^+) > r(Ln^{3+})$.

Loading the aqueous phase with an "inert" salt is an approach to decrease the macrocycle tendency to distribute into the aqueous phase; however, the excess of anion may stimulate the recovery of trace lanthanides from a solution loaded with other metals. The difficulty is to find a sufficiently "inert" cation because, at the concentration sufficient to produce the desired salting effect, the cation may compete with the macrocycle and lanthanide distribution will be lowered.

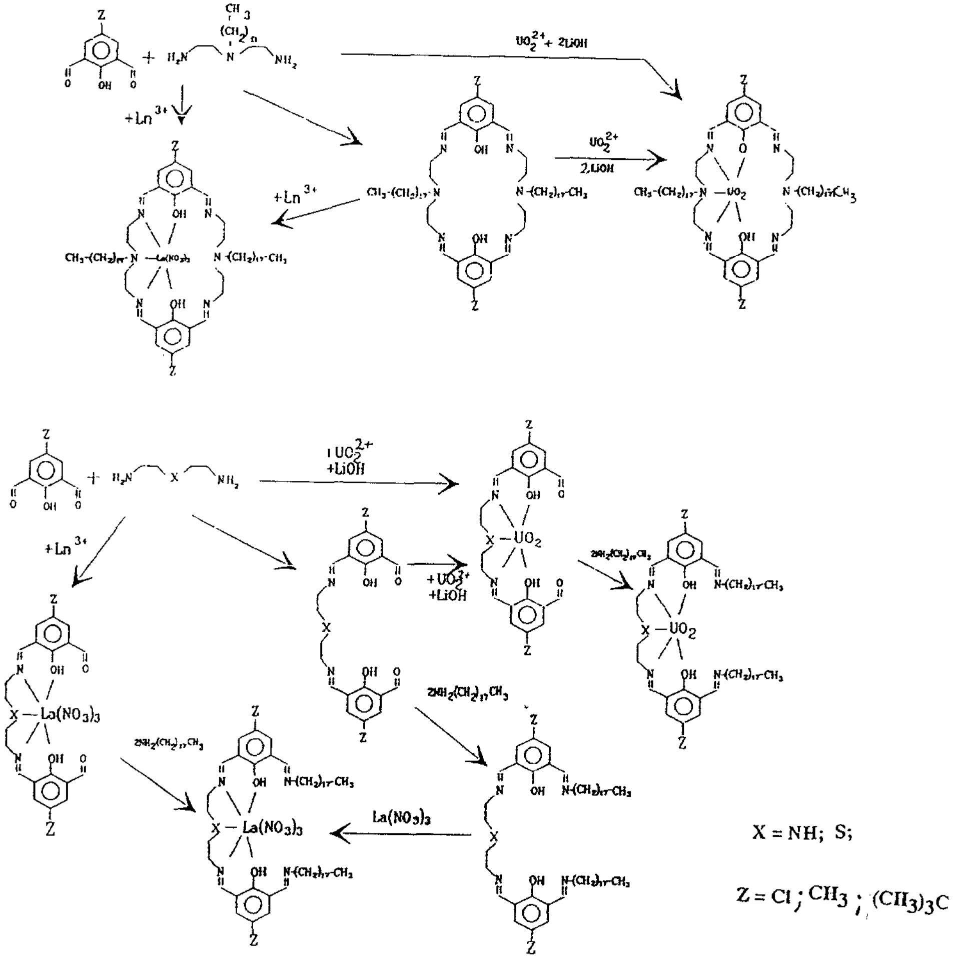

Scheme 25.

For Dy–La mixtures, the best results have been obtained in nitrate medium and in the presence of an excess of ammonium nitrate (which might act as a salting-out agent, decreasing the water activity and facilitating the breaking of the bond between the central metal ion and the coordinated water molecule); moreover, this proves that the ammonium ion is not extracted with the ligand. For example, *D*(Dy) increases from 8.6 to 24 and *D*(La) from 0.24 to 0.55 (contact time, 30 min) with an excess of NH_4NO_3 in the feed (*D* is the distribution coefficient defined as $[M_{org}]/[M_{aqu}]$). The presence of Li^+ decreases both Dy and La extraction owing to a probable competitive extraction of Li^+ with H_2-**48** and H_2-**49.** Under the same experimental conditions (excess of NH_4^+), Dy and La were extracted to a lower extent from chloride medium.

The selectivity of the macrocycles for Dy and Eu over La is very high and, from mixtures of these ions, it is possible to extract preferentially either Dy or Eu over La. The evaluated separation factors are as follows: $S(\text{Dy–La}) = 44$ and $S(\text{Eu–La}) = 37$. On the contrary, both extractants exhibit a slight selectivity for Dy over Eu in the same conditions as reported above with a separation factor $S(\text{Dy–Eu})$ of 2. From these competitive extraction experiments, the macrocyclic ligands exhibit the following order of affinity for the rare earth tested: $\text{Dy} > \text{Eu} \gg \text{La}$.

The distribution ratio $D(\text{Ln})$ vs. the corresponding ionic radius shows that, the larger the ionic radius is, the lower the D value will be: $D(\text{Ln}) > 3$ for $r \leqslant 0.95$ Å (in nitrate medium with excess of NH_4^+). Several problems arise from the acid transportation through the membrane. The important advantage found in using these compounds is that the ligands are efficient in the extraction of lanthanides in the trivalent state without addition of a synergic agent as required with the neutral crown ethers [106,107,132].

It was shown that it is also possible to use a mixture containing aliphatic and aromatic hydrocarbons as the organic phase. The results obtained in this case are in line with those obtained with xylene or industrial diluents (Solvesso 150 or Isopar G).

It was found that the condensation of 1,2-diaminoethane with 2,6-diacetyl- or 2,6-diformylpyridine in the presence of uranyl(VI) salts in a 2:2:1 molar ratio yields $[UO_2(\mathbf{38})](X)_2$ and $[UO_2(\mathbf{65})](X)_2$ ($X \equiv NO_3^-, ClO_4^-$) [129,130].

IR, NMR, magnetic circular dichroism and crystal field studies suggest an effective D_{6h} site symmetry for the central metal ion. This facile preparation shows that actinide can function as a very effective templating agent for the synthesis of macrocycles with medium cavity size.

Furthermore, the exceptional inertness of the complexes toward release of UO_2^{2+} ion in solution, even in the presence of acids or strongly competing ligands, suggests that systems of this type may be used advantageously when effective sequestering of the actinide ions is an important requirement [129].

In a new approach to the molecular recognition of metal oxo cations (particularly UO_2^{2+}), a ligand design strategy was introduced that provides at least one hydrogen bond donor for interaction with oxo group(s) as well as conventional electron pair donor ligands for coordination to the metal centre.

The oxo groups are utilized as a means of providing both additional binding strength and selectivity in forming the ion–ligand complex. The dipolar nature of the metal–oxygen bond produces a partial negative charge on the oxo group that can be exploited in the design of specific complexing agents. Supplying a hydrogen bond donor group to interact with an oxo group within a ligand that also provides donor groups for coordination to the metal centre is a means of improving molecular recognition.

The partial negative charge on each of the uranyl(VI) oxygen atoms makes the UO_2^{2+} group a potential hydrogen bond acceptor. Both stability and selectivity of uranyl(VI) chelates can be enhanced when provision is made for oxo group interaction in addition to coordinative interactions to the metal centre. The gain in stability contributed by a hydrogen bond may be small in relation to the metal binding interactions, but the net gain in specificity can be expected to be significant since a positively charged hydrogen bond donor group both contributes to the stability of the uranyl complex and at the same time destabilizes complexes with non-oxo cations through electrostatic repulsion. Thus the overall increase in selectivity is expected to exceed the hydrogen bond energy in a defined structure.

This approach, described as stereognostic coordination chemistry [133], is exemplified in the design of four tripodal ligands: tris[2-(2-carboxyphenoxy)ethylamine (H_3-**74a**), tris[3-(2-carboxyphenoxy)propyl]amine (H_3-**74b**), tris[3-(2-carboxynaphthyl-3-oxy)propyl]amine (H_3-**74c**), and tris[3-(2-carboxy-4-octadecylphenoxy)propyl]amine (H_3-**74d**).

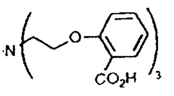

H_3-**74a**

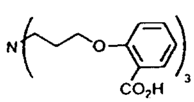

H_3-**74b**

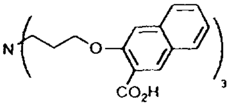

H_3-**74c**

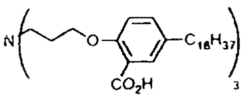

H_3-**74d**

The ligands H_3-**74a**, H_3-**74b** and H_3-**74c** form 1:1 complexes with UO_2^{2+}. The bidentate coordination of carboxyl groups of these compounds is indicated by IR spectra, which offer support for the presence of a hydrogen bond to the uranyl group. The proposed geometry of the resulting uranyl complexes with such ligands is presented schematically in Fig. 56.

It was expected that increasing the ligand cavity size by incorporating an aromatic ring as part of the ligand arm would increase ligand rigidity, thereby offsetting the entropic disadvantage of the long ligand arm.

It was shown that more than five intervening atoms between the tertiary nitrogen atom and the carboxylate groups are required for metal ion

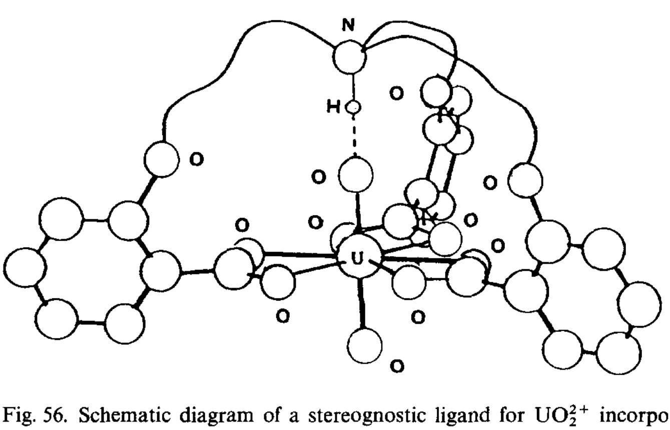

Fig. 56. Schematic diagram of a stereognostic ligand for UO_2^{2+} incorporating three donor carboxylate groups and an ammonium hydrogen bond donor.

incorporation and monomeric complex formation. Solvent extractions of aqueous UO_2^{2+} into chloroform solutions of the ligands have shown them to be powerful extactants. In the case of the very hydrophobic ligand H_3-**74d**, the stoichiometry of the complexation reaction is shown to be a 1:1 UO_2–ligand complex formed by the release of 3 protons. The extraction is quantitative at pH 2.5, and an effective extraction coefficient of about 10^{11} is estimated for neutral aqueous solutions of UO_2^{2+} [133].

In recent years, considerable effort has been devoted to uranyl-binding pyrrole-containing complexes, and the three systems reported in Scheme 26(a) have been proposed: superphthalocyanine (1), pentaphyrin (2) and sapphyrin (3). In each of these ligands, the uranyl(VI) ion is chelated in a saddle-shaped pentagonal planar arrangement and, in the case of sapphyrin, uranyl chelation also induced a chemical modification of the ligand framework.

More recently, a pyrrole-containing "phorphyrin-like" system, incorporating a hexagonal planar Schiff base and related uranyl(VI) complex (4), has been prepared (Fig. 57(a)) [134].

The macrocyclic uranyl(VI) complex has been obtained by the metal template condensation of 3,4-diethylpyrrole-2,5-dicarbaldehyde and 4,5-diamino-1,2-dimethoxybenzene in the presence of uranyl(VI) nitrate or by the preformed ligand and the same uranyl(VI) salt. The quite simple NMR spectrum of the complex is consistent with the very symmetrical structure obtained by X-ray diffractometry (Fig. 57(b)).

The uranyl cation is coordinated to all six nitrogen atoms in a planar fashion. Although not formally aromatic, the complex is remarkably planar. The structure of this complex is thus very different from the saddle-shaped conformation seen in the uranyl chelates of the formally aromatic "expanded porphyrin" ligands (1) and (2) (Fig. 57(a)). As a result in part of this planarity, the coordination geometry about the uranium atom is hexagonal bipyramidal.

This uranyl complex appears to be quite stable, undergoing no apparent decomposition or demetallation when stirred for several hours in a solution of chloroform and trifluoroacetic acid. In fact, exposure to these conditions leads solely to protonation (not demetallation) as evidenced by the fact that adding triethylamine serves to regenerate quantitatively the starting complex. In addition, heating complex (4) to 300°C fails to effect any apparent decomposition.

Preliminary results on the coordination properties of lanthanide(III) ions are consistent with La(III), Eu(III), and Gd(III) all being effectively chelated by this pyrrole-containing porphyrin-like system [134].

The even more "expanded" porphyrin (5) of Fig. 57(a) has been synthesized by a nitric-acid-catalyzed [2 + 2] condensation between 4,4′-diethyl-5,5′-diformyl-3,3′-dimethyl-2,2′-bipyrrole and 1,2-diamino-4,5-dimethoxybenzene, followed by dissolution of the crude product in CH_2Cl_2 containing a few drops of triethylamine [134]. This macrocycle binds methanol in solution and in the solid state and provides an

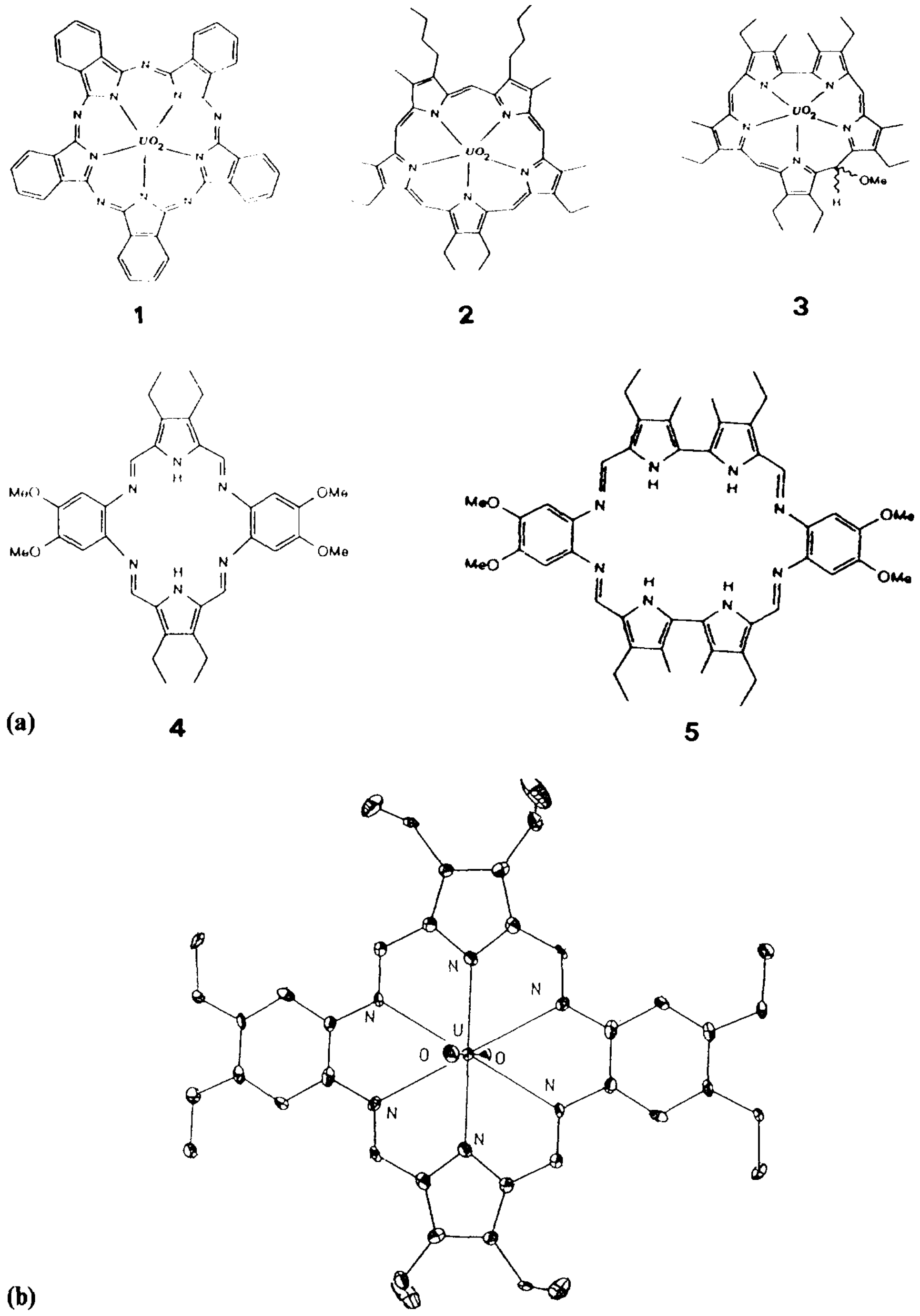

Fig. 57. (a) A series of "porphyrin-like" systems and (b) a view of the uranyl(VI) complex (4).

excellent example of neutral substrate complexation with an expanded porphyrin, as confirmed by an X-ray diffraction analysis [134] which reveals a 2:1 complex with methanol. The methanol molecules lie above and below the macrocycle. The bipyrrole hydrogen atoms are hydrogen bonded to the methanol oxygen atoms. The methanol hydrogen atom is also involved in a bifurcated hydrogen bond with the imine nitrogen atoms [134].

5. DINUCLEAR COMPLEXES

In recent years, binucleating macrocyclic and/or macroacyclic compounds have been extensively studied since these structural units are thought to be involved in a variety of biochemical and industrial processes. The preparation of complexes which contain two transition metal ions separated by distances of 3.5–6 Å is of considerable interest; at these distances no direct interaction between the metal ions is expected, yet a substrate could interact simultaneously with both ions.

Studies on the activation of small molecules (especially oxygen) have received considerable impetus through the use of bimetallic complexes as activators. The simultaneous presence of two metal ions at a suitable distance from each other is a prerequisite for the formation of an activation space necessary for the coordination of oxygen and/or organic substrates and for their subsequent oxidation. It was found that pairs of clusters of metal ions are sometimes capable of mediating certain chemical reactions either better than or in a different way from isolated centres [11].

Macrocyclic and macroacyclic ligands have also been used for the generation of compounds with specific spectroscopic and magnetic properties. It was found that complexes containing magnetic metal centres exhibit magnetic properties which are not simply the sum of those of the individual ions surrounded by their nearest-neighbour ligands. These properties result from both the nature and the magnitude of the interactions between the metal ions within the molecular unit. Using compartmental ligands, binuclear complexes can be synthesized where the two metal centres, if paramagnetic, can interact with each other through the endogenous and/or the exogenous bridges in a ferromagnetic or antiferromagnetic way. By changing the type of ligand, the distance between the two chambers and/or the paramagnetic centres, it is possible to vary considerably the magnetic interaction, and particular complexes are good models for the fabrication of a molecular ferromagnet.

Thus the organization provided by an appropriately designed binucleating ligand may confer unusual structural features and/or magnetic, optical, catalytic properties.

The large variety of complexes obtained by binucleating ligands has been recently divided into two groups: (i) complexes with metals sharing at least one donor atom of ligands containing adjacent sites in which the central donor atom provides a bridge; ligands providing these complexes have collectively been termed

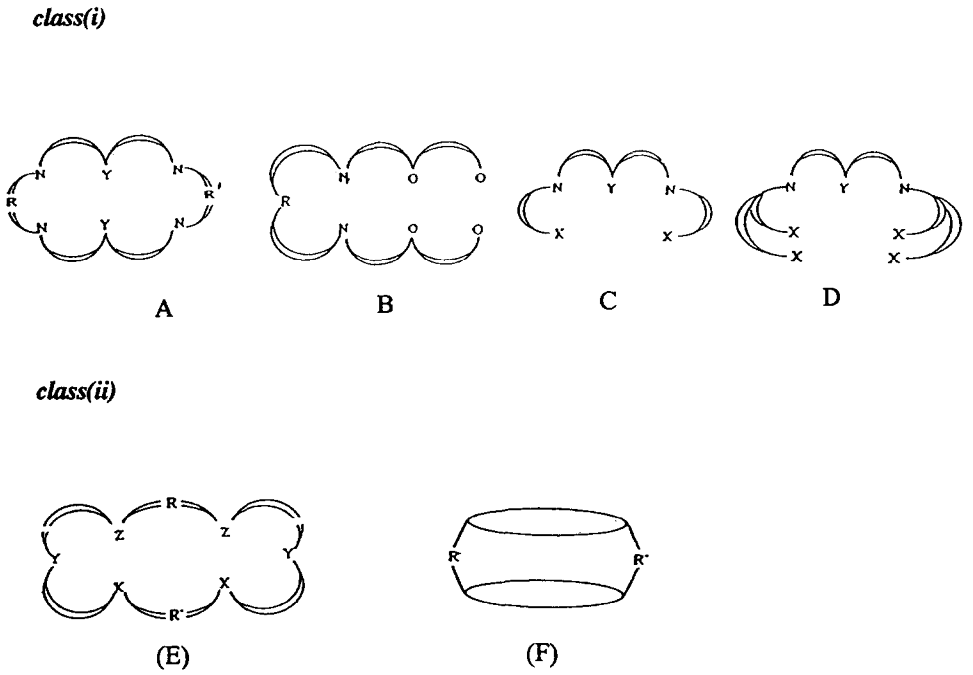

Scheme 26.

compartmental ligands; (ii) complexes in which the donor atoms are not shared; these complexes thus derive from ligands having isolated donor sets [10].

Ligands suitable to give the most appropriate structural arrangement of the metal ions for obtaining the above-mentioned properties are reported in Scheme 26.

Type A are macrocycles derived from [2 + 2] condensation polyamines, type B are side-off acyclic ligands in which a [1 + 2] condensation occurs, type C are end-off acyclic ligands in which a [2 + 1] condensation occurs (in the related metal complexes, Y provides an endogeneous bridge; a further exogeneous bridge may be provided by a mono- or bidentate anion), type D are polypodal ligands. The chains R and R′ can contain additional donor atoms (NH, S, O, PPh etc.) producing a multiplicity of different compartments. Compounds E and F contain remote chambers; in E the compartments are connected by aliphatic or aromatic chains while in F the two macrocycles are constrained in a stack configuration.

The dicopper complex $[Cu_2(\mathbf{75})(H_2O)_2](BF_4)_2$ (Fig. 58(a)) (H_2-**75** is the macrocycle derived by condensation of ethylenediamine and 2,6-diacetyl-4-methylphenol) is an example of a macrocyclic [2 + 2] compound [131]. The entire binuclear cation, apart from the apical water molecule, is roughly planar; the copper atoms are five coordinated in a square pyramidal configuration.

Another example is represented by the zinc-templated cyclocondensation of 1,3-propanediamine and 2,6-diformyl-4-methyl phenol which leads to the synthesis

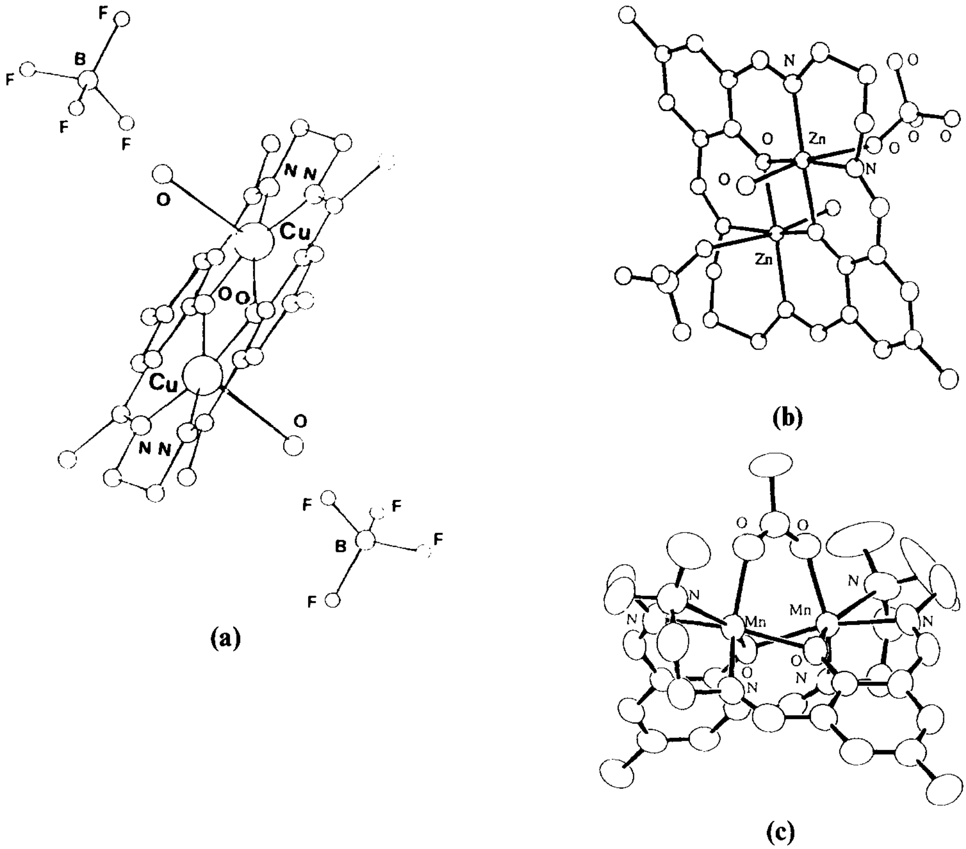

Fig. 58. Structures of (a) $[Cu_2(\mathbf{75})(H_2O)_2](BF_4)_2$, (b) $[Zn_2(\mathbf{75'})(H_2O)_2(ClO_4)_2]$ and (c) $[Mn_2(\mathbf{75''})(CH_3COO)]^+$.

of dinuclear zinc complexes of the corresponding $[Zn_2(\mathbf{75'})(H_2O)_2(ClO_4)_2]$ Robson tetramine Schiff base macrocycle [131]. The X-ray crystal structure of the perchlorate complex revealed the presence of two independent molecules. One molecule has present two six-coordinate zinc atoms separated by 3.17 Å; the coordination geometry is derived from four macrocyclic ligand donors, a water molecule and a monodentate perchlorate anion. The zinc atoms in the second molecule have only a weak interaction with the anion and so each metal is five coordinate, interacting with four macrocyclic ligand donors and a water molecule. The coordination geometry at each metal may be regarded as distorted octahedral in one molecule and distorted square pyramidal in the other molecule. The phenolate oxygen atoms act as bridging ligands in each molecule (Fig. 58(b)) [131].

The macrocyclic size has been enlarged and/or the denticity increased to incorporate identical or different d and/or f metal ions. Using ligands such as H_2-**75**″,

$[M_2(\mathbf{75}'')]^{n+}$, $[UO_2M(\mathbf{75}'')]^{n+}$, or $[MM'(\mathbf{75}'')]^{n+}$ complexes have been prepared and their properties studied [131].

Recently the manganese(II) complexes $[Mn_2(\mathbf{75}'')(RCOO)](ClO_4)$ have been synthesized and the X-ray structure of $[Mn_2(\mathbf{75}'')(CH_3COO)](ClO_4)$ has been solved [131].

The macrocyclic Schiff base acts as an octadentate N_6O_2 ligand and an acetate anion bridge the two manganese(II) ions, which are coordinated also by two bridging phenolic oxygen atoms and three nitrogen atoms. The whole coordination geometry around each manganese ion is roughly octahedral but severely deformed [131].

Electrochemical measurements of these complexes revealed that both the substituents of the phenol ring and those on the ligating acetate effectively control the redox properties of the manganese(II) centre [131]. Such fine tuning of redox properties may be useful to construct functional modes of Mn-containing redox enzymes.

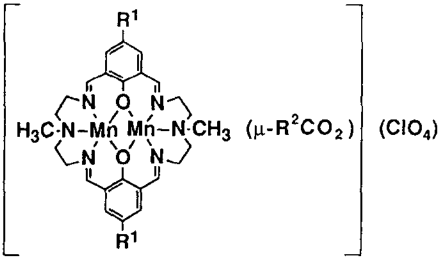

R^1	R^2
CH_3,	CH_3
OCH_3	$ClCH_2$
H,	Cl_2CH
F,	Cl_3C
Br	F_3C

$[Mn_2(\mathbf{75}'')(RCOO)](ClO_4)$

The macrocycles derived by the [2 + 2] condensation of 2,6-diformyl-4-methylphenol and a diamine have been synthesized by either direct template reaction [135] or stepwise template reaction [136–138].

Stepwise template reaction was found very useful for the synthesis of [2 + 2] macrocycles of dissimilar lateral chains [136,138]; it helps also in the preparation of heterodinuclear and heteropolynuclear complexes [136–138].

[2 + 2] macrocyclic $[CuPb(\mathbf{76})]^{2+}$ complexes, where the macrocycle contains ethylenediamine and 1,5-diamino-3-azapentane as the amine precursor, have been prepared by condensation of the copper(II) diformylethylenediimine acyclic complex with 1,5-diamino-3-azapentane.

The macrocycle has been isolated as Cu(II)Pb(II) complexes differing in the counteranion and solvation. X-ray structure analysis for a complex $[CuPb(\mathbf{76})(CH_3COO)](BPh_4)\cdot CH_3CN$ shows that the Cu is at the four coordination site and adopts a nearly planar geometry. The Pb assumes a six-coordinate surrounding with two phenolic oxygen atoms, three nitrogen atoms, and an acetate oxygen atom. The acetonitrile is free from coordination (Fig. 59).

The Pb(II) ion is readily replaced by a divalent transition metal ion to afford

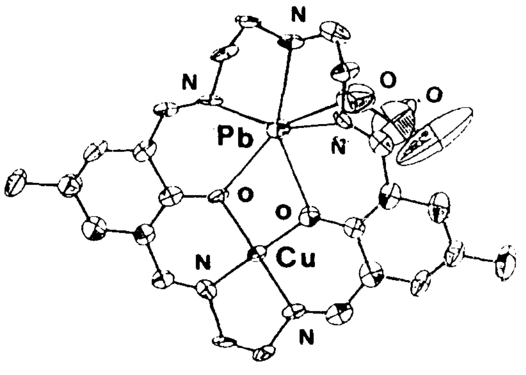

Fig. 59. Structure of $[CuPb(76)(CH_3COO)][BPh_4] \cdot CH_3CN$.

Cu(II)M(II) complexes (M ≡ Mn, Co, Zn). An antiferromagnetic spin coupling operates within a molecule for M ≡ Mn or Co. Electrochemical studies of the complexes show that complexes containing Cu(I)M(II) and Cu(III)M(II) can be obtained.

Dinuclear copper(II) complexes with half-saturated and fully saturated compartmental macrocycles have been prepared through the reaction procedure of Scheme 27 [139,140] with the aim to obtain more flexible systems.

Analogously to the related Schiff bases systems, these reduced ligands can give rise to a large variety of mononuclear, homo- or heterodinuclear complexes.

The addition of 1 equivalent of H_2-77 to an ethanol solution of $[VO(OEt)_3]$ yields an orange–yellow compound of composition $[VO(77)] \cdot H_2O$. The formation of a vanadyl(IV) complex from a vanadium(V) precursor indicates that the ligand anion stabilizes the neutral [VO(77)] species [139].

The reaction between H_2-77 and vanadyl sulphate (1:1) in methanol affords $[VO(H_2\text{-}77)(SO_4)] \cdot 3H_2O$ [139]. When 1 equivalent of H_2-77 is treated with 2 equivalents of vanadyl sulphate in the presence of 2 equivalents of triethylamine the homodinuclear complex $[(VO)_2(77)(\mu\text{-}SO_4)] \cdot MeOH \cdot 3H_2O$ is obtained together with $[VO(H_2\text{-}77)(SO_4)] \cdot 3H_2O$ [139].

The heterodinuclear complex $[VOZn(77)(SO_4)] \cdot 4H_2O$ was obtained by treating $[VO(H_2\text{-}77)(SO_4)] \cdot 3H_2O$ with zinc perchlorate and triethylamine [139].

The electron spin resonance (ESR) and IR spectra of $[VO(77)] \cdot H_2O$ have indicated stacking of the molecules owing to $\cdots V{=}O \cdots V{=}O \cdots$ interactions. In complexes $[VO(H_2\text{-}77)(SO_4)] \cdot 3H_2O$ and $[VOZn(77)(SO_4)] \cdot 4H_2O$ the unidentate sulphate is bound to the octahedral vanadium and two of the secondary amino groups in $[VO(H_2\text{-}77)(SO_4)] \cdot 3H_2O$ are protonated. Both of these complexes undergo oxidation to produce oxovanadium(V) species with $E_{1/2} = 0.40$ V for $[VO(H_2\text{-}77)(SO_4)] \cdot 3H_2O$ and 0.455 V for $[VOZn(77)(SO_4)] \cdot 4H_2O$ vs. saturated calomel electrode (SCE). Fairly strong antiferromagnetic exchange interaction ($J = -128\ cm^{-1}$) has been found in $[(VO)_2 77)(\mu\text{-}SO_4)] \cdot MeOH \cdot 3H_2O$. The crystal

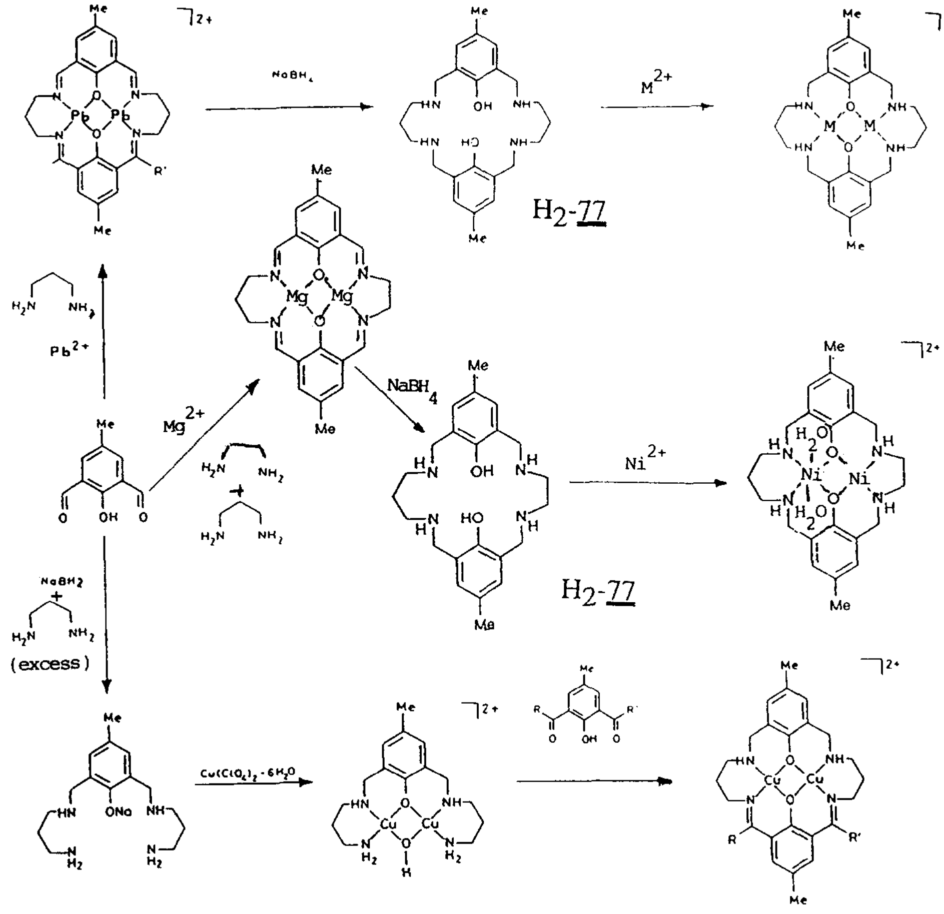

Scheme 27.

structure of $[(VO)_2(77)(\mu\text{-}SO_4)]\cdot MeOH\cdot 3H_2O$ shows that the two octahedral vanadium centres in the complex, separated by 3.077 Å, are bridged by sulphate and have a *syn* oxo configuration (Fig. 60(a)) [139].

The crystal structure of $[Cu_2(77)(ClO_4)_2]$ (Fig. 60(b)) consists of two copper(II) centres bridged by two phenoxide oxygen atoms with two secondary amine nitrogen donors completing the distorted CuN_2O_2 plane. Relatively short Cu–O and Cu–N separations exist in the CuN_2O_2 planes, while long perturbations involving bidentate bridging perchlorate best describe the copper coordination spheres as severely distorted, axially elongated, octahedra. The equatorial CuN_2O_2 chromophore is twisted and the copper centre lies in the mean plane of the N_2O_2 donor set, separated by 2.993 Å [139,140].

The structure of the related system $[Cu_2(77)(CH_3OH)_2](ClO_4)_2$, prepared in dry methanol [139,140], consists of two square pyramidal copper(II) centres bridged

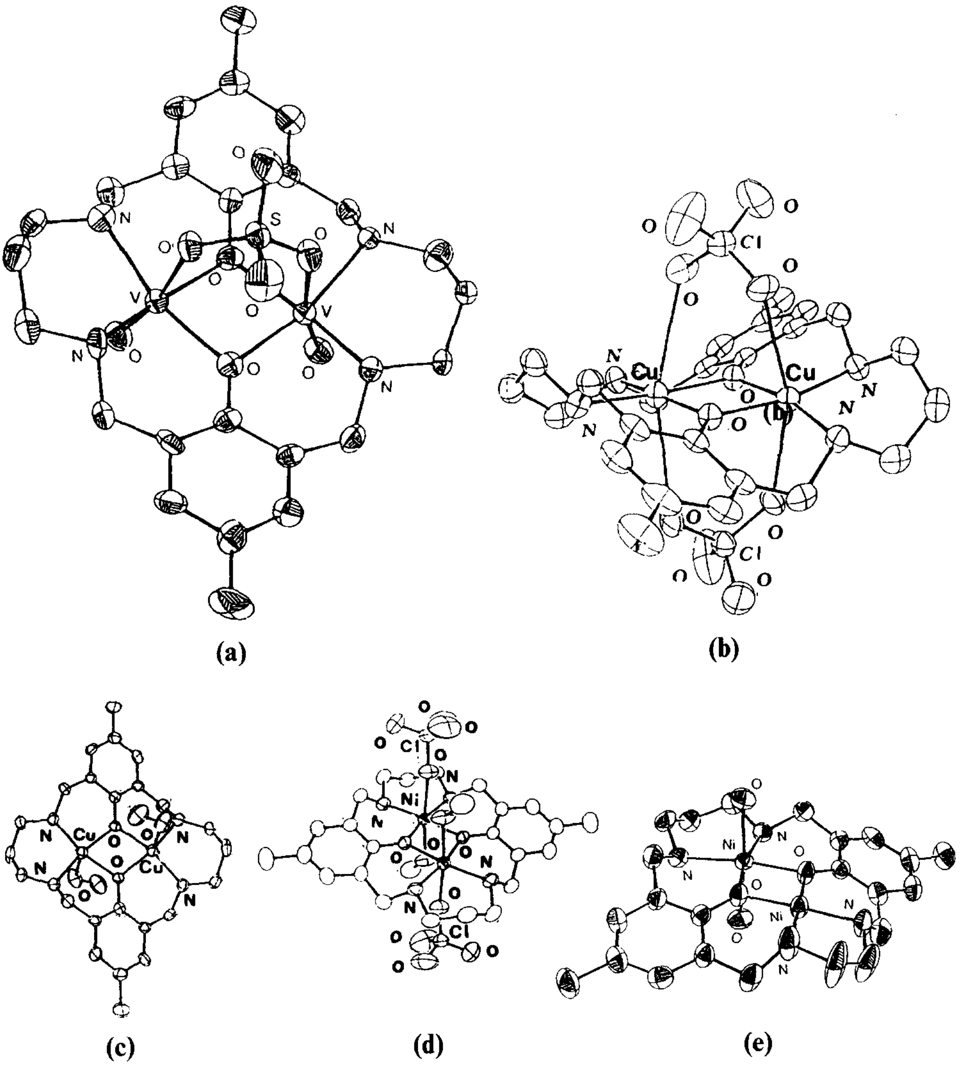

Fig. 60. Structures of (a) $[(VO)_2(77)(\mu\text{-}SO_4)]$, (b) $[Cu_2(77)(ClO_4)_2]$, (c) $[Cu_2(77)(CH_3OH)_2](ClO_4)_2$, (d) $[Ni(77)(CH_3OH)_2(ClO_4)_2]$ and (e) $[Ni_2(77')(H_2O)_2]^{2+}$.

by two phenoxide oxygen atoms with two secondary amine nitrogen donors completing the distorted CuN_2O_2 plane. The copper centre is displaced from the mean plane of the N_2O_2 atoms toward the coordinated methanol and the two copper centres are separated by 3.088 Å. The methanol molecules are bound in a trans fashion, above and below the dinuclear centre, and the methanol–copper interaction is relatively weak (Fig. 60(c)) [139,140].

The structure of $[Cu_2(77)(CH_3OH)](ClO_4)_2$ is very similar to that of the complex $[Cu_2(77)Cl_2]\cdot 6H_2O$, which involves a trans arrangement of two axially bound chlorine atoms about a binuclear centre. Similar distortions were observed in the CuN_2O_2 planes [139,140].

A noticeable feature of these dicopper(II) compounds is that they undergo four one-electron transfers to generate dicopper species with oxidation states varying between 1+ and 3+.

$[Ni(77)(CH_3OH)_2(ClO_4)_2]$ consists of two Ni(II) centres bridged by two phenoxide oxygen atoms with two secondary amine nitrogen donors completing the NiN_2O_2 plane. Each of the metal centres obtains pseudo-octahedral environments by interacting with trans axially disposed methanol molecules and perchlorate ions. The deviation of the metal centres from the mean plane of the N_2O_2 donor sets does not exceed 0.029 Å. The complex molecule contains a centre of symmetry thereby marking the two metal ions chemically and crystallographically equivalent in the solid state. The two metal centres are separated by 3.135 Å [140] (Fig. 60(d)).

In $[Ni_2(77)(py)]_2(ClO_4)_2$, the two nickel(II) centres are in a square pyramidal configuration with N_2O_2 in planar donor sets, involving two phenoxide bridges and two trans axially disposed pyridines. The distance between the two nickel centres is 3.206 Å [140].

The asymmetric macrocycle H_2-**77′** was synthesized by the sequential addition of 1 equivalent each of 1,2-diaminoethane and 1,3-diaminopropane to a boiling methanol solution containing $Mg(NO_3)_2 \cdot 6H_2O$, $Mg(CH_3CO_2)_2 \cdot 4H_2O$ and 2-hydroxy-5-methylbenzene-1,3-dicarbaldehyde (1:1:2) over a period of several hours. After reduction of the dimagnesium Schiff base macrocyclic complex thus formed with $NaBH_4$, the metal-free H_2-**77′** was separated by sequestering magnesium with disodium ethylenediaminetetraacetate. It is important to note that if the order of addition of the diamines is reversed, instead of H_2-**77′**, solely H_2-**77** is obtained [140].

Although treatment of $Ni(ClO_4)_2 \cdot 6H_2O$ with triethylamine gave a deep red solution of $[Ni(77)(H_2O)_2]^{2+}$, the perchlorate salt was not amenable to crystallization. Several counteranions were tried but only the iodide salt turned out to afford single crystals [140].

$[Ni(77)(H_2O)_2](I)_2$ is a mixed spin state complex in which one nickel(II) is square planar in the smaller N_2O_2 chamber and the other nickel(II) is octahedral in the larger N_2O_2 chamber (Fig. 6(e)). On the reaction with pyridine, $[Ni(77)(H_2O)_2](I)_2$ produces the square planar–square pyramidal $[Ni_2(77)(py)](I)_2$ [140].

For $[Ni(77)(CH_3OH)_2(ClO_4)_2]$ in dimethylsulphoxide with a glassy carbon electrode, the two one-electron reduction steps ($E_{1/2} = -1.32, -1.65$ V (SCE)) occur quasi-reversibly. The $Ni^{II}Ni^{I}$ species were not stable on the coulometric time scale. The cyclic voltammogram of $[Ni(77)(CH_3OH)_2(ClO_4)_2]$ in MeCN with a Pt electrode at positive potential range (Fig. 4) exhibits two reversible one-electron oxidation steps ($E_{1/2} = 0.94, 1.08$ V (SCE)). The occurrence of these two waves at the indicated potentials was also observed in differential-pulse voltammetric measurements. Controlled-potential electrolysis at 1.3 V consumed 2 equivalents of charge implicating the two-electron oxidation $[Ni(\mathbf{77})(CH_3OH)_2(ClO_4)_2]$ to a dinickel(III) species. The ligand itself and $[Zn_2(\mathbf{77})(H_2O)_2](ClO_4)_2$ do not exhibit any electrochemical response in the entire potential range from -2.0 to $+1.7$ V. The stability of the mixed-valence $Ni^{II}Ni^{I}$ and $Ni^{II}Ni^{III}$ species can be related to their conproportionation constants K_{con}. A greater value of K_{con} indicates greater stability of the mixed-valence species with respect to the isovalent species. Although $K_{con} = 3.8 \times 10^5$ for the reduction process implies considerable stability of the $Ni^{II}Ni^{I}$ species, a much lower value of K_{con} (2.3×10^2) for the oxidation process suggests easier access to the dinickel(III) species [140].

Strong antiferromagnetic interactions occur in these unsaturated and saturated copper(II) complexes.

The reaction of H_2-**77** with $CuCl_2$ forms green–brown crystals of the trinuclear complex $[Cu_2(\mathbf{77})(CuCl_4)]$ [139,140]. Conductance measurements in dmso indicate that this trinuclear compound is a 1 : 1 electrode. The dissociation of this complex is perhaps most likely to occur with the formation of the cation $[Cu_2(\mathbf{77})]^{2+}$ and a solvated chlorocuprate anion.

The non-symmetric ligands (type B) can give rise to mono- or heterobinuclear positional isomers by complexation (see Scheme 28a).

The potentially hexadentate compartmental side-off Schiff bases react with metal acetates to give complexes which show clearly the coordination selectivity patterns available. In the case of the uranyl cation, the metal site of the outer O_2O_2 compartment with a solvent molecule occupies the seventh site of a pentagonal bipyramid. This is confirmed by X-ray structural analysis of $UO_2(H_2\text{-}\mathbf{78})(MeOH)$ (Fig. 61(a)) [141] and of $UO_2(H_2\text{-}\mathbf{79})(dmf)$ (Fig. 61(b)) [142].

The crystal structure of $UO_2(H_2\text{-}\mathbf{78})MeOH$ [141] consists of discrete units which are involved in hydrogen bonding. Surprisingly, the chemical composition of the ligand is not the same in the two molecules of the asymmetric unit (A and B); whereas in A, the ligand has the expected formula with the nitrogen atoms bonded through a $-CH_2-CH_2-$ aliphatic chain, in B there is a $-CH{=}CH-$ chain. The two resulting complexes are consequently similar but chemically different and this explains the presence of eight molecules in a cell which has only four equivalent positions. Apart from this, the main structural features are the same in A and B, with the uranium atoms seven coordinated in a slightly distorted pentagonal bipyramid geometry.

In $UO_2(H_2\text{-}\mathbf{79})(dmf)$ [142], the uranyl(VI) ion occupies the outer O_2O_2 compartment which is inclined by 19° with respect to the inner N_2O_2 site. The five oxygen atoms, equatorially bonded to the O–U–O group, are coplanar as are the four N_2O_2 atoms of the inner site.

Positional isomers of the mononuclear complex of copper(II) with H_4-**79** have been prepared [7,69]. When $CHCl_3$–EtOH was used, the green O_2O_2 isomer was obtained, while in refluxing methanol the light brown N_2O_2 isomer was obtained.

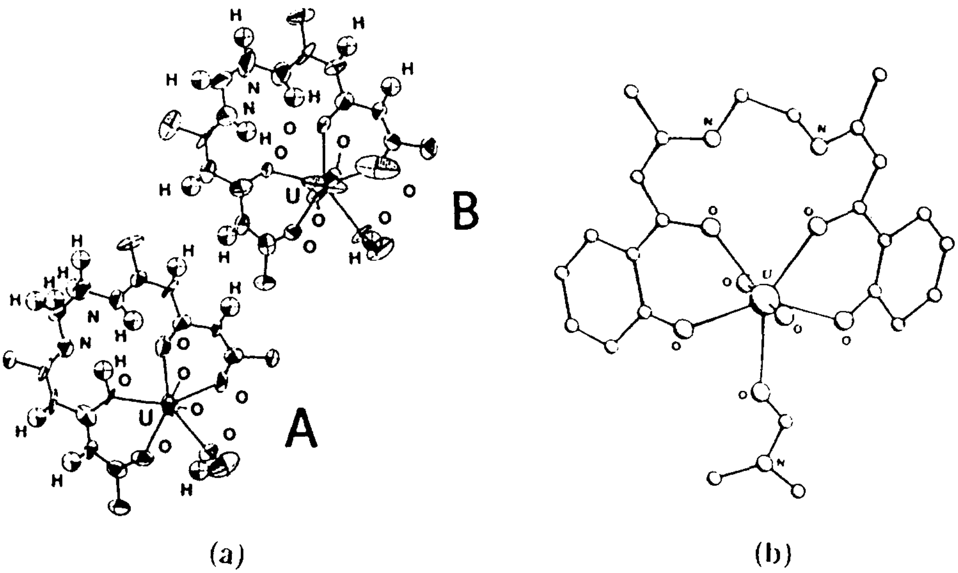

(a) (b)

Fig. 61. Structures of (a) $UO_2(H_2$-**78**)(MeOH) and (b) $UO_2(H_2$-**79**)(dmf).

For Ni(H_2-**79**), the magnetic measurements can easily distinguish between the two positional mononuclear isomers, the nickel(II) being diamagnetic in the N_2O_2 set and paramagnetic in the O_2O_2 set. The complex is diamagnetic, showing that the nickel(II) ion is coordinated to two nitrogen and two oxygen atoms in a square planar configuration as confirmed by an X-ray investigation [7,69].

In a similar way, mononuclear dioxouranium(VI), nickel(II) and copper(II) complexes with the ligand H_4-**80** or H_4-**81** have been prepared.

By using the side-off compartmental ligands, it has been possible to prepare heterobinuclear complexes as the site occupancy of the metal can be guaranteed [143]. Using the pure mononuclear isomers, the second metal ion was easily introduced in the desired chamber (Scheme 28(b)).

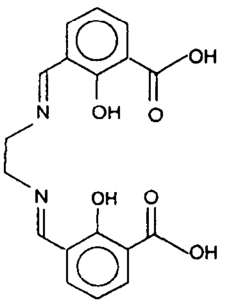

H_4-**80**

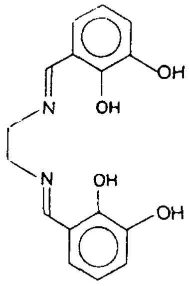

H_4-**81**

For these heterodinuclear complexes, there is the opportunity for positional isomerism to occur; however, the dioxouranium has been found to occupy only the outer donor set (Scheme 28). The X-ray structures of $CuUO_2$(**79**)$(dmso)_2$ (Fig. 62(a)) and $NiUO_2$(**79**)(dmso) (Fig. 62(b)) have been solved [143]. The crystals were obtained from dmso and, for each complex, the dioxouranium(VI) moiety lies in the O_2O_2 set and is further bonded to a molecule of dmso.

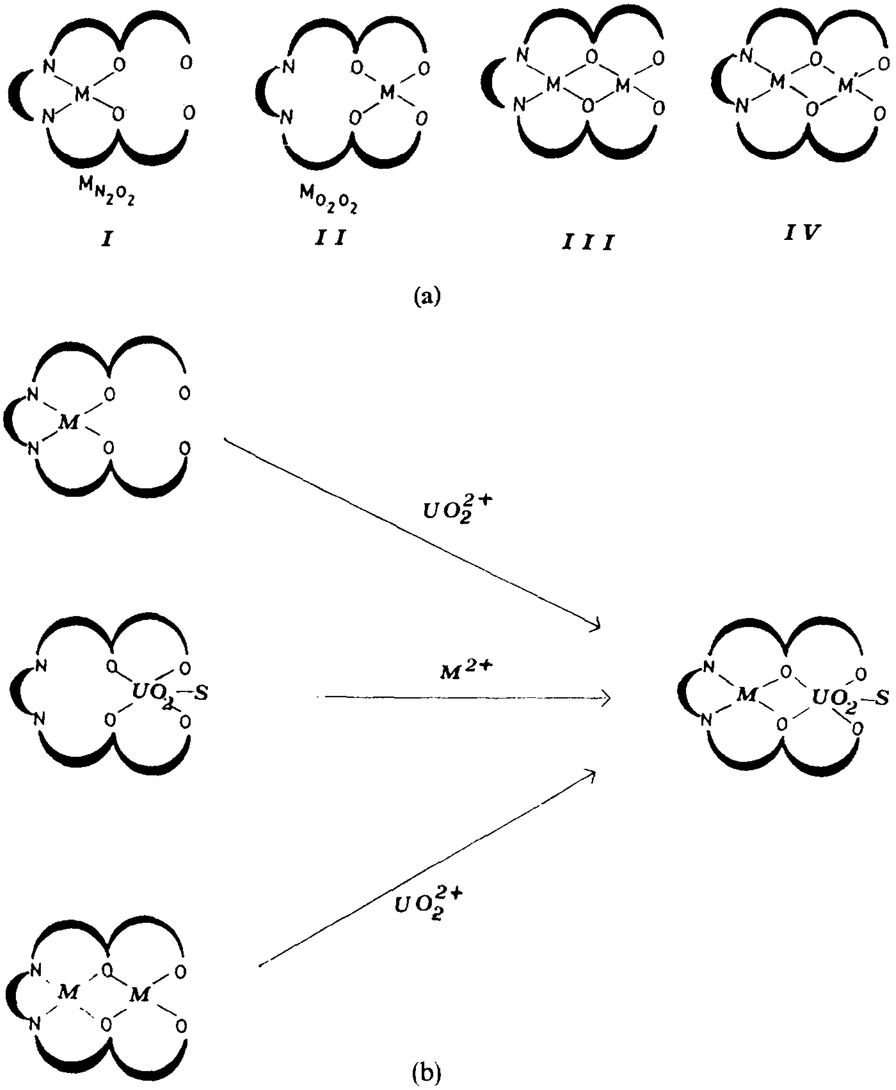

Scheme 28. (a) Schematic representation of mononuclear (I and II) and heterodinuclear (III and IV) positional isomers. (b) The possible pathways for the formation of heterobinuclear complexes containing UO_2^{2+}.

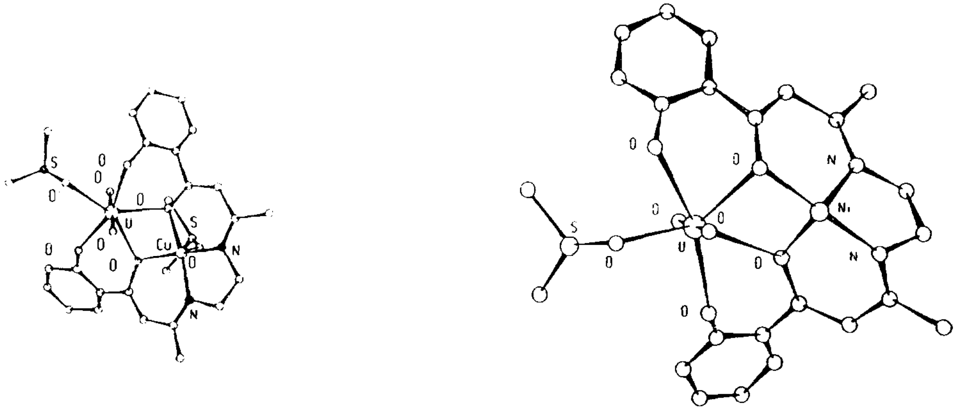

Fig. 62. Structures of (a) $[CuUO_2(\mathbf{79})(dmso)_2]$ and (b) $[NiUO_2(\mathbf{79})(dmso)]$.

In the two complexes, the polyhedron around the uranium atom is a slightly distorted pentagonal bipyramid. The five oxygen atoms equatorially bonded to uranium are not coplanar, but their regularly alternating disposition indicates the presence of a puckered arrangement. The copper(II) and the nickel(II) are retained in the inner N_2O_2 chamber; the copper(II) ion is five coordinated being also bonded to a dmso molecule. The nickel(II) ion is four coordinated but not square planar as expected.

Extension of these principles to the compartmental ligands derived from facultative diamines is shown in Scheme 28(b). As well as using the sequential reaction pathway, it was found that both copper and nickel homodinuclear complexes can undergo a transmetallation reaction with uranyl salts leading to the formation of heterobinuclear products. These heterodinuclear complexes are identical to those prepared by the stepwise procedure.

With the ligand H_4-**82**, $Pd(CH_3COO)_2$ gives positional isomers when $R \equiv C_6H_5$ (the N_2O_2 isomer being in a much greater abundance than the O_2O_2 isomer and only the N_2O_2 isomer when $R \equiv$ *tert*-butyl. The site selectivity of palladium(II) for the N_2O_2 site and of UO_2^{2+} for the O_2O_2 site makes the formation of heterobinuclear complexes with only one positional isomer straightforward.

A range of bimetallic liquid crystals exhibiting the same coordination moiety of H_4-**82** or the closely related β,δ-triketone precursors (Fig. 63) has been prepared [144]. They display columnar structures; the liquid crystalline phases of the compounds II and III of Fig. 63 have a very similar structure which is the result of average correlation with alternating molecules of II being rotated by 90° and alternating molecules of III being rotated by 180°. The antiparallel organization of III results in stacking in the columns with non-equivalent metal centres stacked in an alternating structure. This special organization is under investigation as a method to produce ferrimagnetic materials [144].

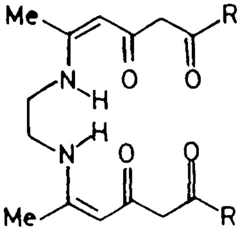

H_4-82

R
-C_6H_5
tert-C_4H_9

The complex $Na_2[Cu_2(\mathbf{83})(OH)] \cdot 11H_2O$ (Fig. 64) (H_4-**83** is the Schiff base obtained by condensation of 2,6-diformyl-4-chlorophenol and (±)1-aminoethane phosphonic acid in the presence of NaOH) is an example of [1 + 2] end-off acyclic complexes (type C). The copper ions are five-coordinated square pyramidal. A

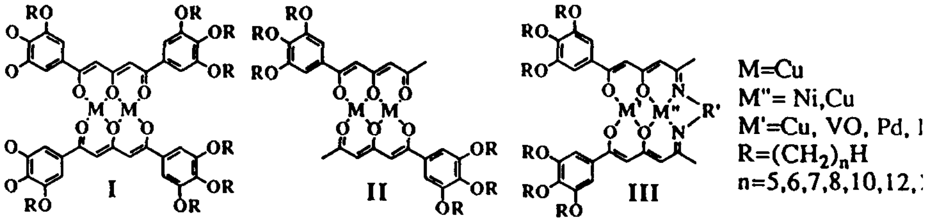

Fig. 63. Structures of bimetallic liquid crystals.

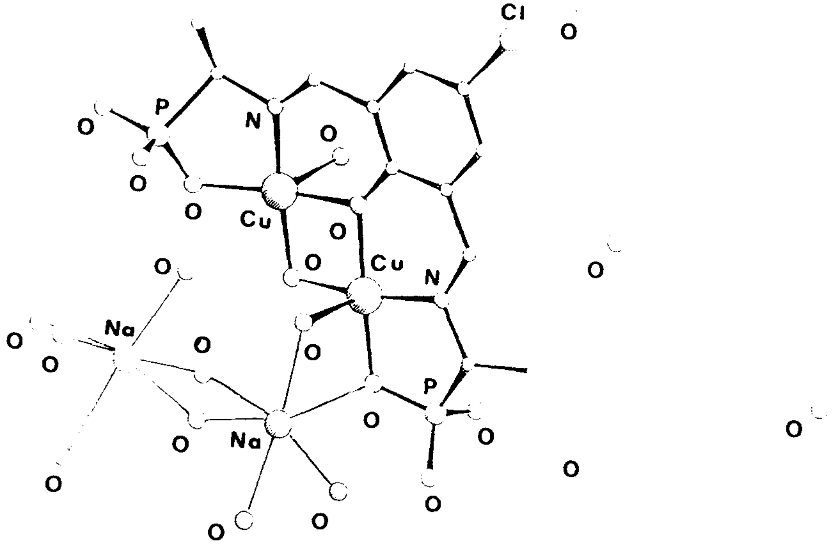

Fig. 64. Structure of $[Na_2Cu_2(\mathbf{83})(OH)] \cdot 11H_2O$.

phenolate oxygen provides the endogenous bridge while an OH^- group provides the exogenous bridge. Two water molecules are in the apical position [145].

The introduction of different pendant arms into the 2 and 6 positions of 4-substituted phenol leads to the formation of dissymmetrical Schiff bases [146]. One approach starts from 4-bromosalicylaldehyde and introduces first a methyleneamine group on the unsubstituted 2 position through the Mannich reaction and then an imine function on the 6 position by reaction of a primary amine with the free carbonyl group [146] (Scheme 29(a)).

The molecular structure of the dinuclear copper(II) cation in $[Cu_2(\mathbf{84a})(\mu\text{-}Br)(\mu\text{-}HCO_2)]_2[Cu_2Br_4]$ (Fig. 65(a)) reveals the constitution of the deprotonated Schiff base ligand with the phenolate group acting as an endogenous bridge. In addition, there are two exogenous bridges: a formate and a bromide. Each copper ion is five coordinated and the donor sets are completed by two nitrogen atoms from the sidearms of the ligand. Although both sidearms are N_2 chelates, the chemical environments they provide are different. The geometry of one copper(II) ion is distorted square pyramidal with the bridging bromide as the apical ligand. The geometry of the second copper(II) ion is significantly distorted from both square-based pyramidal and trigonal bipyramidal. The dinuclear copper(I) anion $[Cu_2Br_4]^{2-}$ is a planar species in which the metal geometry is trigonal planar with two of the bromides acting as asymmetric bridges. The magnetic behaviour of this complex is characteristic of a pair of copper atoms interacting antiferromagnetically ($2J = -42\ cm^{-1}$) (Scheme 29(a)) [146].

A second approach is based on the efficient protection of one of the two aldehyde functions of 2,6-diformyl-4-methylphenol by lanthanide(III) ions, owing to their oxophilic character [146]. Thus asymmetric Schiff bases H-**84b** and H_4-**84c** and related mononuclear gadolinium(III) and dinuclear copper(II) complexes have been prepared according to Scheme 29(b). The structure of $[Gd(H\text{-}\mathbf{84b})_2(H_2O)_4](ClO_4)_3 \cdot 4H_2O$ consists of $[Gd(H\text{-}\mathbf{84b})_2(H_2O)_4]^{3+}$ cations, perchlorate and chlorate anions and non-coordinated water molecules. The Gd atom is surrounded by eight oxygen atoms, four belonging to water molecules and the other four to the carbonyl and phenolic functions of the two **84b** ligands. The coordination sphere of the gadolinium(III) ion is very close to a perfect square antiprism (Fig. 65(b)) [146].

H-**84b** may be obtained also by self-condensation of the formyl and amino precursor in alcohol; the subsequent condensation at the free carbonyl group gives rise to asymmetric acyclic ligands of the type H-**84c**.

The structure of the dicopper(II) complex $[Cu_2(\mathbf{84c})(OH)](ClO_4)_2 \cdot H_2O$ (Fig. 64(c)) shows that both copper atoms are in square pyramidal surroundings. The apical position of one copper atom is occupied by the oxygen atom of a perchlorate group; this copper ion is slightly pulled out from the basal plane in the direction of the perchlorate group. The apical position of the second copper atom is occupied by a water molecule [146].

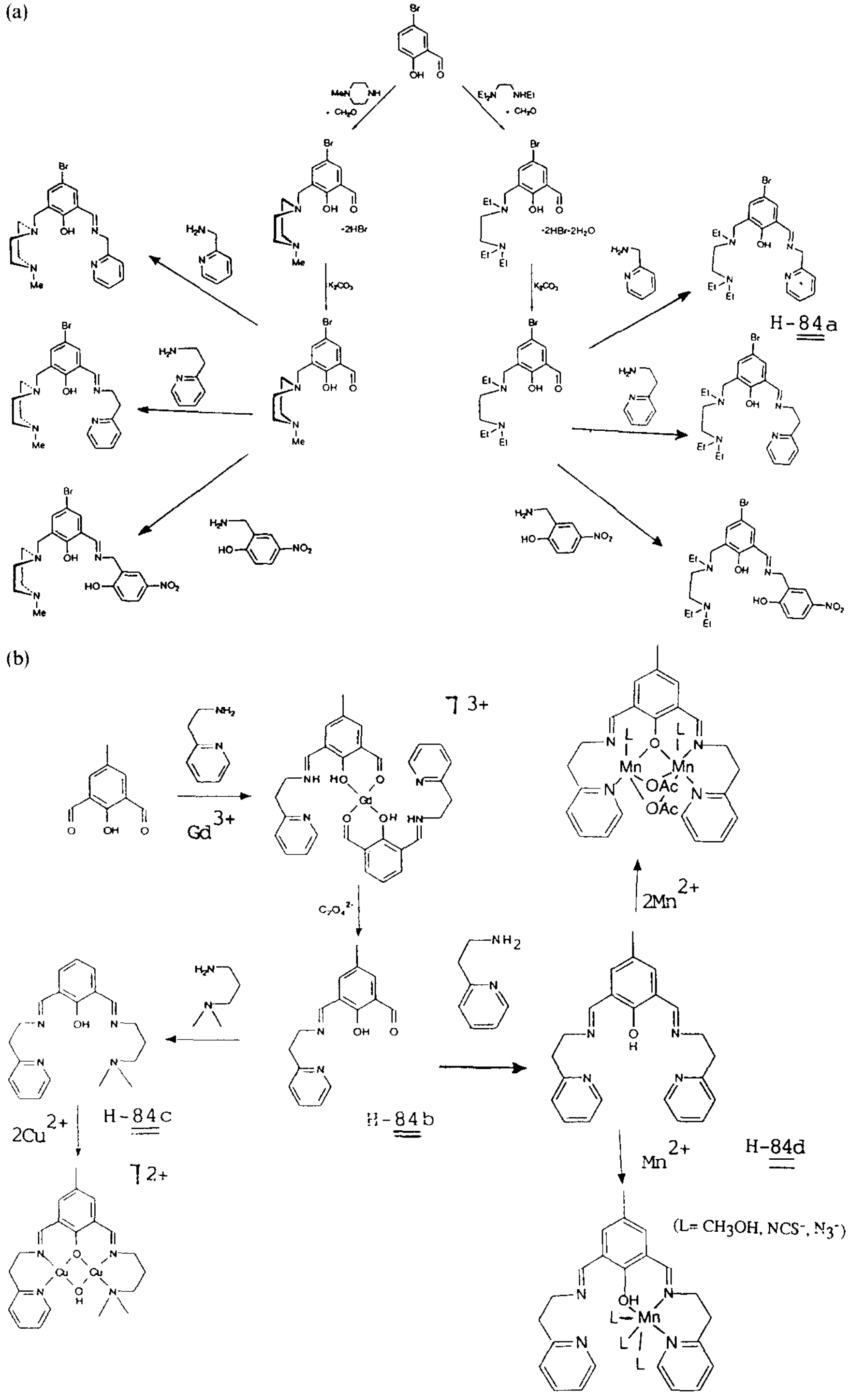
(a)
Br
OH
O
· CH2O
-2HBr
-2HBr·2H2O
K2CO3
H-84a
(b)
Gd3+
3+
Gd
C2O4 2-
2Mn2+
Mn
OAc
L
H-84b
H-84c
H-84d
2Cu2+
2+
Cu
Mn2+
(L= CH3OH, NCS-, N3-)

Scheme 29.

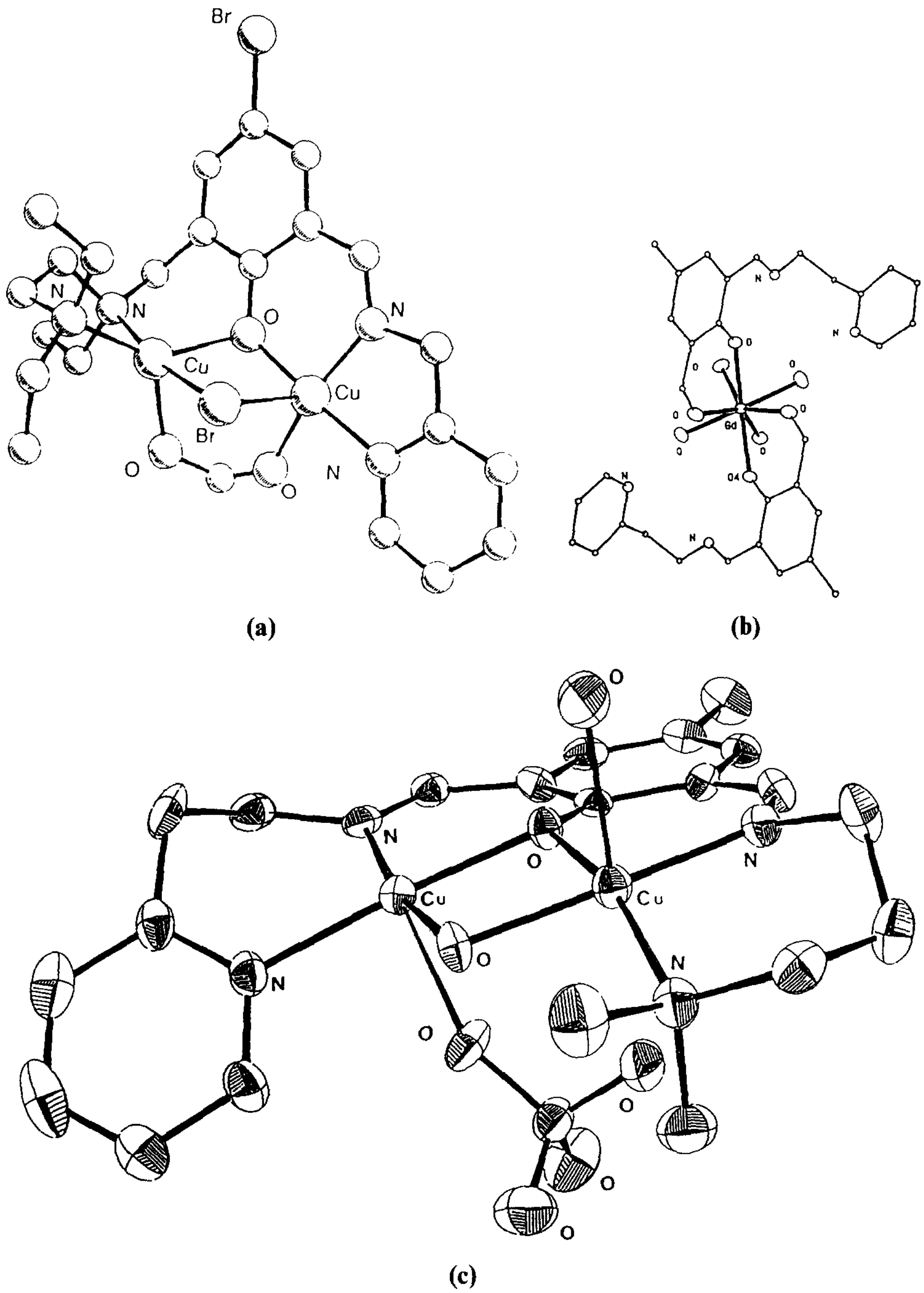

Fig. 65. Structures of (a) $[Cu_2(\mathbf{84a})(\mu\text{-}Br)(\mu\text{-}HCO_2)]^+$, (b) $[Gd(\mathbf{84b})_2(H_2O)_4]^{3+}$ and (c) $[Cu_2(\mathbf{84c})(OH)]^{2+}$.

2,6-bis[*N*-(2-pyridylethyl)iminomethyl]-4-methylphenol H-**84d** can form mononuclear manganese(II) [Mn(H-**84d**)$(NCS)_2(H_2O)$] or manganese(III) [Mn(H-**84d**)$(N_3)_3$] complexes in addition to the homodinuclear manganese(II) [Mn_2(**84d**)$(CH_3COO)_2(CH_3OH)$](ClO_4) and [Mn_2(**84d**)$(CH_3COO)_2(NCS)$] or the homodinuclear manganese(II)–manganese(III) [Mn_2(**84d**)$(CH_3COO)_2(CH_3OH)_2$]$(ClO_4)_2$, [Mn_2(**84d**)$(CH_3COO)_2(NCS)_2$] and [Mn_2(**84d**)$(CH_3COO)_2(N_3)_2$]·$2CH_3OH$ [146].

The dinuclear complexes [Mn_2(**84d**)$(CH_3COO)_2(CH_3OH)$](ClO_4), [Mn_2(**84d**)$(CH_3COO)_2(NCS)_2$] and [Mn_2(**84d**)$(CH_3COO)_2(N_3)_3$]·$2(CH_3OH)$ have a μ-phenoxo-di-μ-acetato bridged dinuclear structure. The first and the second complexes have one manganese ion five coordinated and the other six coordinated, while in the third complex the two manganese ions are in an octahedral environment. In the mononuclear complexes the manganese ions are six coordinated in a distorted octahedral environment [146].

These mononuclear compounds can be excellent precursors in the syntheses of heterodinuclear or heteropolynuclear complexes [146].

While the side-off ligands have been successfully used in the preparation of homo- and heterodinuclear complexes containing lanthanide and actinide ions, the end-off ligands seem not to be suitable for coordination of lanthanides and actinides owing to their coordination geometry and ionic radius which are considerably different from those of the d metal ions used for the synthesis of dinuclear complexes. For instance, thorium(IV) is usually eight or nine coordinated in square antiprismatic, dodecahedral, monocapped square antiprismatic, or trigonal tricapped prismatic coordination geometry.

The reaction of the Schiff base H_3-**85** (obtained by condensation of 2,6-diformyl-4-chlorophenol with *o*-aminophenol) with the appropriate lanthanide(III) nitrate ($Ln \equiv La \rightarrow Yb$) in the presence of the stoichiometric amount of base (LiOH) produces the complex Ln(**85**)·nH_2O ($Ln \equiv$ La, Sm, Pr, Eu, Gd, Tb, Dy, Yb; $n =$ 0, 1) [69,147].

It is difficult for H_3-**85** to behave as a pentadentate ligand towards one lanthanide ion. Although this should occur, there is a coordination insaturation about the metal ion even considering the solvent molecules present. Consequently an oligomerization of the complex could be suggested.

The binucleating behaviour of H_3-**85** with f ions was demonstrated for the complex Mg[Th_2(**85**)$_3$]$_2$·$6H_2O$ [147] obtained by reaction of the preformed ligands or of the diformyl- and amino precursor with $Th(NO_3)_4 \cdot 4H_2O$ in the presence of LiOH and $Mg(CH_3COO)_2 \cdot 4H_2O$. Each anion is a dinuclear unit (Fig. 66) in which two Th atoms are bridged by three oxygen atoms from three different ligands. Each ligand, which is trianionic pentadentate, is coordinated with two atoms of the first Th atom, with two atoms to the second Th atom and with the central oxygen atom to both Th atoms. The two independent Th atoms are nonacoordinated in

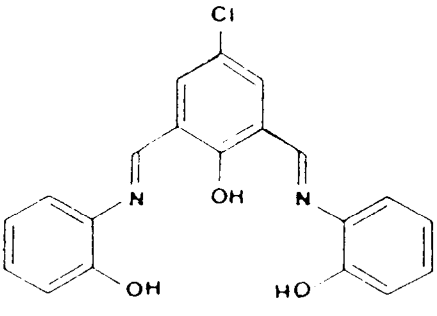

H_3-**85**

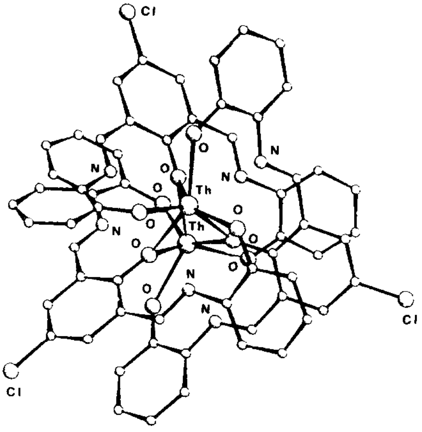

Fig. 66. Structure of $[Th_2(\mathbf{85})_3]_2^{2-}$.

a slightly distorted tricapped trigonal prism. The Mg^{2+} cations are octahedrally surrounded by six water molecules [147].

The magnetic moments of the lanthanide complexes Ln(**85**)-nH_2O are lower than expected (this could be caused by oligomerization) and it was possible to prepare complexes of the type $Mg_3[Ln_2(\mathbf{85})_3]_2 \cdot H_2O$ or $Li_3[Ln_2(\mathbf{85})_3] \cdot H_2O$ where the anionic stoichiometry is the same as that of the thorium complex. It was thus suggested that also in these complexes the ligand H_3-**85** has a compartmental behaviour [69,147].

Several polypodal ligands (type D) have been prepared and used for dinuclear complexation. These complexes, owing to their flexibility, appear to be very promising agents in oxygen activation and in oxidation reactions. The ligands (Scheme 26) contain ionizable (i.e. COOOH) or neutral (i.e. pyridine) groups in the pendant arms X while the central bridging group Y is a phenolic or an alcoholic OH.

Many further examples of complexes belonging to the different types of ligands reported in Scheme 26 have been reviewed in the recent literature [10,12].

When symmetric ligands or similar ions are used, particular experimental procedures must be used in order to avoid reactions of the type

$$2[M_aM_bL]^{n+} \rightarrow [M_aM_aL]^{n+} + [M_bM_bL]^{n+}$$

Homobinuclear complexes have been found to catalyse the *o*-quinone formation from the corresponding *o*-diphenol and the epoxidation of olefins better than the analogous mononuclear complexes. Heterobinuclear metal centres seem to be necessary for the asymmetric activation of CO_2 [11].

The specific spectroscopic and magnetic properties of lanthanide(III) ions have made them essential components in the preparation of new materials and ideal as probes in studies of biological systems. These investigations have been often carried out with the help of macrocyclic ligands.

It has been shown that it is possible to introduce two lanthanide ions into a macrocyclic cavity; for instance, Schiff bases obtained by condensation of 2,6-diformyl-4-substituted phenols with the facultative diamines NH_2–$(CH_2)_2$–X–$(CH_2)_2$–X–$(CH_2)_2$–NH_2 (X ≡ NH, O) provide a coordination moiety large enough to allow the preparation of homo- and heterodinuclear complexes [147–150].

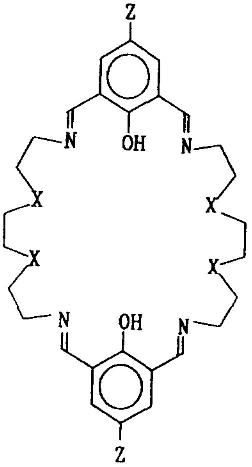

H_2-**86** (Z=CH_3, X=NH)
H_2-**87** (Z=CH_3, X=O)
H_2-**88** (Z=Cl, X=O)

The homodinuclear Gd_2(**87**)$(NO_3)_4 \cdot H_2O$ complex has a propeller conformation with approximate non-crystallographic D_2 symmetry with a crystallographic 2-fold axis passing through the centre, and normal to the mean plane, of the macrocycle. Both gadolinium atoms lie within the macrocycle and are bridged by the two phenolate oxygen atoms. Each gadolinium atom is ten coordinated, being bound to two nitrogen and two oxygen atoms of the macrocycle, four nitrate oxygen atoms and two phenolate oxygen atoms [150] (Fig. 67).

In particular, homo- and heterodinuclear lanthanide(III) complexes of the type Ln_2(**88**)$(NO_3)_4 \cdot nH_2O$ (Ln ≡ La, Pr, Sm, Eu, Gd, Tb, Dy; $n = 1, 2$) and Ln^1_x–Ln^2_{2-x}(**88**)$(NO_3)_4 \cdot nH_2O$ (Ln^1–Ln^2 ≡ La–Sm, La–Gd, La–Dy, La–Eu, Dy–Gd, Dy–Eu, Gd–Eu, Gd–Tb, Eu–Tb, La–Tb; $n = 1, 2$) have been synthesized and their possible structure and the interaction between the metal ions have been inferred from spectroscopic, mass spectrometry and magnetic data together with scanning electron microprobe analyses.

With these heterodinuclear complexes, the study of the energy transfer from the ligand to the two different lanthanide ions inside the macrocycle and from one lanthanide ion to other is feasible. Such energy transfer has been well defined especially for the complex EuTb(**88**)$(NO_3)_4$ [149]. The processes absorption of the ligand → energy transfer to the europium(III) → emission have been studied also for

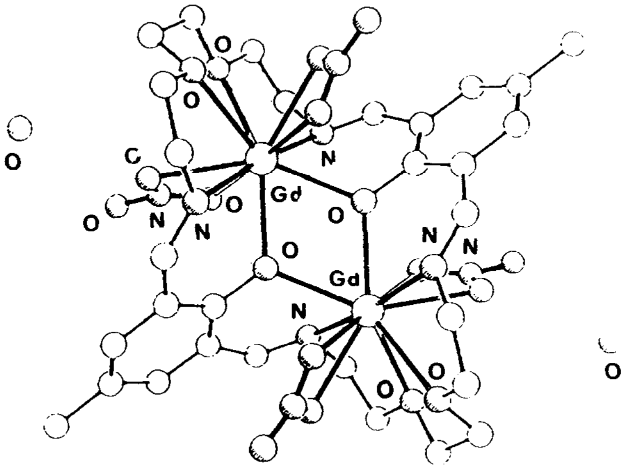

Fig. 67. The molecular structure of $Gd_2(\mathbf{87})(NO_3)_4 \cdot H_2O$.

the mononuclear europium(III) nitrate complex with the macrocycle B of Scheme 16 obtained by condensation of 2,6-diformyl-4-chlorophenol and 1,5-diamino-3-azapentane [101].

Spectroscopic investigations on heterodinuclear species have quantified the ligand→Ln(III) and Tb(III) to Eu(III) energy transfers also for an evaluation of the intermetallic distance [149]. The reported Gd–Gd distance (3.97 Å) for the complexes $[Gd_2(\mathbf{87})(NO_3)_4] \cdot 2H_2O$ is considerably shorter than that estimated for the similar complexes with H_2-**88**. Moreover, in the Eu–Eu complex with H_2-**87**, the lifetime is much shorter than the lifetime reported for the complex with H_2-**88**. It was suggested that the different R substituent may induce a different conformation of the ligand and hence different $Ln \cdots Ln$ distances [149,150].

The series of these heterodinuclear lanthanide(III) complexes has been more recently enlarged and the composition of compounds of the type $[(Ln_{1-x}Eu_x)_2(\mathbf{87})(NO_3)_4] \cdot H_2O$ and $[(Eu_{1-x}Tb_x)_2(\mathbf{87})(NO_3)_4] \cdot H_2O$ inferred by neutron activation analyses [150]. It was suggested that formation of $LnEu(\mathbf{87})(NO_3)_4 \cdot H_2O$ is more favourable than that of $LnTb(\mathbf{87})(NO_3)_4 \cdot H_2O$. In both cases the cation discrimination index, computed as the ratio of probabilities of Ln^{3+} incorporation into the crystalline heterolanthanide compounds, is in favour of the larger Ln^{3+} ion [150].

Luminescence decay dynamics of the $[(Sm_{1-x}Eu_x)_2(\mathbf{87})(NO_3)_4] \cdot H_2O$ and $[(Pr_{1-x}Tb_x)_2(\mathbf{87})(NO_3)_4] \cdot H_2O$ systems ($0 < x < 1$) reveals two microscopic environments for Eu^{3+} and Tb^{3+} which were attributed to homodinuclear molecules, $[Ln_2(\mathbf{87})(NO_3)_4] \cdot H_2O$ ($Ln \equiv Eu$ or Tb) (slow component), and heterodinuclear molecules $[SmEu(\mathbf{87})(NO_3)_4] \cdot H_2O$ and $[PrTb(\mathbf{87})(NO_3)_4] \cdot H_2O$ (fast component). The luminescence decay rate constants for intramolecularly coupled Eu–Sm and Pr–Tb pairs are $8200\ s^{-1}$ and $12\,500\ s^{-1}$ which yield coupling constants *a* of

2.9×10^{-53} $m^6 s^{-1}$ and 4.7×10^{-53} $m^6 s^{-1}$ respectively when dominant dipolar interactions are assumed. No exchange interactions are evident despite the presence of a phenolate linkage shared by the heteroatoms only about 4 Å apart. The ratio of Eu–Eu to Eu–Sm cation pairing selectivity constants of 1:1·5 (expected ratio for random pairing is 1:2) supports the intervention of molecular recognition processes favouring the homo- to hetero-paired species in the ion pairing events leading to $[(Sm_{1-x}Eu_x)_2(\mathbf{87})(NO_3)_4]\cdot H_2O$ compounds [150].

It was found that in the binuclear complexes $[(Ln_2(\mathbf{86})(NO_3)_4]\cdot nH_2O$ one metal ion can be leached out of **86**; this is accompanied by hydrolysis of **86** to 2,6-diformyl-*p*-cresol in water. However, in mildly acidic alcoholic solutions (with limited amounts of water) partial hydrolysis of **86** occurs along with condensation at the adjacent secondary nitrogen sites. This is evidenced by the isolation (from a mixture of several products) and characterization by single-crystal X-ray crystallography of mononuclear praseodymium and neodymium complexes of a 3:1 zwitterionic Schiff base $(H_n\text{-}\mathbf{89})^{(n-3)+}$ [150].

In the case of praseodymium, the complex crystallizes as $[Pr(H_3\text{-}\mathbf{89})(NO_3)(OH)]_2(ClO_4)_2\cdot NaNO_3\cdot 2H_2O$ with three of the four nitrogen sites probably protonated and coordination to Pr^{3+} afforded by the three phenolic and three aldehyde sites of **89**, a bidentate nitrate anion and a hydroxyl group as shown in Fig. 68(a). The coordination polyhedron of Pr^{3+} is best described as a distorted monocapped dodecahedron in this case.

As shown in Fig. 68(a), **89** is constituted by three molecules of 2,6-diformyl-*p*-cresol and one molecule of triethylenetetramine which utilizes two primary and a pair of adjacent secondary amino groups for condensation with the carbonyls.

In the case of neodymium, the complex appears to crystallize as $[Nd(H_3\text{-}\mathbf{89})(NO_3)(OH)_2][NO_3]_2$ with three of the four nitrogen sites of **89** probably protonated and the Nd^{3+} coordination polyhedron made up of the three phenolate and three aldehyde sites of **89** as well as a bidentate nitrate anion and a water molecule as shown in Fig. 68(b). The Nd^{3+} coordination polyhedron may also be thought of as a distorted monocapped dodecahedron [150].

The acid-catalysed condensation of 2,6-diformyl-*p*-cresol and diethylenetetramine at low temperature with $Pr(NO_3)_3$ as template agent produces the complex $Pr(\mathbf{89'})(NO_3)_2\cdot CH_3OH$, where the noncondensed carbonyl group has been acetylated under mild acid conditions [150].

Compounds of lanthanum and neodymium, isolated from more acid solutions, have a water molecule substituting a methanol molecule to give $Ln(\mathbf{89'})(NO_3)_2\cdot H_2O$.

The decacoordination polyhedron about praseodymium(III) is constituted by one phenolate oxygen atom, an imine nitrogen atom and three amino nitrogen atoms from the Schiff base, two bidentate nitrate anions from the Schiff base, two bidentate nitrate anions and a molecule of methanol. This decacoordination geometry has

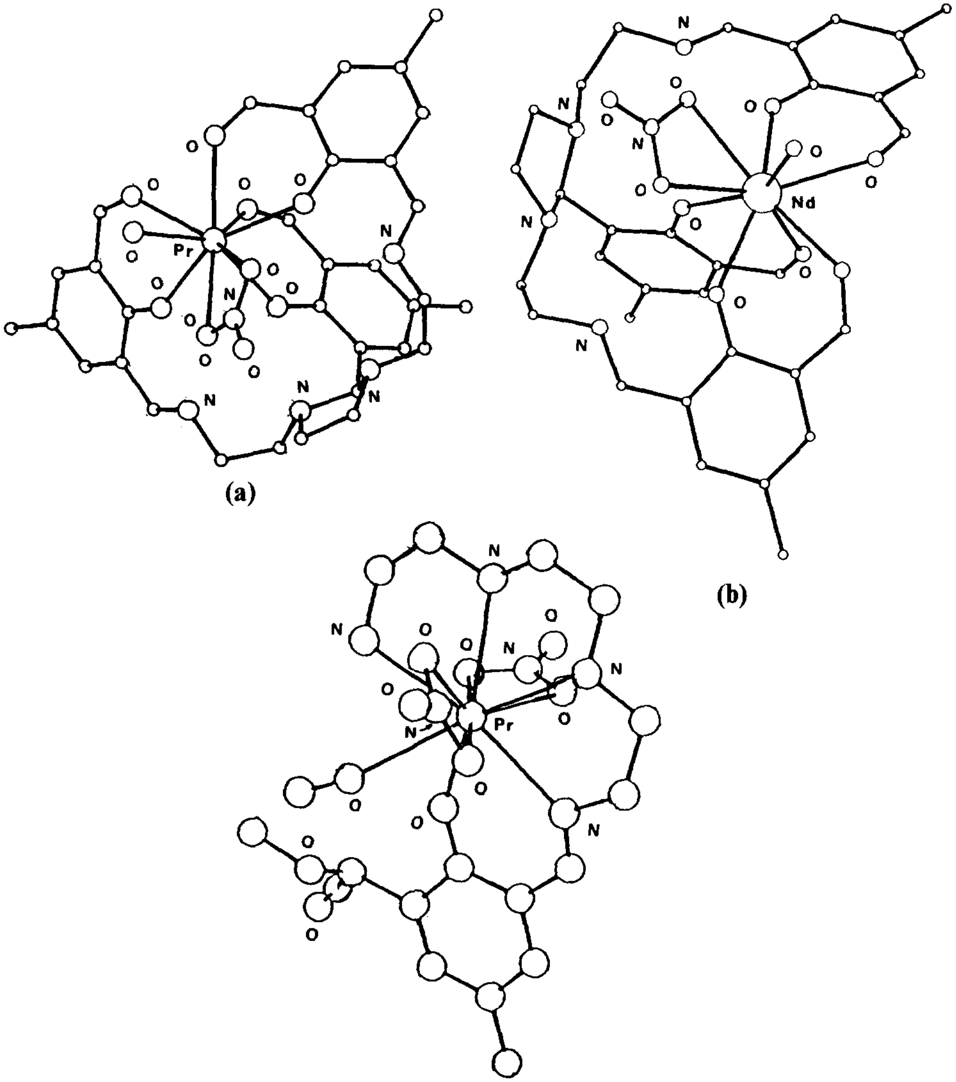

Fig. 68. Structures of (a) $[Pr(H_3$-**89**$)(NO_3)(OH)_2]^{2-}$, (b) $[Nd(H_3$-**89**$)(NO_3)(OH)_2][NO_3]_2$ and (c) Pr(**89′**)$(NO_3)_2 \cdot CH_3OH$.

been described as a distorted D_{4d} bicapped square antiprism or as a distorted bicapped dodecahedron of D_2 symmetry [150] (Fig. 68(c)).

These homo- and heterodinuclear complexes have been used as useful precursors in the formation of crystallographically pure oxides (Ln_2O_3 or $Ln^1Ln^2O_3$) by their thermal decomposition. Thus, in the decomposition of [DyEu(**88**)$(NO_3)_4] \cdot H_2O$, the water molecule is lost at 80–100°C. At about 600°C,

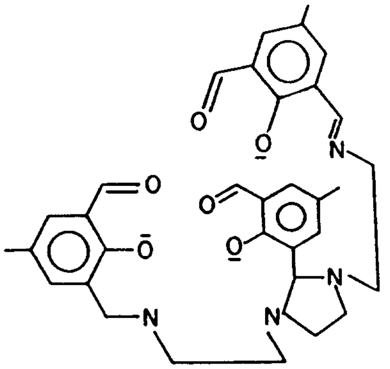

$(H_n\text{-}\underline{89})^{(n-3)+}$

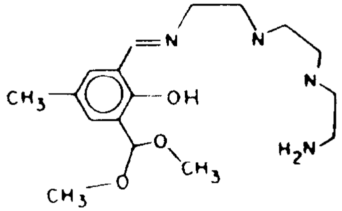

H-$\underline{89}$'

there is a range of stability of the formed sample which has been determined to be $DyEuO_2CO_3$. At about 1200°C $DyEuO_3$ was formed in a cubic symmetry while, at about 1600°C, $DyEuO_3$ with a monoclinic symmetry was obtained [151].

The acyclic compartmental ligands H_4-**81**, H_4-**90** and H_4-**91**, especially designed for the simultaneous coordination of a d and an f metal ion, have been obtained by condensation of 2,3-dihydroxybenzaldehyde with the appropriate diamine in alcoholic solution; they contain an inner N_2O_2 chamber particularly designed for a d transition metal ion and an outer O_2O_2 site too large for such an ion but suitable for an f ion, as confirmed by the X-ray structure of H_4-**90** [71].

Consequently it is possible to produce well-defined compounds without positional isomers or undesired species. The preparation of mono- and heterodinuclear complexes follows the reaction sequence reported in Scheme 30 [152,153].

X-ray data reveal that, in the mononuclear complexes, copper(II) and nickel(II) are square planar N_2O_2 isomers and evidence the correct size of the outer O_2O_2 chamber for the coordination of large metal ions such as f ions or barium. The condensation reaction of 2,3-dihydroxybenzaldehyde and ethylenediamine, using uranyl(VI) or lanthanide(III) ions as templating agents leads to the formation of $UO_2(H_2$-**81**$)(MeOH)$ and $Ln(H_4$-**81**$)(NO_3)_3$; the Schiff base coordinates as neutral in the lanthanide(III) complex and as dinegative in the uranyl(VI) complex. In these complexes, the metal ion is suggested to be in the outer O_2O_2 compartment with a solvent molecule occupying the fifth equatorial site of a pentagonal bipyramidal for the uranyl(VI) compounds and with nitrate anions filling the coordination sphere for the lanthanide(III) compounds. The outer O_2O_2 preference for uranyl(VI) ion in complexes with the potentially hexadentate side-off Schiff bases H_4-**78** and H_4-**79** has been already ascertained by X-ray structural analyses [141,142].

Heterodinuclear d–f complexes can be obtained by reaction of the mononuclear

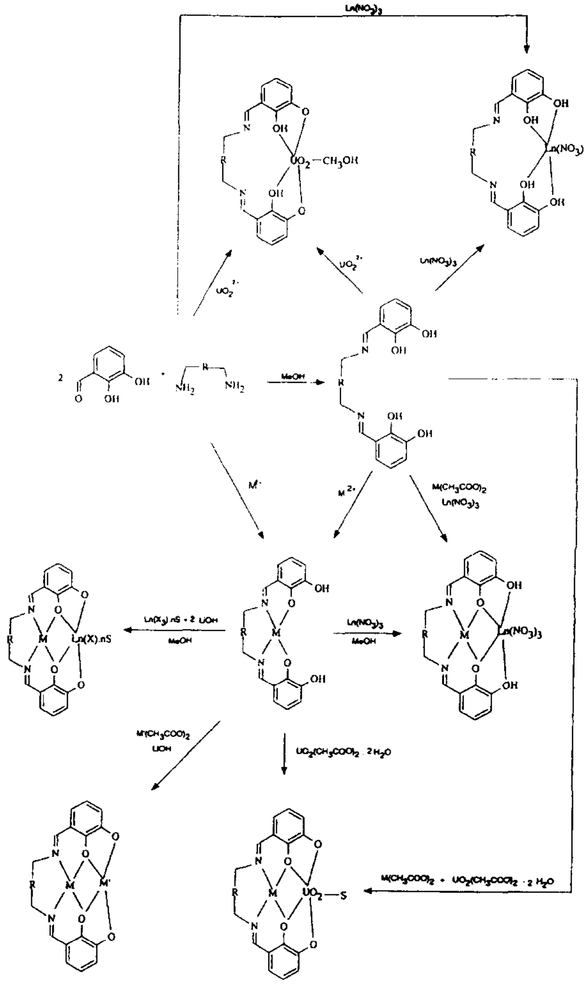

	R
H_4-**81**	$-CH_2CH_2$
H_4-**90**	$-CH_2C(CH_3)_2CH_2-$
H_4-**91**	$-C(CH_3)_2CH_2-$

$X = NO_3^-, Cl^-, CH_3COO^-, ClO_4^-$

Scheme 30.

d complexes with uranyl(VI) in coordinating solvents and with lanthanide(III) or barium(II) ions in methanol and in presence of a base.

The enhanced selectivity of the two chambers of these ligands towards the different metal ions is evidenced by their capability to form pure heterodinuclear complexes also when a transition metal ion (i.e. copper(II) or nickel(II)) and an f metal ion (i.e. lanthanum(III) or uranyl(VI)) are added in sequence to the ligands without previous separation and purification of the mononuclear species. The transition metal ion always occupies the inner chamber and the f ion the outer chamber [154].

An X-ray investigation of crystals of [CuY(**81**)(NO_3)(dmso)] (Fig. 69), grown from a dimethylsulphoxide–methanol solution, shows that the copper(II) is tetraco-

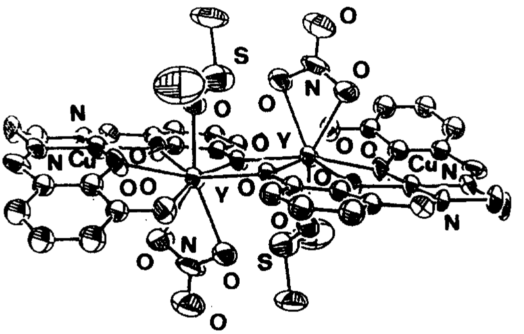

Fig. 69. Structure of [CuY(**81**)(NO_3)(dmso)]$_2$.

ordinated in the inner N_2O_2 chamber while the yttrium(III) is eight coordinated in the outer O_2O_2 site. The complex is a tetranuclear asymmetric unit, two yttrium ions being held together by phenolate oxygen bridges. The coordination of each yttrium(III) ion is completed by the oxygen atoms, a bidentate nitrate ion and a dimethylsulphoxide molecule. These heterodinuclear complexes have been used as precursor in the synthesis, by thermal decomposition, of mixed oxides; for example CuLa(**81**)(NO_3) produces $CuLa_2O_4$ with an orthorhombic symmetry [152].

This oligomerization, via the phenolic oxygen atoms of the outer chamber, can be prevented by the addition of anions which fill the coordination sphere about the lanthanide(III) ion with the consequent formation of monomeric species, as found for CuLn(H_2-**81**)(NO_3)$_3$.

X-ray powder diffraction studies on copper(II)–yttrium(III) and copper(II)–gadolinium(III) complexes [CuLn(**81**)(NO_3)(S)] (S ≡ MeOH, H_2O) show that they are isostructural [154,155]. Hence both can be assumed to be tetranuclear, with a structure quite similar to that found for [CuY(**81**)(NO_3)(dmso)]$_2$. Preliminary X-ray structural data confirm that the complexes MLn(H_2-**81**)(NO_3)$_3$ are dinuclear: the copper(II)$\cdots$lanthanide(III) distances are comparable in both tetranuclear and dinuclear structures [154,155].

Copper(II)–lanthanoid(III) complexes with *N,N′*-bis(3-carboxysalicylidene)-1,2-ethanediamine or with the similar 2-propanediamine and 1,5-diethylenetriamine have been prepared by reaction in methanol of the mononuclear copper(II) complex with La(NO_3)$_3$ in the presence of the LiOH. The copper(II) ion is bound at the inside N_2O_2 site while the lanthanoid ion occupies the outer O_2O_2 chamber [152,153].

The temperature dependence of the magnetic susceptibility of NiGd(H_2-**81**)(NO_3)$_3$ and CuGd(H_2-**81**)(NO_3)$_3$ complexes was measured in the 2.5–200 K and 2.65–100 K ranges respectively. The former derivative follows a Curie behaviour down to 15 K: below this temperature saturation effect might be at the origin of a slight deviation. The observed magnetic moment ($7.55\mu_B$) is slightly lower than those expected for isolated Gd(III) ions ($7.80\mu_B$), but in any case is indicative that the Ni(II) ion is in a square planar environment and, therefore, in a low spin configuration. The lower value of the effective magnetic moment is probably due to the presence of some unreacted Ni(II) monomer.

The $\chi(T)$ values for CuGd(H_2-**81**)(NO_3)$_3$ increase on lowering the temperature, pass through a maximum at about 4.7 K and then decrease. The sample used for the analysis of the magnetic behaviour was chosen on the basis of the lowest level of monomeric impurity. The best fit parameters obtained by using an isotropic spin hamiltonian ($H = J_{CuGd}S_1S_2$), corrected to account for the amount of monomeric species, were $J_{CuGd} = -1.59(3)\ \mathrm{cm}^{-1}$ and an amount of Cu(II) monomer of 6.9(2)% with fixed $g = 2.05$ and $g = 1.98$ values for Cu(II) and Gd(III) ions respectively.

The magnetic behaviour of the tetranuclear [CuGd(**81**)(NO_3)(H_2O)]$_2$ is similar to that of the dimeric system. Again, on lowering the temperature an increase in the $\chi(T)$ values is observed with a maximum around 14.5 K: the decrease below this temperature is more dramatic than in the previous case. Assuming that the molecular structure of the compound is similar to that of the yttrium analogue, the magnetic behaviour can be interpreted as due to the magnetic coupling in a tetrameric linear unit where one Gd–Gd and two equivalent Gd–Cu interactions are operative. The best fit parameters using the appropriate spin hamiltonian ($H = J_{CuGd}(S_1S_2 + S_3S_4) + J_{CuGd}S_2S_3$) and including a term to account for the presence of the external magnetic field are $J_{CuGd} = -3.76(4)\ \mathrm{cm}^{-1}$ and $J_{GdGd} = 0.16(5)\ \mathrm{cm}^{-1}$ with the previously reported g values for the two ions.

In agreement with previous findings, a ferromagnetic interaction is, even in this system, operative within the Gd(III)–Cu(II) pairs with a mechanism which does not depend on the geometry and nature of the bridging atoms. This result seems to confirm the presence of a spin polarization mechanism in 3d–4f pairs. The observed antiferromagnetic Gd(III)–Gd(III) coupling is weak, but in any case the observed coupling constant is indicative that some exchange mechanism is operative together with the pure dipolar mechanism.

The copper(II), nickel(II), iron(III), uranyl(VI) and lanthanide(III) complexes with the similar Schiff bases H_2-**92a** to H_2-**92e** have been used for a study of the recognition properties of the external O_2O_2 chamber and for the preparation of heteropolynuclear complexes [156]. In particular, the 1:1 addition complexes between the mononuclear nickel(II) compounds of H_2-**92a** to H_2-**92c** with Sn(R)$_2$(Cl)$_2$ (R ≡ Me or Ph), Sn(*n*-butyl)(Cl)$_3$ or $SnCl_4$ have been found to be generally monoaqua adducts of the tin Lewis acids with the water engaged in hydrogen bonding with the methoxy and phenolic oxygen atoms of the Schiff base ligand. Crystal structure determinations revealed that the monoaqua adducts of dimethyltin dichloride which exist in the structures [Ni(**92a**)·Sn(CH_3)$_2$(Cl)$_2$(H_2O)] and {[Ni(**92b**)·Sn(CH_3)$_2$(Cl)$_2$(H_2O)]}$_2$ differ in that, in the former tin is in a trigonal bipyramidal environment, whereas in the latter it is in an octahedral environment as a result of an intermolecular Sn···Cl contact of 3.615 Å [156] (Fig. 70).

When the inner coordination chamber is enlarged and contains an additional

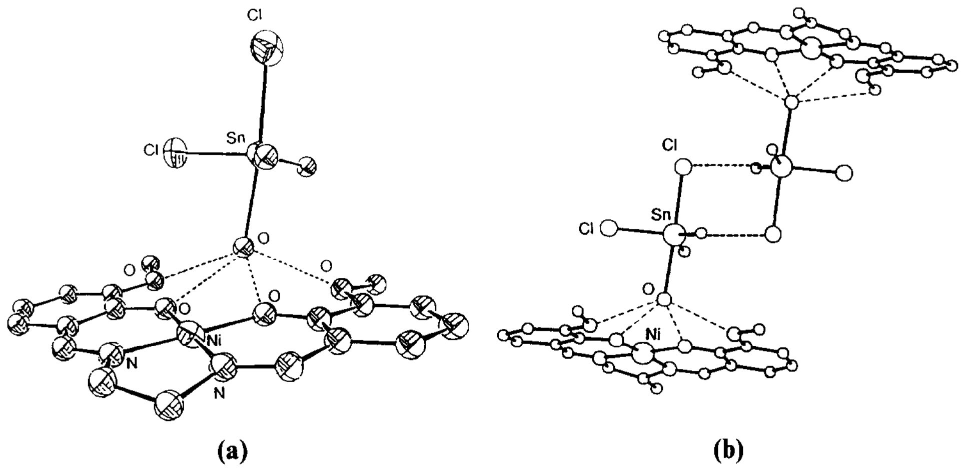

Fig. 70. Structures of (a) [Ni(**92a**)·$Sn(CH_3)_2(Cl)_2(H_2O)$] and (b) [Ni(**92b**)·$Sn(CH_3)_2(Cl)_2(H_2O)]_2$.

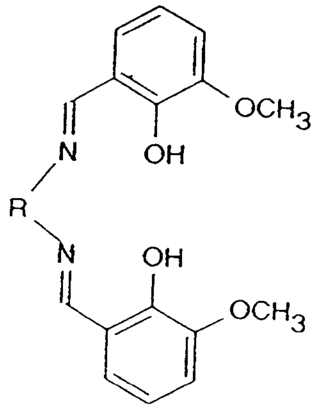

R	
CH_2CH_2	H_2-92a
$(CH_3)CHCH_2$	H_2-92b
C_6H_4	H_2-92c
$-CH_2CH_2CH_2-$	H_2-92d
$CH_2CH_2NCH_2CH_2$ $(CH_2)_{11}CH_3$	H_2-92e

donor atom, it is possible to accommodate an f ion in this coordination site. Mono- and homodinuclear uranyl(VI) complexes have been prepared by reaction of uranyl(VI) salts with the ligands H_4-**92** and H_4-**93**, obtained by condensation of 1,5-diamino-3-azapentane or 1,5-diamino-3-thiapentane with 2-formylsalycylic acid [157]. It was also verified that Schiff bases, with a donor set N_3O_2, coordinate the lanthanide ions [157] roughly in their equatorial plane; thus the two coordination chambers N_3O_2 and O_2O_2 of H_4-**93a** and H_4-**93b** seem to be suitable for an easy coordination of 4f ions.

Homodinuclear lanthanide(III) complexes have been obtained by reaction of the preformed ligands with the appropriate lanthanide(III) salt or by a template procedure (Scheme 30) [154].

The effective magnetic moment of $[Gd_2(\mathbf{93a})(NO_3)_2]\cdot4H_2O$ decreases with decreasing temperature, passing from $10.97\mu_B$ at room temperature to $7.96\mu_B$ at

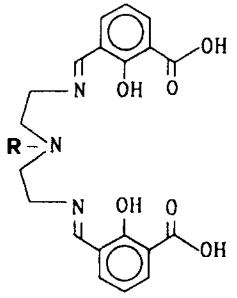

R	
$CH_3(CH_2)_{11}$-	H_4-**93**a
H	H_4-**93**b

4.2 K. The room temperature value is slightly lower than expected for a pair of non-interacting $S = 7/2$ ions ($11.17\mu_B$). The significative decrease in the $\chi(T)$ values as the temperature is lowered indicates that lower spin multiplicity states are occupied at lower temperatures and consequently that some magnetic interactions are operative between the gadolinium ions in the complex. Using the isotropic hamiltonian ($H = JS_1S_2$), it is possible to derive the expression for the magnetic susceptibility. A least-squares fitting procedure of the experimental data, maintaining the g factor at the fixed value of 1.975, yielded an antiferromagnetic interaction with a coupling constant $J = 0.211(4)$ cm^{-1} with an agreement factor $R = 0.011$. If a Gd–Gd distance of 3.8 Å is assumed by comparison with similar complexes, it is possible to calculate in the point dipolar approximation a value of 0.032 cm^{-1} for the dipolar interaction. This value, one order of magnitude lower than the coupling constant derived by the fitting procedure, indicates that a superexchange mechanism through the bridging atoms is operative in this compound [154].

Attempts to prepare mono- and heterodinuclear lanthanide(III) complexes with these ligands failed, whereas a successful procedure was followed with the ligands H_4-**94** to H_4-**96** (Scheme 31) [154,155,157].

The mononuclear lanthanide(III) complexes, where the Schiff base behaves as neutral pentadentate, undergo transmetallation reaction when treated with uranyl(VI) salts, giving rise to the mononuclear and homodinuclear uranyl(VI) complexes.

In the mononuclear complex $UO_2(H_2$-**94**$)\cdot$dmf, the ligand binds equatorially to UO_2^{2+} using the inner coordination chamber leading to seven-coordinated uranium in the distorted bipyramidal coordination geometry. The dmf molecule is hydrogen bonded to the phenolic oxygen atoms of the ligand. The ability of H_4-**94** to H_4-**96** to act as compartmental dinucleating agents toward f ions has also been verified on the complexes $(UO_2)_2$(**94**)(dmso) and $(UO_2)_2$(**94**)(dmf). The chelating ligand coordinates the inner UO_2^{2+} as in $UO_2(H_2$-**94**$)\cdot$dmf while the outer UO_2^{2+} is

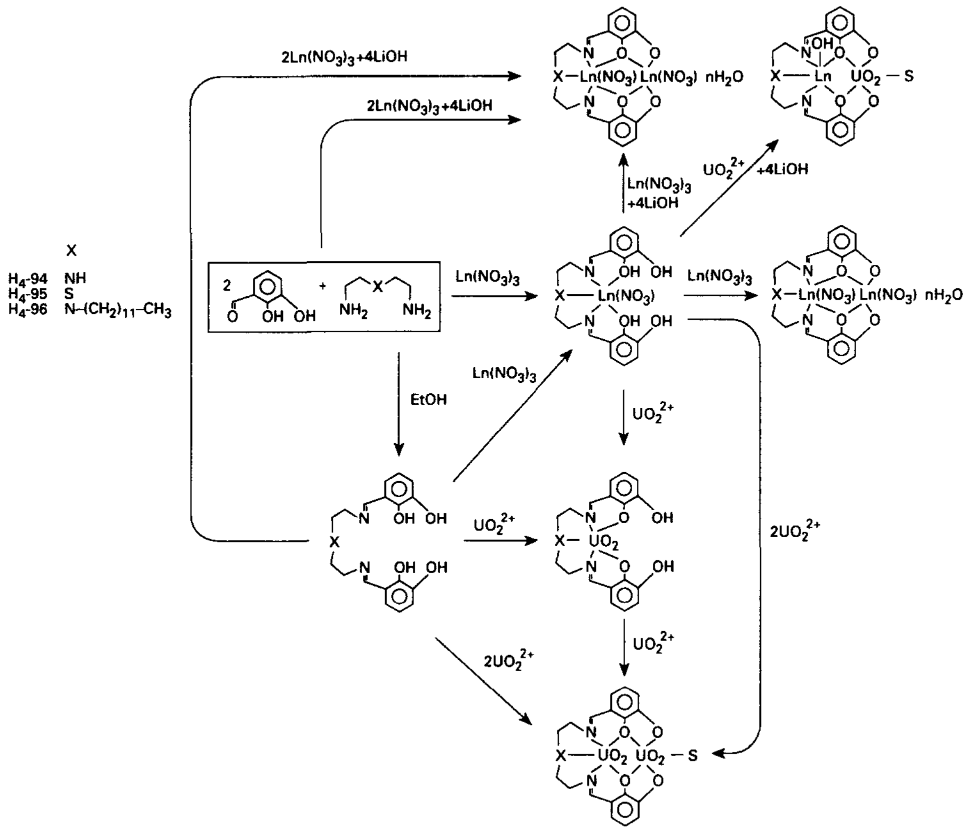

Scheme 31.

coordinated by four oxygen atoms of the dinucleating ligand and by the oxygen atom of the solvent molecule (Fig. 71) [155].

Differently from the outer linear UO_2^{2+} group in the dinuclear $(UO_2)_2$(**94**)(S) complexes, which reaches its equatorial penta coordination through the coordination of a solvent molecule (dmso, dmf, H_2O etc.), the outer lanthanide(III) can reach its coordination saturation through oligomerization. Thus in the lanthanide(III) complexes with H_4-**92** to H_4-**96** a dimerization through the phenolic oxygen atoms which fill the coordination sphere about the rare earth metal ion has been suggested. This causes low solubility also for the complexes derived from H_4-**92** to H_4-**96** in spite of the introduction of a long aliphatic chain [154].

A number of novel heterodinucleating ligands have been synthesized by Ba^{2+}-templated 1:1 macrocyclization of the appropriate dialdehydes with the suitable diamines reported in Scheme 32. The ligands have both a cavity suitable for complexation of transition metal cations and a cavity for complexation of alkali or alkaline earth metal cations. The resulting barium complexes could be converted into the

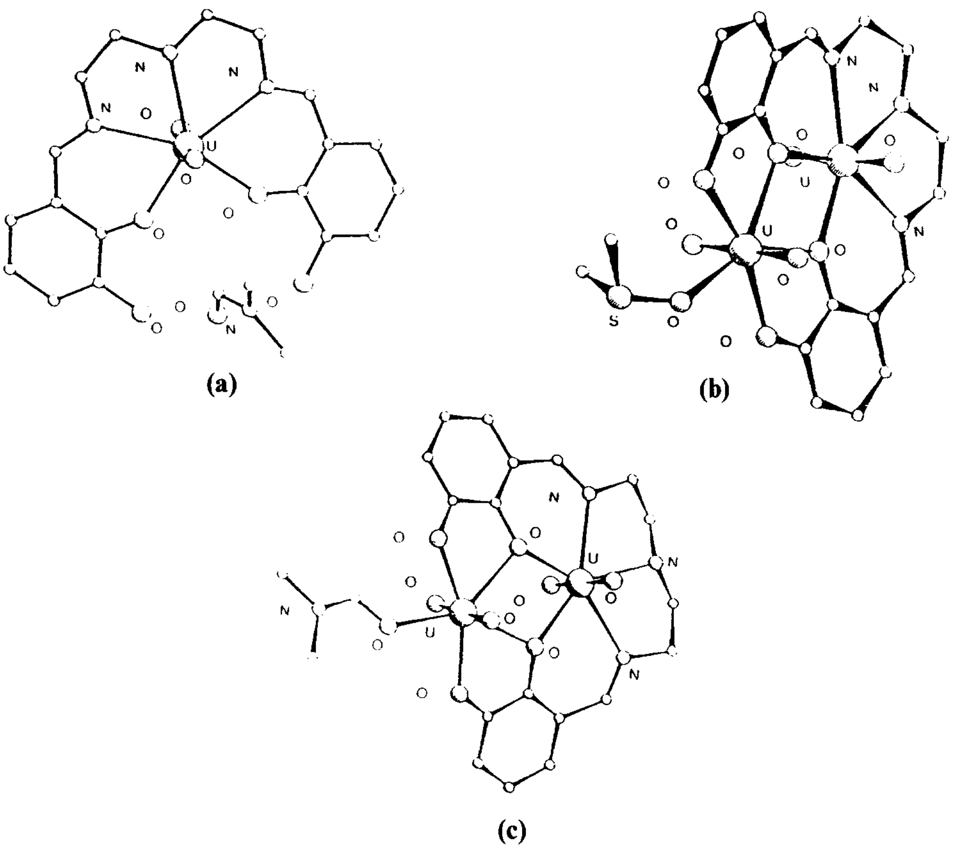

Fig. 71. Structures of (a) $UO_2(H_2\text{-}\mathbf{94})$, (b) $(UO_2)_2(\mathbf{94})$(dmso) and (c) $(UO_2)_2(\mathbf{94})$(dmf).

heterodinuclear complexes on reaction with nickel, copper, or zinc acetate. The mono transition metal complexes could be obtained by removing the barium salt from the polyether cavity [158,159].

The dinuclear cyclic ligands of Scheme 32 have a rather flexible polyethylene glycol unit that forms the hard cavity. In order to make this cavity more rigid, a terphenyl unit was incorporated for the construction of preorganized hemispherands (Scheme 33) [159,160].

In the structure of the nickel–barium complex $NiBa(\mathbf{97})(ClO_4)_2 \cdot MeOH$ (Fig. 72), the nickel cation has a square planar coordination while the barium cation is complexed in the polyether cavity. The polyether chain is completely folded around the barium in order to allow the coordination of the two phenolate oxygen and eight ether oxygen atoms. The eleventh coordination site is occupied by a perchlorate anion. The nickel–barium distance is 3.70 Å.

In $NiBa(\mathbf{98})(CF_3SO_3)_2 \cdot H_2O$ (Fig. 73), the barium cation is nine-fold coordinated by two phenolic oxygen atoms, four ether oxygen atoms, two triflate anions,

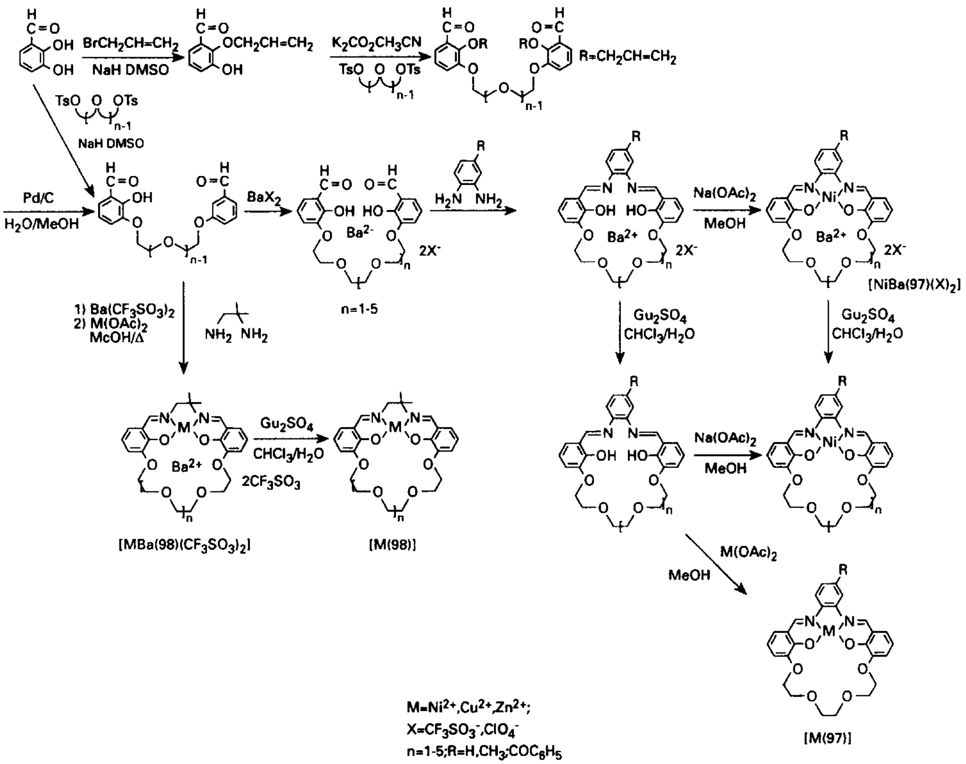

Scheme 32.

and one water molecule. The crown ether cavity is obviously too small for barium, and therefore the barium ion is complexed in a perching fashion. A triflate ion occupies one apical position while the other is occupied by water. The distance between the two metal ions is 3.69 Å.

In the dinuclear complex NaNi(**99**)(picrate) (Fig. 74), the nickel cation also has a square planar coordination while the six macrocyclic oxygen atoms coordinate the sodium cation, giving an encapsulated complex. The two apical positions are occupied by two picrate anions, one coordinating with an oxygen atom and the other with an oxygen atom of a *p*-nitro group. The sodium seems to induce a slight contraction of the ligand. The contraction is also reflected in the somewhat shorter distance of the four atoms complexing the nickel cation. The distance between the two metal ions is 3.63 Å.

In ZnBa(**100**)$(CF_3SO_3)_2 \cdot 3$dmf (Fig. 75) the zinc cation has a square pyramidal coordination that is formed by the two nitrogen atoms, the two phenolate oxygen atoms of the macrocycle, and an oxygen atom of dimethylformamide at the axial position. The zinc cation is displaced by 0.39 Å out of the mean plane of the four coordinating atoms of the macrocycle toward the coordinated carbonyl of dimethyl-

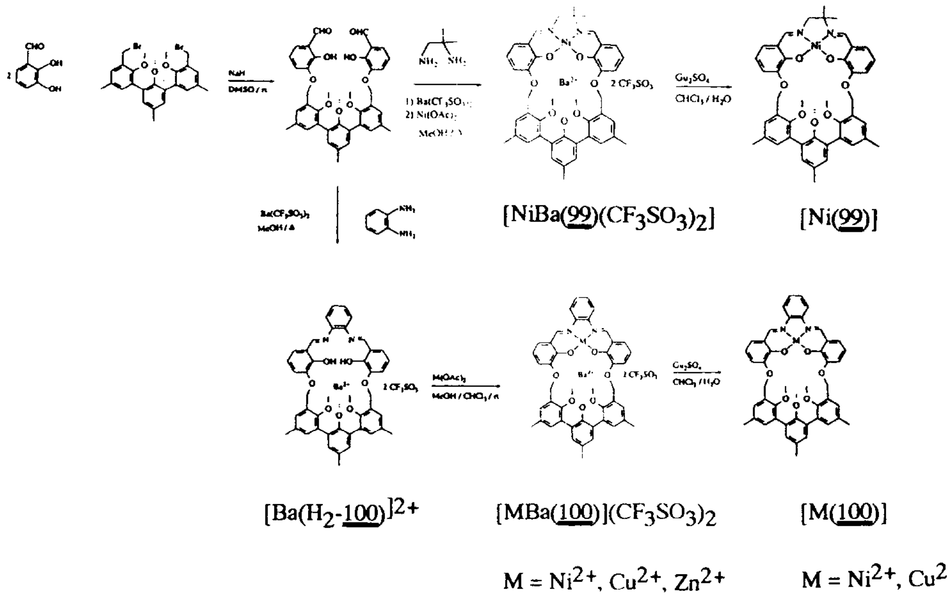

[NiBa(99)(CF$_3$SO$_3$)$_2$] [Ni(99)]

[Ba(H$_2$-100)]$^{2+}$ [MBa(100)](CF$_3$SO$_3$)$_2$ [M(100)]

M = Ni^{2+}, Cu^{2+}, Zn^{2+} M = Ni^{2+}, Cu^{2+}

Scheme 33.

formamide. The barium cation is complexed in the polyether cavity by the two phenolate oxygen, the two benzylic oxygen, and the three alternating methoxy oxygen atoms.

In addition to these seven oxygen atoms of the macrocycle, two molecules of dimethylformamide are coordinated to the barium at the same side as the dimethylformamide coordinated to the zinc. The tenth coordination site is occupied by a triflate anion. The distance between the two metal ions is 3.63 Å.

Electrochemical studies show that the redox properties of the complexed transition metal cation are strongly affected by the complexation of a hard cation in the polyether cavity. Cyclic voltammetry showed that the one-electron reduction of the nickel–barium, copper–barium and nickel complexes is chemically reversible but electrochemically irreversible at the applied scan rates. The two-electron reduction of the zinc–barium complex is both electrochemically and chemically irreversible. The ESR measurements also showed the influence of complexed hard cations on the properties of the complexed copper cation [158,159].

Dinucleating ligands containing quite different coordination sites which allow the easy formation of heterodinuclear complexes have also been synthesized by combining porphyrin with bipyridine, Schiff bases or crown ether systems [161,162]. In particular, Schiff base condensation of bis(salicylaldehyde)-linked porphyrins and ethylenediamine under high dilution gave salen-capped porphyrins **101a** and **101b** in high yields [162,163]. For the preparation of heterodinuclear complexes, the difference in affinity between the salen and the porphyrin ligands was utilized. Thus,

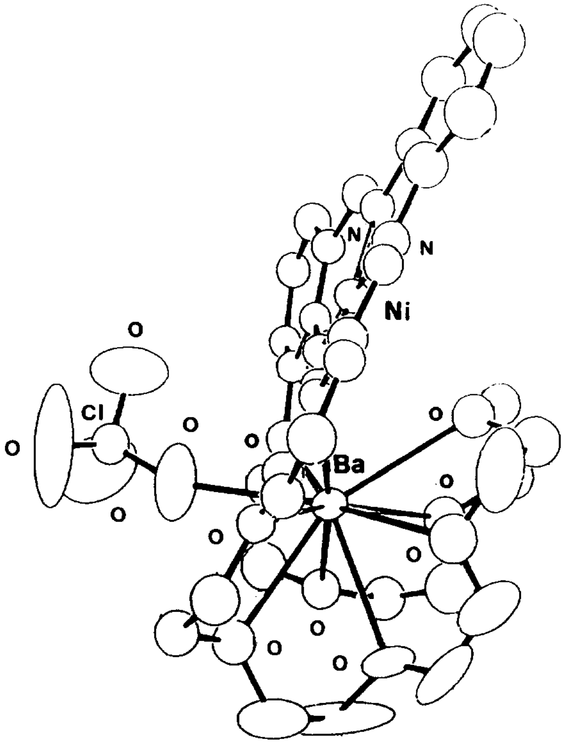

Fig. 72. Structure of NiBa(**97**)$(ClO_4)_2 \cdot$ MeOH.

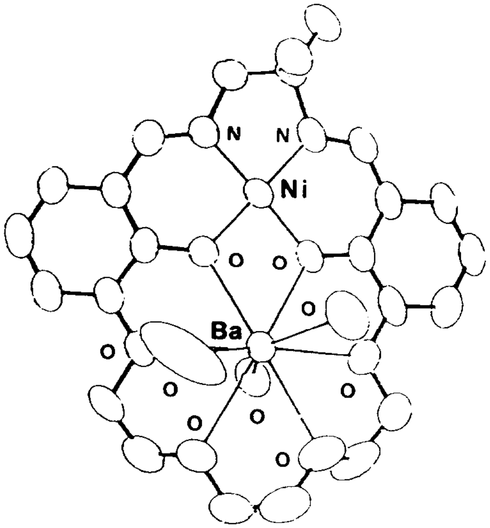

Fig. 73. Structure of NiBa(**98**)$(CF_3SO_3)_2 \cdot H_2O$.

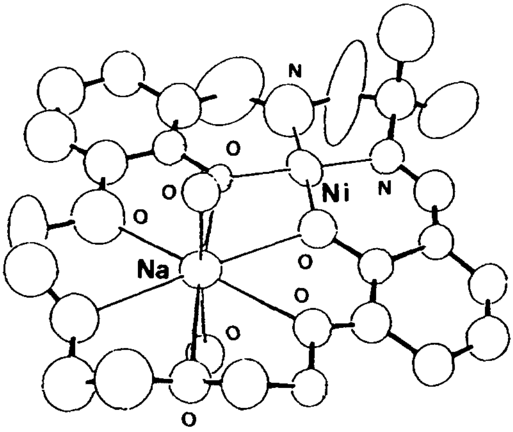

Fig. 74. View of NaNi(**98**)(picrate) (only the coordinated oxygen atoms of the two picrate anions are shown for clarity).

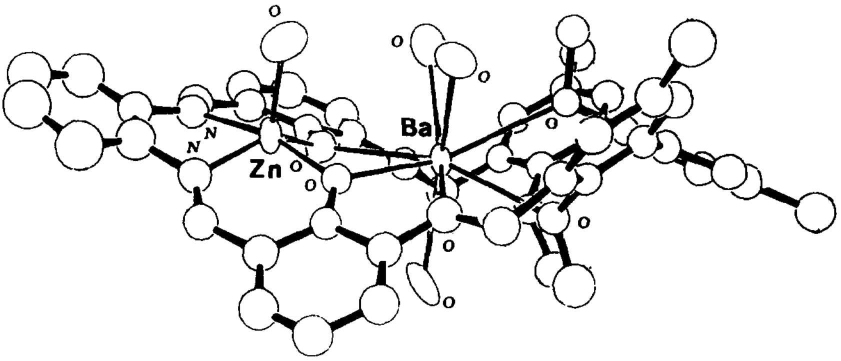

Fig. 75. Structure of ZnBa(**100**)$(CF_3SO_3)_2 \cdot 3$dmf (only the coordinated oxygen atoms of the three dimethylformamide molecules and of the coordinated anion are shown for clarity).

treatment of the salen–porphyrin ligands with nickel(II) acetate in dichloromethane at room temperature resulted in the insertion of nickel(II) into the salen site only with excess nickel acetate, but in refluxing chloroform both sites were metallated to give the corresponding bis-nickel complexes. In contrast, zinc(II) was selectively inserted into the porphyrin site on treatment with zinc(II) acetate in dichloromethane at room temperature. This behaviour may be ascribed to the affinity of the salen ligand for the nickel(II) ion and that of the porphyrin ligand for the zinc(II) acetate to give nickel–salen–zinc–porphyrin complexes in nearly quantitative yields. The porphyrin π electronic state of these Ni–salen-capped Zn porphyrins was perturbed by their Ni–salen cap. The parallel or perpendicular orientation of the two coordinating moieties was studied by ^{1}H NMR, UV–visible spectra, fluorescence, and cyclic voltammetry measurements.

A binucleating macrocyclic ligand which embodies six- and four-coordinate

101a n=2
101b n=3

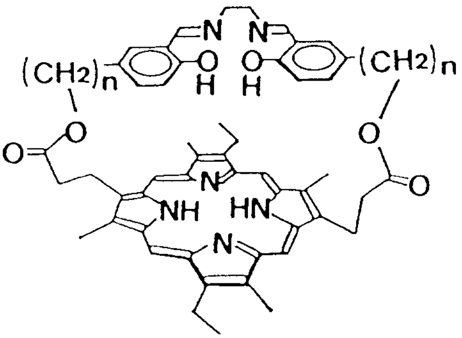

sites and related homo- and heterodimetallic complexes of Zn(II),Co(II), and Mn(II) have been prepared according to the reaction shown in Scheme 34 [163].

The mononuclear complexes M(**A**) of Scheme 34 were readily prepared by allowing the acyclic ligand H_2-**A** to react with the metal acetate and triethylamine in alcohol solvents. In this way, the generally insoluble complexes of Zn(II), Co(II), and Mn(II) were prepared, and oxidation of the Co(II) complex with $[FeCp_2]PF_6$ gave the Co(III) species. The diamagnetic Zn(II) and Co(II) complexes had ^1H NMR spectra which confirmed that the compounds possess a 2-fold rotation axis, supporting the prediction that the mononuclear complexes have the structure M(**A**) of Scheme 34.

Addition of 2 equivalents of $M(OAc)_2$ to H_2-**A** followed by reaction with either ethylenediamine or *o*-phenylenediamine yielded intractable products; the same procedure employing the larger 1,3-diaminopropane formed the homodinuclear complexes which, by addition of NH_4PF_6, have been recovered as crystalline products with varying amounts of solvent of crystallization. The subsequent addition of chloride ions gives the monochloro homodinuclear species $[M_2(\mathbf{B})(Cl)]PF_6$ of Scheme 34 [163].

The acyclic complex M(**A**) was cyclized with 1,3-diaminopropane under acid catalysis, and then the second metal was added. The complexes were inert to O_2 in the solid state but displayed variable reactivity in acetonitrile solution. Exposure of $[ZnMn(\mathbf{B})(Cl)]^+$ and $[Mn_2(\mathbf{B})(Cl)]^+$ to air in acetonitrile caused the yellow solutions to turn brown, the latter complex reacting faster. After air was bubbled through the solution for 24 h, the mixed-valence complex $[Mn_2(\mathbf{B})(\mu\text{-}Cl)(Cl)]PF_6$ was isolated as brown–black crystals from the dimanganese(II) precursor [143]. This complex contains Mn(III) in the open site and the Mn(II) is retained in the closed site. The same Mn(II)–Mn(III) complexes can be prepared by the addition of $[FeCp_2]^+$ in the presence of Cl^- ions. Attempts to prepare an Mn(III)–Mn(III) species by the addition of amounts in excess of 2 equivalents of $[FeCp_2]^+$ yielded the same Mn(II)–Mn(III) product, suggesting that the oxidation of the closed-site Mn(II) is more difficult after the Mn(II) in the open site has been oxidized.

$[ZnMn(\mathbf{B})(Cl)]^+$ gives a brown powder which consists of the starting material

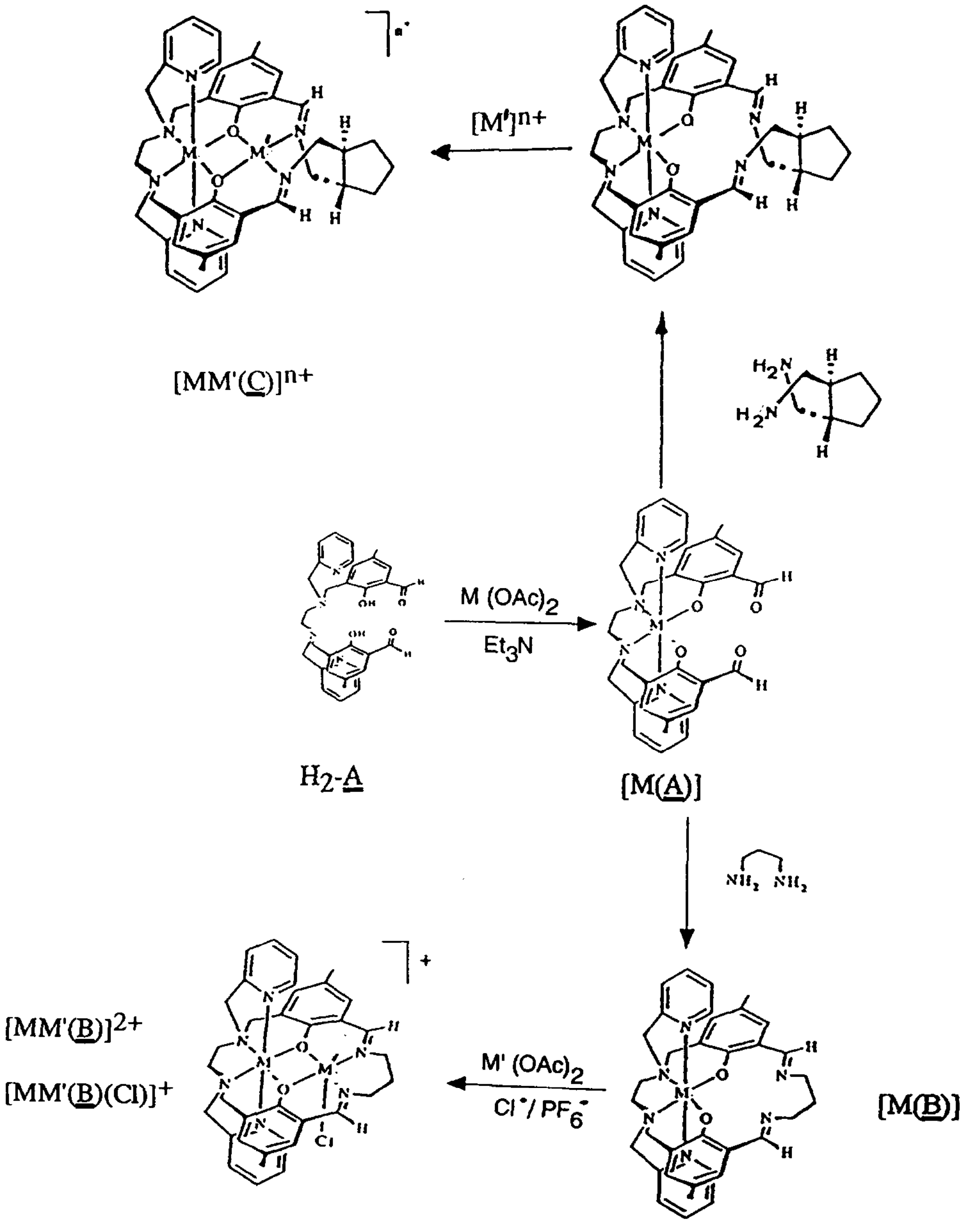

Scheme 34. Mononuclear, homo- and heterodinuclear complexes prepared from a macrocyclic compartmental ligand containing a six- and a four-coordinate site.

and probably MnO_2. Addition of varying equivalents of $[FeCp_2]^+$ to a solution of $[ZnMn(B)(Cl)]^+$ led to the same products as were observed for the reaction with O_2.

$[ZnCo(\mathbf{B})(Cl)]^+$ and $[Co_2(\mathbf{B})(Cl)]^+$ species were essentially inert to O_2 in acetonitrile solutions. Under similar conditions, the $[Co_2(\mathbf{B})]^{2+}$ complex slowly darkened over several days but no clean products could be isolated.

As expected the dizinc complex is not a catalyst for epoxidation and the dicobalt species exhibits marginal catalytic activity. The manganese species, however, are effective catalysts.

The open-site manganese species, $[ZnMn(\mathbf{B})(Cl)]^+$, and the corresponding complex with the closed-site manganese $[MnZn(\mathbf{B})(Cl)]^+$ have similar catalytic activity although the ratios of epoxide to aldehyde are different. This result suggests that the manganese in the sexadentate site dissociates one of the pyridyl ligands to open a site for forming the catalytically active oxo species.

The dimanganese species are the most effective catalysts. The two dimanganese complexes lead essentially to the same product ratios, and both catalysts consume 90% of the substrate. It seems probable, therefore, that the same catalytically active intermediate is being generated from the two dimanganese catalytic precursors. The fact that the mixed-valent dimanganese complex has a much faster initial rate may reflect the greater ease of attaining the catalytically active species for the mixed-valent catalyst precursor. At the midpoint of reaction, both catalysts have similar rates. All the catalysts become ineffective after a varying number of turnovers, which is probably associated with the destruction of the ligand. A comparison of the catalysis using the similar mononuclear Schiff base complex [Mn(saltn)] (H_2saltn ≡ *N,N′*-salicylidene-1,3-diaminopropane) with the two dimanganese complexes indicates that the bimetallic systems produce catalysts which have greater turnover numbers, different product ratios and faster rates.

Single-crystal X-ray diffraction structures of the bimetallic complexes $[Mn_2(\mathbf{B})(Cl)]PF_6$, $[Co_2(\mathbf{B})(Cl)](PF_6)_2$, $[Co_2(\mathbf{B})](PF_6)_2$ and $[Mn_2(\mathbf{B})(\mu\text{-}Cl)(Cl)]$-$PF_6$, were determined [163] (Fig. 76). Although the monomeric species $[Zn(\mathbf{A})]$ and $[Co(\mathbf{A})]^+$ have a C_2 symmetrical arrangement of the chelate arms, all the bimetallic macrocyclic systems have an unsymmetrical arrangement of ligands at the closed site where both pyridyl ligands lie on the same side of the mean molecular plane. In all the structures, the closed site resembles a trigonal prismatic structure, whereas the open site is square pyramidal or square planar. In the case of the mixed-valence structure $[Mn_2(\mathbf{B})(\mu\text{-}Cl)(Cl)]PF_6$, the Mn^{III} in the open site is octahedral and the closed site resembles a trigonal prismatic geometry having one disconnected phenolic bridging ligand. The $[Co_2(\mathbf{B})Cl]^+$ and $[Mn_2(\mathbf{B})(Cl)]^+$ ions are isostructural.

That the unsymmetrical structures are not caused by the presence of a chloro group in the open site is suggested by the fact that the $[Co_2(\mathbf{B})(Cl)]^+$ and $[Co_2(\mathbf{B})]^{2+}$ ions have similar unsymmetrical structures. Thus there is an inherent feature of the binucleating macrocyclic ligand that causes the asymmetry. As revealed in the structures, the trimethylene diimine link prefers to adopt a chair conformation. This,

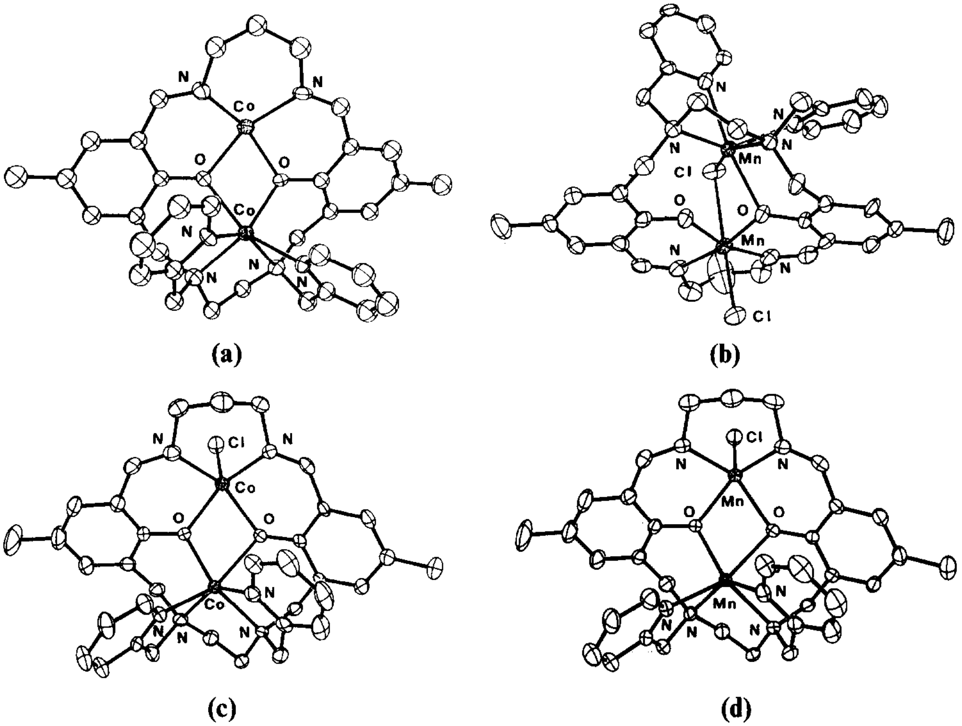

Fig. 76. Structures of (a) $[Co_2(\mathbf{B})](PF_6)_2$, (b) $[Mn_2(\mathbf{B})(\mu\text{-}Cl)(Cl)]PF_6$, (c) $[Co_2(\mathbf{B})(Cl)]PF_6$ and (d) $[Mn_2(\mathbf{B})(Cl)]PF_6$ (H_2-**B** is the macrocycle reported in Scheme 34).

in turn, forces the phenolic groups to adopt a conformation where these bridging groups lie on the same side of the mean macrocyclic plane. As a consequence, these transmitted steric imperatives cause both of the pyridyl ligands to dispose themselves to the same side of the mean molecular plane opposite to that of the phenolic groups.

It was suggested that to obtain a symmetrical closed-site structure where one pyridyl ligand lies above the other below the mean macrocyclic plane, the bite angles associated with the ethylenediamine and/or trimethylene diimine links need to be expanded [163].

Complexes $[MM'(\mathbf{C})]^{n+}$ containing chiral ligands have been prepared by a procedure similar to that employed for $[MM'(\mathbf{B})]^{n+}$ (Scheme 34). The topology and stereochemistry of these complexes are controlled by the introduction of a chiral diimine moiety into the macrocyclic portion of the ligand. By varying the metal combinations, it is possible to tune the redox properties of these complexes and to develop appropriate systems for dioxygen activation and for asymmetric epoxidation [163].

Tripodal heptadentate amine phenol ligands H_3-**102** prepared by KBH_4 reduction of the corresponding Schiff bases form with lanthanide(III) nitrate dinuclear complexes in the presence of base [164].

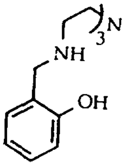

H_3-**102**

The dinuclear complex $[Gd(\mathbf{102})]_2 \cdot 2CHCl_3$ has a distorted bicapped octahedral (or cubic) coordination geometry around each gadolinium atom which is coordinated by an N_4O_4 donor set. The two gadolinium atoms are bridged by two phenolate O atoms, one from each heptadentate ligand. The Gd–Gd separation is 3.9841 Å [164].

From the structure of $[Gd(\mathbf{102})]_2 \cdot 2CHCl_3$, it seems that the formation of the dinuclear complex is caused by the higher coordination requirements of lanthanide ions and/or by the small cavity of the heptadentate ligand. There are two ways to prevent this dimerization: one is to introduce bulky groups onto aromatic benzene rings at the 3 position and the other is to increase the length of the chelating "arms".

A variable temperature (4.2–83 K) magnetic susceptibility study of the $[Gd(\mathbf{102})]_2 \cdot 2CHCl_3$ complex revealed a good fit of the data to two very weakly antiferromagnetically coupled $S = 7/2$ ions ($g = 2.00$, $-J = 0.045$ cm^{-1}) [164].

6. TRINUCLEAR COMPLEXES

The interaction of O_2 with mono- and dinuclear copper complexes has been extensively studied. Most recently, attention has been devoted also to tricopper clusters as they may be of importance in a number of the multicopper blue oxidases and laccases [165,166]. These multicopper blue oxidases catalyse the four-electron reduction of dioxygen to water with concomitant one-electron oxidation of a variety of substrates, such as polyphenols, aromatic polyamines, and ascorbate [167–169]. These enzymes have been described as containing different types of copper environments, designated as type 1, type 2 and type 3 centres, based on their spectroscopic properties [170]. An important and recent X-ray structural determination on oxidized ascorbate oxidase from zucchini unambiguously demonstrated the existence of this trinuclear centre [35]. The functional unit has four copper ions bound in mononuclear and trinuclear moieties. The isolated type 1 "blue" copper is bound to two histidines, a cysteine and a methionine ligand while the trinuclear cluster has a biologically unprecedented structure with the three copper ions arranged in a near isosceles triangle.

In a biomimetic approach to understand the function of the trinuclear copper cluster in the molecular mechanism of the four-electron reduction of dioxygen to water in multicopper oxidases [171], the tricopper(I) complex

$[Cu_3(\mathbf{103})(PPh_3)_2](PF_6)_3 \cdot 2CH_3CN$ was synthesized by reaction of $[Cu(CH_3CN)_4](PF_6)$ with the ligand **103** under Ar in CH_2Cl_2 containing PPh_3. Two of the copper(I) ions are found in a distorted tetrahedral environment with coordination to the tertiary amino, the pyridyl nitrogen and the phosphorus atoms of the triphenylphosphine ligand. The third copper(I) ion possesses a distorted trigonal pyramidal coordination with ligation to two pyridyl and two amino nitrogen atoms (Fig. 77) [171].

The new trinuclear copper(I) complex $[Cu_3(\mathbf{104})](PF_6)_3$ obtained by reaction of the preformed ligand with $[Cu(CH_3CN)_4]PF_6$ reacts with O_2 at −80°C in CH_2Cl_2–CH_3CN (9:1) to produce the hexanuclear cluster $[Cu_3(\mathbf{105})(OH)_2](PF_6)_3 \cdot 2H_2O$ of Scheme 35 [172].

In this complex the ligand has been hydroxylated as confirmed by the X-ray structure of the azide analogue $[Cu_3(\mathbf{105})(OH)(N_3)]_2(PF_6)_6$. The molecule is centrosymmetric and consists of two types of copper ion environments. Two copper ions exist as a dinuclear Cu(II) pair with bridging phenoxo and μ-1,1-azido ligands. The third Cu(II) ion is pentacoordinated with near-planar ligation to the tridentate bis[2-(2-pyridyl)ethyl]amine moiety and hydroxide ligand. There is longer axial interaction with the hydroxide ligand which connects to the symmetry-related copper atom and second trinuclear unit (Fig. 78). On the basis of EPR and conductance measurements, the hexanuclear structure is retained in CH_3CN and CH_2Cl_2 solution while in coordinating solvents such as DMF and MeOH the unit breaks, giving trinuclear units $[Cu_3(\mathbf{105})(OH)_2]^{3+}$.

The barium(II) complex $Ba(\mathbf{106})(ClO_4)_2 \cdot H_2O$ has been obtained by reaction

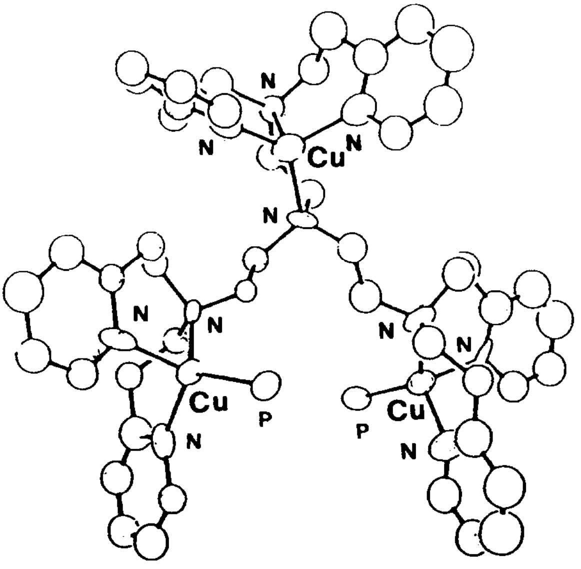

Fig. 77. Structure of $[Cu_3(\mathbf{103})(PPh_3)_2]^{3+}$.

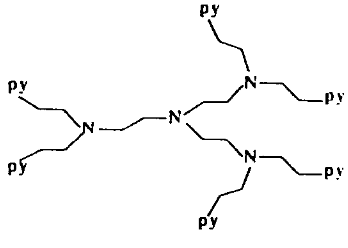

103

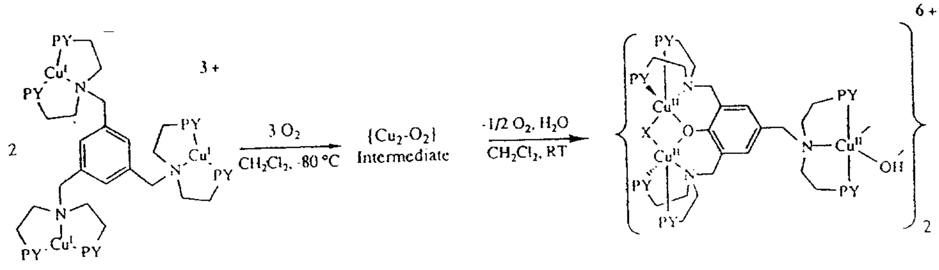

$[Cu_3(\mathbf{104})]^{3+}$

$[Cu_3(\mathbf{105})(OH)(X)]_2^{6+}$
$X = OH^-, NO_3^-$

Scheme 35.

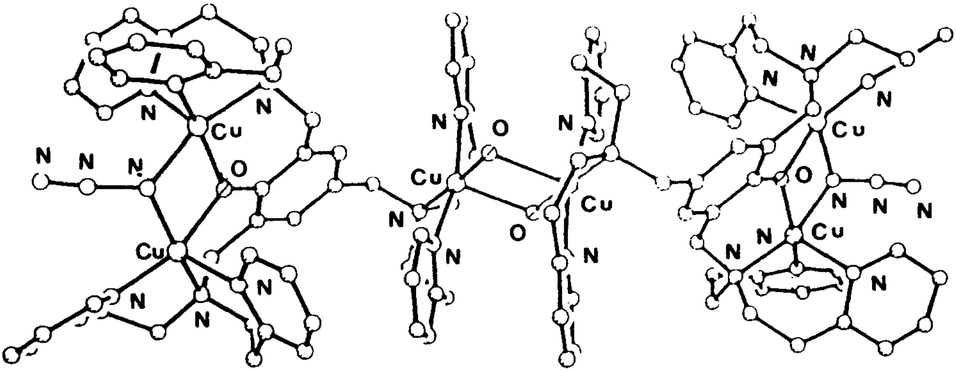

Fig. 78. Perspective view of $\{[Cu_3(\mathbf{105})(N_3)(OH)]\}_2^{6+}$.

of 2,6-diacetylpyridine with *N*,*N*-bis(2-aminoethyl)-1,2-ethanediamine in the presence of barium diperchlorate as the templating device [31]. Transmetallation reaction with copper(II) or silver(I) ions produces the corresponding dinuclear complexes [34,173,174] (Scheme 36).

The structure of $[Ag_2(\mathbf{106})](BF_4)$ [174] (Fig. 79(a)) has two six-coordinated silver(I) ions (3.167 Å) bound in the pyridine diimine moieties of the macrocycle. One of the imino nitrogen atoms within each pyridine diimine fragment bridges two silver ions while the other is bound only to a simple ion. The coordination about each silver ion is completed by the primary amines of the pendent arm. The overall configuration of $[Ag_2(\mathbf{106})]^{2+}$ is folded so as to form a cleft with the metal atoms well hidden at one end [174].

By condensation of the disilver complex $[Ag_2(\mathbf{106})]^{2+}$ with salicylaldehyde the corresponding Schiff base was prepared. The subsequent transmetallation reaction with hydrated copper(II) salts in methanol and acetonitrile gives $[Cu_3(OH)(\mathbf{107a})(H_2O)](ClO_4)_3 \cdot 2H_2O$ [34,174], whose structure (Fig. 79) has a

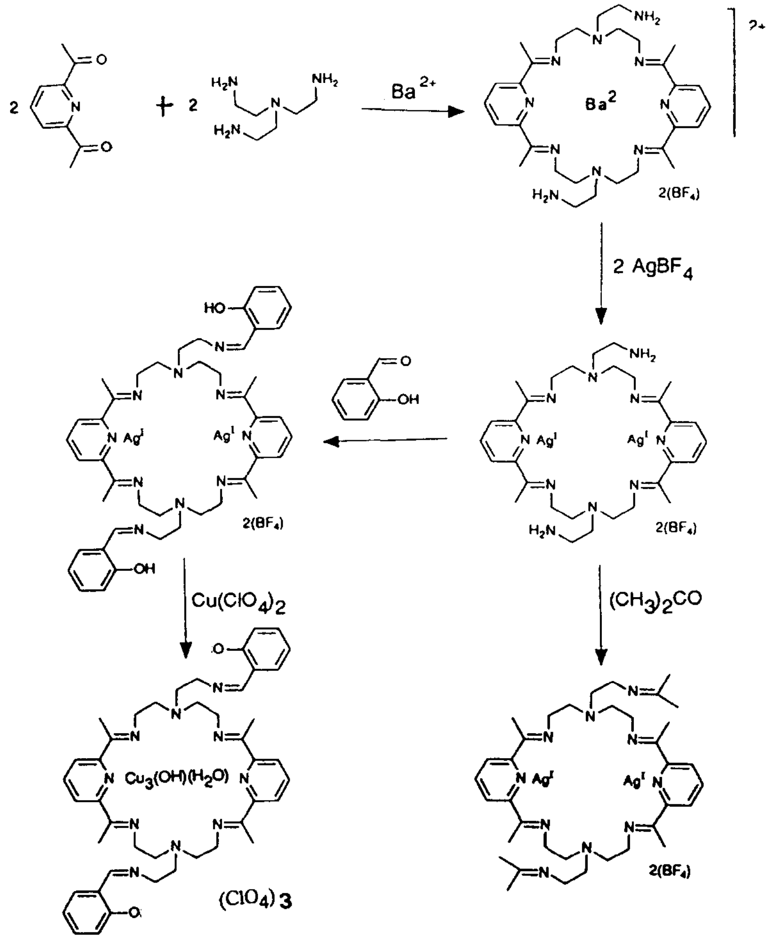

Scheme 36. Reaction pathway for the formation of mononuclear, homodinuclear and homotrinuclear complexes.

triangulo-copper(II) cluster held within the ligand perimeter, which resembles the trinuclear copper(II) site found in ascorbate oxidase [171] (Scheme 36).

$[Cu_3(OH)(\mathbf{107b})(H_2O)](ClO_4)_3 \cdot 2H_2O$ consists of a type-3-like centre, Cu(1) and Cu(2), and a type-2-like atom Cu(3). The type-2-like copper atom is 4.9 and 5.9 Å from the two copper atoms of the type-3-like centre; they are 3.6 Å apart and bridged by a hydroxy group, the origin of which appears to be water from the reaction medium, with the two copper(II) atoms acting in concert, as a superacid pair, to promote the generation of a nucleophile (Fig. 79(a)). The room temperature magnetic moment of the *triangulo* complex was $1.66\mu_B$ per Cu atom suggesting that some magnetic coupling is occurring, presumably within the type-3-like centre. The two copper atoms constituting the type-3-like centre are found in distorted square

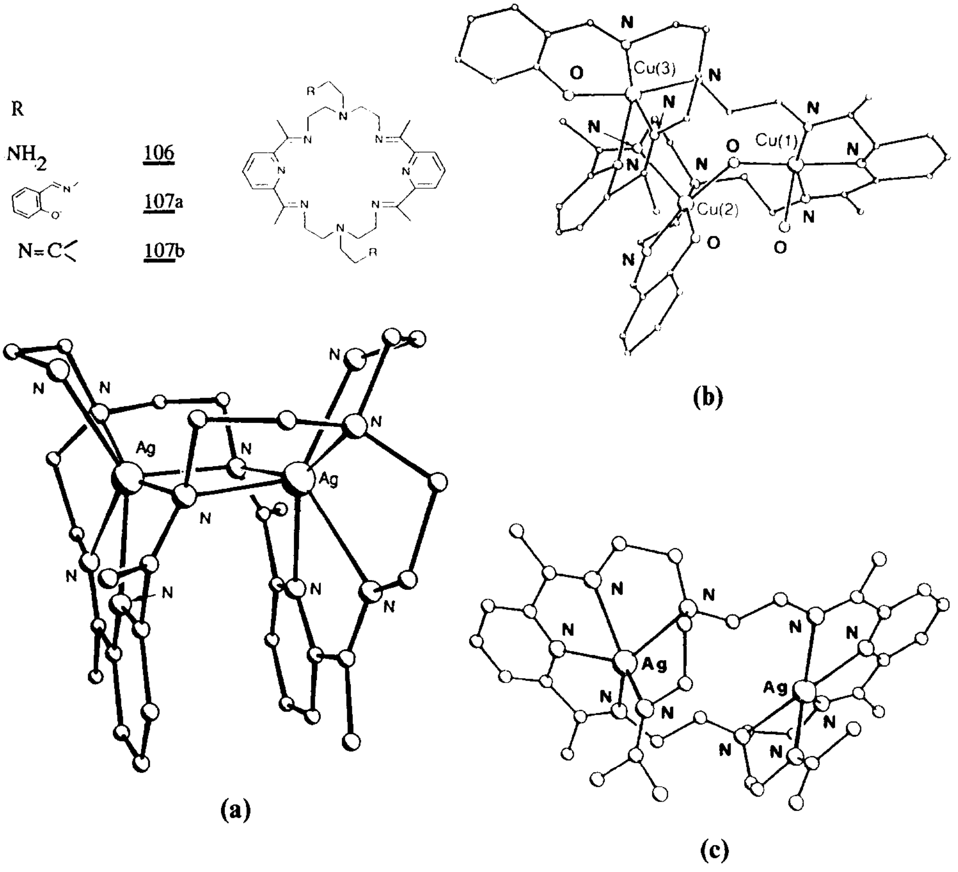

Fig. 79. Structures of (a) $[Ag_2(\mathbf{106})]^{2+}$, (b) $[Cu_3(\mathbf{107a})(OH)H_2O]^{3+}$ and (c) $[Ag_2(\mathbf{107b})](BF_4)_2$.

pyramidal coordination geometries. The type-2-like copper atom also has a distorted square pyramidal coordination environment.

A study of the magnetic properties shows that the trinuclear copper(II) complex can be regarded as a mononuclear site non-interacting with an antiferromagnetically moderately coupled ($2J = -202\ cm^{-1}$) copper(II) pair [174].

The nature of the complex suggests that it be regarded as a first-generation model for the triangular copper(II) sites found in ascorbate oxidase and proposed for multicopper oxidases such as laccase.

The reaction of $[Ag_2(\mathbf{106})](BF_4)_2$ with acetone in methanol gave a yellow crystalline product where two molecules of acetone had condensed to the amine groups of the macrocycle giving rise to the bis(*N*-isopropylidene) compound $[Ag_2(\mathbf{107b})](BF_4)_2$ as confirmed by the X-ray structure [173,174] (Fig. 79(b)). The structure of the dication shows that each silver atom forms five interactions with nitrogen atoms of the macrocycle; the silver–silver distance is 5.378 Å. The overall conformation of the macrocyclic dication is open and, although somewhat folded, no cleft is formed; none of the nitrogen atoms forms bridges between the silver atoms. In this respect, the structure is remarkably different both from that of the precursor molecule $[Ag_2(\mathbf{106})](BF_4)_2$, in which there is a silver–silver separation of 3.17 Å and the conformation of the macrocycle forms a deep cleft with two bridging macrocyclic imino nitrogen atoms, and from those of related disilver(I) complexes derived from bibracchial tetramine Schiff-base macrocycles (Scheme 36).

Also, in the structure of a *triangulo*-Cu_3 complex $[Cu_3(\mathbf{107a})(OH)H_2O]$-$(ClO_4)_3 \cdot 2H_2O$, the cleft-like nature of $[Ag_2(\mathbf{106})](BF_4)_2$ is lost. The nature of $[Ag_2(\mathbf{107b})](BF_4)_2$ suggests that this change in molecular geometry occurs during the formation of the disilver intermediate $[Ag_2(\mathbf{107a})](ClO_4)_2$ prior to the transmetallation reaction leading to the *triangulo*-Cu_3 complex.

Well defined heterotrinuclear complexes have been prepared and fully characterized by using the macrocyclic ligands of Scheme 37 obtained as barium complexes by [2 + 2] cyclization of the appropriate dialdehyde with 1,2-diaminobenzene, in the presence of Ba^{2+} as a templating agent. The subsequent reaction of the barium complex with copper(II) or nickel(II) acetate yields the heterotrinuclear complexes [175,176].

Mononuclear barium and trinuclear dicopper–barium and dinickel–barium complexes have been analysed by X-ray crystallography [175]. In $Ba(\mathbf{108})(CF_3SO_3)_2$ (Fig. 80) the H_4-**108** macrocycle is folded around the barium, thereby allowing coordination by all ten oxygen atoms of the macrocycle. The eleventh position around the barium ion is occupied by an oxygen atom of a triflate ion. The two conjugated *N,N'*-*o*-phenylene-bis(salicylidenaminato) (salophen) units are not planar. The structure of the dicopper–barium complex $Cu_2Ba(\mathbf{108})(CF_3SO_3)_2 \cdot 2H_2O$

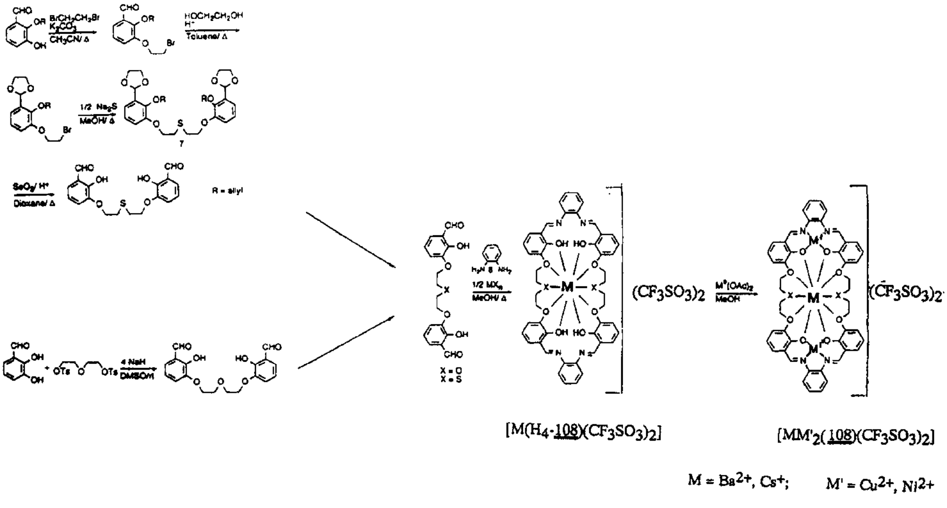

Scheme 37.

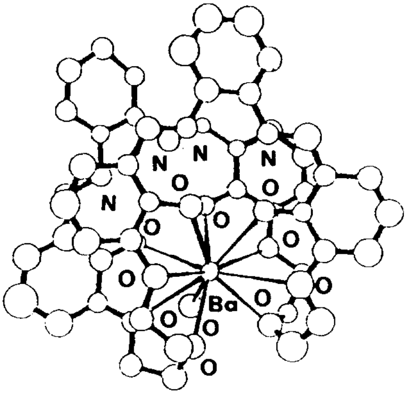

Fig. 80. Structure of $Ba(H_4\text{-}\mathbf{108})(CF_3SO_3)_2$.

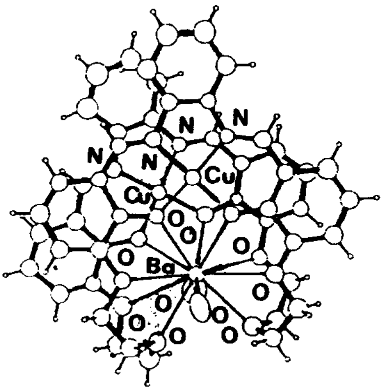

Fig. 81. Structure of $Cu_2Ba(\mathbf{108})(CF_3SO_3)_2 \cdot 2H_2O$.

(Fig. 81) shows that the two copper cations are complexed in a square planar fashion in the salophen units. The barium cation is complexed in the polyether cavity by nine oxygen atoms of the macrocyclic ring and by weak coordination of the remaining $ArOCH_2$ oxygen atom. In addition to these 10 oxygen atoms of the macrocycle, a triflate anion and a water molecule are also coordinated. The conjugated systems exhibit a much smaller deviation from planarity than mononuclear barium complex. The metal–metal distances in this complex are 3.70 and 3.85 Å for $Ba^{2+} \cdots Cu^{2+}$ and 3.50 Å for $Cu^{2+} \cdots Cu^{2+}$.

The structure of $Ni_2Ba(\mathbf{108})(CF_3SO_3)_2 \cdot H_2O \cdot$dmso (Fig. 82) shows that the nickel cations are complexed in the salophen unit in a square planar fashion. The barium cation has an 11-fold coordination. In addition to the 10 oxygen atoms of the macrocyclic ring a water molecule is coordinated. The salophen units are not

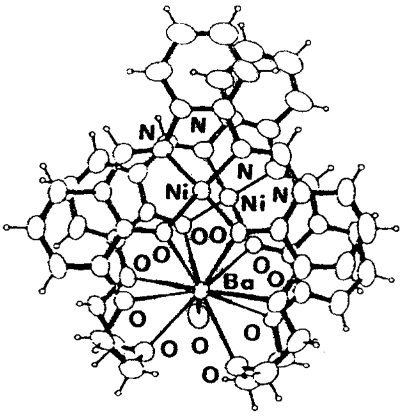

Fig. 82. Structure of $Ni_2Ba(\mathbf{108})(CF_3SO_3)_2 \cdot H_2O \cdot$dmso.

completely planar; the metal–metal distances in this complex are 3.66 and 3.73 Å for $Ba^{2+} \cdots Ni^{2+}$ and 3.42 Å for $Ni^{2+} \cdots Ni^{2+}$. The Ni^{2+}–Ba^{2+}–Ni^{2+} angle is 55.1°.

The striking result in these three structures is that, by the complete surrounding of the barium cation, the two salophen units are brought into close proximity in a parallel stacking orientation.

The electrochemistry of the copper-containing heterotrinuclear complexes shows that there is an interaction between the two copper cations. It is therefore likely that also in solution the conformation is folded, similar to the structure in the solid state. Coulometry revealed that these complexes undergo a reduction with two electrons, and cyclic voltammetry showed that the reduction–oxidation processes are chemically reversible.

The electrochemical behaviour of the nickel-containing heterotrinuclear complexes is complicated by adsorption phenomena at the mercury electrode. Significant differences due to variation in the hard cation and structural variation in the ligand have been observed for both the copper- and the nickel-containing heterotrinuclear complexes.

The ESR spectra of the copper-containing trinuclear complex in methanol are in agreement with the electrochemical results and confirm that the conformation of the molecules remains intact. Even the addition of exogenous ligands, which might bridge the two Cu(II) cations, does not alter the structure of the complexes; only in the case of the dicopper–caesium has complex partial decomposition been found in MeOH.

It was also suggested that the unpaired electrons are not completely located on Cu(II), but as a result of covalency are delocalized over the salophen units.

The template synthesis of heterotrinuclear complexes of the compartmental macrocyclic ligands H_2-**109** and H_2-**110** has been reported [71,177].

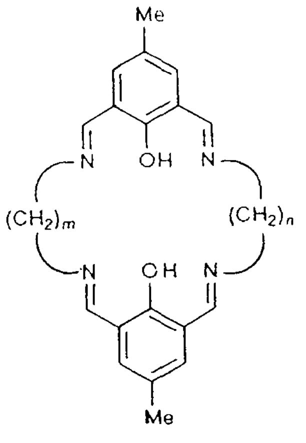

H_2-109

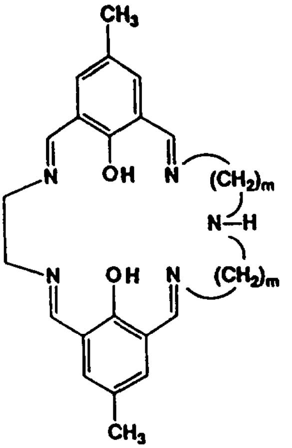

H_2-109'

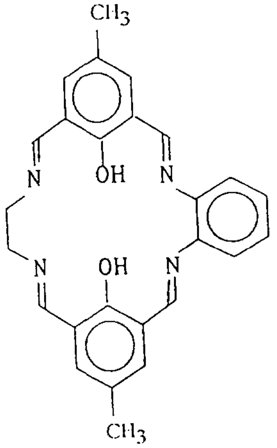

H_2-109"

The reaction of [*N,N'*-ethylene- or *N,N'*-propane-1,3-diylbis(3-formyl-5-methylsalicylideneiminato)]–M(II) (M ≡ Cu or Ni) and a diamine (ethylenediamine, propane-1,3-diamine, butane-1,4-diamine or pentane-1,5-diamine) in the presence of PbX_2 ($X \equiv ClO_4^-$, PF_6^-, BPh_4^- or BF_4^-) gives the macrocyclic complexes $\{Pb[M(\mathbf{109})]_2\}X_2$.

When the aliphatic chains are CH_2CH_2, it is impossible to obtain M_2Pb heterotrinuclear complexes probably because the second N_2O_2 cavity, constructed with ethylenediamine, is too small and rigid to incorporate a large lead(II) ion.

$\{Pb[Cu(\mathbf{109})]_2\}(ClO_4)_2 \cdot dmf$ is composed of the trinuclear complex cation $\{Pb[Cu(\mathbf{109})]_2\}^{2+}$, two perchlorate ions, and a dmf molecule. Two Cu(**109**) entities in the cation are structurally similar to each other, the copper(II) ion being bound at one of the N_2O_2 sites. The other N_2O_2 site of Cu(**109**) is coordinated to the lead(II) ion. The lead(II) ion is sandwiched between two quadridentate Cu(**109**) molecules forming eight coordination. The configuration around the Pb may be approximated by a square antiprism. The Cu $\cdots$ Pb separations are 3.442 and 3.424 Å (Fig. 83(a)).

The Ni_2Pb complexes are diamagnetic while the magnetic moment (per Cu atom) of the Cu_2Pb complexes falls in the range $(1.78–1.90)\mu_B$ and is temperature independent, suggesting no interaction between the two copper(II) ions, in line with the Cu–Cu separation (about 6 Å) found for $\{Pb[Cu_2(\mathbf{109})]_2\}(ClO_4)_2 \cdot dmf$ [177].

It must be noted that the template synthesis $[Pb_2(\mathbf{109})](NO_3)_2$, using lead(II) ion as template, is practicable [140,142]. The crystal structure of the analogous perchlorate complex $[Pb_2(\mathbf{109})](ClO_4)_2$ [177] shows that the two lead(II) ions are bound at the N_2O_2 coordination sites, sharing the bridging phenolic oxygen atoms. A perchlorate anion bridges two neighbouring macrocyclic molecules. One of the

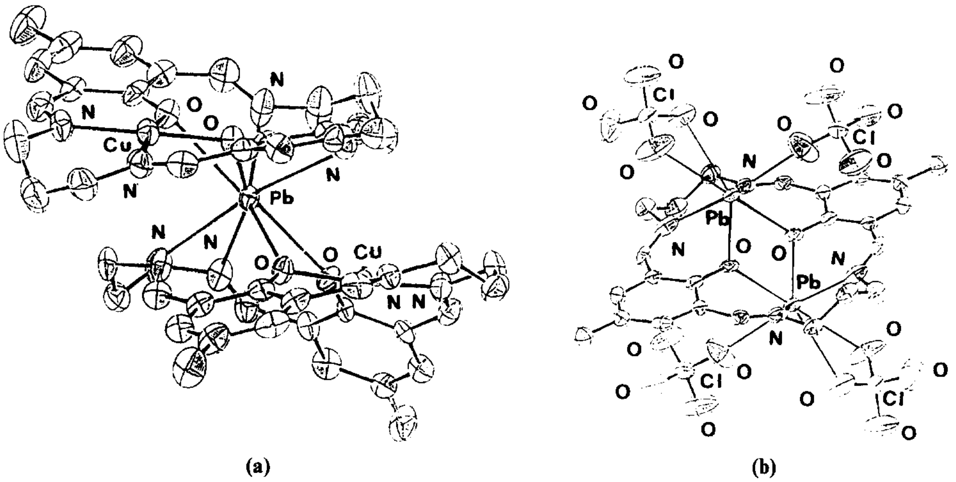

Fig. 83. Structures of (a) $\{Pb[Cu_2(\mathbf{109})]_2\}(ClO_4)_2 \cdot dmf$ and (b) $[Pb_2(\mathbf{109})](ClO_4)_2$.

perchlorate oxygen atoms coordinates to the Pb ion of the macrocyclic molecule and two of them coordinate to the Pb ion of the neighbouring macrocyclic molecule. Thus, the geometry around each metal can be regarded as seven coordination. Each lead(II) ion deviates considerably from the least-squares N_2O_2 plane (1.28 Å) owing to the mismatch between the size of the coordination cavity and the radius of the metal ion. This result suggests a high flexibility of lead(II) ion in coordination (Fig. 83(b)).

When one of the coordination chambers is enlarged as in H_2-**109′**, dinuclear or polynuclear complexes of the type CuM(**109′**)(X)(Y) ((X)(Y) ≡ $(ClO_4)_2$, $(NO_3)(PF_6)$, $(CH_3COO)(BF_4)$) have been obtained [178].

The structure of [CuPb(**109′**)(CH_3COO)](BF_4)dmf (Fig. 84(a)) consists of a dimeric cation $[CuPb(\mathbf{109'})(CH_3COO)]^{2+}$ bridged by acetate groups, tetraphenylborate ions, and dmf molecules. The Cu is located at the 4 coordination site formed with the ethylene chain and assumes a planar environment. The Pb is at the

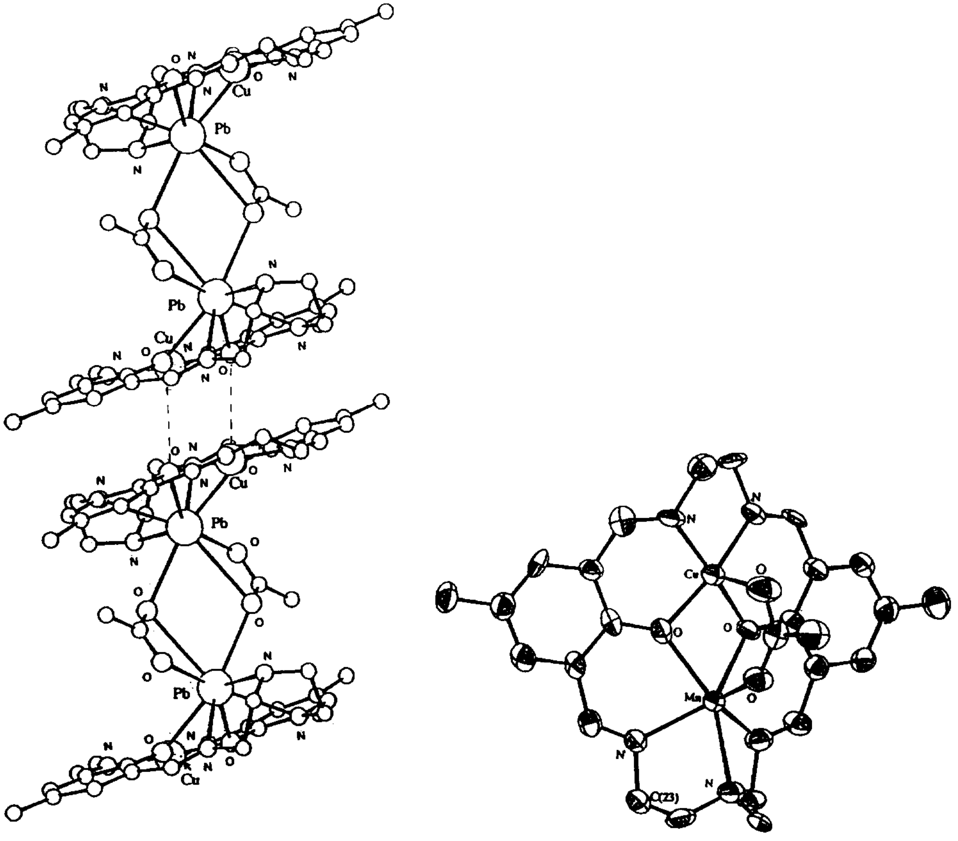

(a) (b)

Fig. 84. Structures of (a) $[CuPb(\mathbf{109'})(CH_3COO)]_n^+$ and (b) $[CuMn(\mathbf{109'})(CH_3COO)]^+$.

5 coordination site formed with the $-(CH_2)_2NH(CH_2)_2-$ chain and assumes an eight-coordinate structure also involving three acetate oxygen atoms. The Cu–Pb separation, bridged by two phenolic oxygen atoms, is 3.577 Å. In the crystal, the dimeric cations further interact through out-of-plane bonding between the $[CuN_2O_2]$ entities forming a column along the *a* axis [178].

The CuPb(**109′**)(X)(Y) complexes react with MSO_4 (M ≡ Mn, Fe, Co, Ni, Cu, Zn) to form the corresponding CuM(**109′**)(X)(Y) complexes [178]. The structure of [CuMn(**109′**)(CH_3COO)](BF_4) shows the Cu(II) and Mn(II) ions reside at the 4 and 5 coordination sites of the macrocycle respectively, and the acetate group bridges the two metal ions providing a nearly square pyramidal geometry for the Cu and a highly distorted six-coordinate environment for the Mn. The Cu–Mn separation is 3.122 Å [178] (Fig. 84(b)).

The cryomagnetic investigation (4.2–300 K) for the CuMn, CuFe, CuCo, CuNi, and CuCu complexes reveal the operation of an antiferromagnetic spin exchange interaction within each molecule. The cyclic voltammograms of the CuM complexes indicate Cu(II)/Cu(I) reduction near −0.8 V (SCE) and oxidation at the ligand centre near +1.3 V. The oxidation of the Fe(II) of the CuFe complex occurs at +0.64 V whereas the Mn(II) ion of the CuMn complex and the Co(II) ion of the CuCo complex are hardly oxidized [178].

Recently, heterodinuclear CuPb complexes of macrocyclic analogues of H_2-**109**, in which one lateral bridge is a simple alkane chain, $-(CH_2)_n-$ ($n = 2, 3$), and another bridge is a hydroxyl-containing chain, $-(CH_2)_nCH(OH)(CH_2)_n-$ ($n = 1$ or 2), have been obtained. In these CuPb complexes, the second donor site of the macrocycles can incorporate a lead(II) ion by coordination of the hydroxy oxygen to the metal ion [179].

An analogous configuration has been proposed for the copper(II)–lanthanum(III) complex, Cu_2La(**109″**)$(NO_3)_2(OH)$, prepared by template condensation of [*N*,*N*′-phenylene-bis(3-formyl-5-chlorosalicylideneiminato]-copper(II) with 1,2-diaminoethane in the presence of $La(NO_3)_3 \cdot 6H_2O$ [71]. Again the ligand, owing to the reduced cavity, is believed to coordinate the lanthanum(III) ion through oxygen and nitrogen atoms above and below the equatorial plane. The lability of this complex in solution may be caused by the N_2O_2 site not involved in the coordination to the copper(II) ion: it could be too small and not flexible enough for a strong coordination to the 4f ion [71].

Unsymmetrical macrocycles, capable of binding three or more metal ions in close proximity, providing different types of metal-binding environments, have been synthesized [180]. The precursor dilead(II) complex, $\{[Pb_2$(**110**)$(Cl)](ClO_4)_2\}_n$, which is central to the synthesis of the desired trimetallic complex was obtained from the reaction of Scheme 38. $\{[Pb_2$(**110**)$(Cl)](ClO_4)_2\}_n$ adopts a polymeric chain structure (Fig. 85). The two lead ions are in crystallographically independent but chemically similar coordination environments. They are bridged by the phenolic "head" unit, so each lead ion occupies one "side" of the macrocycle and is bound

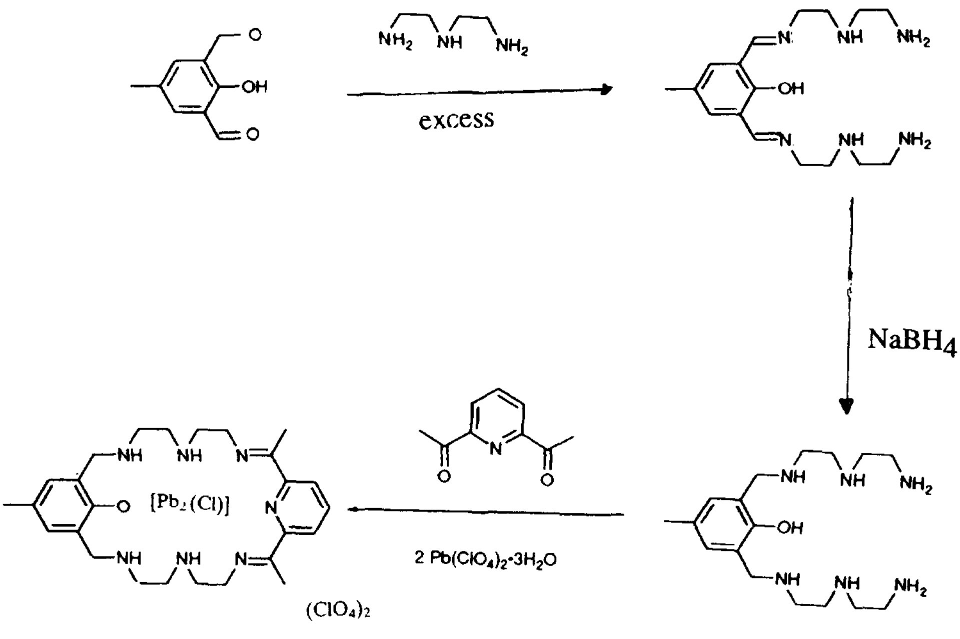

$\{[Pb_2(\mathbf{110})(Cl)](ClO_4)_2\}_n$

Scheme 38.

by a chloride ion, a phenolic oxygen atom, two amine nitrogen atoms, one imine nitrogen atom and weakly by the bridging pyridine nitrogen atom. The result is a distorted six-coordinate geometry about lead. There are also weak interactions with the perchlorate anions. The chloride ion bridges the lead ions in adjacent macrocycles; the macrocycle is far from planar. This twist occurs so that the macrocycle may bind to the two lead ions. Bonds to the phenolic "head" of the macrocycle are somewhat shorter than those to the pyridine nitrogen atom does interact weakly with the lead ions, and in so doing it forms an unusual bridge [180].

The formation of a weak bridging interaction is facilitated by macrocyclic constraints, which hold the pyridine nitrogen atom in close proximity to the lead ions. **110** was designed to bind three transition metal ions so when templated on two large lead ions, which bind at the phenolic "head" of the macrocycle, the pyridine nitrogen atom is left "available" for such an interaction.

Transmetallation reactions of $\{[Pb_2(\mathbf{110})(Cl)](ClO_4)_2\}_n$ with a wide variety of transition metal ions indicate that trinuclear complexes are formed when the large lead ions are replaced by smaller transition metal ions.

One recently isolated example of this is the emerald green tricopper(II) complex of **110**, $Cu_3(\mathbf{110})(OH)(ClO_4)_4(H_2O)$. The IR spectrum shows that the macrocycle

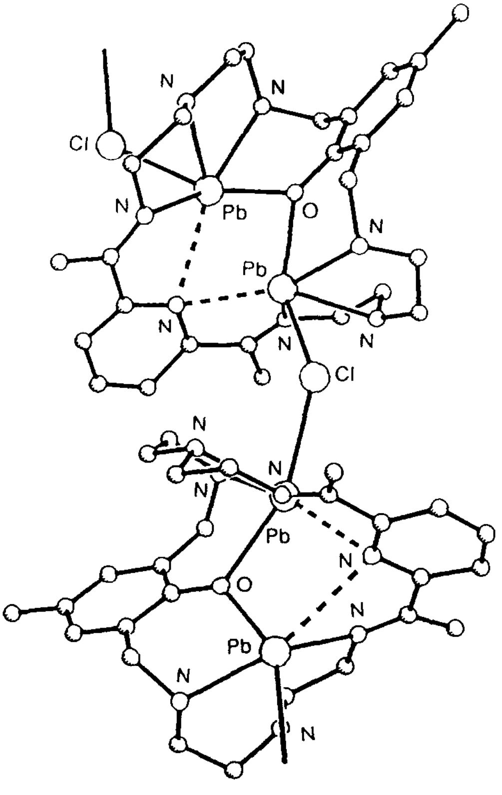

Fig. 85. Structure of $\{[Pb_2(\mathbf{110})(Cl)](ClO_4)_2\}_n$.

remains intact and fast atom bombardment mass spectrometry gives a cluster of peaks corresponding to $[Cu_3(\mathbf{110})(OH)(ClO_4)_3]^+$: the fragmentation pattern is consistent with the stepwise loss of perchlorate from this species [180].

Most of the above trinuclear complexes are formed by a chelating ligand L forming mononuclear complexes of the type ML_2. These mononuclear complexes, acting as ligands toward transition metal ions, afford homo- or heterotrinuclear complexes of the formula $[ML_2]_2M'$. Only a few trinuclear complexes have been described with a true trinucleating ligand.

The design and preparation of heteropolynuclear complexes with trinucleating ligands present some interesting problems. To accomplish a controlled synthesis, it is necessary to direct different metal ions, with specificity, to different binding sites within the ligand molecule.

1,7-diphenyl-1,3,5,7-heptanetetraone and 1,3-bis(2-hydroxyphenyl)-1,3-propanedione have a high specificity in the achievement of this controlled synthesis. The first ligand represents the highest of the series of β-polyketones in which the well-known 1,3-diketones are the simplest members and 1,3,5-triketones the intermediate members. They may be altered by varying the terminal R and R′, replacing hydrogen atoms on the backbone carbon atoms with other groups, replacing the ketonic oxygen atoms with other electron pair donors and increasing the number of ketone groups. These ligands are readily enolizable and form polyanionic species in the presence of a base. By use of a homologous series of ligands, a homologous series of chelates may be presented in which the major structural features are constant.

There are many papers on 1,3,5-triketonate chelates, and their properties (magnetic, optical, redox, catalytic, etc.), together with those of the related Schiff base complexes, have been studied in detail and also reviewed [181].

The triketones are ligands which are not particularly suitable for the formation of binuclear uranyl(VI) complexes, as the seven-coordinate pentagonal bipyramidal geometry around this ion imposes constraints on these chelating ligands. On the contrary, no problem arises for the preparation of mononuclear complexes. The structure of a mononuclear uranyl(VI) complex with 1,5-diphenyl-1,3,5-pentanetrione (Fig. 86(a)) consists of discrete neutral molecules in which the uranium is seven-coordinate in the usual pentagonal bipyramidal arrangement [182]. Two triketonate ligands in a cis configuration and one methanolic oxygen atom complete the equatorial pentacoordination. Under somewhat stringent conditions, addition of $(C_2H_5)_3N$ as a base, a trinuclear species has been found for bis(triethylammonium) tris (2,2′,8,8′-tetramethyl-3,5,7-nonanetrionato-μ_3-oxo-tris (dioxouranate) (Fig. 86(b)). This compound contains a nearly equilateral triangle of UO_2^{2+} ions with a central O^{2-} ion trigonally bonded to the three uranium atoms and the terminal oxygen atom bound to one uranium atom and the terminal oxygen atom

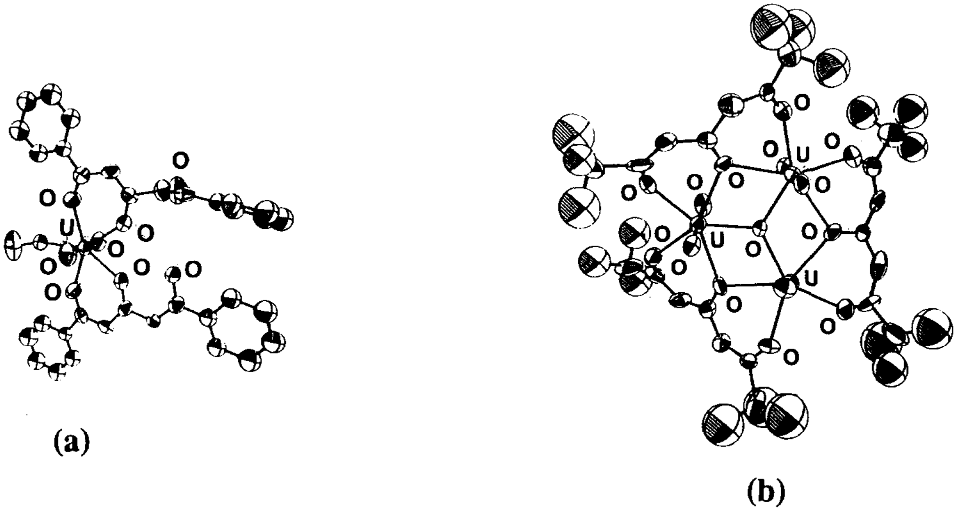

Fig. 86. (a) The molecular structure of bis[1,5-diphenyl-1,3,5-pentanetrionato](methanol)bisdioxouranium(VI) (b) The trinuclear structure of the anion of the complex bis(triethylammonium)-tris(2,2′,-8,8′-tetramethyl-3,5,7-nonanetrionato)-μ_3-oxo-tris(dioxouranate).

bound to one uranium atom. Each uranium atom is seven coordinate in a nearly pentagonal bipyramidal geometry [182].

Homotrinuclear or homodinuclear copper(II), nickel(II) and cobalt(II) complexes have been prepared by reaction of 1,3,5,7-heptanetetra and the appropriate metal salt in methanol–water or acetone–water solution and in the presence of base. Isolation of complexes with two or three metal ions appears to depend on preparative details such as the solvent, temperature and base used.

Magnetic data indicate that trinuclear copper(II) complex exhibits a reduced magnetic moment due to strong antiferromagnetic interactions, while the binuclear complex exhibits a normal magnetic behaviour typical of isolated copper(II) ions. The lack of free carbonyl absorptions in the IR spectra of the binuclear complexes supports the conclusion that, in these compounds, the metal ions occupy the external chambers and are separated rather than adjacent to one another in the inner coordination sites [183].

Several isomorphous heterotrinuclear bis[1,7-diphenyl-1,3,5,7-heptanetetetra-onato(3)]bisdioxouranium(VI)M(II)-4-tetrapyridine complexes $[(UO_2)_2M(\mathbf{111})_2(py)_4]$ (M(II) ≡ Zn, Cu, Ni, Co, Fe, Mn) have been prepared and characterized [184,185]. Two uranyl(VI) ions occupy the terminal coordination positions in the molecules with four ketonate oxygen atoms and one pyridine nitrogen constituting the five equatorial donor atoms in a distorted pentagonal bipyrimidal coordination geometry; the divalent transition metal ion occupies the central position and is bound to four ketonate oxygen atoms, which all act as bridging atoms between the transition metal and uranium atom. In addition pyridine nitrogen atoms occupy the fifth and sixth coordination position above and below the plane of the tetraketonates (Fig. 87).

It was suggested that a reasonable precursor to the observed product is the binuclear uranyl(VI) complex $UO_2(H\text{-}\mathbf{111})_2(S)_2$.

This could explain the ease and specificity with which these heterotrinuclear complexes are obtained from solutions containing 2:2:1 ratios of ligand:

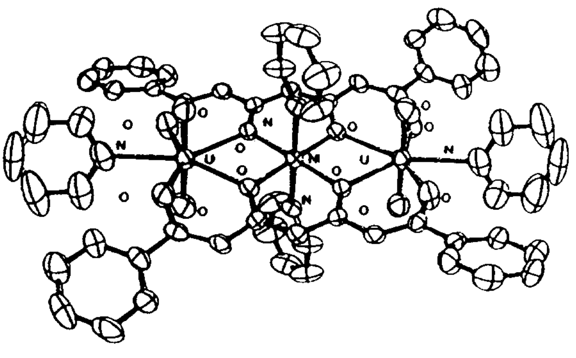

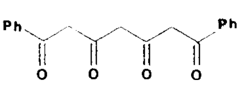

H3-**111**

Fig. 87. Structure of $[(UO_2)_2M(\mathbf{111})_2(py)_4]$ (M ≡ Zn^{2+}, Cu^{2+}, Ni^{2+}, Co^{2+}, Fe^{2+}, Mn^{2+}).

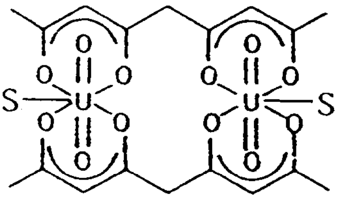

$UO_2(H\text{-}\mathbf{111})_2(S)_2$

$UO_2^{2+}:M^{2+}$. Indeed, attempts were made to prepare 1:1 $UO_2^{2+}:M^{2+}$ and 1:2 $UO_2^{2+}:M^{2+}$ bi- and trinuclear complexes by changing the reaction stoichiometries; however, the only products isolated were the $[(UO_2)_2M(\mathbf{111})_2(py)_4]$ complexes.

1,3-bis(2-hydroxyphenyl)-1,3-propanedione(H_3-**112**) forms pure mononuclear complexes with divalent transition metal ions of the formula $M(H_2\text{-}\mathbf{112})_2$ [186]. The divalent metal ion is coordinated in a square planar fashion by two β-diketone moieties, corresponding to two (H_2-**112**) ligands.

Usually, the coordinated metal fixes two solvent molecules to achieve the hexacoordination around the metal ion [187]. On the contrary, the anionic complex $[Li(H_2\text{-}\mathbf{112})_2]^-$ exhibits a tetrahedral coordination [188], while the Cr(III) and Fe(III) compounds present an octahedral coordination around the metal ion [189].

As a result of their planar structure, only the mononuclear complexes with divalent metal ions are able to afford polynuclear compounds. These are synthesized by treating the mononuclear precursors with a different (heterotrinuclear) or alike (homotrinuclear) metallic salt in a strong basic medium to deprotonate the phenolic groups. The synthetic experimental conditions are critical because mixtures of homotrinuclear compounds, $[MMM(\mathbf{112})_2]$ or $[M'M'M'(\mathbf{112})_2]$, could be obtained probably because of the strong basic medium employed. Compounds of the formula $[(UO_2)_2M(\mathbf{112})_2\cdot(py)_4]\cdot 2py$ are synthesized from the corresponding isomerically pure mononuclear precursors $M(\mathbf{112})_2$ (M ≡ Ni, Co, Zn) by treating them with uranyl acetate in a strong basic medium. The structures of $[(UO_2)_2M(\mathbf{112})_2\cdot(py)_4]\cdot 2py$ (M ≡ Co, Ni) complexes are identical [190] (Fig. 88). The tetragonally distorted octahedrally coordinated divalent metal ion M

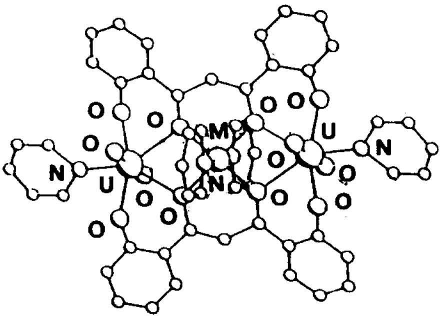

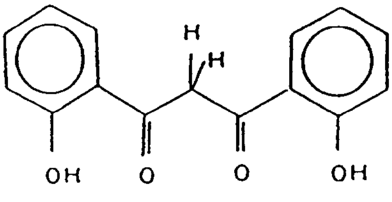

$H_3\text{-}\mathbf{112}$

Fig. 88. Perspective view of $[(UO_2)_2M(\mathbf{112})_2(py)_4]_2\cdot 2py$ (M ≡ Co, Ni).

($M \equiv$ Ni, Co) is placed at the crystallographic inversion centre. It is coordinated with two pyridine groups in the axial direction and by four oxygen atoms of the β-diketone moieties of the two **112** ligands in the basal plane. The uranyl ions occupy the outer coordination positions with two ketonic oxygen atoms, two phenolic oxygen atoms, and one pyridine nitrogen atom constituting the five equatorial donor atoms in a distorted pentagonal bipyramidal coordination sphere geometry. The ligand molecule and the three metal atoms are essentially coplanar. Two additional pyridine molecules are occupying interstitial lattice positions. Again the specificity of this controlled synthesis is achieved because the outer positions are the only position accessible to form the unusual seven coordination of the uranium atoms in these compounds.

By introduction of slight changes in the experimental conditions, a large series of compounds have been obtained, corresponding to mixtures of homotrinuclear species [190]. The boiling temperature used and the relatively long time required to dissolve the mononuclear complex in the presence of a large concentration of triethylamine favour reorganization to yield homotrinuclear complexes. To minimize this reorganization problem, NaH in dry THF at room temperature was used but no analytically pure heterotrinuclear complexes were obtained. Surprisingly, when these heterotrinuclear complexes (CoNiCo, CoZnMn, MnZnMn) are treated with pyridine, outer homodinuclear complexes are obtained, leaving a vacancy in the central position [190].

7. POLYNUCLEAR SYSTEMS

Complexes containing several metal centres in some predetermined arrangement can exhibit quite peculiar chemical and/or physical behaviour. Multielectron reduction or oxidation of substrates may be possible. The relatively accessible arrangement of the four metal centres provided by the organizing ligand may enable substrates to be brought under the influence of two or three or even all four metals simultaneously; only a modest $2e^-$ change per metal is then required for the transfer of up to $8e^-$ either to or from the substrate. Thus for example, the interaction of appropriate complexes with substrates such as O_2 and N_2, which are of considerable chemical, biological, and industrial importance, could prove interesting and useful. Tetramanganese derivatives may provide realistic and useful models for the dioxygen-generating component of the photosynthetic system, which appears to involve four manganese centres in close proximity [191–195].

Preordered arrangement of several metal ions can be dominated by the use of different synthetic strategies:

(i) a single ligand, which can secure into its coordination moiety the desired metal ions;

(ii) macrocyclic or macroacyclic ligands (especially dinucleating) which contain bridging groups capable of binding several metal ions as well as mediating magnetic and/or electronic interaction among them;

(iii) suitable simpler complexes which can act as building blocks for the preparation of more sophisticated systems;

(iv) suitable bridging ligands (Cl^-, ClO_4^-, N_3^- etc.).

The X-ray structure of the copper–yttrium complex [CuY(**81**)(NO_3)(dmso)]$_2$ shows the ability of the phenolato oxygen atoms to act as bridging groups giving rise to polynuclear species.

The interaction of copper salts with the ligand H_2-**113**, obtained by condensation of 3,4-dihydroxybenzaldehyde with 2-aminomethylpyridine, allows the isolation of a nitrate [{Cu(H-**113**)(NO_3)}$_4$], a chloro [{Cu(**113**)Cl}$_2$] and an acetate [{Cu(**113**)(CH_3CO_2)}$_4$] derivative. The acetate complex [{Cu(**114**)(CH_3CO_2)$_2$}$_2$] of a ligand (H_2-**114**) prepared from 2-(2′-aminoethyl)pyridine has been isolated and its structure solved by X-ray diffractometry [195].

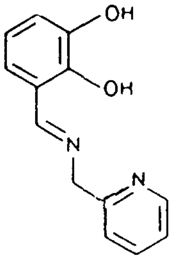

H_2-**113**

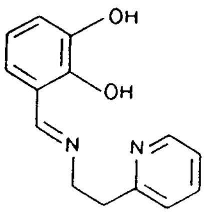

H_2-**114**

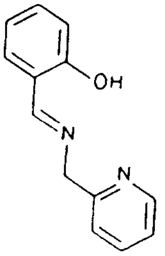

H-**115**

The tetranuclear arrangement of [Cu_2(**114**)(CH_3COO)$_2$]$_2$ results from the dimerization of two dinuclear units comprising one copper atom in the chelate O_2 site and one in the lateral site N_2O. Both oxygen atoms are deprotonated. The two copper ions are thus bridged by one ligand oxygen atom and two acetates complete the bridging network. The fifth ligand is provided by a catechol oxygen from another binuclear unit. The geometries of the two copper sites are quite different. The environment around one copper atom is approximately a trigonal bipyramid while the coordination around the other copper atom is close to a square pyramid (Fig. 89).

The complex [Cu(H-**113**)(NO_3)]$_4$ is tetranuclear and adopts a distorted cubic arrangement, the four copper atoms being bridged by four catecholate oxygen atoms (Fig. 90).

The temperature dependence of the magnetic susceptibility of the [Cu(H-**113**)(NO_3)]$_4$ over the range 6–300 K evidences an antiferromagnetically coupled tetranuclear copper cluster where all four copper atoms are coupled.

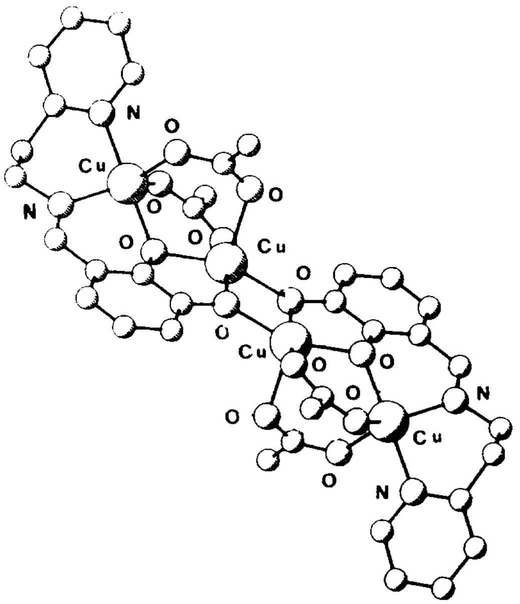

Fig. 89. Structure of compound [{Cu_2(**114**)($CH_3COO)_2$}$_2$].

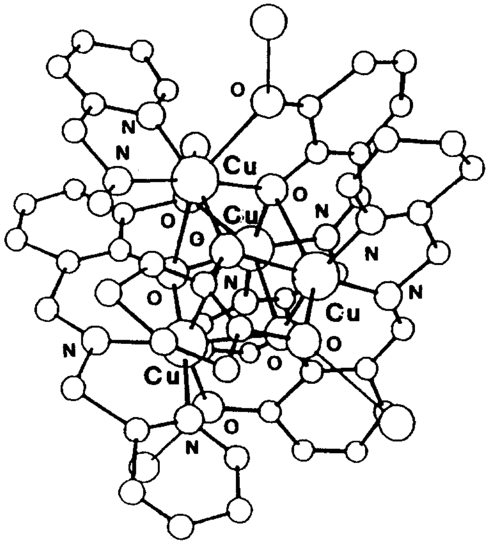

Fig. 90. Structure of [Cu(H-**113**)($NO_3)_4]_4$.

Also the hydroxo oxygen atom can behave as a bridging group leading to the formation of μ_3-OH polynuclear complexes from basically binuclear coordination entities.

One of the species obtained by reaction of the ligand H_3-**116** with cobalt(II) acetate is the tetranuclear compound [Co_2(**116**)(OH)(CH_3COO)]$_2$ (Fig. 91(a)) which

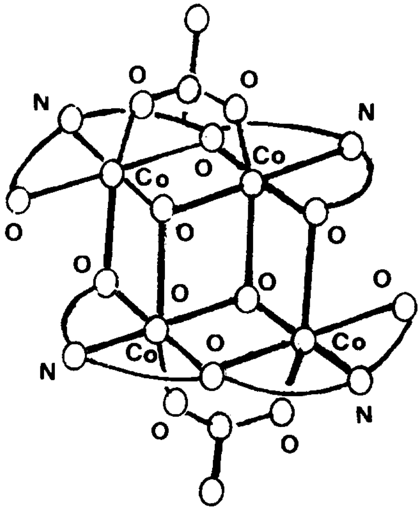

(a)

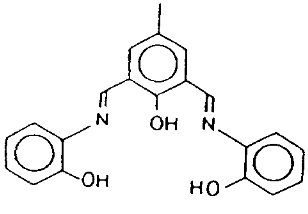

H3-116

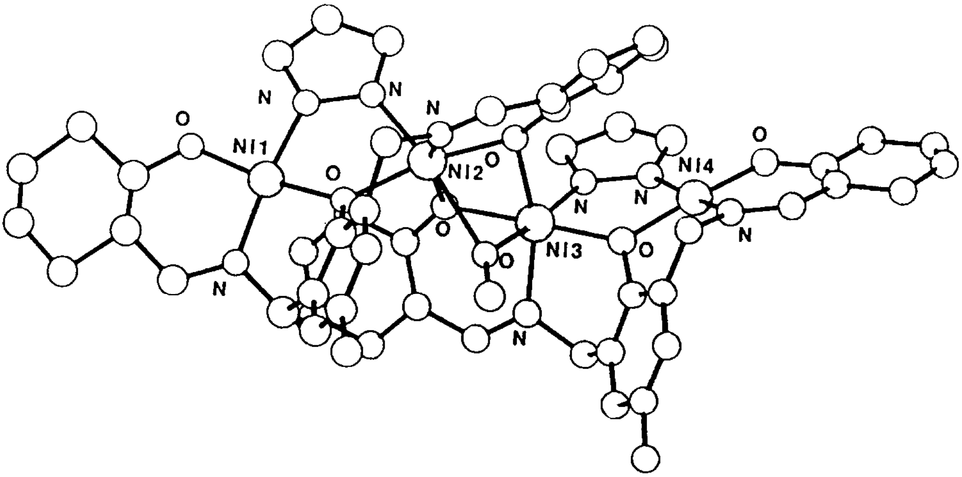

(b)

Fig. 91. Structures of (a) $[Co^{II}Co^{III}(\mathbf{116})(OH)(CH_3COO)]_2$ and (b) $[Ni_4(\mathbf{116})(pyrazolate)_2(CH_3OH)]$.

includes two $[Co^{II}Co^{III}(\mathbf{116})(OH)(CH_3COO)]$ moieties bridged by two μ_3-hydroxo oxygen atoms. In the binuclear unit, the Co(II) and Co(III) ions are bridged through the central phenolate oxygen atom of **116**, the acetate group and one hydroxo group. Fron molecular weight and conductivity measurements, the analogous nickel(II) complexes were assumed to involve similar neutral tetranuclear species [196].

The tetranuclear complex [Ni_4(**116**)(pyrazolate)$_2$(CH_3OH)] has been obtained by reaction of H_3-**116**, $Ni(ClO_4)_2 \cdot 6H_2O$ and triethylamine in methanol [196].

The structure (Fig. 91(b)) has a zigzag tetranuclear unit which is formed by association of the two dinuclear molecules by virtue of a phenoxo oxygen atom and two nitrogen atoms of the pyrazolate ion. Similarly, the Ni3 and Ni4 atoms are bridged by a phenoxo oxygen atom and two pyrazolate nitrogen atoms. These dinuclear units are connected by phenoxo oxygen atoms and a methanol oxygen atom forming a face-shared bioctahedron. The Ni–Ni separations are 3.416 Å, 3.002 Å and 3.418(4) Å for Ni1–Ni2, Ni2–Ni3 and Ni3–Ni4 respectively. The coordination geometries of the Ni2 and Ni3 atoms are distorted octahedra, while the environments of the Ni1 and Ni4 atoms are close to square planar. These structural features indicate that the Ni2 and Ni3 atoms are high spin (paramagnetic) Ni(II), and the Ni1 and Ni4 atoms are low spin (diamagnetic) Ni(II) atoms [196].

The effective magnetic moment of [Ni_4(**116**)(pyrazolate)$_2$(CH_3OH)] ($2.24\mu_B$ (Ni atom)$^{-1}$ at 300 K) is smaller than the spin-only value for high spin nickel(II); variable-temperature magnetic susceptibility data, over the temperature range 80–300 K, gave $J = -4.71$ cm^{-1} and $g = 2.25$ and have been interpreted as due to magnetic interaction between the two paramagnetic Ni2 and Ni3 centres [196].

On reacting H_3-**116** with $Mn(CH_3COO)_2 \cdot 4H_2O$ in a nitrogen atmosphere and in MeOH, the dodecanuclear manganese(II) complex [$(Mn)_{12}$(**116**)$_6$$(OH)_4$($CH_3COO$)$_2$] was obtained and characterized by X-ray diffractometry [197]. The unit cell of these crystals includes four asymmetric dodecanuclear units. Each dodecanuclear asymmetric aggregate is built from six binuclear units whose space arrangement corresponds to a 10 Å radius sphere. The 12 manganese(II) ions constitute two crowns of six metal ions held together by 22 oxygen atoms pertaining to the six **116** ligands or to the four hydroxy moieties. Each crown is capped by a bridging acetate anion in a bisbidentate coordination mode. Each of the 12 manganese(II) ions is oxygen bridged to four nearest manganese neighbours with Mn–Mn distances ranging from 3.16 to 4.14 Å. This structural arrangement affords a predominance of the antiferromagnetic interactions in the aggregate ($J = -3$ cm^{-1}); the ESR spectra of this dodecanuclear manganese(II) aggregate reveal the first example of inhomogeneous exchange narrowing in frozen solution [197] (Fig. 92).

Using the compartmental ligand H_3-**117**, the tetranuclear complex [Cu_2(**117**)(OH)(dmso)(H_2O)]$_2$ was obtained from dimethylsulphoxide [198]. The molecule, formed by two binuclear parallel units held together by two μ_3-OH bridges, adopts a chair conformation. One copper atom of the binuclear unit is five coordinated in a square pyramidal arrangement, while the second copper atom is square planar (Fig. 93).

A similar tetranuclear structure has been obtained for the copper(II) complex with the ligand 2,6-diformyl-4-methylphenol-di(benzoylhydrazone) [199].

The hexanuclear copper(II) complex [Cu_3(**118**)(OH)(dmf)]$_2$(μ-Cl)-

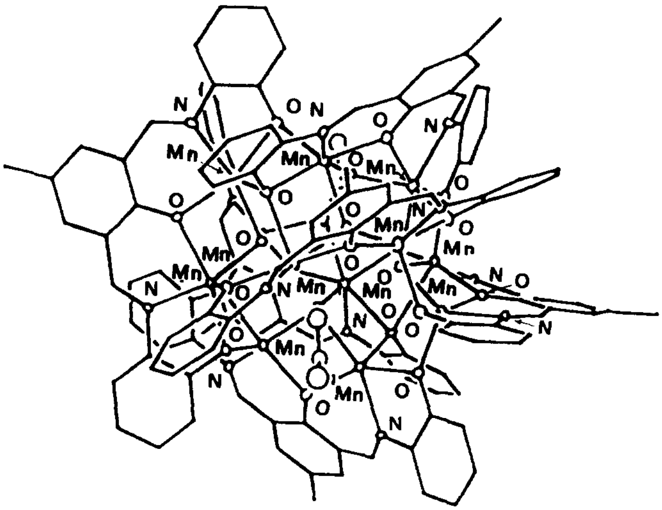

Fig. 92. View of the dodecanuclear aggregate $[(Mn)_{12}(\mathbf{116})_6(OH)_4(CH_3COO_2)_2]$.

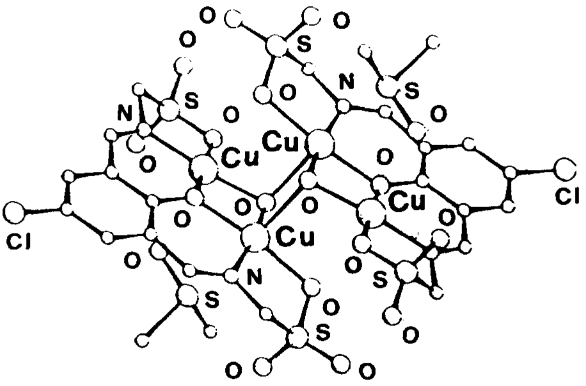

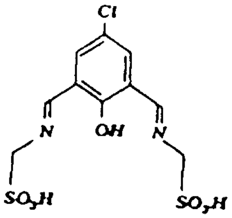

H_3-**117**

Fig. 93. Structure of $[Cu_2(\mathbf{117})(OH)(dmso)(H_2O)]_2$.

(μ-**118**)] · 2dmf, where H_3-**118** is 4-nitro-2,6-bis[salicylideneamino)methyl]phenol consists of two μ_3-$Cu_3(OH)$ cores held by three peripheral bridging ligands and an μ-chloro bridge [200] (Fig. 94).

When 2,6-diformyl-4-methylthiophenol is used as keto precursor, the corresponding compartmental Schiff bases are capable of binding two soft metal ions. Several palladium(II) complexes have been prepared and their reactivity or catalytic behaviour studied [11]. Generally, these complexes are prepared by reaction of $Pd(CH_3COO)_2$ with an S-protected Schiff base, in which metal-promoted S deprotection and complex formation occur in a "one-pot" reaction (Scheme 39).

The reaction of the dipalladium(II) complex $Pd_2(\mathbf{119})(CH_3COO)$ with PPh_3

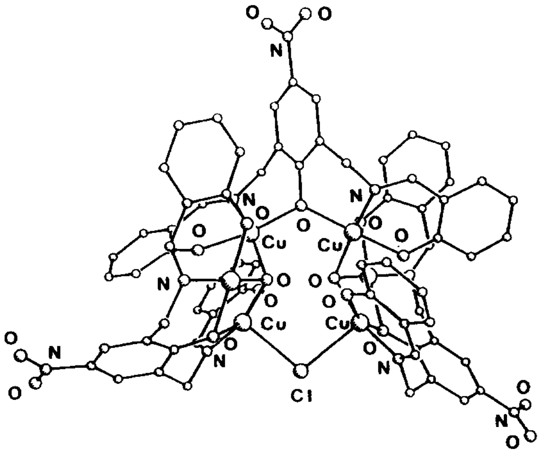

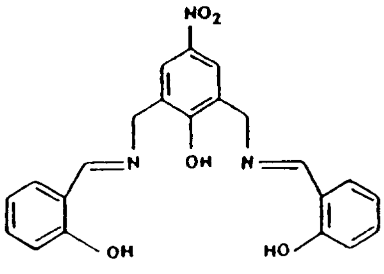

H3-118

Fig. 94. Structure of $\{[Cu_3(\mathbf{118})(dmf)]_2(\mu\text{-}Cl)(\mu\text{-}\mathbf{118})\}$.

in refluxing toluene led to the oxidation of one Schiff base side arm to a benzoxazole with the formation of Pd(**120**)(PPh_3). The same complex was obtained also by deliberate oxidation with $Pb(CH_3COO)_4$ of Pd(H-**119**)(PPh_3). Reaction of $AgClO_4$ either with Pd(H-**119**)(PPh_3) or with Pd(**120**)(PPh_3) gives $[PdAg(\mathbf{120})(PPh_3)]_2(ClO_4)_2$ whose structure contains centrosymmetric dimeric cations in which monomeric $[PdAg(\mathbf{120})(PPh_3)]^+$ units are linked together by bonds from the sulphur of one to the silver of the other. The Ag–S–Ag angle (61.9°) is unusually acute and the Ag ··· Ag distance (2.779 Å) is very short (Fig. 95) [201].

The tetranuclear manganese(III) complex $[(Mn_4(\mathbf{121})_2(CH_3O)_4(CH_3OH)_4]$-$(ClO_4)_2 \cdot 4CH_3OH$ was obtained by reaction of 3,5-bis(salicylideneamino)methylpyrazole (H_3-**121**) with manganese(II) acetate and sodium perchlorate [202].

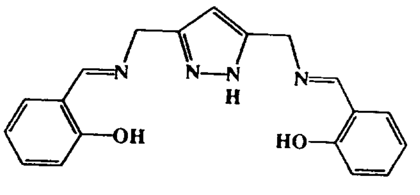

H3-121

The crystal structure reveals the presence of the centrosymmetric complex cation $[Mn_4(\mathbf{121})_2(CH_3O)_4(CH_3OH)_4]^{2+}$ with four linearly arrayed Mn(III) ions. Each terminal Mn(III) ion is bound at one NNO coordination site of **121** through a pyrazolate nitrogen atom and salicylideneaminate nitrogen and oxygen atoms and assumes a distorted octahedral geometry together with two methanol oxygen atoms and one methoxide oxygen atom acting as a bridge to the adjacent internal Mn(III)

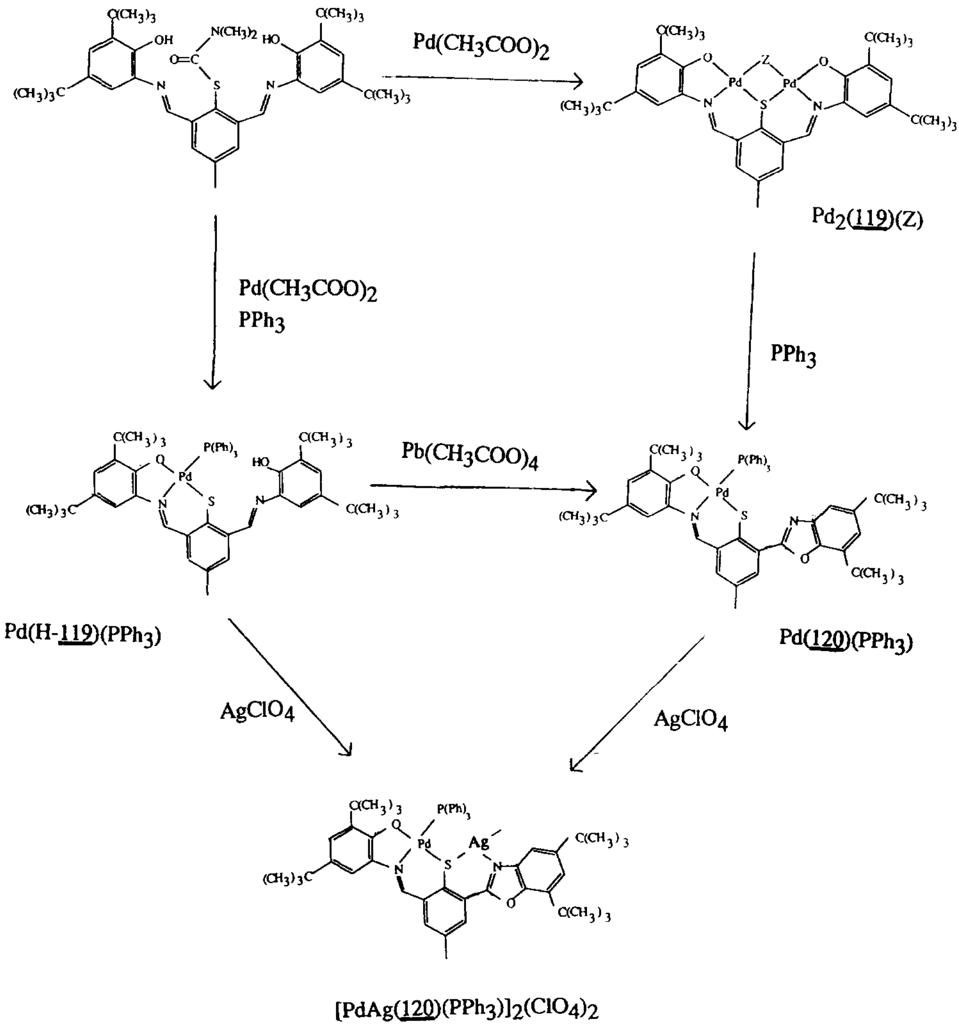

Scheme 39.

ion. The pyrazolate nitrogen atom of the other NNO site coordinates to the adjacent internal Mn(III) ion, but the salicylideneamine nitrogen and oxygen atoms are associated with coordination to another internal Mn(III) ion. The separation between the terminal and internal Mn(III) ions, bridged by the pyrazolate group and methoxide ion, is 3.485 Å. The two internal Mn(III) ions are bridged to each other by two methoxide oxygen atoms (Mn–Mn = 3.127 Å), and each metal assumes a distorted octahedral configuration (Fig. 96).

1,5-bis(salicylideneamino)-3-pentanol (H_3-**122**) reacts with $Mn(CH_3COO)_3 \cdot$-$2H_2O$ and sodium cyanate in methanol to form the dinuclear [(Mn_2(**122**)-

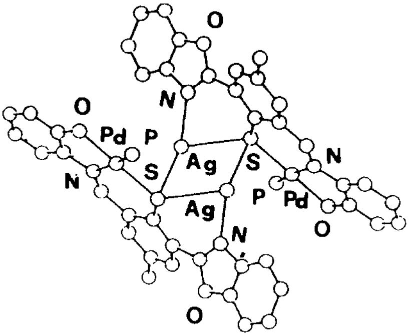

Fig. 95. Structure of $[PdAg(\mathbf{120})(PPh_3)]_2^{2+}$.

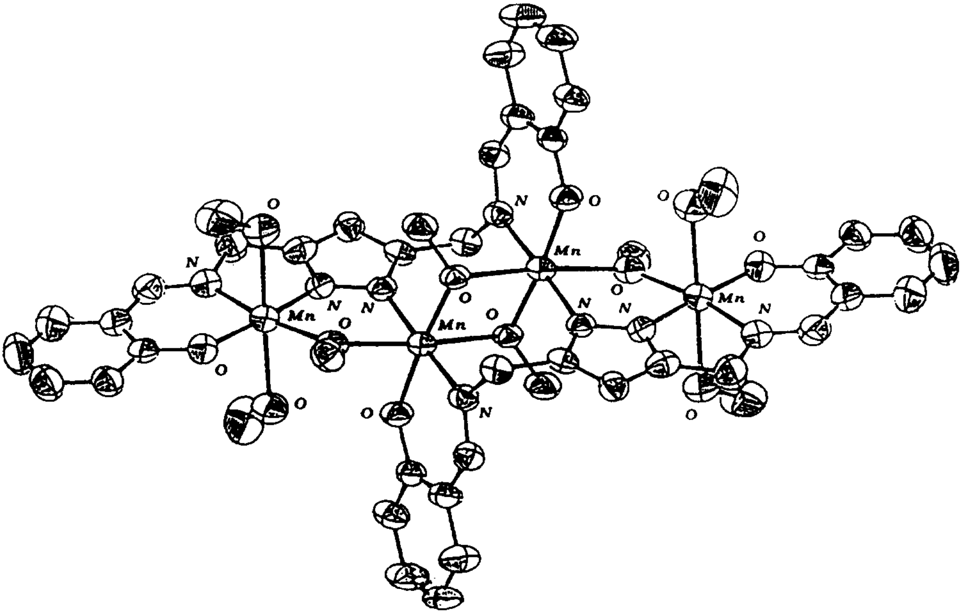

Fig. 96. Structure of $[(Mn_4(\mathbf{121})_2(CH_3O)_4(CH_3OH)_4]^{2+}$.

$(CH_3O)(NCO)_2(H_2O)_2]$ and the tetranuclear $[Mn_4(\mathbf{122})_2(O)_2(CH_3COO)_2]\cdot$-$4H_2O\cdot 2CH_3OH$ [203] (Fig. 97(a)).

In the dinculear complex, the Mn ··· Mn separation is 2.98 Å. The coordination geometries are elongated octahedra for both manganese ions. The square plane around each manganese ion is formed by NO_3 donor atoms of **122** and the bridging-methoxy oxygen atoms. The elongated octahedral coordination is achieved by the weak coordinations of cyanate ion and a water molecule at the apical positions.

In the binuclear half of the tetranuclear complex, the two manganese atoms are bridged by the alkoxy oxygen atom of **122**, the oxo ion and the acetate ion. The

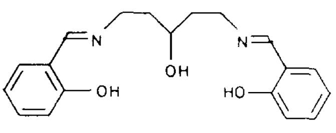

H_3-**122**

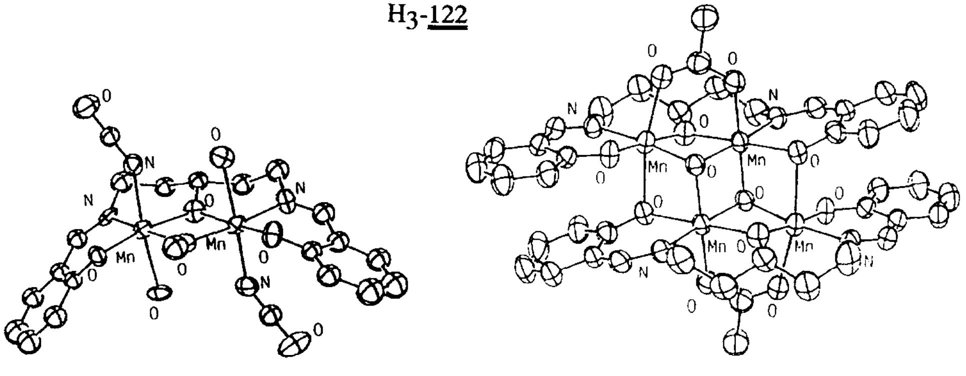

(a)

(b)

Fig. 97. Structures of (a) $[Mn_2(\mathbf{122})(CH_3O)(NCO)_2(H_2O)_2]$ and (b) $[Mn_4(\mathbf{122})_2(O)_2(CH_3COO)_2]$.

two binuclear halves are held together through the oxo ions and the phenoxo oxygen atoms of **122**. Both of the manganese atoms have elongated octahedral MnO_5N geometries. The square plane of one manganese atom is formed by NO_2 donor atoms of **122** and the bridging oxo ion, whereas that of the other manganese atom is formed by an N atom of **122**, two bridging oxo ions, and one oxygen atom of the acetate ion.

This manganese complex has a layered structure consisting of four edge-sharing pseudo-octahedra (MnO_5N), with Mn · · · Mn distances of 2.875 Å and 3.122 Å, with oxo ion bridges between the metal centres whose coordination environment has O donors mainly (Fig. 97(b)). These features are in harmony with those observed for the manganese site in the oxygen evolution centre (OEC) of the photosystem II of green plants.

Magnetic susceptibility measurements on these dinuclear and tetranuclear manganese complexes indicate magnetic moments of $4.08\mu_B$ (Mn atom)$^{-1}$ and $4.32\mu_B$ (Mn atom)$^{-1}$ respectively at room temperature. They decrase to $2.47\mu_B$ (Mn atom)$^{-1}$ and $3.56\mu_B$ (Mn atom)$^{-1}$ respectively at liquid nitrogen temperature, with net antiferromagnetic interactions within the molecules.

On the contrary, the reaction of the smaller 1,3-bis(salicylideneamino)-2-propanol and its ring-chloro-substituted derivatives or of the related formyl and amine precursors with manganese(II) salts in the presence of base does not form the tetranuclear units but the dinuclear manganese(III) complexes of Fig. 98(a) [203].

Each trianionic ligands distributes the five donor atoms between the two metals.

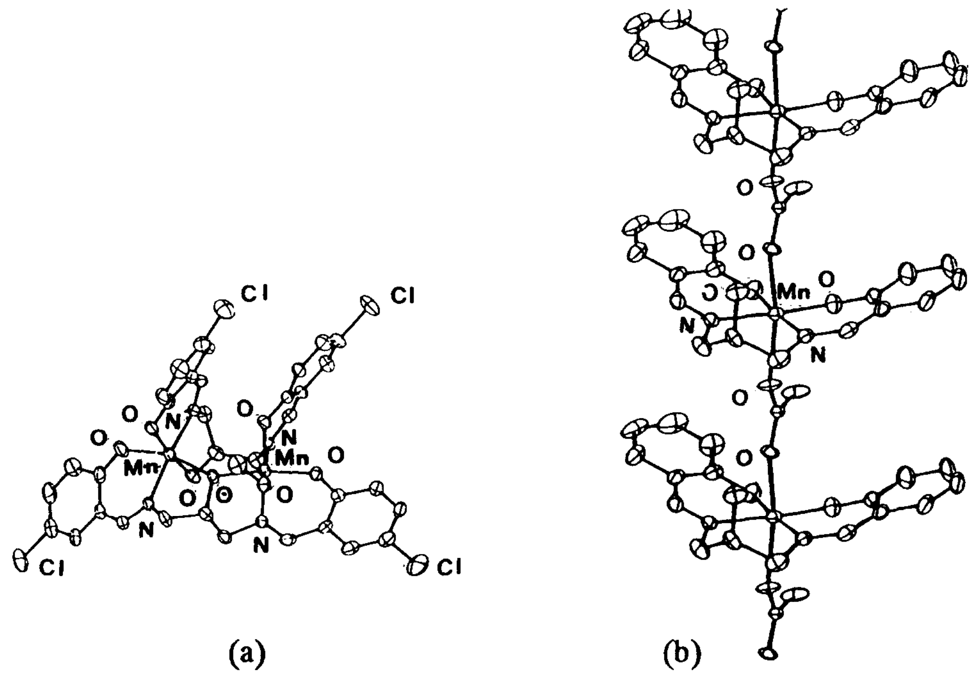

Fig. 98. Structures of (a) the dinuclear and (b) the polymeric acetate chain manganese(III) complexes with the Schiff base 1,3-bis(salicylidene amino)-2-propanol.

One Schiff base acts as a symmetrical binucleating ligand with imino phenolate oxygen and nitrogen atoms coordinated to one manganese atom and the other two oxygen and nitrogen phenolate atoms coordinated to the second manganese atom. The alkoxide oxygen atom acts as an unsymmetric bridge between the two metals. As a result, the manganese(III) ions exhibit a very large separation. The second ligand acts as tridentate about one manganese atom with the oxygen and nitrogen phenolate atoms and with the alkoxide oxygen atom, which is tethered by an ethylene bridged to a bidentate chelating agent, with the remaining oxygen and nitrogen phenolate atoms encapsulating the second manganese atom, whose sixth coordination position is filled by a solvent molecule.

The reaction of 1,3-bis(salicylideneamino)-2-propanol with 3 equivalents of base and 1 equivalent of $Mn(OAc)_3 \cdot 4H_2O$ produced crystals of the polymeric manganese acetate chain reported in Fig. 98(b). Each manganese(III) in the chain has an equatorial plane composed of the two phenolate oxygen atoms and two imine nitrogen atoms of the ligand. The manganese atoms also lie on a mirror plane together with the central backbone carbon and hydroxyl group and the axial acetates. The alcohol oxygen on the ligand backbone is protonated and uncoordinated. The acetate bridges are in anti–anti orientation [203].

The similar bis(benzoylacetone)-1,3-diimino-propan-2-ol (H_3-**122′**) reacts with manganese(II) acetate in the presence of sodium perchlorate and triethylamine to form black crystals of the trinuclear manganese(III) complex $[Mn_3(\mathbf{122'})_2(CH_3O)_2(CH_3OH)(C_2H_5OH)]$–$(ClO_4)\cdot CH_3OH$ of Fig. 99 [203].

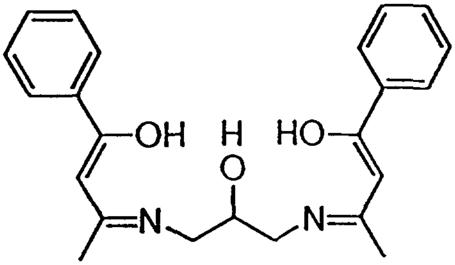

H-<u>122'</u>

The three Mn atoms occupy the corners of an isosceles triangle. The Mn1 and Mn3 atoms are bridged by an alkoxo oxygen atom of a dinucleating ligand and the Mn2 and Mn3 atoms are bridged by an alkoxo oxygen atom of the other dinucleating ligand. Mn1 and Mn2 are also bridged by two methoxo oxygen atoms of the trinuclear manganese(III) complex with bis(benzylacetone-1,3-diiminopropan-2-ol atoms. For Mn3, each dinucleating ligand is tridentate and acts as a meridional bis chelate with one keto oxygen, one imine nitrogen, and one alkoxo oxygen atom in a distorted octahedron. The Mn1 and Mn2 atoms have an elongated octahedral geometry. Each square plane is formed by NO_2 donor atoms of **122'** and the bridging-

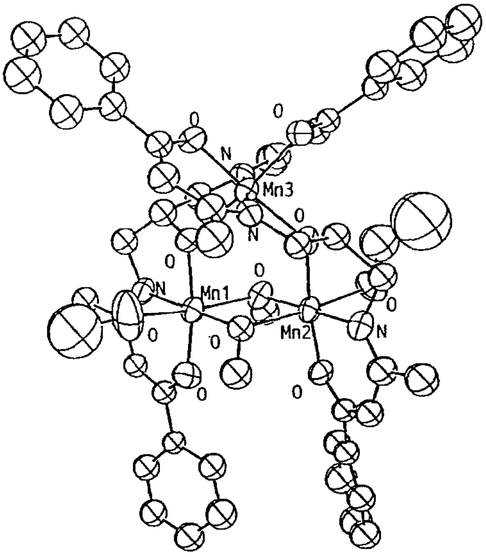

Fig. 99. Structure of $[Mn_3(\mathbf{122'})_2(CH_3O)_2(CH_3OH)(C_2H_5OH)]^+$.

methoxo oxygen atom occupies one site of the apical position. The elongated octahedral coordination is achieved by the weak coordination of a methanol molecule (for Mn1) or an ethanol molecule (for Mn2).

The room temperature magnetic moment ($7.31\mu_B$ molecule^{-1}) for this trinuclear manganese complex is smaller than the spin-only value expected for a three high spin d^4 system. The magnetic susceptibility data measured over a temperature range 80–300 K give a significant antiferromagnetic coupling between Mn1 and Mn2 [203].

A series of tetranuclear manganese complexes has been prepared by the related, not Schiff base ligand 1,5-bis[bis(2-pyriidylmethyl)amino]-3-pentanol (H-**123**) obtained by alkylation of 2-hydroxy-1,3-diaminopropane with 2-(chloromethyl)-pyridine.

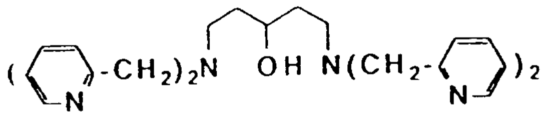

H-123

A dimer of di(μ-oxo)dimanganese(III, IV) dimers was prepared with two coordinated water molecules, $[\{Mn_2(\mathbf{123})(O)_2(H_2O)\}_2](CF_3SO_3)_4 \cdot 6H_2O$, was prepared by reaction of H-**123** with $Mn(NO_3)_2 \cdot 9H_2O$ in the presence of NEt_3 and $Na(CF_3SO_3)$ [204]. Two crystallographically independent tetranuclear complexes are present in the unit cell whose structures are slightly different from each other. The molecular structure of the cation consists of two di(μ-oxo)Mn_2 dimers linked by two **123** bridges to form a dimer of dimers with a bilayered structure. Two Mn⟨OO⟩Mn planes are not faced directly but offset. Two di(μ-oxo)Mn_2 dimers in tetranuclear structure are crystallographically equivalent, since the complex cation possesses an inversion centre. All manganese ions are in distorted octahedra. The oxidation states of the manganese ions in the dimer have been assigned to be 3 and 4. Two water molecules coordinate to manganese(III) ions. The effective magnetic moments of the complex at 300 K and 80 K are $3.50\mu_B$ and $2.51\mu_B$ respectively, indicating the presence of antiferromagnetic interaction between manganese ions. Since two di(μ-oxo)Mn_2(III, IV) dimers are separated by ca. 5.9 Å and there is no bridging group providing the superexchange interaction between dimers, it is reasonable to assume that the exchange interaction between the two dimers is negligible. The J value ($J = -142\ cm^{-1}$) is comparable with those of di(μ-oxo)Mn_2(III, IV) complexes [204].

H-**123** reacts with $Mn(OAc)_3$ in the presence of NEt_3 and $NaClO_4$ to give $\{[Mn_2(\mathbf{123})(CH_3COO)(H_2O)]_2O\}^{4+}$ [205], whose structure (Fig. 100(a)) consists of a pair of $Mn^{II}Mn^{III}$ complexes linked by a single oxo bridge between the Mn^{III} ions. Trapped valence is clearly indicated as bond distances to one manganese are as expected for Mn^{II} atom and likewise the other manganese can be assigned as the

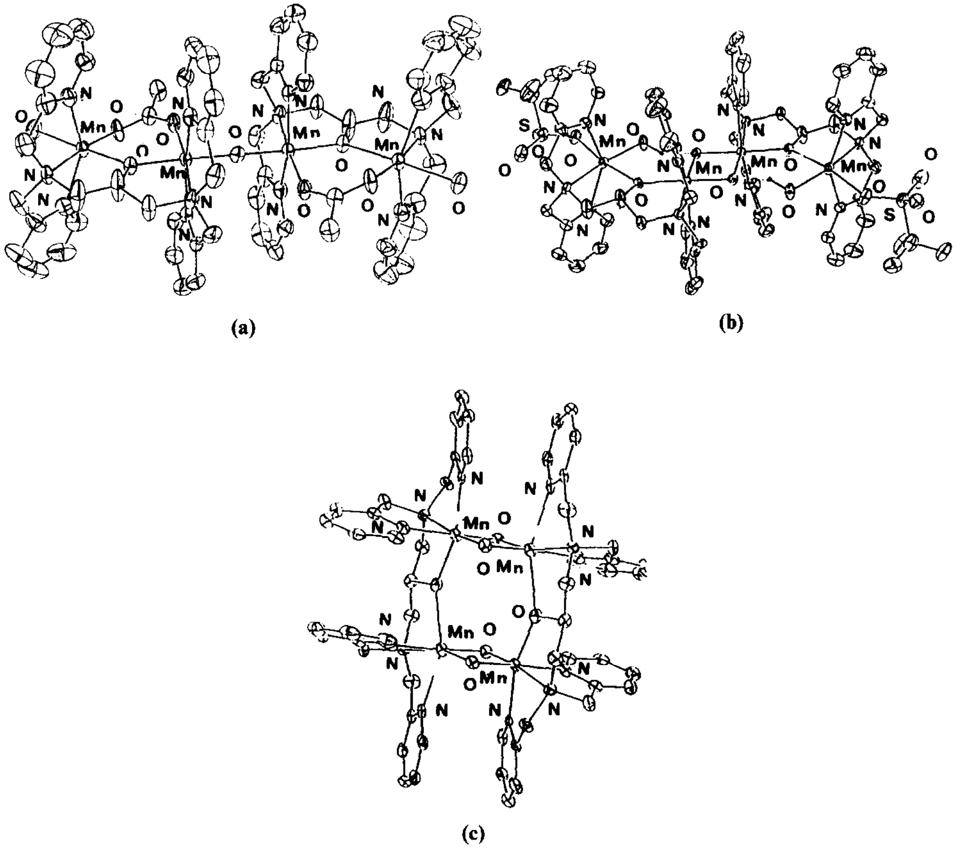

(a) (b)

(c)

Fig. 100. Structures of (a) $\{[Mn_2(\mathbf{123})(CH_3COO)(H_2O)]_2O\}^{4+}$, (b) $[Mn_4O_2(\mathbf{123})(H_2O)_2(CF_3SO_3)_2]^{3+}$ and (c) $[(Mn_2O_2)_2(\mathbf{123})_2]^{4+}$.

Mn^{III} ion. A notable feature of this structure is that the tridentate N_3 ends of the **123** ligand bind in a meridional fashion.

Susceptibility measurements of a powdered sample of $\{[Mn_2(\mathbf{123})(CH_3COO)(H_2O)]_2O\}^{4+}$ indicate that antiferromagnetic interactions within the aggregate are operative. This magnetic behaviour is consistent with relatively weak antiferromagnetic interactions between Mn^{II} and Mn^{III} atoms, as observed for several $Mn^{II}Mn^{III}$ binuclear species, and moderately strong antiferromagnetic coupling between Mn^{III} ions.

According to the cyclic voltammogram of $\{[Mn_2(\mathbf{123})(CH_3COO)(H_2O)]_2O\}^{4+}$ in CH_3CN solution, three quasi-reversible redox waves with $E_{1/2}$ values of approximately 0.83, 1.05, and 1.35 V (SCE) are evident. When an electrode was poised at 0.5 V (SCE) in a MeCN solution of $\{[Mn_2(\mathbf{123})(CH_3COO)(H_2O)]_2O\}^{4+}$, very little current passed and no UV–visible spectral changes occurred, while at higher voltages distinct spectral changes were observed. Thus the cyclic voltammetric waves can be assigned tentatively as shown below although oxidation of coordinated H_2O cannot be ruled out.

The separation between the first two oxidation processes in $\{[Mn_2(\mathbf{123})(CH_3COO)(H_2O)]_2O\}^{4+}$ (about 0.2 V) is substantially less than in other binuclear species possibly as a result of the weak interaction between the two Mn^{II} ions oxidized in the proposed first two cyclic voltammetric processes for $\{[Mn_2(\mathbf{123})(CH_3COO)(H_2O)]_2O\}^{4+}$.

Crystals of $[Mn_4(O)_2(\mathbf{123})_2(H_2O)_2(CF_3SO_3)_2](CF_3SO_3)_3 \cdot CHCl_3$, prepared by air oxidation of $Mn(ClO_4)_2 \cdot 6H_2O$, H-**123** and Et_3N, consist of an inversion-symmetric cationic tetranuclear complex with two of the triflate anions coordinated to manganese atoms (Fig. 100(b)). For this tetranuclear complex, the $Mn^{II}Mn^{III}Mn^{IV}Mn^{II}$ oxidation state assignment was proposed [205]. The coordinated water molecules in the complex are involved in an intermolecular hydrogen bonding interaction to the bridging oxo moieties with contacts of 2.596 Å.

Cyclic voltammetry of $[Mn_4(O)_2(\mathbf{123})_2(H_2O)_2(CF_3SO_3)_2]^{3+}$ in CH_3CN solution, using (Et_4N)–(ClO_4) as supporting electrolyte, reveals two quasi-reversible redox waves with $E_{1/2}$ values of 0.36 V ($E_{pa} - E_{pc} = 0.24$ V) and 0.87 V ($E_{pa} - E_{pc} = 0.27$ V) (SCE). On the basis of spectroelectrochemical studies, the wave at 0.87 V is assigned to an oxidation of $[Mn_4(O)_2(\mathbf{123})_2(H_2O)_2(CF_3SO_3)_2]^{3+}$ and the wave at 0.36 V is assigned to a reduction to the $Mn_2^{III}Mn_2^{II}$ oxidation level. Magnetic susceptibility measurements on a solid sample of $[Mn_4O_2(\mathbf{123})_2(H_2O)_2(CF_3SO_3)_2]^{3+}$ indicate a magnetic moment of $8.7\mu_B$ per molecule at 279 K decreasing to $6.6\mu_B$ at 7 K consistent with net antiferromagnetic interactions within the tetranuclear aggregate.

Vapour diffusion of acetate into a CH_3CN solution of $[Mn_4(O)_2(\mathbf{123})_2(H_2O)_2(CF_3SO_3)_2](ClO_4)_3$ at room temperature yielded the crystalline material $[Mn_2O_2)_2(\mathbf{123})_2](ClO_4)_4$ which was recrystallized from CH_3CN producing $[Mn_4(O)_4(\mathbf{123})_2](ClO_4)_4 \cdot 3H_2O \cdot 2CH_3COCH_3$ [205].

The complex is a trapped mixed-valence species that is reasonably well ordered in the crystal lattice and consists of a pair of $\{Mn^{III}Mn^{IV}O_2\}^{3+}$ cores. In the structure of this complex, the ligand binds in a facial manner (Fig. 100(c)).

2,6-bis[(dimethylamino)methyl]-4-methylphenol (H-**123′**) reacts with *n*-butyllithium to afford the trinuclear compound $(Li(\mathbf{123'})]_3$ [205] and with KH and BaI_2 to afford the tetranuclear oxo cluster $[Ba_4(\mathbf{123'})(\mu_4\text{-}O)_6]$ [205].

In $[Li(\mathbf{123'})]_3$ there is an almost perfectly planar quasi-aromatic Li_3O_3 six-membered ring (Fig. 101(a)). Adjacent lithium atoms are N coordinated by different CH_2NMe_2 substituents of their mutually O-bridging phenolate ligand. The orientation of these ligands with respect to the Li_3O_3 ring provides a “propeller-like” molecule with each trimer having screw-type chirality. Both enantiomers are present in the crystal structure.

Cryoscopic measurements in benzene show that the trinuclear structure is maintained also in solution [205]. When three equivalents of LiI are added to a benzene solution of $[Li(\mathbf{123'})]_3$ at 120°C, $[Li_4(\mathbf{123'})_2(I)_2]$ is obtained. This tetra-

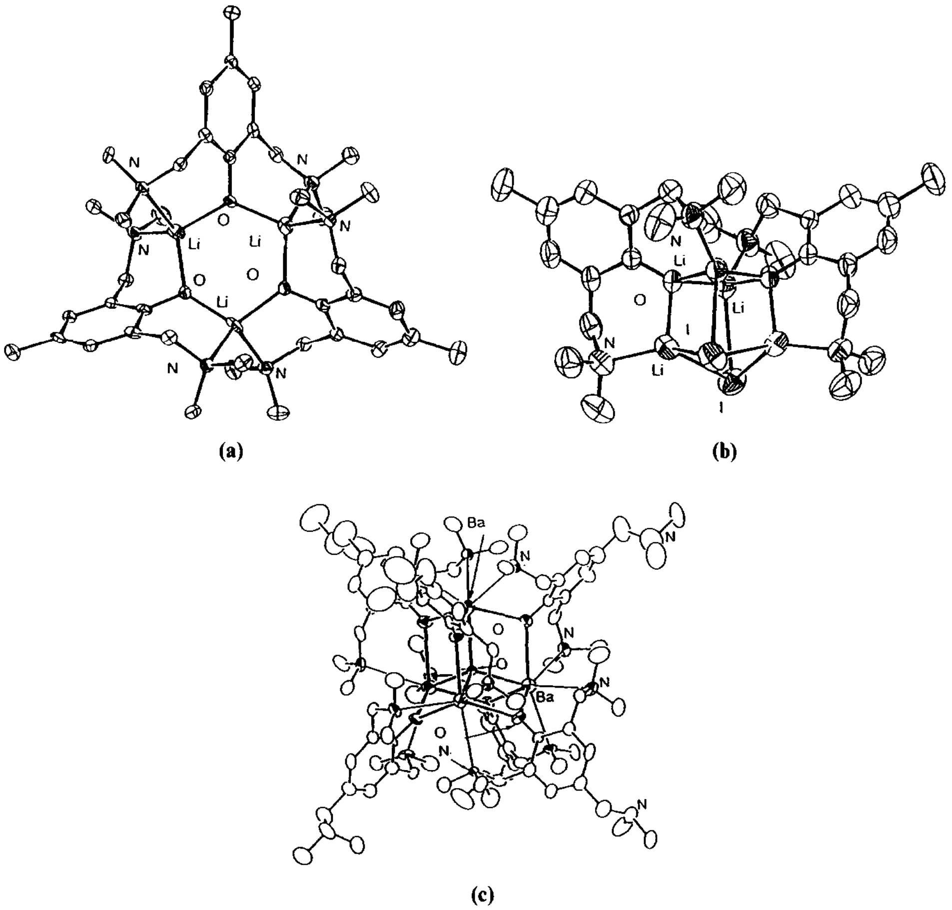

Fig. 101. Structures of (a) $[Li(\mathbf{123'})]_3$, (b) $[Li_4(\mathbf{123'})_2(I)_2]$ and (c) $[Ba_4(\mathbf{123'})(\mu_4\text{-}O)_6]\cdot 3$ toluene.

nuclear complex has been described as a distorted Li_4 tetrahedron with two iodide atoms and the two oxygen atoms of the phenolate ligands coordinating above the four Li_3 faces. The four tertiary amine substituents are all coordinated to different lithium atoms which have a tetrahedral coordination sphere, two with an I, O_2, N environment and two with an I_2, O, N environment. Chemically the structure can be seen as a dimer of two lithium phenolate units each of which contains one molecule of LiI caught by a coordinating amine group [205] (Fig. 101(b)).

$[Ba_4(\mathbf{123'})(\mu_4\text{-}O)_6]\cdot$3toluene [205] (Fig. 101(c)) consists of a tetranuclear cluster of barium atoms encapsulating a μ_4-oxo ligand. Bridging phenolic O groups span each edge of the tetrahedron, and the nitrogen atoms of the *ortho*-dimethylaminomethyl groups also coordinate to the barium atoms, giving each metal a formal coordination number of 7. Three molecules of toluene per cluster are found in the lattice.

On the basis of the results reported above –OH groups were inserted into the coordination moiety of ligands in order to favour the formation of polynuclear species.

The mononuclear $Ba(SCN)_2$ complex of the [2 + 2] macrocycle **45** undergoes a transmetallation reaction with $Cu(ClO_4)_2$ to produce a bimetallic copper complex in which a proton is lost from one OH group and the alkoxide bridges both copper ions. In the crystal, the OH group forms an hydrogen bond with a molecule staked below [206] (Scheme 40).

Structural studies in solution evidence that, when lanthanum nitrate is used as a template in the reaction of 2,6-diacetylpyridine and 1,3-diamino-2-hydroxypropane, the [3 + 3] macrocycle **124** containing three lanthanum ions is the predominant species formed. ^1H NMR decoupling and nuclear Overhauser effect difference spectroscopy confirm the presence of a two-fold axis of symmetry where two sides of the macrocycle are identical and different from the third. This triangular array has recently been confirmed by X-ray structure analysis [207].

In a parallel work [207], the same condensation reaction, in the presence of LnX_3 ($X \equiv NO_3^-$, Ln ≡ La, Pr; $X \equiv NCS^-$, Ln ≡ La, Pr, Nd, Sm, Eu) was reported to produce Ln(**45**-2*H*)$(X)_4$ where a [2 + 2] macrocycle is obtained, but a more recent study [207] has confirmed the formation of [3 + 3] lanthanide complexes of the type [Ln_3(**124**)$(OH)_2(NO_3)_4$]·nH_2O ($n = 4$–7) or [Ln_3(**124**)(OH)-$(NCS)_5$]·$7H_2O$ (Ln ≡ La, Pr, Eu, Gd) [207].

The discrepancy between La_3(**124**)$(NO_3)_6$ and La(**124**)$(OH)_2(NO_3)_4$ may be due to a partial hydrolysis of the hexanitrato complex during its preparation or recrystallization by water.

The X-ray structural determination carried out on crystals of the lanthanum(III) complex grown from water reveals it can be formulated as [Ln_3(**124**)(μ_3-OH)(OH)$(NO_3)_4$]·$7H_2O$. In this structure, the three lanthanum(III) atoms form an equatorial triangle of edge 4 Å. The 30-atom macrocyclic ring is

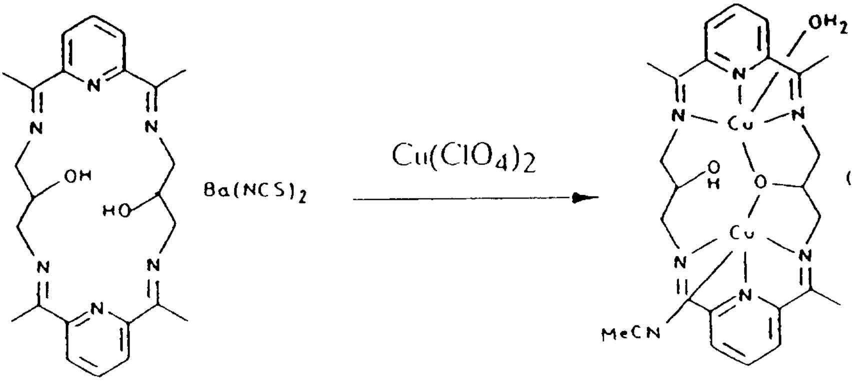

Scheme 40.

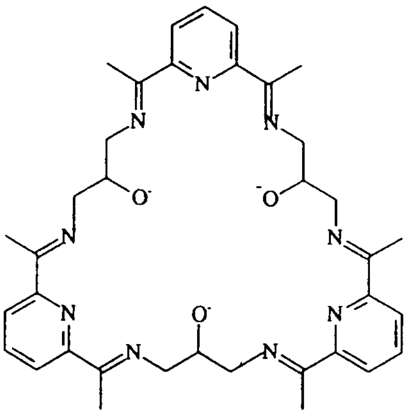

124

made up of three planar 7-atom sections containing the pyridine rings and imine linkages; rotation about the single bonds provides flexibility in the macrocycle. The conformation around one of the $-CH_2-CH(O-)-CH_2-$ chains is different from the other two (Fig. 102).

Each lanthanum is nine coordinate, making five bonds to the macrocycle and four to O atoms of OH^-, NO_3^-, or H_2O. Pairs of [Ln_3(**124**)] are joined by two La–OH–La bridges to make a unit containing six lanthanum atoms lying across a crystallographic inversion centre. There is an extended and intricate network of

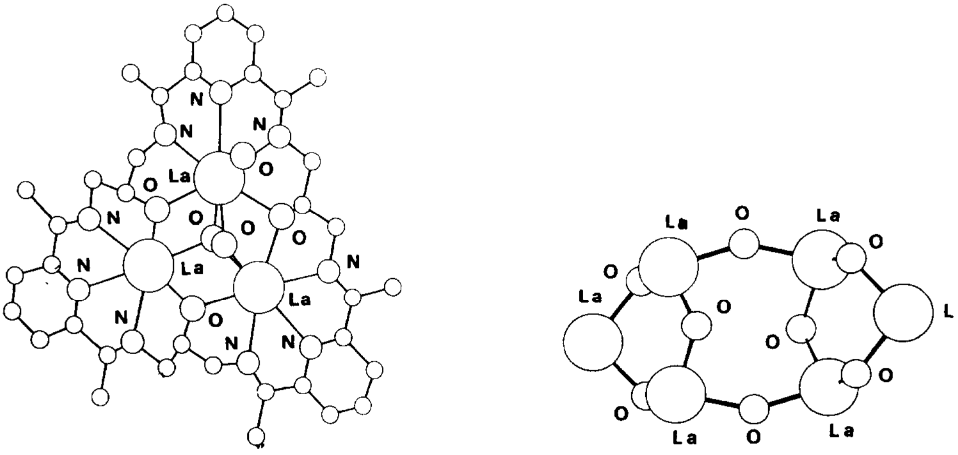

(a)

(b)

Fig. 102. Structure of (a) [Ln_3(**124**)(μ_3-OH)(OH)(NO_3)$_4$] and (b) the two La_3 units linked, across a crystallographic inversion centre, by La–OH–La bridges.

hydrogen bonding involving the non-macrocyclic groups which links the OH^- and NO_3^- ions and lattice molecules.

Magnetic susceptibilities were measured at 297 K for $[Gd_3(\mathbf{124})(OH)_2(NO_3)_4]\cdot4H_2O$ and for $[Pr(\mathbf{124})(NCS)_5(OH)]\cdot7H_2O$. For the praseodymium complex, $\mu = 3.43\mu_B$ per metal ion, which is just within the normal range for Pr^{3+}; the gadolinium complex had $\mu = 6.85\mu_B$, which is significantly less than the spin-only value of $7.94\mu_B$ normally seen for Gd^{3+} complexes.

The reaction of $Ca(NO_3)_2\cdot xH_2O$ with 2,6-diacetylpyridine and 2-hydroxy-1,3-diaminopropane in refluxing methanol produces $[Ca(\mathbf{46})(NO_3)_2]$ where the macrocycle has the ring-contracted structure found in the analogous Pb complex [207].

It has been shown [208] that when $Mn(ClO_4)_2$ is used in a transmetallation reaction of the barium complexes with the [2 + 2] macrocycle **45**, $[Ba(\mathbf{45})(H_2O)]^{2+}$, the [4 + 4] deprotonated macrocycle **125** with four Mn^{2+} ions is formed as a minor product. The four manganese(II) centres, together with the four deprotonated alkoxy groups of the ligand, form a novel cubane-type cluster. Each manganese atom is seven coordinate with approximate pentagonal bipyramidal geometry. The donors in the pentagonal plane are three nitrogen atoms and two alkoxide oxygen atoms while the axial ligands are a third alkoxide and a semicoordinated perchlorate anion ($Mn–OClO_3$, 2.63 Å). There is no evidence for any metal–metal bonding; the shortest manganese–manganese distance is 3.32 Å [208] (Fig. 103).

Transmetallation reaction of $[Ba(\mathbf{45})(H_2O)_2](ClO_4)_2$ with $MnCl_2$ or $Mn(ClO_4)_2$ and NaN_3, followed by a crystallization of the products from dimethylformamide–diethylether or acetonitrile–diethylether respectively, forms the tetramanga-

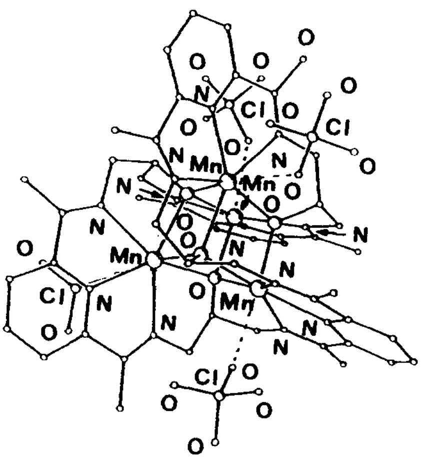

Fig. 103. Structure of $[Mn_4(\mathbf{125})](ClO_4)_4$.

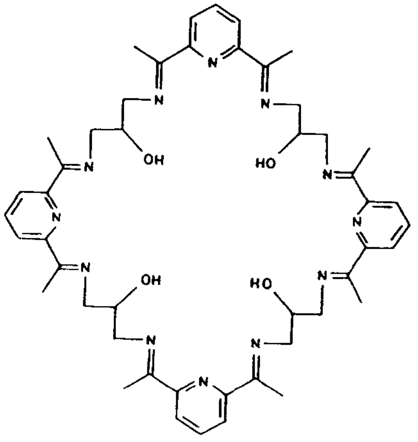

H_4-**125**

nese complexes $[Mn_2(\mathbf{45}\text{-}H)(Cl)_2]_2 \cdot (ClO_4)_2 \cdot 2dmf \cdot H_2O$ and $[Mn_2(\mathbf{45}\text{-}H)(N_3)_2]_2$-$(ClO_4)_2 \cdot 3MeCN$ [208]. The structures of these two complexes (Fig. 104) are quite similar, dimeric with the two macrocyclic units linked through the bridging chloro or azido ligands. There are also hydrogen bonds between alkoxide and alcohol groups on the adjacent monodeprotonated macrocycles. In both cases the two manganese atoms in each macrocycle are also bridged by the anionic ligand and the intramolecular bridge angles are considerably smaller than the intermolecular equivalents. The manganese atoms are all seven coordinated with approximate pentagonal bipyramidal geometry. The pentagonal plane contains three nitrogen and two oxygen donors from the macrocycle and the axial ligands are the exogenous chloro and azido donors. The exogenous ligands all serve to bridge manganese atoms within each macrocycle and of two different dimeric structures.

Both tetramanganese complexes exhibit strong antiferromagnetic coupling; the total magnetic moment drops from $9.55\mu_B$ and $10.79\mu_B$ at 300 K to $2.10\mu_B$ and $3.52\mu_B$ at 6 K for ($[Mn_2(\mathbf{45}\text{-}H)(Cl)_2]_2 \cdot (ClO_4)_2 \cdot 2dmf \cdot H_2O$ and $[Mn_2(\mathbf{45}\text{-}H)(N_3)_2]_2(ClO_4)_2 \cdot 3CH_3CN$ respectively.

Transmetallation reaction of the mononuclear barium complex $[Ba(\mathbf{45})(H_2O)_2](ClO_4)_2$ with $Mn(ClO_4)_2$ and an excess of NaNCS forms the tetranuclear complex $[Mn_4(\mathbf{45}\text{-}2H)(\mathbf{45}\text{-}H)(NCS)_4](NCS)$ which has a dimeric structure with two [2 + 2] macrocyclic units linked together [208] (Fig. 105).

The two halves of the structure are crystallographically independent and have considerable geometrical differences. Each manganese(II) ion is seven coordinate and has approximate pentagonal bipyramidal geometry. In every case the donors in the pentagonal plane are the three nitrogen atoms of a pyridine–diimine unit and two alkoxide donors, all from the same macrocycle. Each manganese atom has the

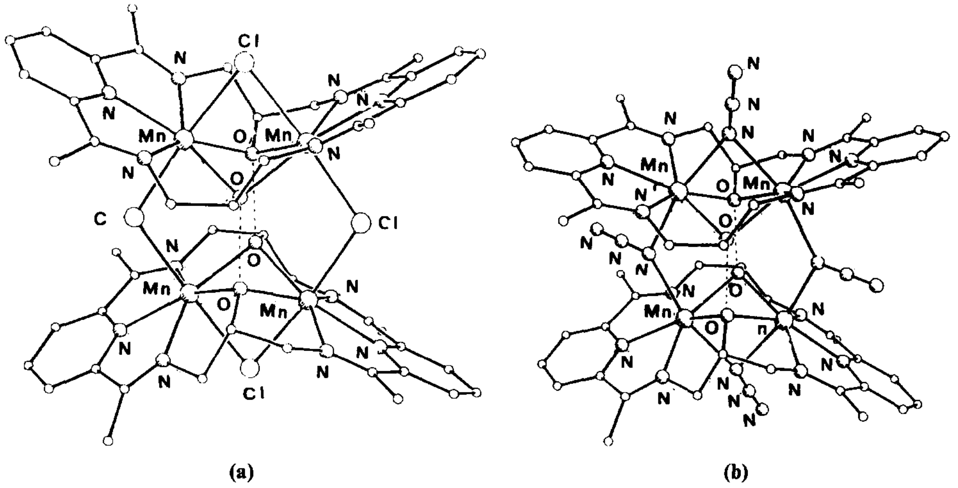

(a) (b)

Fig. 104. Structures of (a) $[Mn_2(\mathbf{45}\text{-}H)(Cl)_2]_2^{2+}$ and (b) $[Mn_2(\mathbf{45}\text{-}H)(N_3)_2]_2^{2+}$.

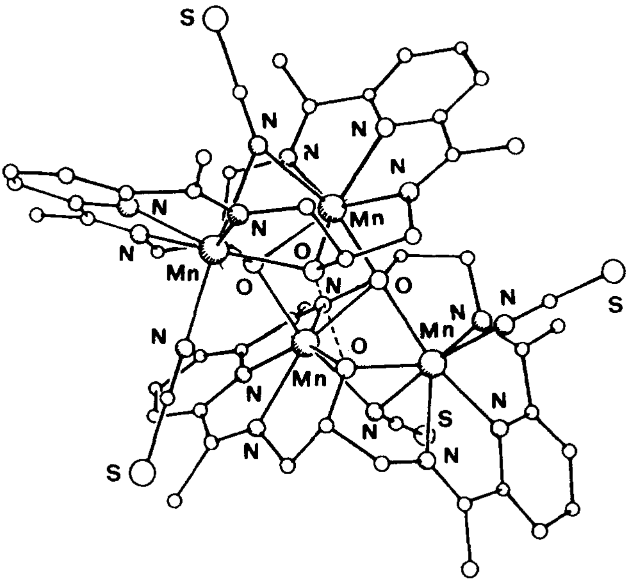

Fig. 105. Structure of $[Mn_4(\mathbf{45}\text{-}2H)(\mathbf{45}\text{-}H)(NCS)_4]^+$.

nitrogen atom of an N-bridged thiocyanate group as one axial ligand. The coordination spheres about two manganese ions are completed by the nitrogen donors of terminally bonded thiocyanates while for the remaining two manganese ions the seventh donor is an alkoxide oxygen atom from the adjacent macrocycle, and it is these two interactions which hold the dimer together. Consequently two alkoxide oxygen atoms are doubly bridging but the other two are triply bridging. The doubly bridging alkoxide oxygen atoms are linked via a hydrogen bond.

The macrocycles themselves are non-planar; each is folded to accommodate the bridging thiocyanate groups by reducing the metal–metal distances to 3.135 Å.

An unusual feature of the structure is the presence of four distinctly different bonding geometries for thiocyanate in addition to the uncoordinated counterion. One of the two terminal thiocyanate groups is bonded in approximately linear fashion whereas the other is distinctly bent. A similar effect is observed for the two bridging thiocyanates.

Using the technique of californium 252 plasma desorption mass spectroscopy it was observed that the barium complex does not contain the [4 + 4] component and hence the larger macrocycle must be formed during the transmetallation reaction with manganese and not in the initial template process [208]. The mechanism reported in Scheme 41 has been proposed for the formation of the [4 + 4] complex [208].

In $[Mn_4(\mathbf{45}\text{-}2H)(\mathbf{45}\text{-}H)(NCS)_4](NCS)$, the two bimetallic macrocyclic units are held together by axial coordination of an alkoxide from one macrocycle to a manganese centre in the second unit. In this complex, only two such “intermolecular”

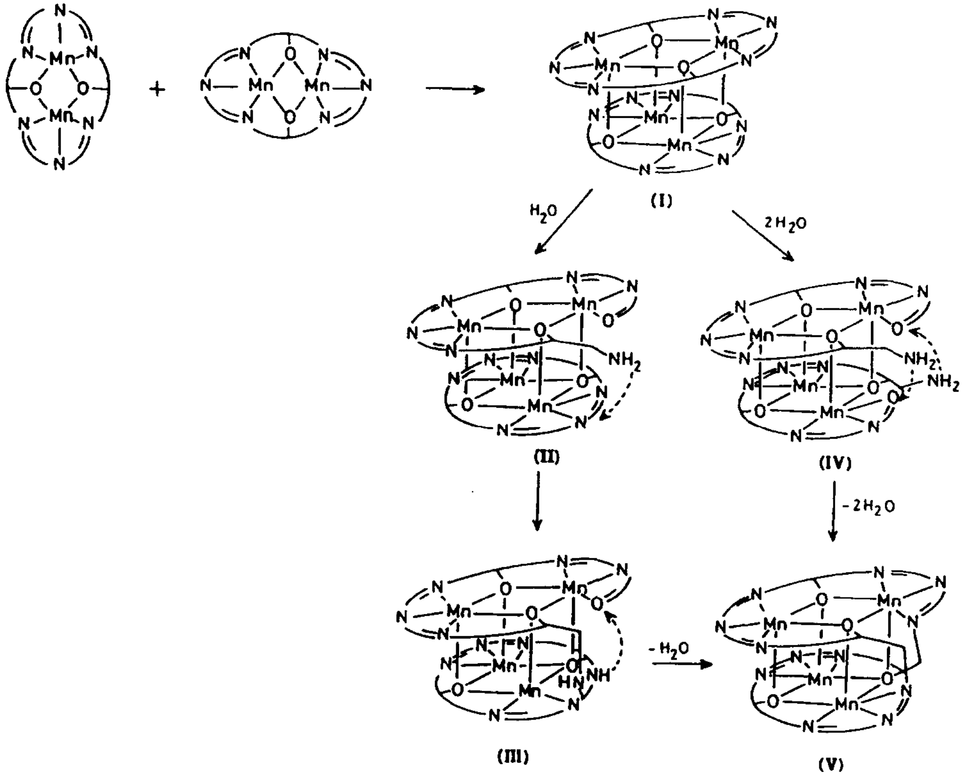

Scheme 41.

bonds are formed because the strongly coordinated thiocyanate ligands occupy the equivalent axial site on the second manganese centre in each [2 + 2] macrocycle. If the terminal thiocyanate groups were not present, four Mn–alkoxide bonds could be formed between two binuclear macrocyclic units in a cofacial orientation (I). The resulting system has the cubane-like core found in (II) but still retains two discrete [2 + 2] ligands. Structure (I) might be expected to exhibit reasonable stability since it is held together by four metal–ligand bonds.

The next step is hydrolysis of an imine bond from one macrocycle to form (II). The terminal amine group is then free to rotate and can add at an imine group on the second macrocycle by nucleophilic attack at the carbon atom, (III). One of the C–N single bonds then breaks, either re-forming (II) or leaving a new intermolecular imine link and releasing another free amine which undergoes a Schiff base condensation with the free carbonyl to form the product (V). Similar attack by nucleophilic amine groups on coordinated imino ligands has been implicated in the mechanism of transamination reactions in related systems.

An alternative route involves the hydrolysis of two imine groups, one in each macrocycle, (IV). Each free amine then attacks the carbonyl of the adjacent ligand to give the product (V). This seems a less likely process since it involves simultaneous hydrolysis of two imine groups in the correct spatial orientation.

The resulting complex (V) has the structure and conformation observed for the [4 + 4] complex (II). In effect, the [4 + 4] macrocycle is formed by a template reaction where the templating moiety is the Mn_4(alkoxide)$_4$ cluster. The cubane core itself forms as a result of the requirement of Mn(II) for a good donor in the axial position. This pseudocubane core then holds the ligands in an orientation favouring the formation of the [4 + 4] macrocycle. [208]

Reaction of 2,6-diacetylpyridine with 1,3-diamino-2-hydroxypropane, in the presence of Mn^{2+} yielded a product with mass spectrum, IR spectrum, and analysis identical to those obtained from the transmetallation reaction. Addition of SCN^- to the template mixture also resulted in the formation of $[Mn_4(\mathbf{45}\text{-}2H)(\mathbf{45}\text{-}H)(NCS)_4](NCS)$. However, the yield of a second, insoluble, carbonyl-containing component was increased with respect to the transmetallation route. The probable explanation of this effect is that the thiocyanate ions, by coordinating to some of the metal sites, reduce the number of sites available for amine or carbonyl coordination. Hence the efficiency of the templating ion is reduced and the insoluble product precipitates before ring closure can occur.

Manganese(II) complexes with the symmetric macrocycle H_2-**109** and the asymmetric macrocycle resulting from the two-step condensation of 2,6-diformyl-4-methylphenol with 1,3-diaminopropane and 1,3-diamino-2-hydroxypropane (H_3-**126**), $[Mn_2(\mathbf{109})(Cl)_2]$, $[Mn_2(H\text{-}\mathbf{126})(Cl)_2]$, $[Mn_2(\mathbf{109})(Br)_2]$ and $[Mn_2(H\text{-}\mathbf{126})(Br)_2]$ [209], have been proposed to be built from isolated binuclear units with an axially distorted square pyramidal geometry around each manganese ion. The manganese ion is displaced out of the macrocyclic ligand plane towards the apical halide anion.

	R
H_2-109	H
H_3-126	OH

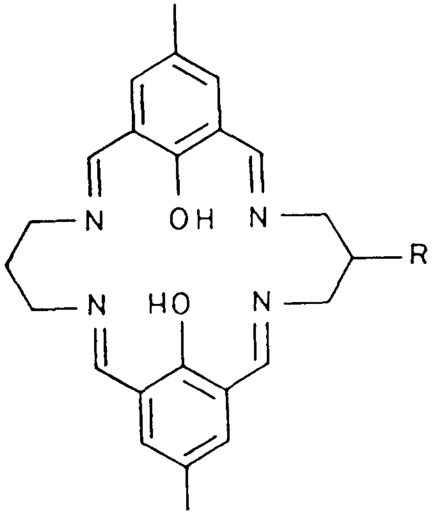

Mn2(H-126)(X)2

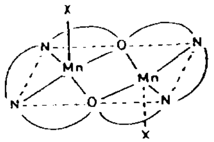

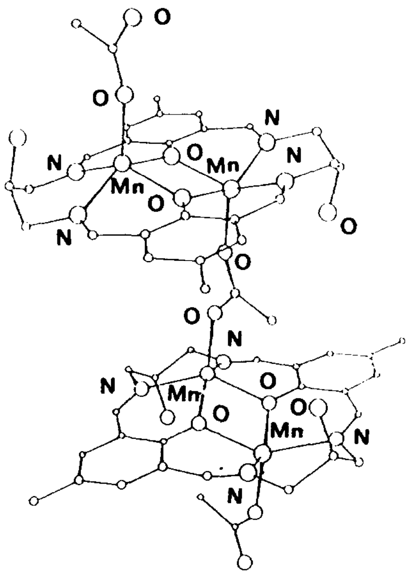

Fig. 106. View of the $[Mn_2(H\text{-}\mathbf{126})(CH_3COO)]^+$ cation chain.

The high spin manganese(II) ions exhibit a very weak intramolecular ferromagnetic exchange interaction ($J = +0.1$ to $+0.3\ cm^{-1}$) in all four complexes.

The X-ray structure of $[Mn_2(H\text{-}\mathbf{126})(CH_3COO)]ClO_4$ shows that, in the cation, two independent binuclear units are bridged by an acetate group to afford infinite chains (Fig. 106). These chains are stacked in planes parallel to the (100) plane. The disordered perchlorate anions are located between these planes.

In both binuclear units, the manganese environment is square pyramidal with two nitrogen and two oxygen atoms from the macrocyclic ligand in the base plane and an oxygen atom from an acetate anion in the apical position. The manganese cation is 0.61 Å above the base plane, towards the acetate ligand. Two pyramids share an $O \cdots O$ edge to form a centrosymmetric binuclear unit with an average Mn–Mn separation of 3.27 Å. The interatomic distance between the manganese atoms separated by the acetate moiety is 6.22 Å. A similar structure has been proposed for $[Mn_2(\mathbf{109})(CH_3COO)](ClO_4)$. In both complexes, a weak antiferromagnetic interaction is operating [209]. $[Mn_2(\mathbf{126})]ClO_4$ is most probably a tetranuclear species including two binuclear units bridged through their alcoholate anions [209]. In this tetranuclear complex the presence of more than one type of antiferromagnetic interaction has been evidenced [209].

Condensation of 1,3-diamino-2-hydroxypropane with 2,6-diformyl-4-methylphenol leads to a mononuclear barium(II) complex [210] but lead(II) mono- and dinuclear complexes [211] of H_4-**127a**. In the mononuclear complexes, the barium ion is coordinated to all four macrocyclic oxygen donors, two diagonally related imine nitrogen atoms and two perchlorate anions; the lead ion is too small to span

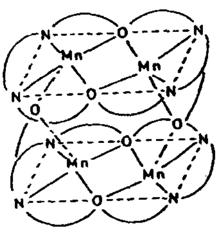

$Mn_4(\underline{126})_2(ClO_4)_2$

the diagonal imine–imine distance (Figs. 107(a) and 107(b)). The structure of the mononuclear lead(II) complex resembles that of the dinuclear analogue; the lead is retained in the same macrocyclic donor set as in the dinuclear complex. This can explain the facile conversion of the dinuclear complex into the mononuclear complex and the free ligand. In both complexes, the lead is five coordinated being bonded to

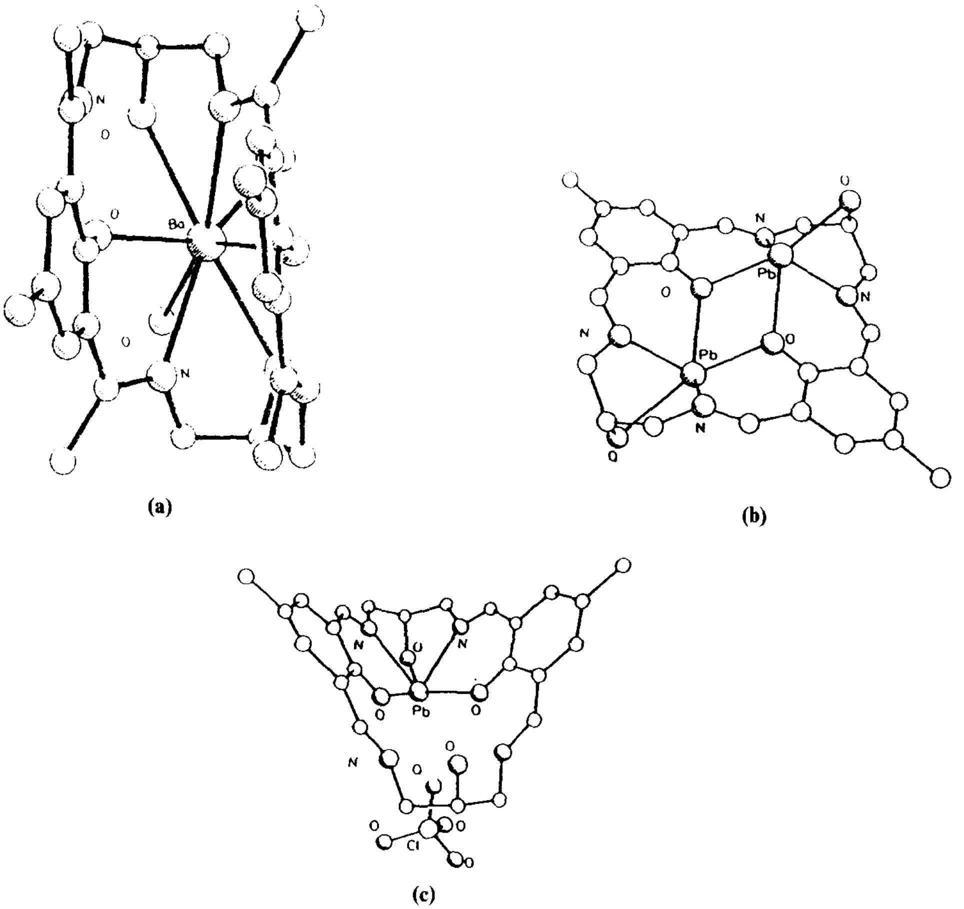

(a)

(b)

(c)

Fig. 107. The structures of (a) $Ba(H_4\text{-}\mathbf{127a})(ClO)_4)_2$ (only the coordination oxygen atom of each of the ClO_4^- ligands is shown), (b) $[Pb_2(H_2\text{-}\mathbf{127a})](ClO_4)_2$ and (c) $[Pb(H_4\text{-}\mathbf{127a})](ClO_4)_2$.

two phenol groups, two imine nitrogen atoms and one pendant alcoholic group (Fig. 107(c)) [211].

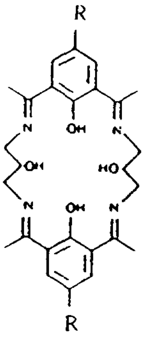

	R
H_4-**127a**	CH_3
H_4-**127b**	$(CH_3)_3C$

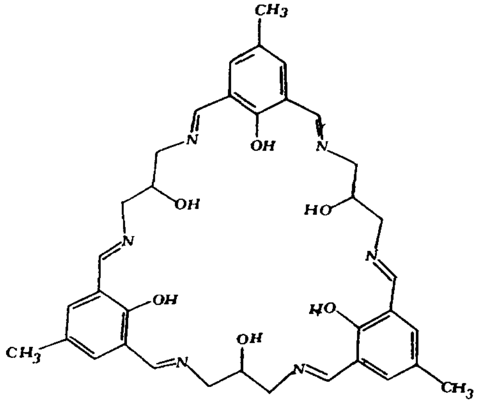

H_6-**127'**

The template condensation of 2,6-diformyl-4-Z-phenol ($Z \equiv CH_3$, $(CH_3)_3C$) and 1,3-diamino-2-hydroxypropane in the presence of copper(II) salts alone produces binuclear [2 + 2′] macrocyclic complexes with no coordination of the secondary alcohol group.

The same template condensation in the presence of copper(II) acetate and excess azide produced the polymeric complexes $[Cu_2(H_2$-**127a**$)][Cu_2(N_3)_6]$, while this template condensation in the presence of CuCl produced an unusual, mixed-oxidation-state species $[Cu_2($**127a**$)][Cu_2Cl_4]$ [167].

In the dinuclear complexes, the copper ions are five coordinated in a slightly distorted square pyramidal geometry as found for $[Cu_2(H_2$-**127a**$)(CH_3OH)(ClO_4)](ClO_4)$ where each copper atom is bonded to two imine nitrogen atoms and two endogenous phenolate oxygen bridges in the basal plane, with a methanol oxygen or perchlorate oxygen atom occupying the fifth, axial position (Fig. 108(a)).

$[Cu_2($**127a**$)][Cu_2Cl_4]$ has a polymeric structure with a fairly flat macrocyclic cation involving two square pyramidal copper(II) ions bridged by phenoxide oxygen atoms. The cations are in turn bridged in a trans-axial fashion by the unusual, flat, $[Cu_2Cl_4]^{2-}$ anion which involves two copper(I) ions. The two copper(II) centres are displaced slightly by 0.225 Å from the mean plane of the equatorial donors toward the "terminal" chlorine atoms of the $[Cu_2Cl_4]^{2-}$ ion. The $[Cu_2Cl_4]^{2-}$ anion is asymmetric with a short copper–chlorine distance linking the two dinuclear ions and longer internal copper–chlorine distances (Fig. 108(b)).

Also, the structure of $[Cu_2(H_2$-**127a**$)][Cu_2(N_3)_6]$ is polymeric (Fig. 108(c)). In the binuclear cation, the two copper(II) centres are bridged internally by phenoxide

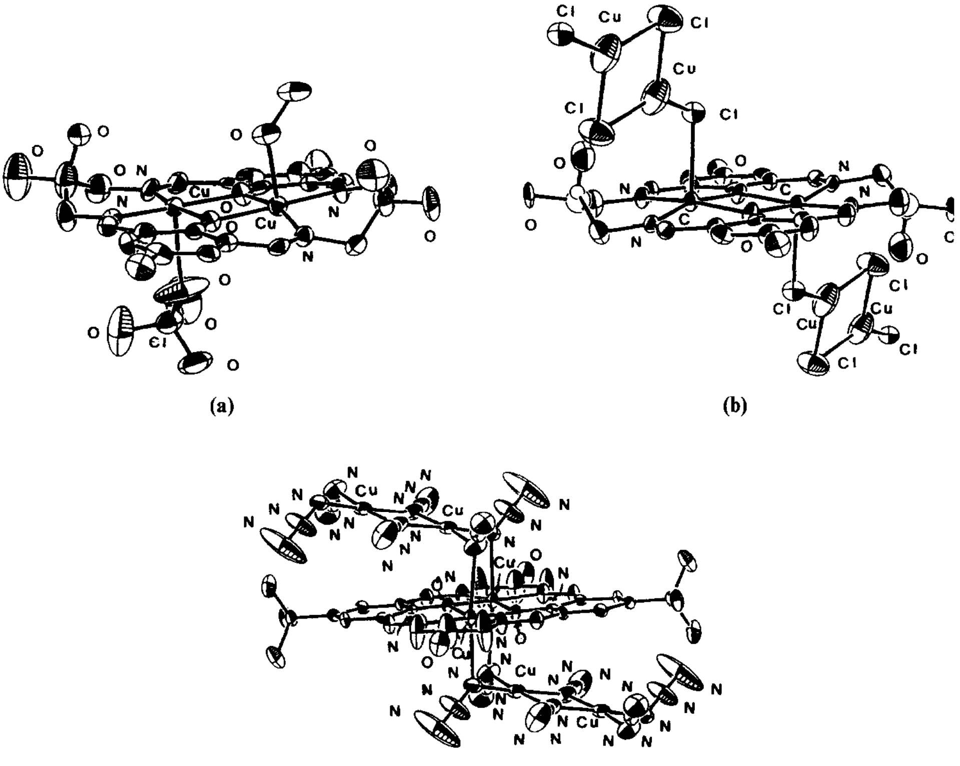

(a) (b)

(c)

Fig. 108. Structures of (a) $[Cu_2(H_2$-**127a**$)(CH_3OH)(ClO_4)]^+$, (b) $[Cu_2($**127a**$)][Cu_2Cl_4]$ and (c) $[Cu_2(H_2$-**127b**$)][Cu_2(N_3)_6]$.

oxygen atoms and no coordination of the secondary alcohol groups. Each copper centre is six coordinated with nitrogen atoms from terminal azide groups on the $[Cu_2(N_3)_6]^{2-}$ anion acting as axial ligands. The structure consists of an alternating, stepped chain of interconnected dinuclear macrocyclic cations $[Cu_2(H_2$-**127b**$)]^{2+}$ bridged axially through 1,1-azide interactions to dinuclear $[Cu_2(N_3)_6]^{2-}$ anions. The basal donor set N_4O_2 of the macrocyclic cation is very close to planar with displacements of the copper centres from this plane of less than 0.03 Å. The unusual hexaazido anion has a chair conformation.

Extended magnetic interactions were observed for the azide derivatives in which intraring antiferromagnetic exchange and independent exchange within the anion are accompanied by extended, antiferromagnetic, intermediate exchange [167].

The reaction of $Cu(NO_3)_2$, 2,6-diformyl-4-methylphenol-1,3-diamino-2-hydroxypropane and $N(Et)_3$ in refluxing methanol, followed by concentration to a small volume produced the dodecanuclear complex $[Cu_6($**127c**$)(\mu_2\text{-}OH)_3]_2 \cdot (NO_3)_6 \cdot 10H_2O$ [167].

The structure of the dimeric cation (Fig. 109) consists of two almost flat, hexagonal macrocyclic rings, each involving an array of six nominally pseudo square planar copper(II) centres. Two hydroxide bridges not only bridge two copper pairs Cu(1), Cu(2) and Cu(5), Cu(6) within the same ring but also provide a bridge to copper atoms Cu(4) and Cu(3) on the other macrocyclic ring.

The molecular symmetry dictates that this intermacrocycle bridges are held together by four axial hydroxide bridges. The relative short interring hydroxide contacts indicate a significant axial interaction and so three copper atoms are bridged in a tripodal arrangement and the geometry at Cu(3) and Cu(4) is square pyramidal. A pair of symmetrically related bidentate nitrate groups, bonded to Cu(1) and Cu(2), are located on the concave (outer) face of the complex. A second pair of disordered and poorly defined nitrate groups also bond to the outer faces at Cu(5) and Cu(6). Five pairs of water molecules and two disordered nitrate anions have been located in the lattice.

The copper atoms are linked within each ring by an alternating single and double bridged arrangement of oxygen atoms (alkoxide and hydroxide plus phenoxide) that resembles a resonance form of benzene.

The symmetric and alternating arrangement of single and double oxygen bridges, linking all the copper magnetic orbitals within each ring, indicates the likelihood of exchange involving the whole hexanuclear ring. Of the two different bridge groups, the single-atom alkoxide bridge (large Cu–O–Cu angle) is considered to dominate the exchange situation [167].

The longer 1,5-diamino-3-hydroxypentane forms the tetrametallic [2 + 2] macrocyclic complexes $[Cu_4(\mathbf{128})(\mu_4\text{-OH})](NO_3)_3 \cdot 2H_2O$, $[Cu_4(\mathbf{128})(\mu_4\text{-OH})]$-

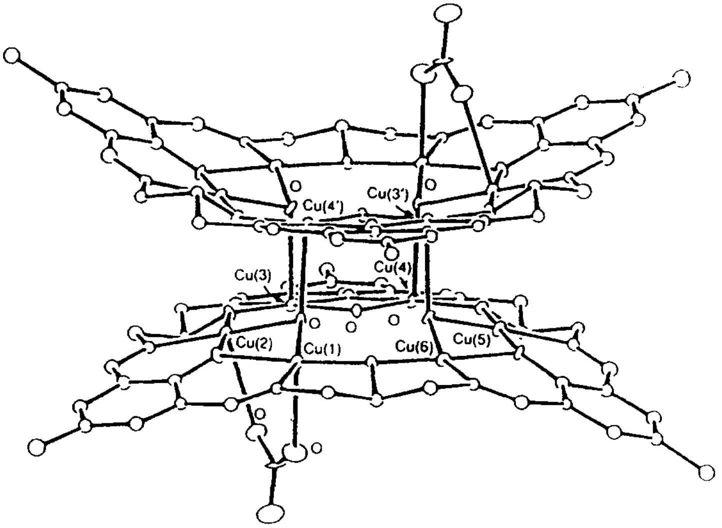

Fig. 109. The structure of $[Cu_6(\mathbf{127c})(\mu_2\text{-OH})_3]_2(NO_3)_6 \cdot 10H_2O$.

$(ClO_4)_3$, $[Cu_4(\mathbf{128})(\mu_4\text{-}OH)(CH_3COO)_3]\cdot 3H_2O$, $[Cu_4(\mathbf{129})(\mu_4\text{-}OH)](NO_3)_3\cdot nH_2O$, ($n=2, 1$), $[Cu_4(\mathbf{129})(\mu_4\text{-}OH)](ClO_4)_3\cdot 2H_2O)$ and $[Cu_4(\mathbf{129})(\mu_4\text{-}OH)(CH_3COO)_3]\cdot 2H_2O$ by condensation in refluxing methanol with 2,6-diformyl-4-*tert*-butylphenol or 2,6-diformyl-4-methylphenol in the presence of the appropriate copper(II) salts [212,213].

The good yields obtained and the general absence of binuclear or polymeric side products is probably a consequence of the strong binucleating ability of the diformylphenol component. Formation of an initial binuclear diformylphenol complex would maintain the carbonyl groups in the correct orientation for macrocyclic formation and ensure that, when the [2 + 2] macrocycle formed, it would contain four copper(II) ions. If these can be accommodated within the ring a tetranuclear complex is isolated; if the macrocycle is too small to bind all four copper ions as is the case when 1,3-diamino-2-hydroxypropane is used in place of 1,5-diamino-3-hydroxypentane, a rearrangement to give the binuclear complex occurs.

The X-ray structure of $[Cu_4(\mathbf{129})(\mu_4\text{-}OH)](NO_3)_3\cdot 2H_2O$ confirms the tetrameric nature of the cation $[Cu_4(\mathbf{129})(\mu_4\text{-}OH)]$ (Fig. 110(a)), which is centrosymmetric with the oxygen atom O(x) on a centre of symmetry. Four Cu(II) ions are bound within the macrocycle, each coordinated to an imine nitrogen, one phenoxide oxygen and one alkoxide oxygen atom, the central hydroxide ion, i.e. O(x), and one axial donor (water or nitrate). The macrocyclic oxygen donors are all deprotonated and bridging so that the square plane about each copper atom shares two edges with the equivalent planes of two neighbouring copper atoms [212].

The Cu···Cu distances (3.000 and 2.953 Å) are quite short but are non-bonding. Structural analyses of the acetate complexes $[Cu_4(\mathbf{128})(\mu_4\text{-}OH)(CH_3\text{-}$

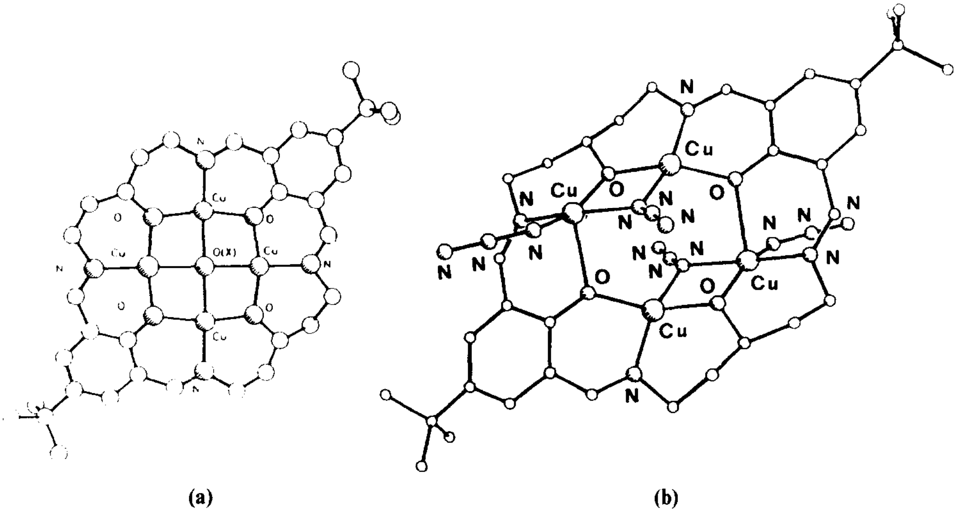

Fig. 110. The structure of (a) $[Cu_4(\mathbf{129})(OH)]^{3+}$ and (b) $[Cu_4(\mathbf{129})(\mu\text{-}N_3)(N_3)_2]$.

COO)] · $3H_2O$ and [Cu_4(**129**)(μ_4-OH)($CH_3COO)_3$] · $2H_2O$ have not yet been obtained. Stoichiometry requires that a hydroxide donor is present in each case, and the IR spectra suggest that the acetate groups are coordinated. It was proposed that the structures of these acetate complexes are similar to that of [Cu_4(**128**)(μ_4-OH)]($NO_3)_3$ · $2H_2O$ but having acetate groups bonded axially to the metal ions. This proposed structure is similar to that determined for [Ni(μ_4-OH)(**128**)($CH_3CO_2)_3$] in which the acetate groups bridge adjacent metal ions [213].

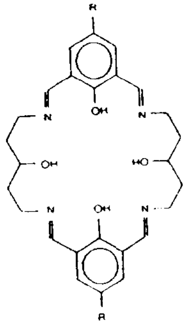

	R
H_4-128	CH_3
H_4-129	$(CH_3)_3C$

Reaction of [Cu_4(**129**)(μ_4-OH)]($NO_3)_3$ · H_2O with NaN_3 forms [Cu_4(**129**)(μ-N_3)($N_3)_2$] · $2CH_3OH$ [213] which differs from the other tetracopper(II) complexes in that it does not contain a central oxygen donor. The μ_4-OH ligand has been replaced by two μ-azido ligands which lie on either side of the macrocyclic plane. The two independent copper atoms have very different coordination environments. Two copper atoms are four coordinate, bonded to alkoxy, phenoxy, imine and μ-azido donors with irregular geometry. The other two copper atoms are five coordinate, having an additional terminal azido ligand; the geometry about these metal ions is approximately square pyramidal but the axial donor is the phenoxy oxygen atom rather than the terminal azide. There is a marked difference between the singly and doubly bridged copper–copper distances, 3.460 Å and 3.045 Å respectively. There are no significant interactions involving the solvate methanol molecules, and the macrocyclic ligand itself is close to planar (Fig. 110(b)). The structure of [Cu_4(**129**)(μ-N_3)($N_3)_2$] · $2CH_3OH$ demonstrates that the central oxygen donor is not required to maintain the tetracopper(II) structure and that the μ_4-OH can be replaced, opening up the possibility of activation of the central moiety.

In the complex [Mn$^{II}_2$Mn$^{II}_2$(128)(O)(CH$_3$COO)$_3$(Cl)(MeOH)]·3MeOH (Fig. 111) obtained from reaction of 2,6-diformyl-4-methyl phenol with 1,5-diamino-3-hydroxypentane dihydrochloride (neutralized with KOH) in the presence of manganese(II) acetate in a methanol–ethanol mixture the macrocycle is non-planar [214].

The mean planes of the two phenol rings are tilted toward each other at an angle of 38.5°. The alcohol and phenol groups of the macrocycle are all deprotonated and each bridges two manganese ions so that the ligand is octadentate. The coordination spheres of the metal ions are completed by a central oxo anion (bound to each manganese ion), three bridging acetate groups, a chloride ion and a methanol molecule. Three other methanol molecules are present in the asymmetric unit but these are not coordinated to the metal complex.

Mn(1) and Mn(3) have very similar coordination and geometry; each is six coordinated and approximately octahedral, coordinated to the macrocycle through one imine nitrogen, one phenoxy oxygen atom and one alkoxy donor. In addition, each is bound to two acetate groups (trans to one another) and to the oxo ion. Five of the six ligands bound to Mn(1) or Mn(3) are bridging and bind to at least one other manganese ion. Mn(2) and Mn(4) are also six coordinate but have less regular geometry than the other metal ions. Mn(4) has the same donor set as Mn(1) or Mn(3) but the acetate groups are cis rather than trans. In the coordination sphere of Mn(2), the acetate groups are replaced by a chloride anion and a methanol group. The manganese centres have a butterfly configuration; each manganese atom has two relatively short interactions with other metal ions and one longer separation. Bond distances about Mn(1) and Mn(3) are very similar and are significantly shorter than equivalent bonds to Mn(2) or Mn(4). Consequently, the original +2 oxidation

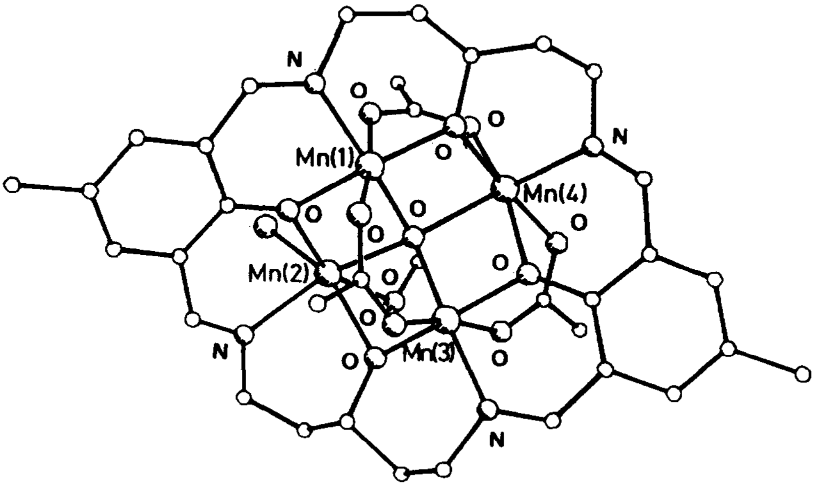

Fig. 111. Structure of [Mn$^{II}_2$Mn$^{II}_2$(128)(O)(CH$_3$COO)$_3$(Cl)(MeOH)].

state is assigned to Mn(2) or Mn(4), whereas Mn(1) and Mn(3) have been oxidized to the +3 level.

The most likely oxidizing agent for this process is molecular oxygen, and this may also be the source of the oxo ligand. The mean magnetic moment falls from $5.12\mu_B$ (Mn atom)$^{-1}$ at 300 K to $4.56\mu_B$ (Mn atom)$^{-1}$ at 93 K. Both of these values are below the mean spin-only moment expected in the absence of any coupling ($5.41\mu_B$ (Mn atom)$^{-1}$).

The tetranickel complex $Ni_4(\mathbf{130})(CH_3COO)_2(CH_3O \cdot H \cdot OCH_3)$ was obtained by template condensation in methanol of 2,6-diformyl-4-methylphenol with 2,6-bis(aminomethyl)-4-methylphenol monohydrochloride in the presence of excess nickel(II) acetate and acetic acid–sodium acetate buffer. X-ray crystallography of green monoclinic crystals of the tetramethanolate grown by vapour diffusion of water into a methanolic solution in the presence of additional nickel acetate reveals four nickel atoms at the corners of the rectangle [215].

A μ_4-hydroxyl group is located with its oxygen atom ca. 0.60 Å above the midpoint of the Ni_4 cluster. An unusual, strongly hydrogen bonded $CH_3OH \cdot O \cdot CH_3$ unit bridges the "face" of the Ni group on the side opposite to the μ_4-OH group, each methoxo oxygen atom being equally attached to two nickel atoms. The arrangement of the macrocyclic ligand resembles a bowl with the Ni_4 group in the bottom. The $CH_3O \cdot H \cdot OCH_3$ unit is inside the bowl. Two acetate units bridge the edges of the Ni_4 group on the outside of the bowl (Fig. 112(a)) [215].

Replacement of the acetate ligands $Ni_4(\mathbf{130})(\mu_4\text{-}OH)(CH_3O \cdot H \cdot OCH_3)(CH_3COO)_2$ either by azide or by methoxide gives derivatives which contain the

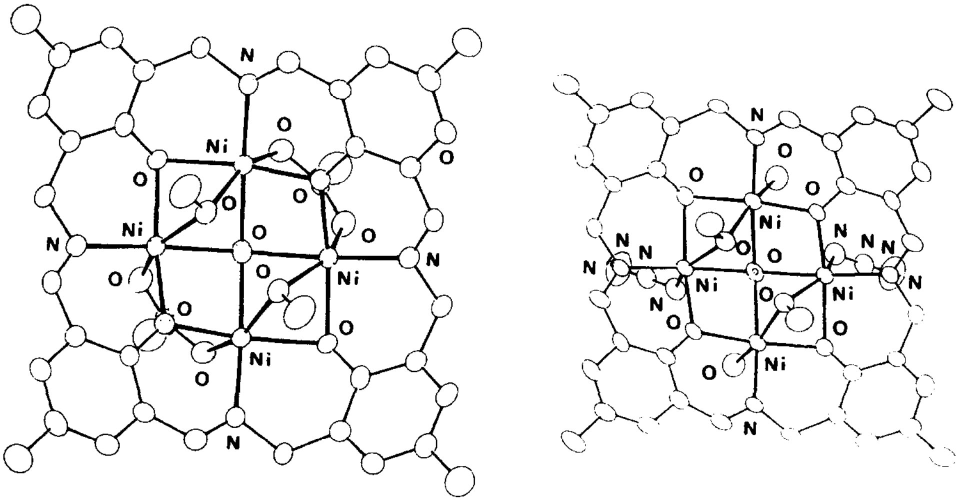

(a) (b)

Fig. 112. The structures of (a) $Ni_4(\mathbf{130})(\mu_4\text{-}OH)(CH_3CO_2)_2(CH_3O \cdot H \cdot OCH_3)_2$ and (b) $Ni_4(\mathbf{130})(\mu_4\text{-}OH)(N_3)_2]CH_3O \cdot H \cdot OCH_3)_2$.

intact $[Ni_4(\mathbf{130})(\mu_4\text{-}OH)(CH_3O \cdot H \cdot OCH_3)]^{2+}$ core present in the acetate complex. Two μ_2 bridging sites on the lower convex side of the bowl, which in the actate complex are occupied by μ_2-acetates, are occupied by H-bonded $(N_3^- \cdot HOH)$ combinations in the azido complex and by H-bonded $(CH_3O \cdot H \cdot OCH_3)^-$ combinations in the methoxo complex (Fig. 112(b)). The three complexes exhibit very similar magnetic properties (300–4.2 K), the Ni_4 group behaving as an essentially non-interacting pair of Ni_2 units within which there is antiferromagnetic coupling with J values of $-33.3\ cm^{-1}$ (acetate), $-28.5\ cm^{-1}$ (azide), and $-30.0\ cm^{-1}$ (methoxo); the coupled pairs are very probably those involving the dialdehyde-derived phenoxide bridges, which are essentially trigonal [215].

A less symmetrical bow-like ligand arrangement is present in $Zn_4(\mathbf{130})(CH_3CO_2)_3(OH) \cdot 2.64CH_3OH \cdot 2.5H_2O$ [215] (Fig. 50). The Zn_4 group is markedly distorted from a square being no longer planar and having a short diagonal, 3.632 Å, and a long diagonal, 4.742 Å. A hydroxo group bridges the short diagonal but it also interacts less strongly with the other two zinc atoms. One acetate bridges the short diagonal on the side opposite to the hydroxo group and on the inside of the bowl. A second acetate bridges an edge of the Zn_4 cluster and the third acetate is monodentate but hydrogen bonded to the hydroxo group. One zinc atom is intermediate between 4 and 5 coordinate, two are 5 coordinate and the fourth is 6 coordinate [215] (Fig. 113).

Reduction of the dihydrochloride macrocyclic Schiff base H_4-**130**, by excess of $NaBH_4$ in ethanol at 0°C, produces the corresponding, but more flexible, tetramino macrocycle H_4-**131** (Scheme 42) [216].

The tetramino macrocycle H_4-**131**, by reaction with zinc acetate in the presence of lithium acetate and tetraethylammonium hydroxide, forms the complex $Zn_4(\mathbf{131})(OH)(CH_3COO)_3$.

The four zinc atoms, not coplanar, are approximately at the corners of a

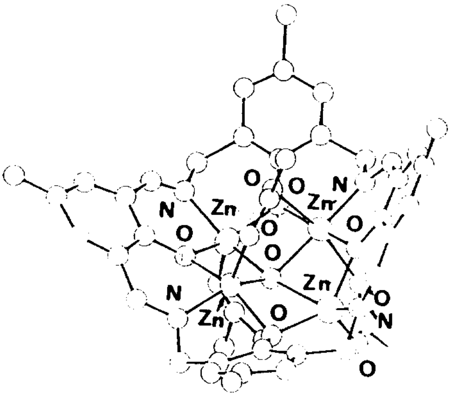

Fig. 113. Structure of $Zn_4(\mathbf{130})(\mu_4\text{-}OH)(CH_3CO_2)_3$.

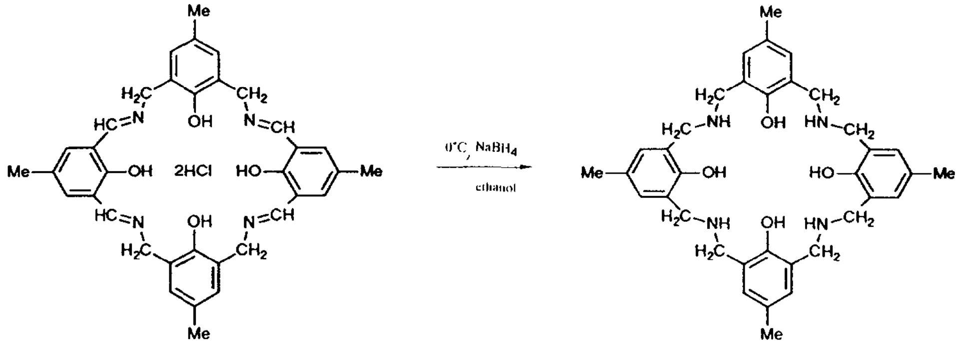

H_4-**130**

H_4-**131**

Scheme 42.

rhombus; one acetate bridges zinc(2) and zinc(3), while the other two acetates are monodentate to zinc(3) and zinc(4).

A coordinating methanol molecule completes an approximately octahedral arrangement around zinc(2) while zinc(3) and zinc(4) are five coordinated and zinc(1) is essentially four coordinated (Fig. 114) [216].

Reaction between 2,6-bis(aminomethyl)-4-methylphenol monohydrochloride, 2,6-diformyl-4-methylphenol, copper(II) acetate monohydrate and an excess of tetrabutylammonium tetrafluoroborate in boiling methanol gave a green crystalline product of the formula $[Cu_6(\mathbf{132})(CH_3COO_2)_2(OH)_2(MeOH)_2(H_2O)](BF_4)$-2.4.4MeOH after the solution had been concentrated and allowed to stand, where

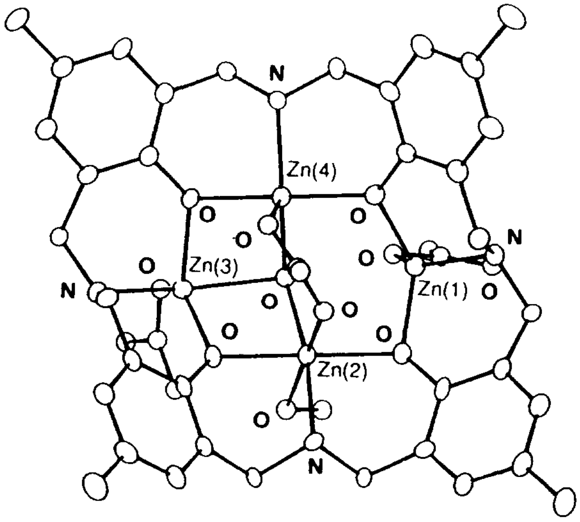

Fig. 114. The structure of $Zn_4(\mathbf{131})(OH)(CH_3COO)_3$.

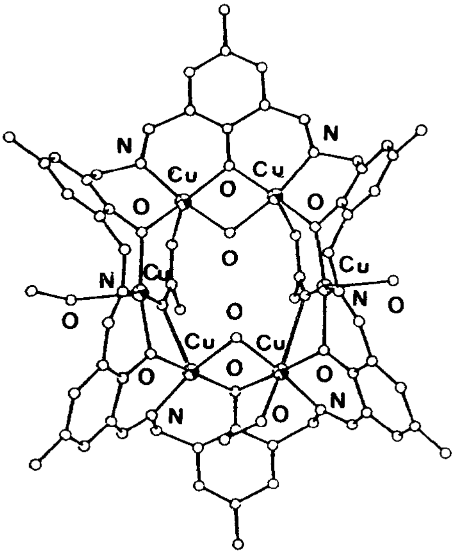

Fig. 115. View of the $[Cu_6(\mathbf{132})(CH_3COO)_2(OH)_2(MeOH)_2(H_2O)]^{2+}$ cation.

H_6-**132** is the [3 + 3] macrocyclic Schiff base derived by condensation of three diamine and three diformyl precursors [217].

The cation shows that two hydroxyl groups, each bridging a pair of copper atoms, which share a dialdehyde-derived phenolate, are the only species within the central cavity formed by the six copper atoms. The two acetates each bridge two copper atoms. Five of the copper atoms are essentially square and an acetate oxygen atom along the direction of elongation (Fig. 115).

By refluxing 2,6-diformyl-4-methylphenol, 1,5-diamino-3-hydroxypentane, and copper(II) perchlorate hexahydrate in ethanol for ca. 24 h, a green product was obtained which was probably $[Cu_4(\mathbf{128})(OH)](ClO_4)_3$. By recrystallization from dimethylformamide–methanol–diethylether solution, this compound produces the octamer $[Cu_4(\mathbf{128})(\mu_5\text{-}O)(ClO_4)]_2(ClO_4)_2$ [109]. The X-ray structure of the cation (Fig. 116) shows that, within each macrocycle, the four atoms are coplanar, and each is coordinated to an imine nitrogen atom, to bridging phenoxide and alkoxide donors, and to a central oxo anion. The coordination sphere of Ox is completed by a copper atom from a second macrocyclic unit together in a centrosymmetric dimer. One perchlorate ion per tetranuclear unit binds as a tripod ligand to the Cu_4 array. Neither the second perchlorate ion nor the solvate water molecule exhibits any significant intermolecular contacts [218].

The octacopper structure is maintained in dmf solution while the unrecrystallized tetramer in the same solvent changes slowly with time and, after approximately 3 days, is identical with that of the octamer. The same spectral change is accomplished within a few seconds in the presence of a base such as triethylamine. Addition of

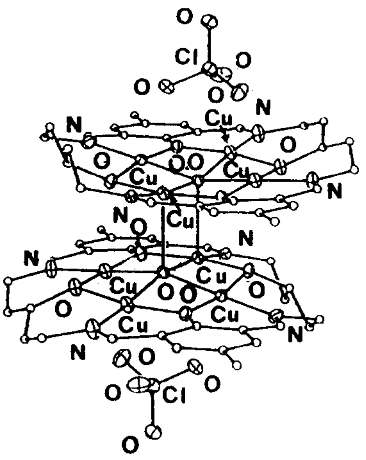

Fig. 116. Perspective view of $[Cu_4(\mathbf{128})(\mu_5\text{-}O)(ClO_4)]_2^{2+}$.

small amounts of acid will reverse the reaction, but excess acid leads to other, as yet unidentified, products. A very similar behaviour is observed for the tetracopper complexes $[Cu_4(\mathbf{129})(OH)](NO_3)_3 \cdot 3H_2O$ and $[Cu_4(\mathbf{129})(OH)](ClO_4)_3 \cdot 2H_2O$ which yield octacopper complexes by recrystallization from dmf with a structure very similar to that of $[Cu_4(\mathbf{128})(O)(ClO_4)]_2(ClO_4)_2$ [218].

The octacopper complexes $[Cu_4(\mathbf{128})(\mu_5\text{-}O)(ClO_4)]_2(ClO_4) \cdot 3\text{dmf}$, $[\{Cu_4(\mathbf{129})(\mu_5\text{-}O)(NO_3)\}_2(NO_3)_2] \cdot 2H_2O$ and $[Cu_4(\mathbf{129})(\mu_5\text{-}O)(ClO_4)]_2(ClO_4)_2$ were prepared either by slow recrystallization of the corresponding tetracopper complex from dimethylformamide–methanol solutions or by treating the tetracopper compound with a base in dry methanol [213].

The most remarkable difference between the structures of the octacopper perchlorate complexes is represented by the geometry of perchlorate bonding. These configurations arise from the geometric mismatch between the square planes.

Cu_4 array and the tetrahedral perchlorate ion represent two ways of maximizing the bonding interaction. In $[Cu_4(\mathbf{128})(\mu_5\text{-}O)(ClO_4)]_2(ClO_4) \cdot 3\text{dmf}$, the anion has bonds to two of the copper atoms which are within the range observed for Cu–O axial bonds, and the third oxygen atom has rather long interactions with the remaining copper atoms. In $[Cu_4(\mathbf{129})(\mu_5\text{-}O)(ClO_4)]_2(ClO_4)_2$, the perchlorate interacts relatively strongly with the three copper centres and only weakly with the fourth. It is significant that, in both complexes, the shortest $Cu\text{–}OClO_3$ bond involves the copper atom which has a strong axial bond to O. Significant interactions involve the second perchlorate anion or the solvate molecules in either structure.

A net antiferromagnetic interaction is observed for each of the complexes and, in general, the octacopper compounds exhibit stronger coupling than their tetracopper equivalents. This may be a consequence of the deviation from tetragonal geometry in the tetracopper complexes which would reduce the orbital overlap and hence the

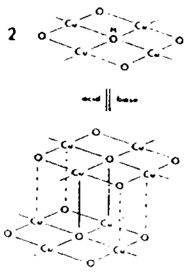

Scheme 43.

extent of antiferromagnetic coupling. The change in the nature of the central oxygen donor is also likely to be significant.

The spectroscopic data imply that both tetrameric complexes undergo slow dimerization in dmf to yield octacopper complexes and that the reaction is promoted by base and reversed by acid (Scheme 43).

In protic solutions such as ethanol the tetracopper monomer with hydroxide at the centre is favoured. In less protic dmf solution the octacopper species is preferred but the rate of the interconversion is slow; addition of base increases the rate by promoting dissociation of the hydroxyl proton [216].

Mixed-valence tetramanganese derivatives of the cyclic Schiff bases obtained by reaction of 2,6-diacetyl pyridine and 1,3-diaminopropane or 1,4-diaminobutane, incorporating both μ-oxo and μ-carboxylate ligands, have been obtained, but poor crystal quality has prevented full refinement of the structures. Preliminary data, however, do indicate appropriate Mn–Mn distances of 2.7 and ca. 3.3 Å (the longer distance being ligand dependent as it is intramacrocyclic). The average oxidation state of manganese in these complexes is 2.5 [218].

Both template condensation of tris(2-aminoethyl)amine with salicylaldehyde and direct treatment of the neutral ligand H_3-**133** with Mn^{III} in CH_3OH–CH_3CN result in deprotonation of the phenol oxygen atoms and isolation of the tetranuclear di-μ-oxo cluster $[Mn_4(\mathbf{133})_2(O)_2]^{2+}$ (as $[MnCl_4]^{2-}$, ClO_4^-, $CF_3SO_3^-$ or Ph_4B^- salts). Identical products were obtained using Mn^{II} salts (after air oxidation of the initial yellow solutions). Fast atom bombardment mass spectra of these products revealed an isotopic cluster centred around $m/z = 1163$, corresponding to $[Mn_4(\mathbf{133})_2(O)_2]^+$: a weaker peak, with intensity dependent on the counterion X, was often observed at m/z corresponding to $[Mn_4(\mathbf{133})_2(O)_2X]^+$.

Crystallographic data on the triflate salt $[Mn_4(\mathbf{133})_2(O)_2][CF_3SO_3]_2 \cdot 2H_2O$ revealed a cluster almost identical to that observed for $[Mn_4(\mathbf{133})_2(O)_2][MnCl_4] \cdot$ 2MeCN or $[Mn_4(\mathbf{133})_2(O)_2](PF_6)_2$ which contain discrete centrosymmetric $[Mn_4(O)_2(\mathbf{133})_2]^{2+}$ cations and $[MnCl_4]^{2-}$ or PF_6^- anions; there is no evidence of any interaction between cations and anions or MeCN solvent molecules (Fig. 117) [218].

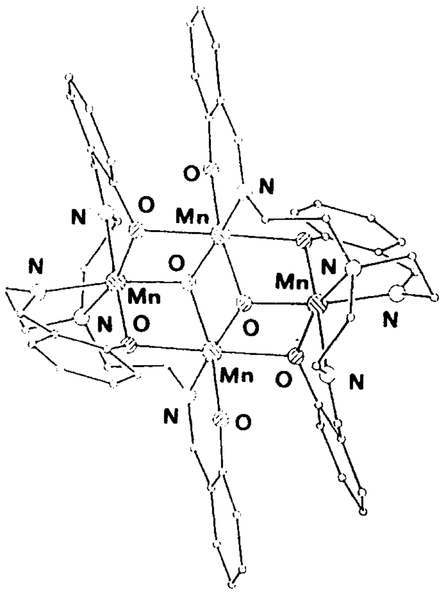

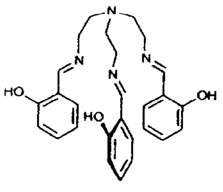

H_3-**133**

Fig. 117. Perspective view of $[Mn_4(\mathbf{133})_2(O)_2]^{2+}$.

Each Mn atom is six coordinate, one manganese atom having an NO_5 donor set while the other manganese atom has an N_3O_3 set. All the donors come from the Schiff base ligands except for the two oxo ions. The oxo and phenoxy groups bridge the four Mn atoms to form two face-sharing incomplete cubanes. The geometry at the Mn atoms approaches octahedral. The Mn–Mn distances range from 2.898 to 3.035 Å. The temperature dependence of magnetic susceptibility of the cluster in the four salts reveals an overall antiferromagnetic interaction, the moment reducing from about 4.5–4.1μ_B (Mn ion)$^{-1}$ at 300 K to about 2μ_B (Mn ion)$^{-1}$ at 4.2 K [218].

The reaction of 2,6-diformyl-4-methylphenol, triethylenetetramine, and copper(II) perchlorate hexahydrate in 2:2:4 molar ratio forms the macrocyclic tetracopper(II) complex $[Cu_4(\mathbf{86})(OH)_2](ClO_4)_4$ [219]. The magnetic susceptibility of $[Cu_4(\mathbf{86})(OH)_2](ClO_4)_4$ obeys the Bleaney–Bowers equation ($J = -280\,cm^{-1}$) indicating that strong antiferromagnetic spin coupling operates within each dicopper(II) unit but the two dicopper(II) units are magnetically independent from each other. The two hydroxide groups, each bridging a pair of copper(II) ions, are facing each other at such a close distance so as to be replaced by an azide ion, affording $[Cu_4(\mathbf{86})(N_3)](ClO_4)_5$.

The magnetic moment of $[Cu_4(\mathbf{86})(N_3)](ClO_4)_5$ also decreases with lowering temperature but does not obey the Bleaney–Bowers equation. This is probably because the magnetic interaction operates among four copper(II) ions through the azide bridge.

The cyclic voltammagram of $[Cu_4(\mathbf{86})(OH)_2](ClO_4)_4$ reveals four redox

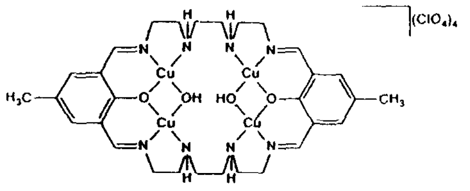

couples in the region from -0.4 to -0.9 V (SCE) which are assigned to the sequential one-electron transfers Cu_4(II,II,II,II)/Cu_4(I,II,II,II)/Cu_4(I,I,II,II)/Cu_4(I,I,I,II)/Cu_4(I,I,I,I). Further, it is suggested that the Cu_4(I,I,I,I) species reduces O_2 to water on the electrode [219].

In a related study on the formation of lead complexes by similar template reaction using 1,9-diamino-3,7-diazanonane in place of 1,8-diamino-3,6-diazaoctane and 2,6-diformyl-4-methylphenol, a condensation occurred between the two secondary amino groups of the tetramine and a carbonyl group of 2,6-diformyl-4-methylphenol to form H_2-**86**′. In order to avoid this condensation, the tetramine 1,8-diamine-3,6-dimethyl-3,6-diazaoctane, alkylated at the seconday amino nitrogen atoms, was successfully used in the template synthesis of the dilead(II) complex [Pb_2(H_2-**86**″)(dmf)$_4$(ClO_4)$_2$](ClO_4)$_2$ [219].

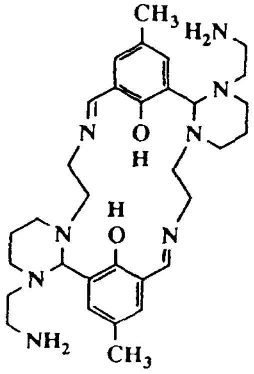

H_2-**86**′

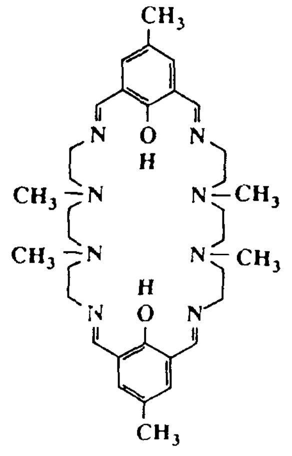

H_2-**86**″

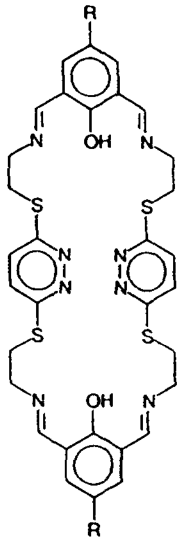

H_2-**86**‴

R = CH_3
R = $C(CH_3)_3$

The structure of [Pb_2(H_2-**86**″)(dmf)$_4$(ClO_4)$_2$]$^{2+}$ shows that the ligand involved in the complex is indeed the 2:2 condensation product of the constituents, 2,6-diformyl-4-methylphenol and 1,8-diamino-3,6-dimethyl-3,6-diazaoctane, and contains two Pb(II) ions. Each Pb(II) ion is bonded to the phenolic oxygen atom, one imino nitrogen atom and two amino nitrogen atoms. The remaining imino nitrogen atoms are free from the coordination of the Pb(II) ions. The significantly short Pb—O bond distance suggests that the phenolic oxygen atom coordinates to the Pb(II) ion in the deprotonated form with the protons attached to the non-coordinated imino nitrogen atoms and hydrogen bonded to the adjacent phenolic oxygen atoms. The open face of the Pb coordination sphere is occupied by two dmf oxygen atoms. Further, a perchlorate oxygen atom interacts with the Pb(II) ion but the Pb—O separation is too large to be taken as a coordination bond. Thus, each Pb(II) ion is six coordinated in a markedly distorted octahedral environment. The two Pb(II) ions are 8.098 Å apart; two perchlorate ions are captured in the crystal lattice [219] (Fig. 118(a)).

Preliminary studies indicate that this dilead(II) complex acts as a good precursor for the formation of tetranuclear complexes containing transition metal ions [219].

The condensation of 2,6-diformyl-4-R-phenol ($R \equiv CH_3$, $-C(CH_3)_3$) with 3,6-bis[(aminoethyl)thio]pyridazine in the presence of copper(II) perchlorate or tetrafluoroborate forms dinuclear complexes [220]. This reaction was carried out

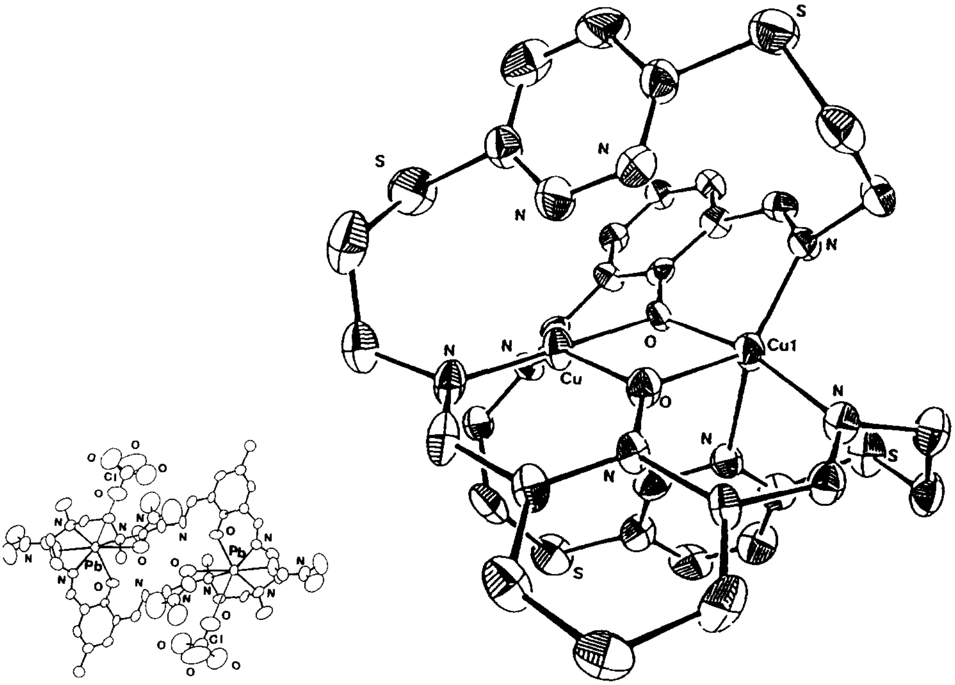

(a) (b)

Fig. 118. Structures of (a) $[Pb_2\text{-}(H_2\text{-}\mathbf{86}'')(dmf)_4(ClO_4)_2]^{2+}$ and (b) $[Cu_2(\mathbf{86}''')]^{2+}$.

with the aim to generate 34-membered $N_8S_4O_2$ macrocycles (H_2-**86‴**) with a high coordination capacity for metal centres.

In these complexes, the macrocycles coordinate with the familiar N_4O_2 equatorial donor set, to two phenoxide-bridged copper(II) centres, but distant axial contacts indicate weak coordination of pyridazine nitrogen atoms as well. The ligand adopts a twist configuration, rotating one phenol group relative to the other, leading to a situation where the pyridazine groups straddle opposite sides of the dinuclear centres (Fig. 118(b)). These complexes exhibit strong antiferromagnetic coupling and redox chemistry involving two one-electron reduction steps at negative potentials (0 to −0.7 V (SCE)). Mixed-valence state (Cu(II)–Cu(I)) species have been generated electrochemically and characterized by ESR spectroscopy [220].

In contrast to this behaviour, if the same condensation reaction is carried out in the presence of other copper(II) salts containing anions with significant coordinating abilities (e.g. Cl, Br, NO_3, CF_3SO_3), 1:1, 17-membered macrocycles are formed which accommodate two copper centres involving phenoxide and methoxide or anion bridges [220].

Rigid and flexible macrocyclic Schiff bases can form dinuclear copper complexes, quite often by metal exchange of the mononuclear barium(II) analogues with copper(I) or copper(II) salts. These copper complexes produce polynuclear species by reaction with O_2 and/or suitable organic substrates. $[Cu_2(\mathbf{134})(RCN)_2](ClO_4)_2$ and $[Cu_2(\mathbf{135})(MeCN)_2]Y_2$ are quite appropriate starting complexes to obtain more complicated structures.

In the cation $[Cu_2(\mathbf{135})(MeCN)_2]^{2+}$, three-coordinate copper(I) ion is bonded to two macrocycle nitrogen donors and to the nitrogen of one MeCN molecule. The stereochemistry is distorted trigonal planar with the copper(I) ions displaced 0.23 Å, on opposite sides, from the N_3 planes. The Cu ··· Cu separation is 3.35 Å [221].

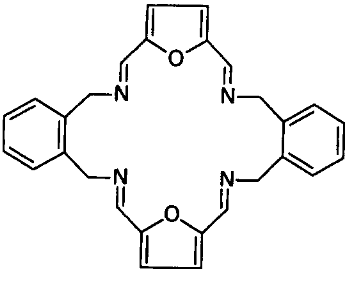

134

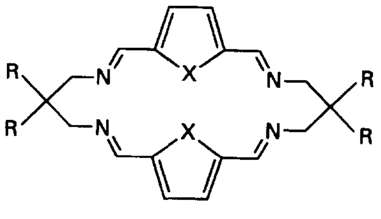

135 X=O, R=H
136 X=O, R=Me
137 X=S, R=H

The consumption by $[Cu_2(\mathbf{135})(MeCN)_2]Y_2$ is only 0.5 ± 0.03 mol O_2 per dicopper(I) unit in the absence of the substrate. It was suggested that each O_2 molecule is associated, in its reduction, with four copper atoms rather than two. Such a situation could occur if the initial coordination of O_2 by $[Cu_2(\mathbf{135})(MeCN)_2]Y_2$ is followed, in the absence of substrate, by fast bimolecular two-electron transfer with a second molecule of $[Cu_2(\mathbf{135})(MeCN)_2]Y_2$ to generate the μ-oxo species according to the reactions

$$Cu^I \cdots Cu^I + O_2 \rightarrow Cu^{II}\text{–}(O_2)^{2-}\text{–}Cu^{II} + Cu^I \cdots Cu^I \rightarrow [Cu^{II}\text{–}O\text{–}Cu^{II}]_2$$

For this oxo species an aggregate of two dimeric units was proposed.

$[Cu_4(\mathbf{135})(OH)_2](ClO_4)_2H_2O$, whose μ-hydroxo-dicopper(II) structural unit was inferred from the antiferromagnetic behaviour ($\mu_{eff}/Cu = 1.37\mu_B$ at 293 K and $0.70\mu_B$ at 93 K), by reaction with phenylacetylene in a MeCN–MeOH (2:1 v/v) solution at reflux for 15 min, gave orange crystals of $[Cu_4(\mathbf{135})_2(CCPh)](ClO_4]_3 0.5dpda$ (dpda = diphenyldiacetylene) followed by white crystals which were shown by chemical analysis and mass and ^1H NMR spectra to be dpda. The total recovered yield of reacted phenylacetylene, i.e. $[CCPh]^- +$ dpda, was 0.95 mol per Cu atom.

The ^1H NMR spectrum of this tetranuclear copper(II) complex in MeCN showed the expected features of the coordinated macrocycle together with a pair of multiplets at δ 7.57 attributable to the coordinated phenylacetylide group. In the structure of $[Cu_4(\mathbf{135})_2(CCPh)][ClO_4]_3 0.5dpda$ (Fig. 119), each macrocycle is bonded to a pair of copper atoms via the four imino nitrogen atoms.

The conformation of each Cu_2N_4 moiety is such that the two metal atoms sit outside the approximate N_4 plane on the open face of the saddle-shaped macrocycle. The four nitrogen atoms of each macrocycle are almost planar. The two pairs of copper atoms are linked via the C–C bond of the phenylacetylide ion. The furan oxygen atoms are not coordinated. The bonding of the two pairs of copper atoms to the acetylide group is different [221].

The dicopper complex $[Cu_2(\mathbf{134})(RCN)_2](ClO_4)_2$ does not react with O_2 in acetonitrile; in DMF, the action of O_2 with this dinuclear macrocyclic complex

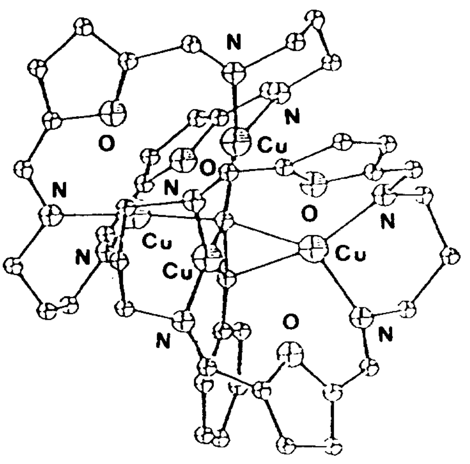

Fig. 119. Structure of $[Cu_4(\mathbf{135})(CCPh)]^{3-}$.

produces a tetranuclear species $[Cu_4(\mathbf{134})_2(OH)](ClO_4)_3H_2O$ whose structure was also determined by X-ray diffraction [222].

Each asymmetric unit contains one $[Cu_2(\mathbf{134})_2(OH)]^{3+}$ cation, three perchlorate anions and two molecules of acetonitrile solvate. The cation contains four coplanar copper(I) ions each coordinated to two imine nitrogen atoms, one from each of the two **134** macrocycles. Within the square plane of the four copper atoms is a hydroxide ion disordered between two positions. In both sites the hydroxide is coordinated to one copper atom with weaker interactions to two other copper atoms.

Each macrocycle is folded in a boat conformation so that the two furan rings are approximately parallel and close enough to suggest some π interaction. Thus there is a planar Cu_4O assembly incorporated in a near-spherical complex ion (Fig. 120). The possible sequence of reactions of Scheme 44 has been proposed [222].

The Cu–Cu distances are too large to allow the hydroxide ion to interact with all four copper ions and this is probably the reason for the observed disorder.

A hexanuclear copper(I) structure was also found in the catalytic oxidation of PhSH to PhSSPh with $[Cu_2(\mathbf{135})(OH)_2](ClO_4)_2H_2O$ or $[Cu_2(\mathbf{135})(OR)_2(MeCN)_2](BPh_4)_2$ (Fig. 121). The cation $[Cu_6(\mathbf{135})_3(SPh)_2]^{2+}$ contains six three-coordinate copper(I) ions linked via two thiolate groups each tetrahedrally bound to three copper atoms and one phenyl carbon atom [10].

By treatment of $Ba(\mathbf{135})(ClO_4)_2 \cdot EtOH$ and $Ca(\mathbf{136})(ClO_4)_2 \cdot EtOH$ with a threefold excess of $[Cu(CH_3CN)_4](ClO_4)$ in CH_3CN–EtOH (2:3) at 60°C and, in the absence of air, the complexes $[Cu_2(\mathbf{135})(CH_3CN)_2](ClO_4)_2$ and

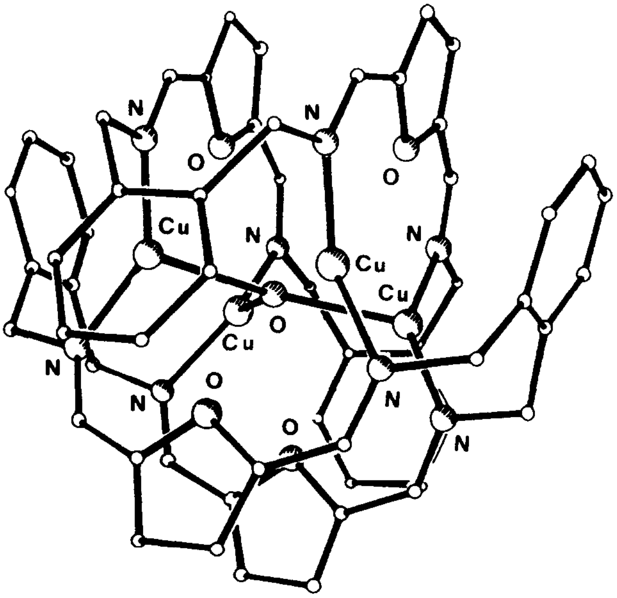

Fig. 120. Structure of $[Cu_4(\mathbf{134})_2(OH)]^{3+}$.

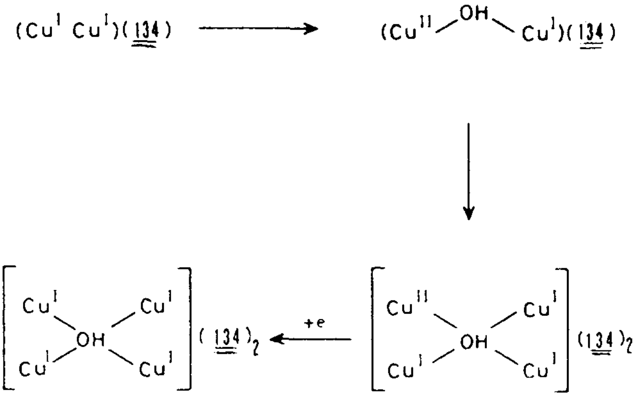

Scheme 44.

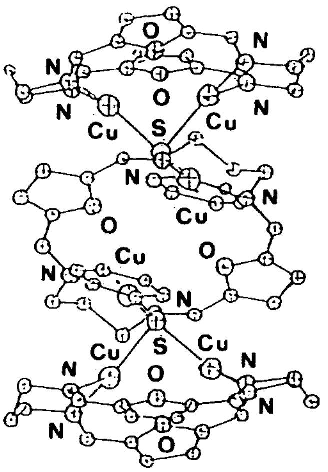

Fig. 121. Structure of $[Cu_6(\mathbf{135})_3(SPh)_2]^{2+}$.

$[Cu_2(\mathbf{136})(CH_3CN)_2]$ have been obtained. When the transmetallation was carried out at reflux temperature in "wet" solvent (1%–2% H_2O) with access to air, the pentanuclear complexes $[Cu_5(\mathbf{136})_2(dmt)_2](ClO_4)_3$ and $[Cu_5(\mathbf{136})(dmt)_2](ClO_4)_3$ and $[Cu_5(\mathbf{137})_2(dmt)_2](ClO_4)_3$ (dmt ≡ 3,5-dimethyl-1,2,4-triazolate anion) were obtained starting from $[Cu(\mathbf{135})(MeCN)_4](ClO_4)_2$ and $[Cu_2(\mathbf{136})(MeCN)_2](ClO_4)_2$ and $[Cu_2(\mathbf{137})(CH_3CN)_2]ClO_4)_2$. Separate experiments established the necessity of both H_2O and O_2 for the formation of the triazolate ring. Moreover, no triazolate was formed when $[Cu(CH_3CN)_4](ClO_4)$ was used in place of the dinuclear complexes $[Cu_2(\mathbf{135})(MeCN)_2](ClO_4)_2$ or $[Cu_2(\mathbf{136})(MeCN)_2](ClO_4)_2$. The use of EtCN in the solvent mixture in place of MeCN afforded the corresponding pentanuclear complexes of 3,5-diethyl-1,2,4-triazolate. The nature of the pentanuclear complex was determined by their independent preparation in the absence of air and water via self-assembly from the dinuclear copper(I) complexes with the ligands **135** to **137** (2 equivalents), pre-prepared Hdmt (2 equivalents) and $[Cu(CH_3CN)_4](ClO_4)$ (1 equivalent). The structure of $[Cu_5(\mathbf{136})_2(dmt)_2](ClO_4)_3$ shows (Fig. 122) that the cation comprises five copper(I) atoms, two molecules of macrocycle and two triazole anions. Four of the copper(I) atoms have a three-coordinate distorted trigonal planar geometry while the central copper(I) atom, positioned at a centre of symmetry, is two coordinate with a linear arrangement. This central copper atom is linked to the two pairs of three-coordinate copper atoms by the two coplanar bridging triazolyl anions [223].

The macrocycle molecules have a non-planar, saddle-shaped conformation. This is reflected in the ^1H NMR spectrum which shows the inequivalence of the CH_3 groups in each saturated segment of the macrocycle (at $\delta = 0.8$ and $\delta = 1.15$) and also in the two protons of the adjacent methylene groups (at $\delta = 3.5$ and $\delta = 4.4$).

The mechanism reported in Scheme 45 has been proposed for the formation of the triazole from acetonitrile. The first step is an aerobic oxidation of the dicopper(I) complex to the di-μ-hydroxodicopper(II) species. This is followed by intramolecular nucleophilic attack by the bridging OH^- groups or intermolecular attack by H_2O at the nitrile carbon atoms.

A concerted nitrile-to-Cu(II) electron transfer at both metal centres with accompanying coupling of the two adjacent nitrogen atoms leads to the species 3 of Scheme 45. The NH_3 needed for the final ring-closure step was supposed to come from a separate metal-promoted hydrolysis of acetonitrile, the intermediate hydrolysis product acetamide having been detected in the reaction mixture [223].

The tetraketones 1,1-(1,3-phenylene)-bis-1,3-butane dione, 1,1-(1,4-phenylene)-bis-1,3-butandione, 1,4-bis(acetoacetyl)pyperazine, *N*-(*o*-toyl)diacetoacetamide and 1,1′-(2,6-pyridyl)-bis-1,3-butanedione (Scheme 46) and related Schiff bases have been

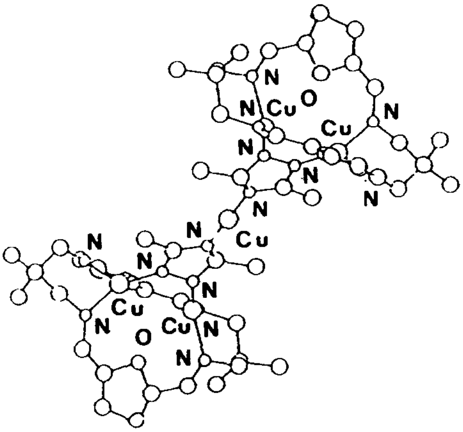

Fig. 122. Structure of $[Cu_5(\mathbf{136})_2(dmt)_2]^{3+}$.

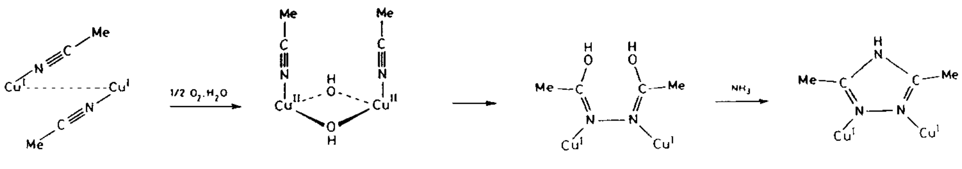

1 2 3 4

Scheme 45. Proposed mechanism for the copper-mediated hydrolysis–oxidation of acetonitrile to 3,5-dimethyl-1,2,4, triazole.

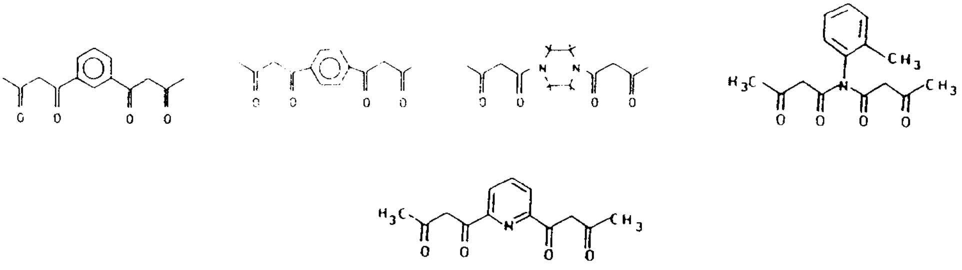

Scheme 46.

synthesized and used in the preparation of polynuclear coordination systems [224,225]. The first two ligands offer two isolated β-diketonate moieties and thus the complexes obtained resemble the β-diketonate complexes. In N-(o-toyl)diacetoacetamide and 1,1-(2,6-pyridyl)-bis-1,3-butanedione, the four ketonic moieties are at the appropriate positions to form homo- or heterotrinuclear complexes (C) in addition to homodinuclear complexes, for which the two alternative structures (A) and (B) reported in the Scheme 47 have been proposed [225].

The dinuclear complexes can be easily converted into the trinuclear by common synthetic procedures. The dinuclear complexes exhibit physicochemical properties typical of isolated β-diketonato compounds while in the trinuclear species (for instance trinuclear copper(II) complexes), significative antiferromagnetic interactions

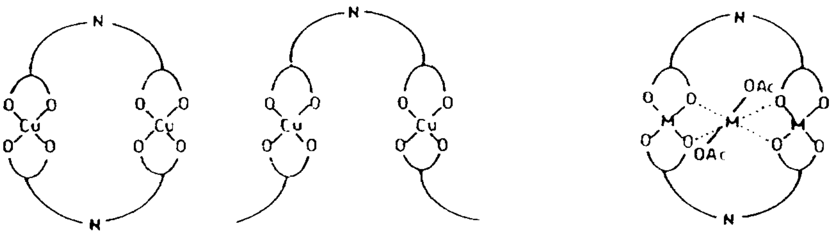

Binuclear (A) Polymer (B) Trinuclear (C)

Scheme 47.

take place indicating the metal ions are held together in adjacent coordination chambers.

With 1,1-(2,6-pyridyl)-bis-1,3-butanedione H_2-**138** the discrete trinuclear complexes $[M_2M'(\mathbf{138})_2]^{2+}$ have been suggested for $M \equiv Zn^{2+}$, Cu^{2+}, Ni^{2+} and $M' \equiv Zn^{2+}$, Ba^{2+} while manganese(II) forms a tetranuclear compound $[Mn_4(\mathbf{138})_2]^{4+}$. This indicates that the central cavity could contain two metal ions as observed for related hexadentate Schiff base macrocycles.

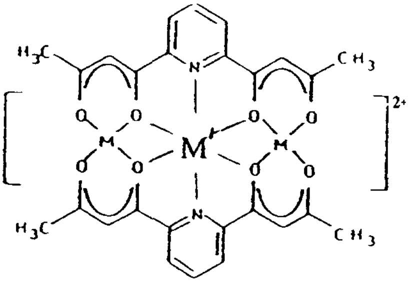

$[M_2M'(\underline{138})_2]^{2+}$ $M=Cu^{2+}, Ni^{2+}, Zn^{2+}$

$M'=Ba^{2+}, Zn^{2+}$

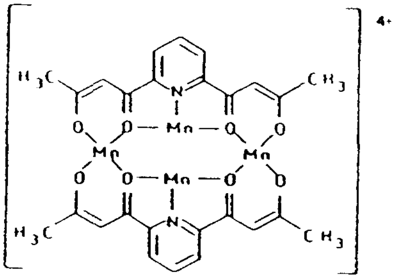

$[Mn_4(\underline{138})_2]^{4+}$

1,1-(2,6-pyridyl)-bis-1,3-butanedione reacts with a series of hydroxyalkyl or hydroxyaryl amines in ethanol to give the Schiff bases H_4-**140** and H_4-**141**. By reaction with copper(II) salts, these Schiff bases produce complexes formulated on the basis of their reduced magnetic moments as polymers of the type $[Cu_4(\mathbf{140})_2]_n$ and $[Cu_4(\mathbf{141})_2]_n$.

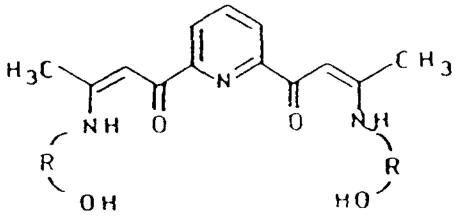

	R
H_4-<u>140</u>	C_6H_4
H_4-<u>141</u>	$(CH_2)_n$ (n=2-5)

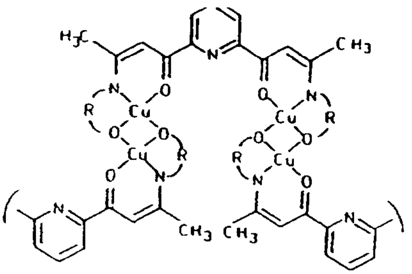

$[Cu_4(\underline{140})_2]_n$ and $[Cu_4(\underline{141})_2]_n$

In some complexes (containing bromide as anion), the ligand behaves as a neutral entity; the copper atoms are coordinated also by bromide ions.

As an extension, the hexaketone 1,3-bis(2-methyl-4,6,8-octanetrione-8-yl) benzene (H_4-**142**) and the homo- and heterotetranuclear complexes $[Cu_4(\mathbf{142})_2(py)_4]_2py$ and $[(UO_2)_2(Zn)_2(\mathbf{142})_2(py)_6]$ have been prepared [226]. In the tetracopper(II) complex, two deprotonated ligands and four copper(II) ions form neutral molecular complexes. The four copper ions are grouped into two sets of two with a metal–metal distance of 6.9 Å across the plane of the phenyl groups and an intragroup metal–metal distance of 3.021 Å. The coordination sphere of the copper ions is composed of four ketonate oxygen atoms in the distorted tetragonal pyramid; within the molecule, the pyridines alternate above and below the plane of the ligand (Fig. 123) [226].

Strong magnetic superexchange between the copper(II) ions in the binuclear units renders the molecule diamagnetic at room temperature. Cyclic voltammetry in pyridine in the range from 0 to 1.2 V yields one quasi-reversible wave with $E_{1/2} = 0.8$ V. Chronoamperometric results show that this wave is due to a four-electron transfer process. Owing to the structural similarity of this complex with bis(1,3,5-triketonate) dicopper(II) complexes, which are known to undergo sequential two-electron transfer, this process can be viewed as two-electron transfer in non-interacting binuclear centres [226].

Minor modification of procedures used to generate the dinuclear compartmental ligands can afford polynucleating ligands, and additional types of reactivities or physicochemical properties stemming from the flexibility may be observed. Thus, the acyclic and macrocyclic Schiff bases of Scheme 48 have been obtained either by self-condensation of the precursors or as metal complexes by template procedures [227,228]. The acyclic ligands H_4-**143** and H_8-**144** have been obtained by condensation of polyamine 1,4- or 1,3-bis[bis(2-aminoethyl)aminomethyl]benzene respectively, with salicylaldehyde or 2,3-dihydroxybenzaldehyde in a molar ratio of 1:4 and in methanol.

A fast atom bombardment mass spectrometry investigation has revealed the presence of the parent peak at the appropriate *m/z* value for both ligands while ^1H and ^{13}CNMR confirm the structure proposed in Scheme 48.

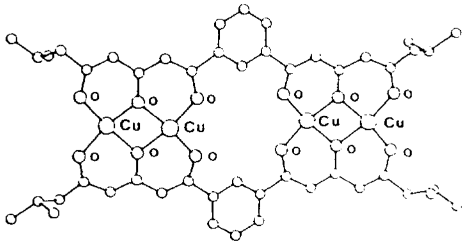

Fig. 123. The structure of $[Cu_4(\mathbf{142})_2(py)_4]$.

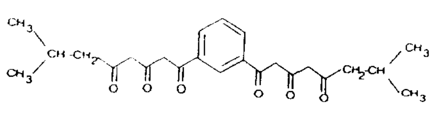

H_4-**142**

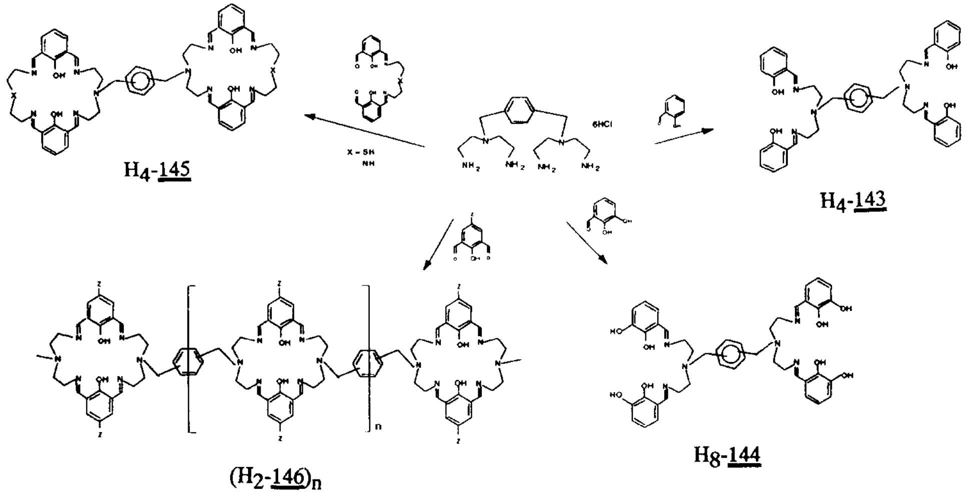

Scheme 48.

The reaction of H_4-**143** and H_8-**144** with $UO_2(CH_3COO)_2 \cdot 2H_2O$ in the appropriate molar ratio in boiling methanol produces the dinuclear $(UO_2)_2$(**143**)$\cdot 2H_2O$ or $(UO_2)_2(H_2$-**144**)$\cdot 2H_2O \cdot$2dmf and the tetranuclear $(UO_2)_4$(**144**)$\cdot 2H_2O \cdot$2dmf complexes.

An X-ray investigation on $(UO_2)_2$(**143**)$\cdot$dmso$\cdot C_6H_6$ shows that the compound forms a centrosymmetric binuclear complex as the benzene ring, bridging the two macroacyclic coordination moieties, is centred on the inversion point [227]. The quasi-linear uranyl(VI) ion is equatorially coordinated in the usual, slightly distorted, bipyramidal pentagonal configuration by the O_2N_3 donor set of the Schiff base ligand forming an irregular puckered pentagon (Fig. 124(a)). The entire molecule can be depicted as a three-step conformation. The two least-squares planes containing the central benzene ring and the equatorial O_2N_3 coordination pentagon are approximately parallel; the two uranium atoms are displaced 1.20 Å and below the central benzene ring plane and are 12.686 Å apart (Fig. 124(b)) [227]. The dmso and

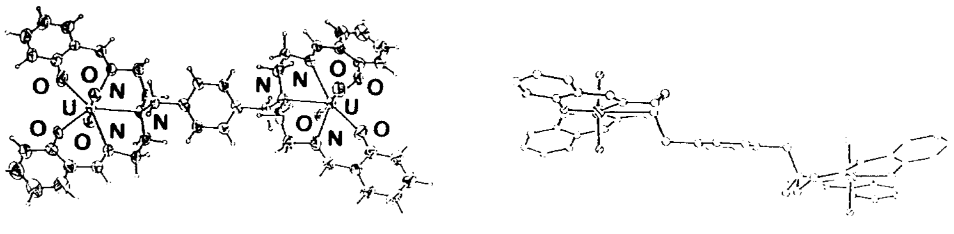

(a) (b)

Fig. 124. (a) The molecular structure and (b) the three step conformation of the complex $(UO_2)_2$(**143**).

benzene molecules do not present any type of interaction with the remaining cell content.

Dinuclear $Ln_2(H_2\text{-}\mathbf{144})(X)_2$ ($X \equiv NO_3^-$, OH^-) and homo- and heterotetranuclear lanthanide(III) complexes, $Ln_4(\mathbf{144})(NO_3)_2(OH)_2$, have been prepared with a procedure similar to that employed for tetrauranyl(VI) analogues.

By reaction of the same polyamines with 2,6-diformylphenols, the "face-to-face" H_4-**145** or polynuclear $(H_2\text{-}\mathbf{146})_n$ compounds have been obtained [228] (Scheme 48). The organic polymer is quite insoluble and hence difficult to characterize fully; the complexes have been obtained only by a template procedure.

A template synthesis was also employed for the preparation of uranyl(VI) and lanthanide(III) complexes with the ligand H_4-**145**. These complexes, $(UO_2)_2(\mathbf{145})$ and $(La)_2(\mathbf{145})(NO_3)_2$, have been synthesized by reaction of the acyclic mononuclear complexes with the hexamine in alchoholic solution.

Very recently the synthesis and characterization of ligands of the type reported in Scheme 49 were carried out [228].

In the heterodinuclear complexes containing lanthanide(III) ions, $[MLn(H_2\text{-}\mathbf{81})(X)_3]$ ($X \equiv NO_3^-, Cl^-, CH_3COO^-$), the anions complete the coordination sphere about the central f ion. When these anions are partially removed by addition of a base (i.e. LiOH), oligomerization occurs, with the formation of tetranuclear species. Also, the "tripodal" heptadentate amine phenol ligand tris((2-hydroxybenzyl)amino)ethylamine forms a homodinuclear eight-coordinate complex with gadolinium(III) nitrate in the presence of base where the two gadolinium atoms are bridged by phenolate oxygen atoms, one from each heptadentate

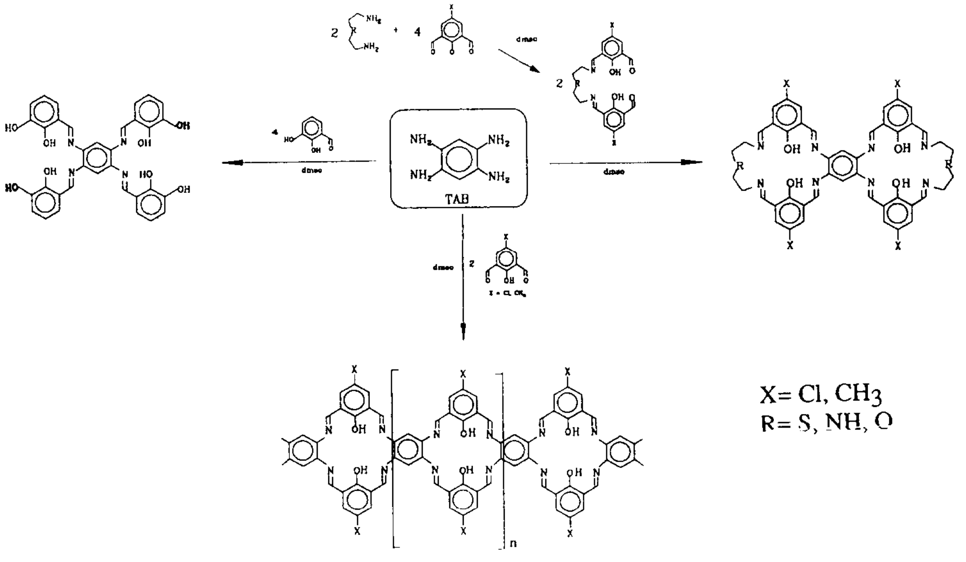

X= Cl, CH3
R= S, NH, O

Scheme 49.

ligand [164]. This seems to be a route for the synthesis of heteropolynuclear complexes with predetermined properties, and preliminary synthetic data show that it is possible to obtain polynuclear complexes by reaction of appropriate polyamines and formyl precursors in the presence of the desired metal ions and bases (Scheme 50).

With these systems (especially that derived from 2,3-dihydroxybenzaldehyde), it seems also possible to prepare pure heteropolynuclear species without prior isolation of monomeric complexes, this being due to the capability of the N_2O_2 and O_2O_2 sites to coordinate preferentially d and f metal ion respectively.

Macrocyclic and macroacyclic receptor molecules that contain an electrochemically responsive signaling function, i.e. a redox-active centre, in close proximity to a host binding site are currently under investigation [229–232]. Depending on the complementary nature of the host cavity, these systems can in principle be designed to recognize electrochemically the binding of any charged or neutral inorganic or organic guest molecules through either space electrostatic interactions or electrostatic communication via various bond linkages between the receptor site and the redox centre [231]. Selective binding of a particular guest molecule coupled with an electrochemical response is of paramount importance for future potential prototypes of new amperometric molecular sensory devices [229–233]. Several of these systems are based on Schiff base hosts [230–235].

Polyfunctionalized macrocyclic and macroacyclic ligands capable of forming polynuclear species have been recently prepared. The macrobicyclic Schiff bases **147** and **148** have been obtained by one-step synthetic methodology of [2 + 3] condensation of tris(2-aminoethyl)amine and ferrocene-1,1′-dicarbaldehyde or 4,4′-diformyl-2,2′-bipyridyl [229]. These Schiff bases are easily reduced using $NaBH_4$ to give **149** and **150** (Scheme 51) [229].

The addition of two equivalents of $[Zn(dmso)_5](ClO_4)_2$ to dimethyl sulphoxide solutions of **147** and **149** led to the isolation of the dinuclear cryptates $[Zn_2(\mathbf{147})](ClO_4)_4$ and $[Zn_2(\mathbf{149})](ClO_4)_4$ respectively.

Electrochemical data suggest the two-coordinated Zn^{2+} guest cations are not

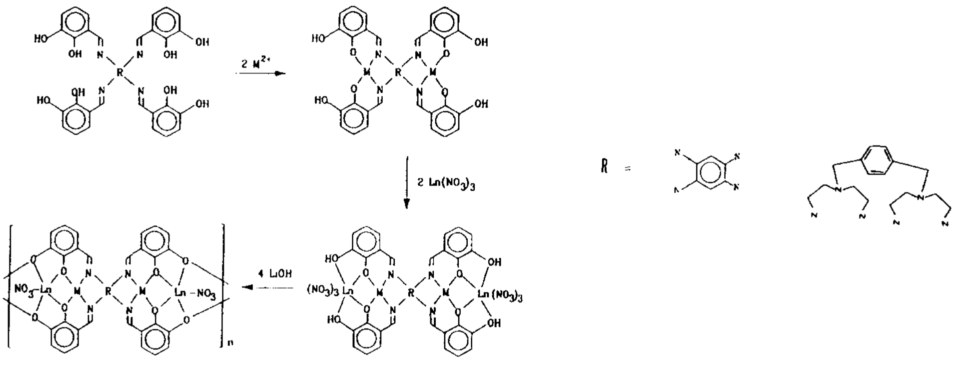

Scheme 50.

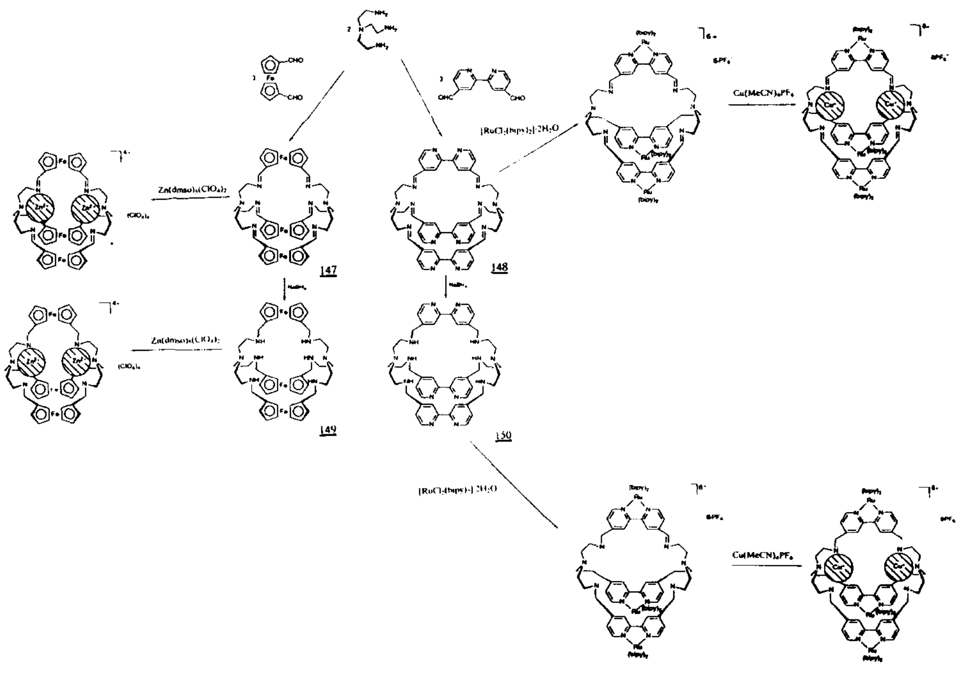

Scheme 51.

electrostatically communicating with the ligand's peripherally linked ferrocene redox centres. The reaction of 3 equivalents of $[RuCl_2(bipy)_2] \cdot 2H_2O$ with 1 equivalent of **148** in dimethylformamide initially gave an intensely coloured deep red solution. Treatment with an excess amount of ammonium hexafluorophosphate precipitated the trimetallic complex $[Ru_3(\mathbf{148})(bipy)_6](PF_6)_6$ containing three externally coordinated ruthenium(II) cations. The addition of two equivalents of $[Cu(MeCN)_4]PF_6$ to an acetonitrile solution of the latter complex gave the heteropolymetallic complex $[Ru_3Cu_2(\mathbf{148})(bipy)_6](PF_6)_8$ containing two internally coordinated copper(I) cations in addition to the three externally bound ruthenium(II) cations. In an analogous stepwise synthetic procedure starting with **150**, the heteropolymetallic $[Ru_3Zn_2(\mathbf{150})(bipy)_6](PF_6)_8$ complex was also successfully isolated. It was suggested that the internally coordinated zinc(II) metal cations do electrostatically communicate and perturb the photo- and electrochemical properties of the externally bound ruthenium(II) cations; for example the metal-to-ligand charge transfer band of $[Ru_3(\mathbf{148})(bipy)_6](PF_6)_6$ is blue shifted in the presence of an excess amount of $Zn(ClO_4)_2$ [229].

The condensation in ethanol or acetonitrile of formylferrocene with polyamines $H_2N(CH_2)_2NH_2$, $NH_2(CH_2)_2X(CH_2)_2NH_2$ ($X \equiv NH$, S, O, $N(CH_2)_{11}CH_3$), $H_2N(CH_2)_2O(CH_2)_2O(CH_2)_2NH_2$ and $H_2N(CH_2)_3\text{–}NN\text{–}(CH_2)_3NH_2$ forms the corresponding Schiff bases (Scheme 52) as confirmed by the X-ray structure of the compound where R ≡ $(CH_2CH_2OCH_2CH_2)$ (Fig. 125(a)) [230,231].

There are two independent molecules of the diferrocenyl ligand in the asymmetric unit. These two molecules are chemically equivalent and show that the ferrocenyl groups are in the eclipsed form; the cyclopentadienyl ring couples are perfectly parallel with Fe–C distances normal. The C=N double bonds of the Schiff base moiety are well localized and are between 1.26 and 1.27 Å. No relevant intra- or intermolecular interactions are present [230].

These Schiff bases can be reduced, as proved for *N,N'*-ethylenebis(ferrocenylidene)amine which forms bis{*N,N'*-ethylenebis[(ferrocenylmethyl)amine]} by reaction with $NaBH_4$ (Scheme 52) [231].

The X-ray structure of the copper(II) dinitrate with bis{*N,N'*-ethylenebis[(ferrocenylmethyl)amine]} shows that the copper(II) ion is in an octahedral surrounding

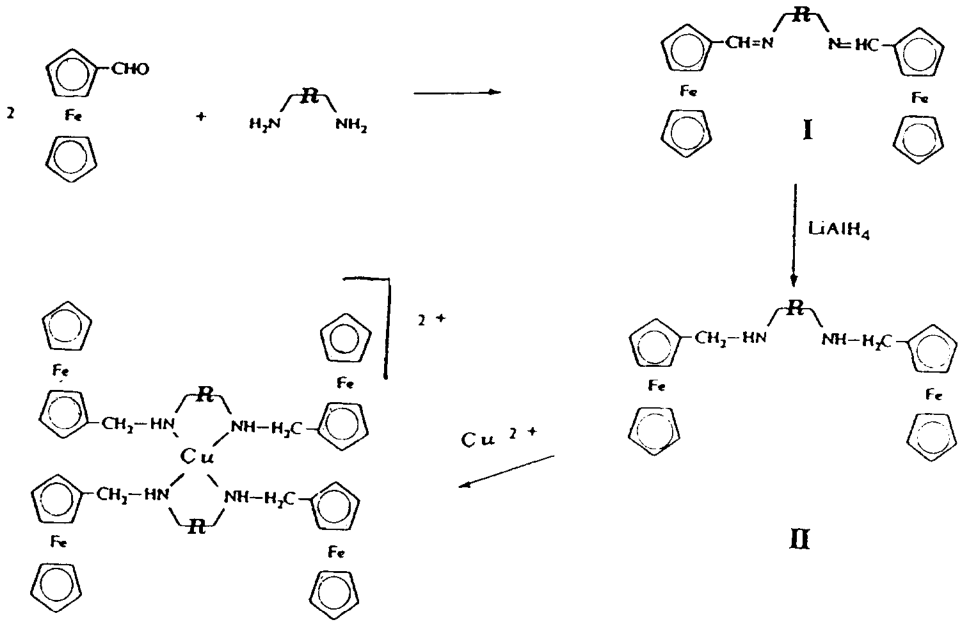

R

$H_2N(CH_2)_2NH_2$
$NH_2(CH_2)_2X(CH_2)_2NH_2$ (X= NH, S, O, $N(CH_2)_{11}CH_3$)
$H_2N(CH_2)_2O(CH_2)_2O(CH_2)_2NH$
$H_2N(CH_2)_3$-N N-$(CH_2)_3NH_2$

Scheme 52.

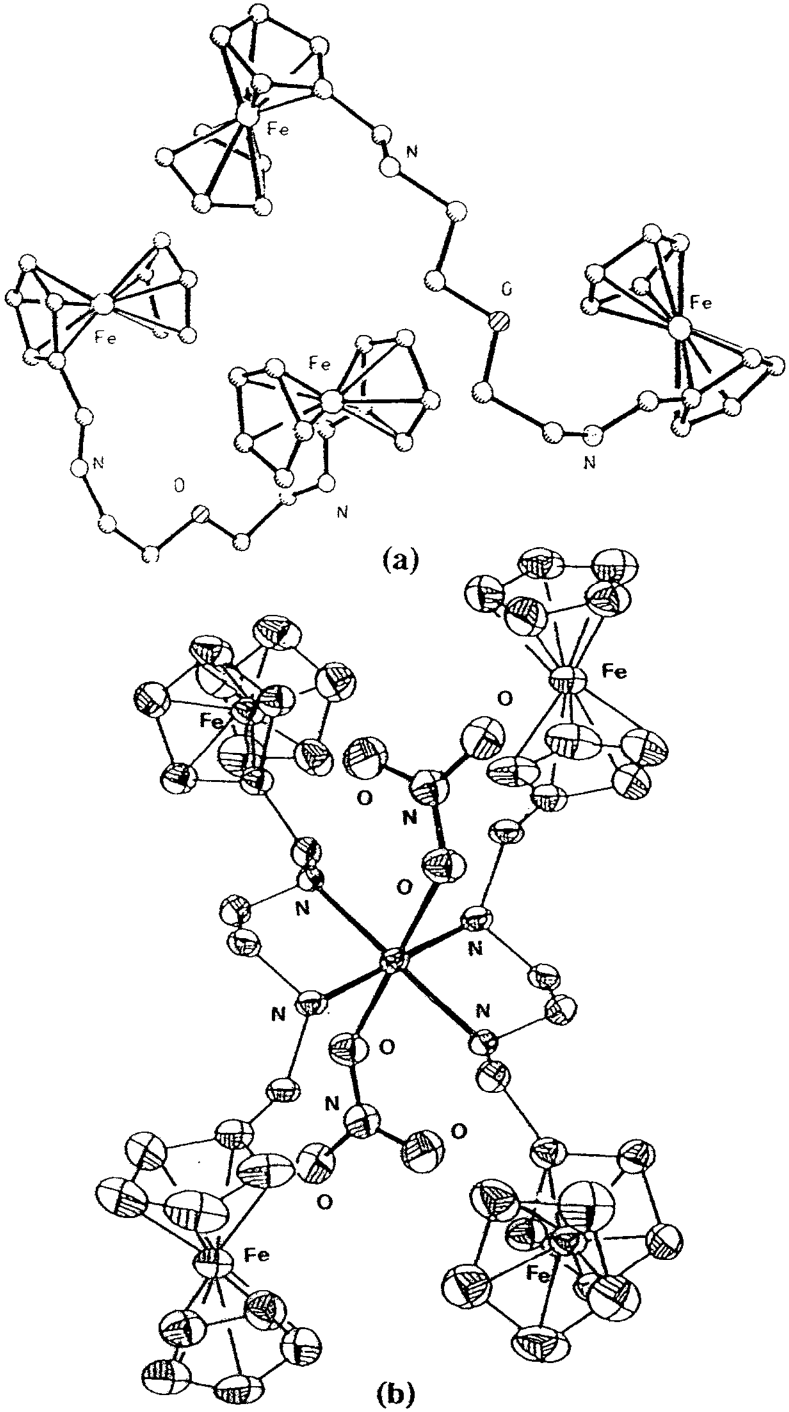

Fig. 125. Structures of (a) diferrocenyl Schiff base reported in Scheme 52 (R ≡ $-(CH_2)_2O(CH_2)_2-$) and (b) bis{*N*,*N*′-ethylene bis[(ferrocenylmethyl)amine]}copper(II) dinitrate.

formed by the four equatorial nitrogen atoms from the two diferrocenyl-containing groups (II), which act as bidentate ligands through the ethylenediamine nitrogen atoms and the two apical oxygen atoms of two nitrate anions. The four nitrogen atoms of the basal plane are planar and the copper atom lies in this plane (Fig. 125(b)) [231].

In this pentanuclear complex the four ferrocene groups oxidize at the same potential as shown by cyclic voltammetry; thus, this compound is a four-electron reservoir potentially capable of acting as a multielectron mediator in redox catalytic reactions. Its electronic properties have been characterized by spectroscopic techniques and variable-temperature magnetic susceptibility measurements [230].

The reaction of formylferrocene with 4,4′-diaminodibenzo-18-crown-6 forms the compound A which yields B by reduction with $NaBH_4$ (Scheme 53(a)).

A similar Schiff base has been obtained by condensation of (4 aminophenyl)-ferrocene with 4-formylbenzo-15-crown-5.

With these Schiff base systems one-wave anodic shifts on the ferrocene redox couple were observed with Na^+, K^+ and Mg^{2+} with magnitudes of shift increasing with increasing charge of the guest cations.

The reduced macrocycle B of Scheme 53(a) contains a saturated linkage between the aza crown system and ferrocenyl redox centre; it was found to serve as an insulator and it is totally electrochemically insensitive to the presence of any alkali metal cation. This is a general behaviour: with these types of ligand systems anodic perturbations of the ferrocene oxidation wave are observed if a conjugated π electron system (–C=C–, –CH=N–) links the heteroatoms of the crown ionophore to the redox centre, and the polarizing power of the guest metal cation is of great importance in determining the magnitude and type (one or two wave) of shift in redox potential of the ferrocenyl redox centre [232].

Similarly the condensation of ferrocene-1,1′-dicarbaldehyde and an appropriate diamine gave the Schiff base products which were easily reduced using $NaBH_4$ to give the corresponding polyazaferrocene macrocyclic ligands (Scheme 53(b)) [232].

X-ray crystallographic investigations on the polyazaferrocene macrocycle where $R \equiv CH_2CH_2NHCH_2CH_2$ confirms the reaction pathway proposed in Scheme 53(b) [232]. The structure consists of discrete molecules as shown in Fig. 126. The $Fe(cp)_2$ unit is eclipsed with Fe–C distances in the range 2.025–2.071 Å. The conformation of the aza methylene linkage indicates approximate C_s symmetry [232].

Preliminary metal coordination investigations with $Ni(ClO_4)_2$, $Cu(BF_4)_2$ and $Zn(ClO_4)_2$ and the polyazaferrocene macrocycles of Scheme 53(b) led to the successful isolation of corresponding complexes whose elemental analyses all suggested 1:1 ligand metal stoichiometry. With zinc, ^{13}C and ^{1}H NMR titration experiments in CD_3CN confirm 1:1 Zn^{2+}:ligand solution stoichiometry [232].

Of particular relevance to chemical sensor technology are the results of electrochemical competition experiments. When an equimolar mixture of Ni^{2+}, Cu^{2+} and Zn^{2+} is added to aqueous electrochemical solutions of the polyazaferrocene macro-

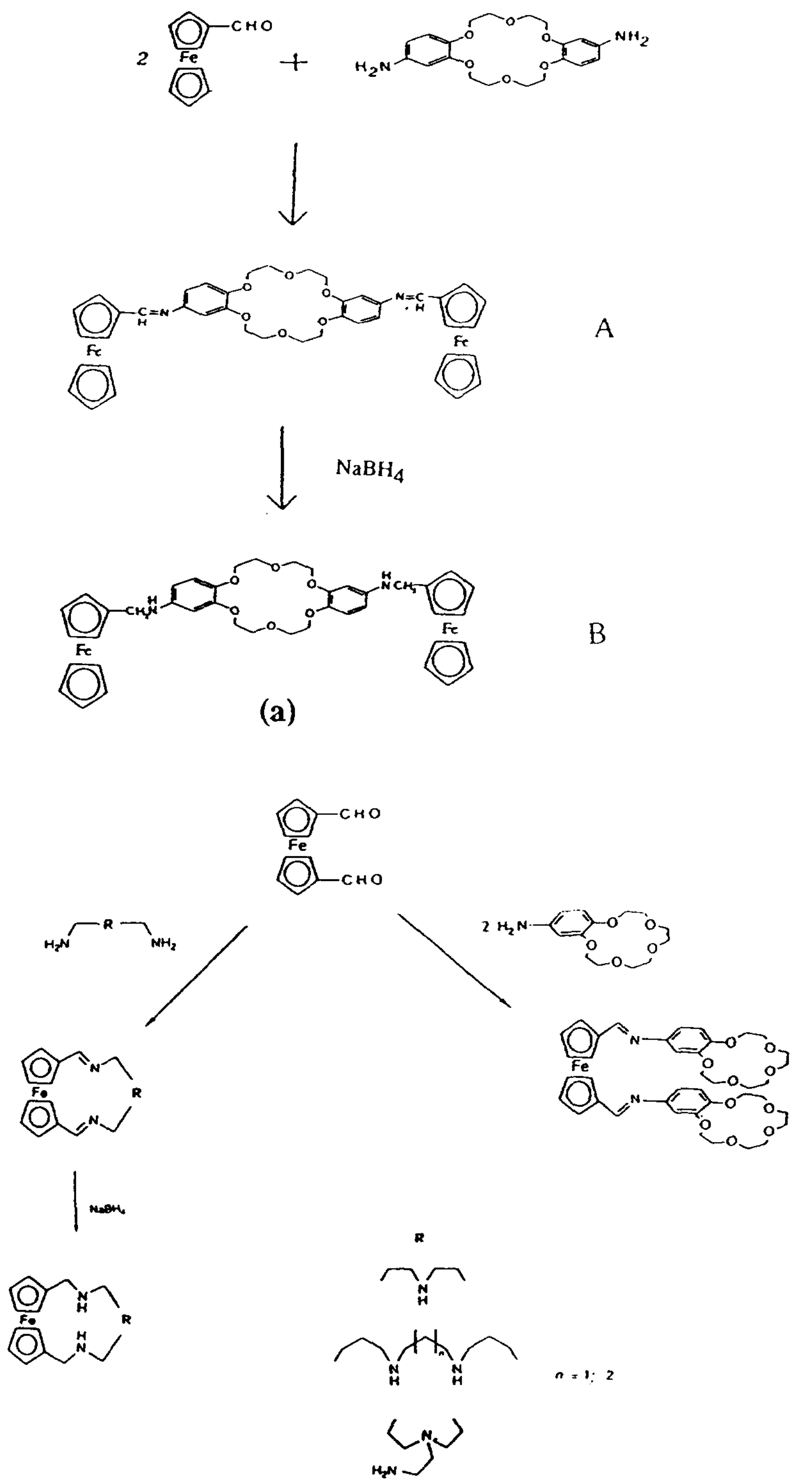

Scheme 53.

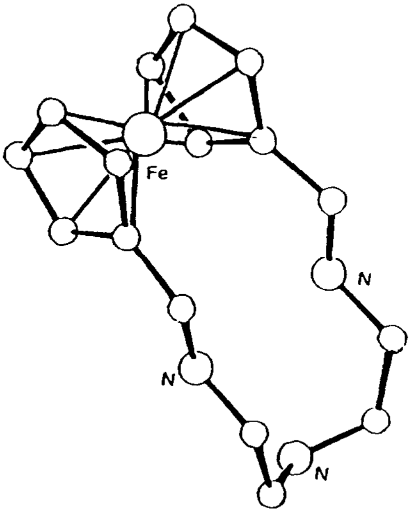

Fig. 126. Structure of a polyazaferrocene macrocycle.

cycles with R ≡ $(CH_2)_3NH(CH_2)_3NH(CH_2)_3$ and R ≡ $(CH_2)_3NH(CH_2)_4NH(CH_2)_3$, the ferrocene–ferricinium redox couple shifts anodically by an amount approximately the same as that induced by the Cu^{2+} cation alone. This result suggests these polyazaferrocene derivatives are first-generation prototype copper-selective amperometric sensors, capable of detecting the Cu^{2+} cation in the presence of Ni^{2+} and Zn^{2+} ions [232].

Macrocyclic polyamines, when protonated, have been shown to complex a variety of inorganic and organic anions via favourable electrostatic and hydrogen bonding interactions. The polyazaferrocene derivatives at appropriate pH values can be protonated to produce polyammonium redox-active macrocycles with the potential of complexing and electrochemically sensing anions. Preliminary anion coordination studies were carried out with the nucleotide adenosine trophosphate (ATP) and hydrogenophosphate (HPO_4^{2-}) using initially ^{31}P NMR spectroscopy. At pH values between 6 and 8 the corresponding pK_a values of the polyazaferrocene derivatives are such that at least two of the nitrogen donor atoms are protonated. ^{31}P NMR titration experiments with the polyazaferrocene macrocycles of Scheme 53(b) and ATP and HPO_4^{2-} reveal that these ligands at pH 6.5 form 1:1 complexes with these anionic guests. Cyclic voltammetric experiments evidence the electrochemical recognition of these phosphate anion guests in water. At pH 6.5 cathodic shifts of 60–80 mV of the ferrocene redox couple of the polyazaferrocene macrocycles of Scheme 53(b) are observed in the presence of ATP and HPO_4^{2-} anions. Consequently these new polyazamacrocyclic ligands have been proposed as novel prototype amperometric sensors for the electrochemical recognition of transition metals and phosphate anions in water [232].

Preliminary studies have shown the Schiff base, obtained according to the Scheme 53(b) by reaction of 1,1′-diformylferrocene and 4-amino-15-benzocrown-5, to be K^+ selective, although not electrochemically well behaved [232].

Schiff base bis crown ether ligands [236–238] that contain alkali and transition metal coordinating sites have been prepared via the condensation of 2 or 3 equivalents of 4-formylbenzo-15-crown-5 with an appropriate di- or triamine (Scheme 54).

Homometallic copper(I) and silver(I) and heteropolymetallic copper(I)–sodium, silver(I)–sodium, and copper(I)–potassium complexes have been isolated. The X-ray structure of the copper(I)–potassium complex with the ligand where $X \equiv CH_2CH_2SCH_2CH_2SCH_2CH_2$ is reported in Fig. 127.

The stoichiometry of this ligand to K^+ guest cations is dependent on the

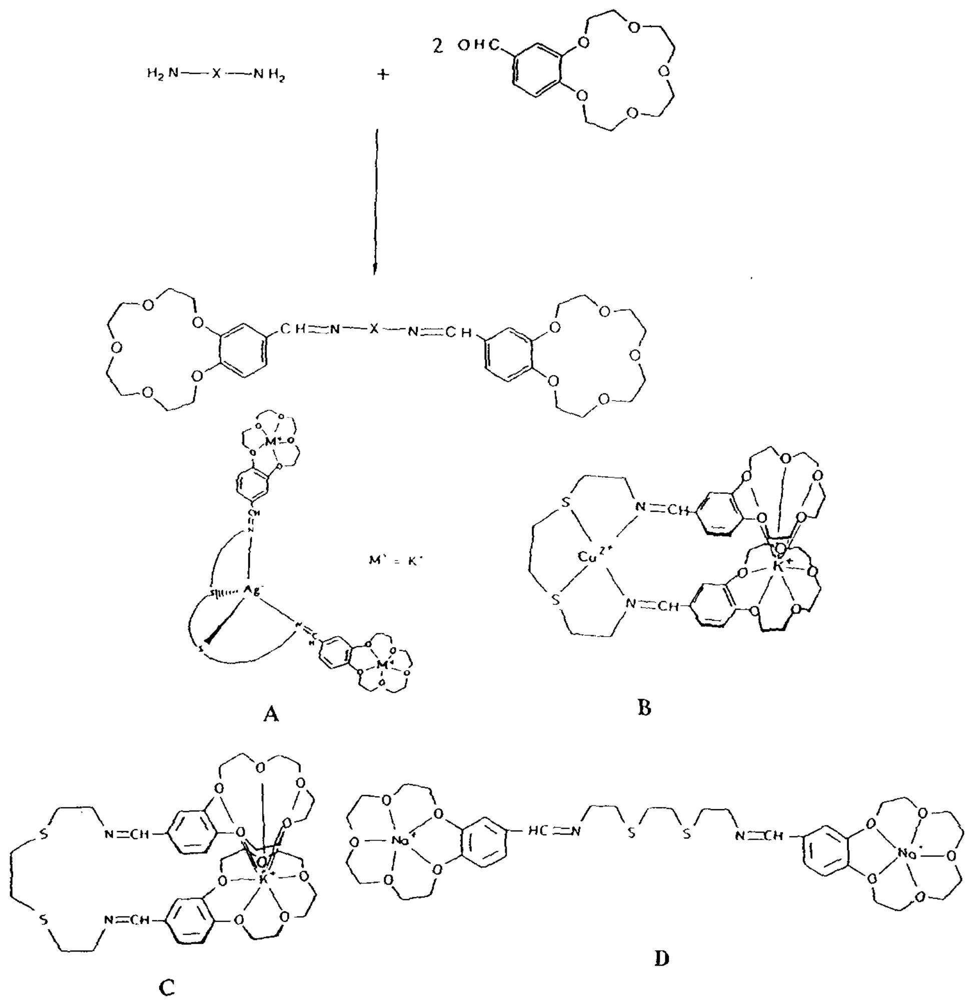

Scheme 54.

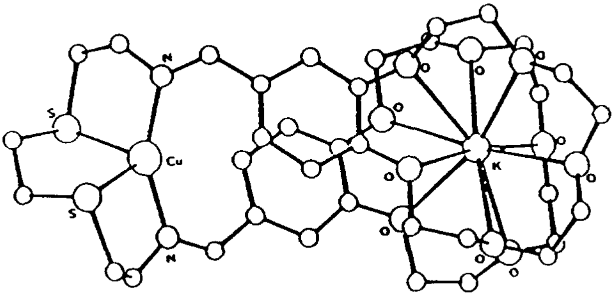

Fig. 127. Structure of the copper–potassium complex with a Schiff base crown ether ligand.

stereochemical requirements of cobound transition metal guests. For example, it forms a 1 : 1 intramolecular sandwich with K^+; however, with tetrahedrally coordinated Ag^+, the subsequent formation of the intramolecular sandwich complex with K^+ is prevented and the polymetallic complex A of Scheme 54 results. With the square planar or tetragonally bound copper(II) complex, however, the stereochemical requirements of this transition metal allow the formation of the preferred 1 : 1 sandwich complex with K^+, B of Scheme 54.

As evidenced in Scheme 54, in the presence of transition metal ions (i.e. Cu^{2+}, Ag^+ etc.), Na^+ forms the dinuclear complex C, while K^+ gives rise to the mononuclear compound D [236].

The Schiff base obtained by condensation of tris(2-aminoethyl)amine with 4-aminobenzene-5-crown-5 forms the tetranuclear copper–sodium complex of Scheme 55. Electrochemical investigations on the homometallic copper complexes of ligands reported in Schemes 54 and 55 revealed that both exhibit irreversible copper(II)/copper(I) redox couples in acetonitrile and dimethylformamide solvents [236,238].

Pentanuclear and hexanuclear complexes containing copper(I) ions and chromium(0) tricarbonyl fragment in the periphery of the molecular entity have been prepared [239,240].

The condensation of 2,2′-bipyridine-6,6′-dicarbaldehyde [241] or 1,10-phenanthroline-2,9-dicarbaldehyde [242] with (*o*-toluidine)tricarbonylchromium [243] in refluxing benzene produces the corresponding Schiff bases **151** and **152** of Scheme 56.

Reaction of **151** with $[Cu(CF_3SO_3)]_2 \cdot C_6H_6$ in dichloromethane resulted in an immediate colour change to deep violet followed by precipitation of the complex $[Cu_2(\mathbf{151})](CF_3SO_3)_2$. After purification of the mother liquor by column chromatography, a second deep red complex $[Cu(\mathbf{151})_2](CF_3SO_3)$ was isolated.

Following the same experimental procedure starting from **152**, complexes $[Cu_2(\mathbf{152})](CF_3SO_3)_2$ and $[Cu(\mathbf{152})_2](CF_3SO_3)$ were isolated [239].

Similarly, the reaction of 1,3-bis(aminomethyl)benzene,1,6-diamineoctane or

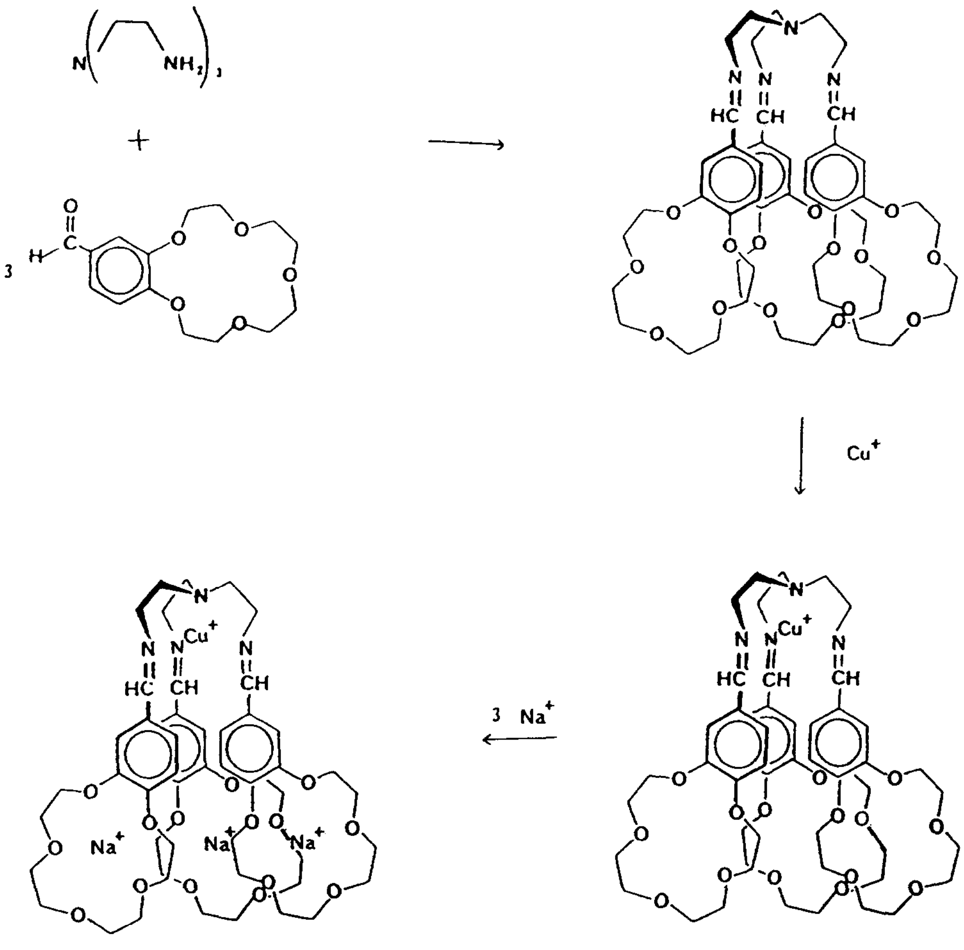

Scheme 55.

tris(aminoethyl)amine with 1,4-diformylbenzene tricarbonyl chromium forms the macrocyclic **153** and **154** and macrobicyclic **155** complexes [240] (Scheme 57).

It is also worth noting that condensation of 1,3-bis(aminomethyl)benzene with terephthaldehyde in anhydrous tetrahydrofuran gave the expected macrocycle which polymerized after a few hours even at low temperature (−30°C). Therefore, the coordination of the tricarbonyl chromium subunits leads to a stabilization of the alkylidenamine bonds probably as a result of both electronic and steric effects.

The one-pot cyclization to form **155** does not require high dilution conditions since the expected product precipitates readily from the reaction mixture.

Treatment of **155** with $[Cu(CH_3CN)_4]ClO_4$ produces the pentanuclear complex $[Cu_2(\mathbf{155})](ClO_4)_2$ whose X-ray structure is shown in Fig. 128.

The hexaimine cavity has an elongated ellipsoidal shape. The two copper atoms

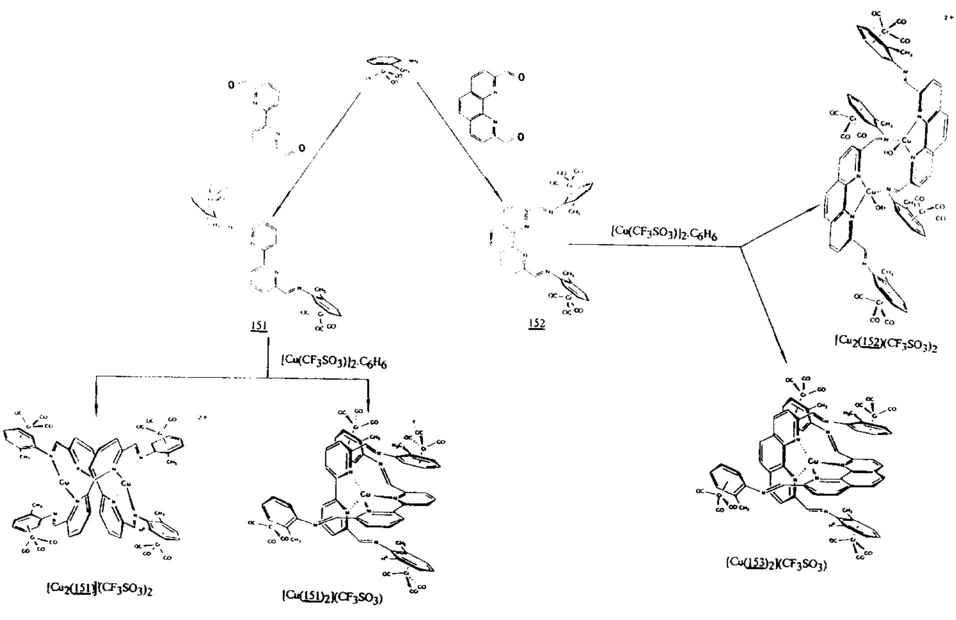

Scheme 56.

are 6.655 Å apart and inside the molecular cavity, whereas the three chromium atoms span a triangle outside the cavity. Each copper(I) ion is similarly coordinated in a distorted tetrahedral fashion to three alkylidenamine nitrogen atoms and to one bridgehead nitrogen atom at a longer distance. The geometry about the three chromium atoms is very similar to that of the closely related complex $[Cr(C_6H_6)(CO)_3]$ [244].

Homo- and heteropolynuclear species have also been obtained by using the ligands H_5-**156** and H_4-**157** [245]. In particular, the reaction H_5-**156** with $Cu(CH_3COO)_2 \cdot H_2O$ forms the mononuclear $Cu(H_3$-**156**$)$ where the metal ion is coordinated into the inner N_2O_2 chamber. $Cu(H_3$-**156**$)$ represents the starting complex for the formation of pure heteropolynuclear complexes [245].

A tetranuclear gadolinium(III)–copper(II) Schiff base complex has been obtained according to Scheme 58 [245].

X-ray microprobe analyses, mass spectra and IR data confirm the compounds proposed in Scheme 58. The distance between copper(II) and gadolinium(III) ions is too long to give rise to significant spin coupling.

Again a mononuclear copper(II) complex is the starting compound to obtain polynuclear species.

A similar approach to the synthesis of organized molecular assembly by preorganized metal complexes subunits was recently proposed [245]. This employs modified macrocyclic complexes that contain appended catechol as functional groups.

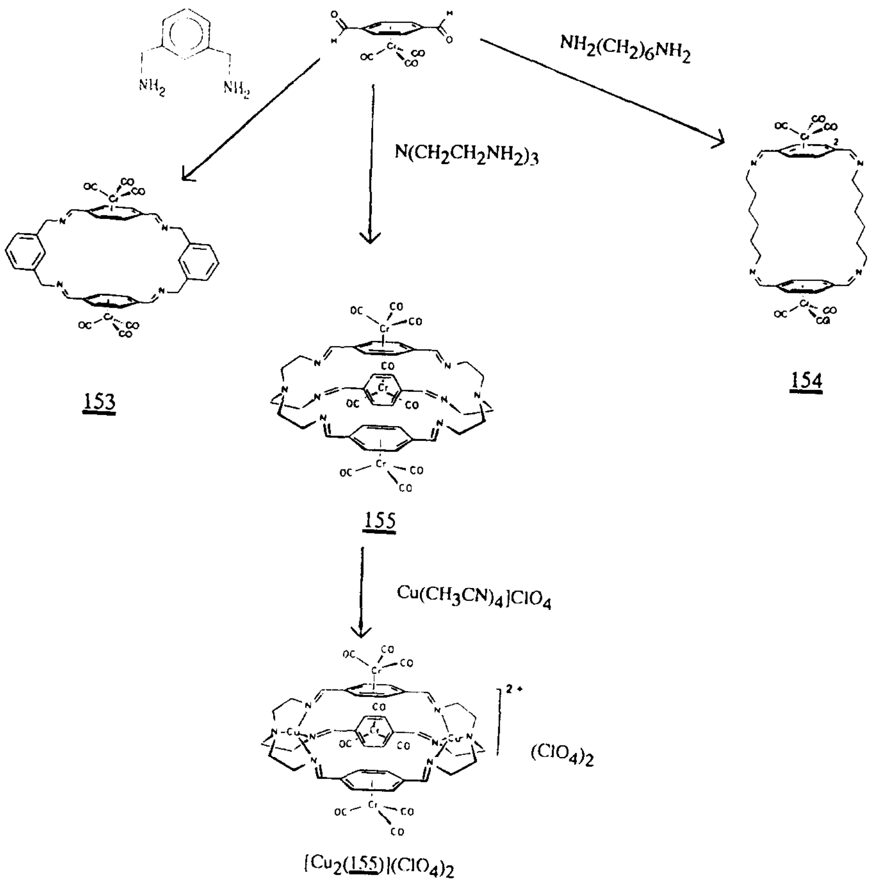

Scheme 57.

The catechol functions can also be oxidized to the related semiquinones as confirmed by X-ray structural determination on a nickel(II) complex [245].

The metallocatecholate and semiquinone complexes readily serve as ligands for other metal ions or coordinatively unsaturated metal complexes to give supramolecules with intramolecular M–M distances in excess of 10 Å [245]. (Scheme 59)

As an example the reactions of the nickel(II) or cobalt(II) complexes of these macrocyclic catecholates M(H_2-**macro**) with $Mo_2O_2S_2(S_2)(dmf)_3$ or $[Mo_2O_2S_2(dmf)_6]^{2+}$, in the presence of base, form $\{[M(\mathbf{macro})][Mo_2O_2S_2(S_2)]\}^{2+}$ and $\{[M(\mathbf{macro})]_2[Mo_2O_2S_2]\}^{2+}$ ($M \equiv Ni^{2+}$, Co^{2+}) respectively [245].

In the structure of the mixed K^+–$[N(CH_2CH_3)_4]^+$ salt of $\{[Ni(\mathbf{macro})]_2[Mo_2O_2S_2]\}^{2+}$ (Fig. 129), the potassium cation is coordinated to the oxygen atoms of three dmf molecules, the catecholate oxygen atoms, and the oxygen atom of one molybdenum oxo group to achieve a six-coordinate geometry. The planarity of the macrocyclic Ni^{2+} complex is retained on coordination to the

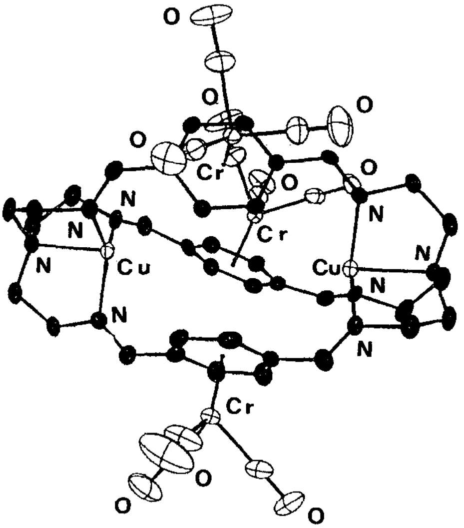

Fig. 128. Structure of $[Cu_2(\mathbf{155})]^{2+}$.

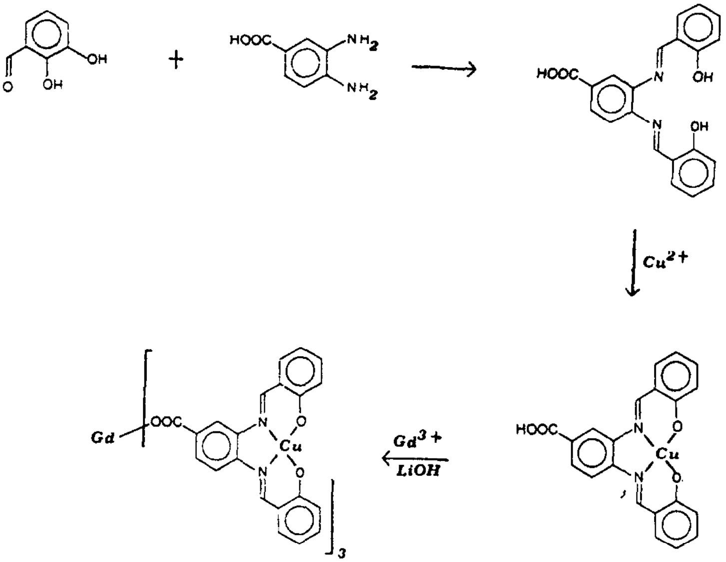

Scheme 58.

$[Mo_2O_2S_2(S_2)]$ unit. The coordination geometries of the Mo atoms are similar to a number of other complexes that contain the *syn*-$[Mo_2O_2S_2]^{2+}$ cores. The intramolecular Mo–Ni distances are 7.87 Å and 10.43 Å respectively [245].

In the polynuclear cation $\{[Ni(\mathbf{macro})]_2[Mo_2O_2S_2]\}^{2+}$ two functionalized macrocyclic nickel(II) complexes are bridged by an $[Mo_2O_2S_2]\}^{2+}$ unit [245].

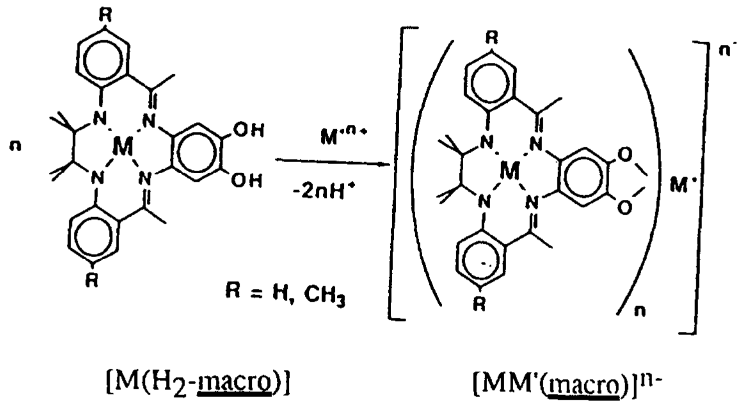

Scheme 59.

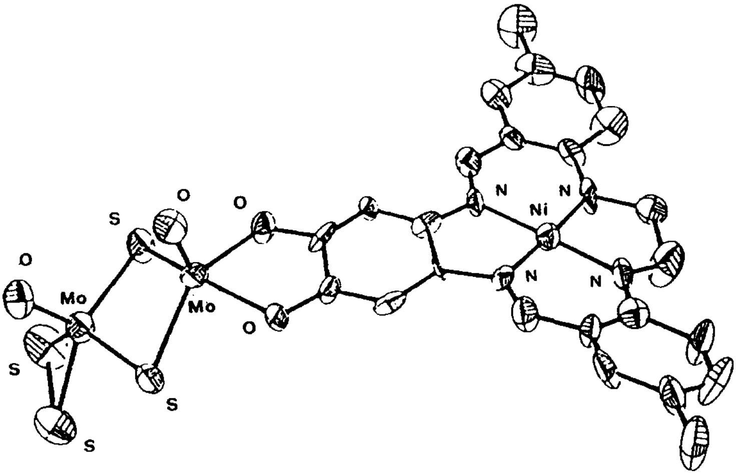

Fig. 129. Structure of $\{[\mathrm{Ni(macro)}]_2[Mo_2O_2S_2]\}^{2+}$.

Polymeric dimolybdenum(IV)–dicopper(II) complexes have been obtained also by the Schiff bases 1,3-dihydroxy-2-methyl-2-(salicylideneamino)propane, 1,3-dihydroxy-2-ethyl-2(salicylideneamino)propane, and tris(hydroxymethyl)(salicylideneamino)methane [246].

The X-ray structure of the complex derived from 1,3-dihydroxy-2-(salicylideneamino)propane reveals a chain structure having a $Cu_2Mo_2O_4$ cubane-like core [246].

The central cubane-like core of the compound has been described as a strongly distorted cube in which four corners are occupied by two copper and two molybdenum atoms. The cube is completed by four oxygen atoms from the two Schiff base molecules and two molybdenum atoms. The copper atoms are bridged by the alkoxy oxygen atoms of the Schiff base with a Cu···Cu distance of 2.951 Å and the molybdenum atoms by the methoxy oxygen atoms with an Mo · · · Mo distance of 3.528 Å; the Mo and Cu atoms are connected by one methoxy and one alkoxy oxygen atom with an average Mo · · · Cu distance of 3.429 Å. The O atom of the Mo=O moiety of each core has a contact to a neighbouring cubane through one copper atom affording an infinite-chain arrangement. The coordination polyhedron of the Mo atom is a distorted octahedron, consisting of oxygen atoms; that of one Cu atom is best described as a distorted square pyramid with significant axial elongation (Fig. 130). The magnetic properties of the compound studied in the 4.2–300 K temperature range correspond to what is expected for a ferromagnetically coupled CuCu pair with a triplet–singlet energy gap of $+30.5\ \mathrm{cm}^{-1}$, being in a triply alkoxo-bridged roof-shaped Cu(II) dimer with a dihedral angle of ca. 151°. The compound has a triple state room temperature ESR spectrum [246].

Tetra- or polynuclear complexes can also be prepared by introducing a spacer between binuclear well-defined entities to study how the degree of coupling, if any, across this spacer is related to size, degree of conjugation, donor atom etc. By this procedure, very interesting polymeric molecular materials have been proposed.

The reaction of *N,N'*-(2-hydroxypropylene)bis(acetylacetoneimine), 4,4'-di-3,5-dimethylpyrazole, nickel salts and KOH in methanol, in 2:1:4:8 ratio, yielded the red–brown tetranuclear compound **158** [247].

The molecular structure of the tetranickel(II) complex confirms the desired

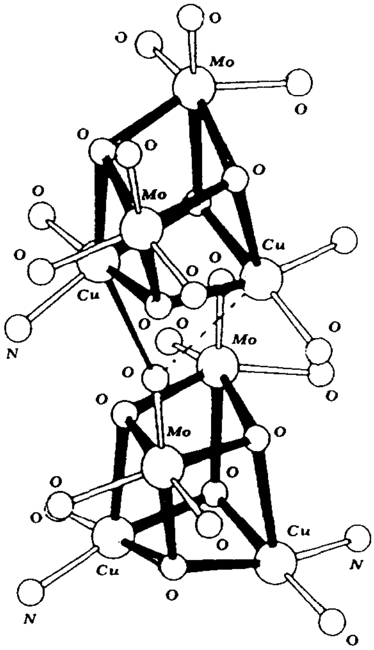

Fig. 130. Two successive cubane-like cores for the dimolybdenum(VI)–dicopper(II) Schiff base chain complex.

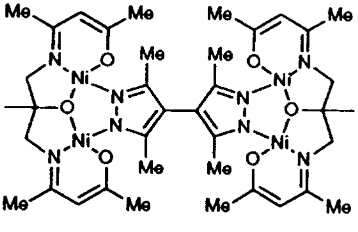

158

pair-of-dimers structure and displays clear twisting around the central single C—C bond brought about by interaction of the 3,3′ and 5,5′ methyl groups on the pyrazoles. Thus, there is no conjugation between the two pyrazole rings of the compound but there is delocalization within each ring. Each *trans*-NiN_2O_2 chromophore is square planar and the two coordination planes within each dinuclear moiety are not coplanar. The endogenous bridging oxygen atoms are up and down in relation to each other. Owing to the twisting around the central C—C linkage, the four Ni atoms are not disposed in a flat rectangular array (Fig. 131).

The analogous tetracopper complex contains one H_2O molecule per tetranuclear moiety. Crystals suitable for X-ray diffraction study have not been obtained to date, but a powder diffractogram shows that it is not isostructural with the complex **158**. Variable-temperature magnetic susceptibility data in the range 295–4.2 K indicate an antiferromagnetic coupling. An intermolecular coupling to adjacent molecules, rather than an intramolecular interaction, was proposed [247].

The chemistry of polyazamacrocycles has been the subject of many recent studies because of interest in the organization of polynuclear metal structures as models of non-haeme polymetallic proteins, molecular recognition, and "supercomplex" formation. Complexation of saturated polyazamacrocycles with seven to twelve nitrogen donor atoms separated by ethylene bridges was studied and the macrocycles

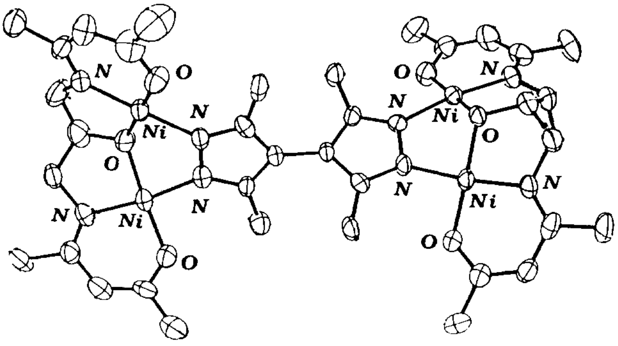

Fig. 131. The structure of the tetranickel complex **158**.

with eight or more nitrogen atoms were shown to afford dinuclear M(II) (M ≡ Cu, Ni or Zn) complexes [248,249].

Dinuclear copper and cobalt complexes of macrocycles with two N_3 coordination sites separated by $[CH_2]_2O[CH_2]_2$ bridges and macrobicycles with two N_4 sites separated by similar bridges were reported [250–254]. Larger macrocycles, 1,4,7,10,13,16,19,22,25,28,31-undecaazacyclotritriacontane and 1,4,7,10,13,16,19,22,25,28,31,34-dodecaazacyclohexatriacontane [255], are suggested to form trinuclear copper(II) complexes in solution. The first well-characterized trinuclear copper(II) was obtained using the macrocycle **159** containing three ethylenediamine entities as donor sites separated by $[CH_2]_2O[CH_2]_2$ bridges [256].

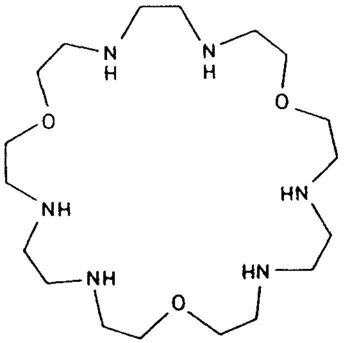

159

The trinuclear complex $[Cu_3(\mathbf{159})(OH)_2](ClO_4)_4(H_2O)$ was isolated as blue crystals by treating a methanol solution of **159** with $Cu(ClO_4)_2 \cdot 6H_2O$ in methanol. Its crystal structure consists of discrete $[Cu_3(\mathbf{159})(OH)_2]^{4+}$ cations, perchlorate anions, and water molecules. The asymmetric unit contains two independent cations which are nearly enantiomorphic; the first is located on the $C6_3$ axis and the second on the C_3 axis. The cation on the $C6_3$ axis is represented in Fig. 132; its molecular symmetry is D_3.

The complex cation has a three-fold symmetry. It contains a central core formed by the assembly of three copper(II) ions and two hydroxo ions by the tritopic macrocycle **159** into a trigonal bipyramidal cluster $[Cu_3(OH)_2]^{4+}$. This cluster is composed of three equivalent Cu^{II} ions bridged by two triply bound μ_3-hydroxo ions; each Cu^{II} atom is coordinated to an ethylenediammine subunit and is held inside the cavity of the macrocycle in a cryptate fashion. The Cu ··· Cu separation in only 2.803 Å. The two μ_3-hydroxo ions are located on a $C6_3$ axis. The coordination polyhedron of each copper is a very elongated octahedron. The macrocycle has a three-bladed propeller-like conformation of three-fold axial symmetry and encircles entirely the cationic core (Fig. 132) [256].

The tetratopic polyazamacrocycle 1,10,19,28-tetraoxa-4,7,13,16,22,25,31,34-octaazacyclohexatricontane (**160**) incorporates four copper(II) ions by reaction with

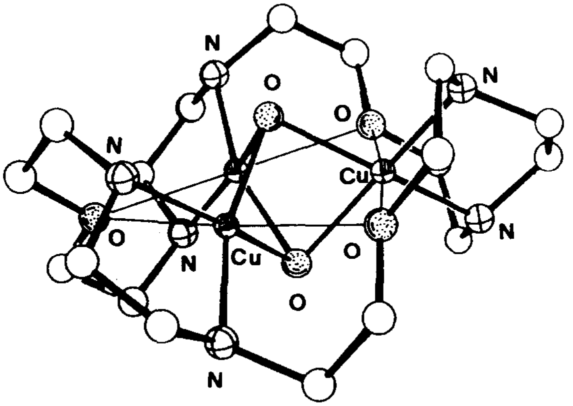

Fig. 132. Structure of $[Cu_3(\mathbf{159})(OH)_2]^{4+}$.

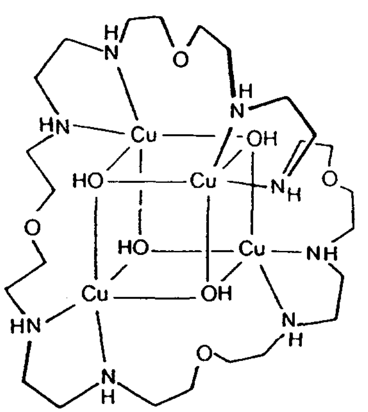

Fig. 133. Probable structure of $[Cu_4(\mathbf{160})(OH)_4]^{4+}$.

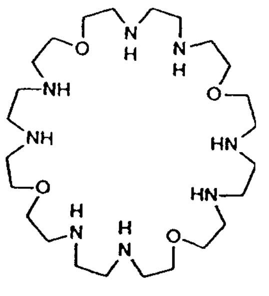

160

copper(II) in the range pH 6–9 [243]. A tetranuclear complex $[Cu_4(\mathbf{160})(OH)_4][ClO_4]_4 \cdot 2H_2O$ was obtained and characterized to be of a cubane-type $Cu_4(OH)_4$ core surrounded by the macrocycle according to IR, visible, fast atom bombardment and ESR spectra, cyclic voltammetry, and cryomagnetic susceptibility [249]. The probable structure of this species is reported in Fig. 133.

Similarly a series of Fe_4S_4 clusters with large methylene **161**, cyclophone **162** and crown ether rings **163** which can serve as models for high potential iron–sulphur proteins have been prepared [257–269]. The redox properties and the role of the macrocyclic moiety to provide a hydrophobic environment around the core in order to stabilize it toward molecular oxygen have been studied [257–269].

There is no doubt that these macrocyclic ligands open new possibilities in the encapsulation of polynuclear species.

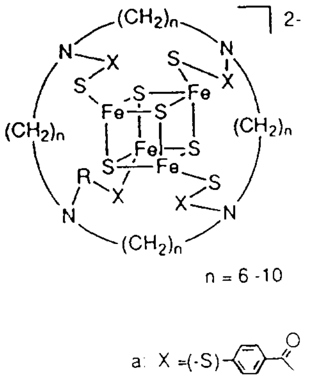

161

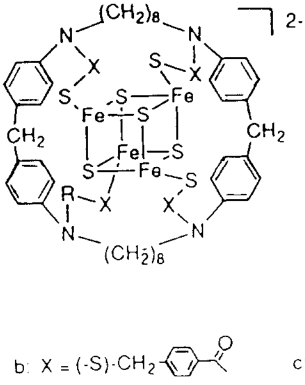

162

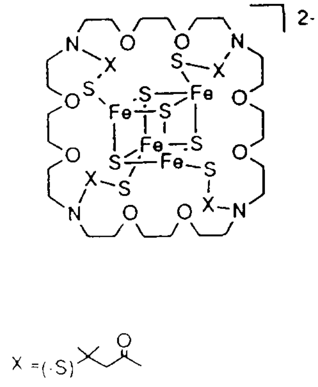

163

8. CONCLUSIONS

The well-known condensation reaction between a carbonyl group and a primary amine has produced a wide range of sophisticated macropolycyclic and/or macropolyacyclic Schiff bases specific for metal ion encapsulation or for the contemporary coordination of two or more metal ions at preordered distances or in well-defined arrays. The different metal ions play a fundamental role in the formation of these compounds. Also, the templating effect of different metal ions and the conditions under which transmetallation reactions take place are of remarkable relevance in obtaining Schiff bases or related compounds containing intramolecular cavities and clefts of appropriate size and shape.

Furthermore, Schiff base formation, followed by a subsequent reduction–demetallation process, leads to a variety of more flexible and stable compounds which contain NH groups and can hence be further functionalized.

C or N functionalization of macrocyclic Schiff bases has produced a series of bibracchial ligands with the correct size for selective metal ion encapsulation, transport and/or separation.

Donor atoms on the side arms can coordinate to a metal ion in its apical position, and the mobility of these arms may allow a highly dynamic complexation and decomplexation of several ions as required, for example, for efficient transport.

These systems can form inclusion complexes in which the substrate is contained inside the molecular cage. Furthermore, they can possess branches, bridges, and connections that allow the construction of a given architecture endowed with desirable dynamic features. They can allow the arrangement of structural groups, binding sites, and reactive functions. Their structural features, controlled by chemical synthesis, determine the stability and the properties of their complexes with inorganic and organic ions and/or neutral molecules.

The results already obtained lead us to believe that several of these systems will be employed in the near future in the separation of metal ions or organic molecules by liquid membrane techniques, in the preparation of new multimetal catalysts, in the easier activation of small molecules and in giving rise to uncommon reactivity or unusual products.

A quite promising task is the design and synthesis of ligands capable of organizing more than two metal centres into predetermined arrangements in order to have multielectron processes or new molecular magnetic or optical devices. Thus, many efforts will be devoted to the development of uni- and polydimensional molecular materials starting from coordination complexes. In order to synthesize these systems, it is necessary to design and prepare organic ligands which can act as fundamental building blocks for the assembly of extended molecular arrays and/or of materials with interesting magnetic, optical or electronic properties. It is also necessary to have a large variety of ligands, quite similar, and progressively more complicated, in order to understand the physicochemical properties of the complexes caused by varying, in a preordained way, the nature and the number of metal ions. Preordered Schiff base compounds can offer interesting advantages in the synthesis of solid state compounds and they have been successfully used as precursors in the preparation of ceramic materials. The use of an appropriate compound favours an intimate mixing of the elements than can allow lower temperature reactions than the traditional ceramic preparative route or the preparation of purer or inaccessible solid state phases. Preparation routes to ceramic materials based on these coordination precursors will receive considerable attention owing to the low cost, the possibility to coat large unusually shaped objects and high homogeneity and purity.

Particular attention will be devoted to characterize as completely as possible reactions that take the molecular starting material to solid state products. Great effort is currently devoted to the attempts to isolate and characterize intermediate products in order to give insight into both the chemistry of formation of a bulk solid and the evolution of the size-dependent physical properties.

In conclusion, Schiff bases are still relevant not only for the preparation of models of the active sites of metalloenzymes and metalloproteins, so helping the understanding of the activation of small molecules in catalytic processes, but also as starting systems to obtain carriers to be used in separation processes of industrial relevance or for new molecular or ceramic materials.

ACKNOWLEDGEMENTS

We thank Progetto Finalizzato CNR Materiali Speciali per Metodologie Avanzate, Progetto Finalizzato CNR Chimica Fine II and European Communities EEC (Contract SC1-0167-C(A)) for financial support.

REFERENCES

1 D.E. Fenton, in A.G. Sykes (Ed.), Advances in Inorganic and Bioinorganic Mechanisms, Vol. 2, Academic Press, London, 1983, p. 187.

2 K.D. Karlin and J. Zubieta, Copper Coordination Chemistry and Biochemistry: Biochemical and Inorganic Perspectives, Adenine Press, 1983.

3 K.D. Karlin and J.Zubieta, Biological and Inorganic Copper Chemistry, Vols. 1 and 2, Adenine Press, 1986.

4 D.E. Fenton, U. Casellato, P.A. Vigato and M. Vidali, Inorg. Chim. Acta, 95 (1984) 187.
D.E. Fenton, U. Casellato, P.A. Vigato and M. Vidali, Inorg. Chim. Acta, 62 (1982) 57.

5 P. Guerriero, P.A. Vigato, D.E. Fenton and P.C. Hellier, Acta Chem. Scand., 46 (1992) 1025.

6 R.D. Willet, D. Gatteschi and O. Kahn, Magneto-structural Correlations in Exchange Coupled Systems, Nato ASI Series, Reidel, Dordrecht, 1983.

7 U. Casellato, P.A. Vigato, D.E. Fenton and M. Vidali, Chem. Soc. Rev., 8 (1979) 199.

8 S.E. Groh, Isr. J. Chem., 15 (1976/1977) 277.

9 F.L. Urbach, in H. Sigel (Ed.), Metal Ions in Biological Systems, No. 13, Copper Proteins, Dekker, Basel, 1981, p. 73, and references cited therein.

10 P. Zanello, S. Tamburini, P.A. Vigato and S.A. Mazzocchin, Coord. Chem. Rev., 77 (1987) 165.

11 P.A. Vigato, S. Tamburini and D.E. Fenton, Coord. Chem. Rev., 106 (1990) 25.

12 D.E. Fenton and P.A. Vigato, Chem. Soc. Rev., 17 (1988) 69.

13 T.M. Sorrell, Tetrahedron, 45 (1989) 3.

14 J.-M. Lehn, Pure Appl. Chem., 50 (1978) 871.

15 J.-M. Lehn, Science, 227 (1985) 849.

16 J.-M. Lehn, Angew. Chem., Int. Edn. Engl., 27 (1988) 89.

17 J.-M. Lehn, Angew. Chem., Int. Edn. Engl., 30 (1990) 1304.

18 K. Henrick, P.A. Tasker and L.L. Lindoy, in S.J. Lippard (Ed.), Progress in Inorganic Chemistry, Vol. 33, Wiley, New York, 1985, p. 1.
L.F. Lindoy, Pure Appl. Chem., 61 (1989) 1575.

19 F. Dejong and D.N. Reinhoudt, Adv. Phys. Org. Chem., 17 (1980) 279.

20 H. Setter and W. Frank, Angew. Chem., 88 (1976) 722.

21 M. Takagi, M. Tazaki and K. Ueno, Chem. Lett., (1978) 1179.

22 M.F. Loncin, J.F. Desereux and E. Merciny, Inorg. Chem., 25 (1986) 2646.

23 D.A. Gutowsky, L. Echegoyen, D.M. Goli, A. Kaifer, R.A. Schulz and G.W. Gokel, J. Am. Chem. Soc., 105 (1983) 6717.

24 S.I. Kang, A. Czech, B.P. Czech, L.E. Stewart and R.A. Bartsch, Anal. Chem., 57 (1985) 1713.

25 J. Strzelbicki and R.A. Bartsch, Anal. Chem., 53 (1981) 2247.

26 Y. Katayama, R. Fukuda and M. Takagi, Anal. Chim. Acta, 185 (1986) 295.

27 T.A. Kaden, Top. Curr. Chem., 121 (1984) 157.

28 R.W. Hay, in E. Kimura (Ed.), Current Topics in Macrocyclic Chemistry in Japan, Hiroshima University, 1987, p. 56.

29 N.W. Alcock, K.P. Balakrishnan, P. Moore and G.A. Pike, J. Chem. Soc., Dalton Trans., (1987) 889.

30 K.A. Arnold, L. Echegoyen, F.R. Fronczek, R.D. Gandour, V.J. Gatto, D. White and G.W. Gokel, J. Am. Chem. Soc., 109 (1987) 3716.

31 D.E. Fenton and G. Rossi, Inorg. Chim. Acta, 98 (1985) L29.

32 V.J. Gatto and G.W. Gokel, J. Am. Chem. Soc., 106 (1984) 8240.

33 H. Adams, N.A. Bailey, W.D. Carlisle, D.E. Fenton and G. Rossi, J. Chem. Soc., Dalton Trans., (1990) 1271.

34 H. Adams, N.A. Bailey, M.J.S. Dwyer, D.E. Fenton, P.C. Hellier and P.D. Hempstead, J. Chem. Soc., Chem. Commun., (1991) 1297.

35 A. Messerschmidt, A. Rossi, R. Ladenstein, R. Hubber, M. Bolognesi, G. Gatti, A. Marchesini, R. Petruzelli and A. Finazzi-Agro, J. Mol. Biol., 206 (1989) 513.

36 J.R. Moran, S. Karbach and D.J. Cram, J. Am. Chem. Soc., 104 (1982) 5826.
D.J. Cram, G.M. Lein, T. Kaneda, R.C. Helgeson, C.B. Knobler, E. Maverick and K.N. Trueblood, J. Am. Chem. Soc., 103 (1981) 6228.
G.M. Lein and D.J. Cram, J. Chem. Soc., Chem. Commun., (1982) 301.
D.J. Cram, T. Kaneda, R.C. Helgeson and G.M. Lein, J. Am. Chem. Soc., 101 (1979) 6752.

37 E. Dalcanale and D.J. Cram, Proc. XI Int. Symp. on Macrocyclic Chemistry, Florence, 1986, A33.
E. Dalcanale, A. Du vosel, P. Soncini and F. Ugozzoli, Proc. Meet. on Macrocyclic and Supramolecular Chemistry in Italy, Parma, 1988, p. 93.

38 C.D. Gutsche, Acc. Chem. Res., 16 (1983) 161, and references cited therein.

39 G.D. Andreetti, R. Ungaro and A. Pochini, J. Chem. Soc., Chem. Commun., (1979) 1005.

40 M. Coruzzi, G.D. Andreetti, V. Bocchi, A. Pochini and R. Ungaro, J. Chem. Soc., Perkin Trans., 2 (1982) 1113.

41 G.D. Andreetti, A. Pochini and R. Ungaro, J. Chem. Soc., Perkin Trans., 2 (1983) 1773.

42 R. Ungaro, A. Pochini, A.G. Andreetti and P. Domiano, J. Chem. Soc., Perkin Trans., 2 (1985) 197.

43 C. Rizzoli, G.D. Andreetti, R. Ungaro and A. Pochini, J. Mol. Struct., 82 (1982) 133.

44 R. Ungaro, A. Pochini, G.D. Andreetti and V. Sangermano, J. Chem. Soc., Perkin Trans., 2 (1984) 1979.

45 S. Shinkai, S. Mori, H. Koreishi, T. Tsubaki and O. Manabe, J. Am. Chem. Soc., 108 (1986) 2409.

46 S. Shinkai, K. Araki, T. Tsubaki and O. Manabe, J. Chem. Soc., Perkin Trans., 1 (1987) 2297.

47 S. Shinkai, K. Araki, S. Shibata and O. Manabe, J. Chem. Soc., Perkin Trans., 1(1989) 195.

48 C.D. Gutsche and K.C. Nam, J. Am. Chem. Soc., 110 (1988) 6153.

49 C.D. Gutsche and I. Alam, Tetrahedron, 44 (1988) 4689.

50 F. Arnaud-Neu, E.M. Collins, M. Deasy, G. Ferguson, S.J. Harris, B. Kaitner, A.J. Lough, M.A. McKervey, E. Marques, B.H. Ruhl, M.-J. Schwing and E.M. Seward, J. Am. Chem. Soc., 111 (1989) 8681.

51 G. Ferguson, B. Kaitner, M.A. McKervey and E.M. Seward, J. Chem. Soc., Chem. Commun., (1987) 587.

52 A. Arduini, E. Ghidini, A. Pochini, R. Ungaro, G.D. Andreetti, G. Calestani and F. Ugozzoli, J. Inclusion Phenom., 6 (1988) 119.

53 C. Alfieri, E. Dradi, A. Pochini, R. Ungaro and G.D. Andreetti, J. Chem. Soc., Chem. Commun., (1983) 1075.
D.N. Reinhoudt, D.J. Dijkstra, P.J.A. in't Veld, K.E. Bugge, S. Harkema, R. Ungaro and E. Ghidini, J. Am. Chem. Soc., 109 (1987) 4761.

54 A. Arduini, A. Pochini, S. Reverberi, R. Ungaro, G.D. Andreetti and F. Ugozzoli, Tetrahedron, 42 (1986) 2089.

55 G. Calestani, F. Ugozzoli, A. Arduini, E. Ghidini and R. Ungaro, J. Chem. Soc., Chem. Commun., (1987) 344.

56 N. Sabbatini, M. Guardigli, A. Mecati, V. Balzani, R. Ungaro, E. Ghidini, A. Casnati and A. Pochini, J. Chem. Soc., Chem. Commun., (1990) 878.

57 G.D. Andreetti, O. Ori, F. Ugozzoli, C. Alfieri, A. Pochini and R. Ungaro, J. Inclusion Phenom., 6 (1988) 523.

58 C. Gutsche, B. Dhawan, K.H. No and R. Muthukrishnan, J. Am. Chem. Soc., 103 (1981) 3782.

59 G.D. Andreetti, R. Ungaro and A. Pochini, J. Chem. Soc., Chem. Commun., (1981) 533.

60 J.M. Harrowfield, M.I. Ogden, W.R. Richmond and A.H. White, J. Chem. Soc., Dalton Trans., (1991) 2153.
J.M. Harrowfield, M.I. Ogden and A.H. White, Aust. J. Chem., 44 (1991) 1237.
J.M. Harrowfield, M.I. Ogden and A.H. White, Aust. J. Chem., 44 (1991) 1249.
J.M. Harrowfield, M.I. Ogden and A.H. White, J. Chem. Soc., Dalton Trans., (1991) 2625.
B.M. Furphy, J.M. Harrowfield, D.L. Kepert, B.W. Skelton, A.H. White and F.R. Wilner, Inorg. Chem., 26 (1987) 4231.
J.C. Bünzli, P. Froidevaux and J.M. Harrowfield, Inorg. Chem., 32 (1993) 3306.

61 Z. Asfari, J.M. Harrowfield, M.I. Ogden, J. Vicens and A.H. White, Angew. Chem., Int. Edn. Engl., 30 (1991) 854.
B.M. Furphy, J.M. Harrowfield, D.L. Kepert, B.W. Skelton, A.H. White and F.R. Wilner, Inorg. Chem., 26 (1987) 4231.
B.M. Furphy, J.M. Harrowfield, M.I. Ogden, B.W. Skelton, A.H. White and F.R. Wilner, J. Chem. Soc., Dalton Trans., (1989) 2217.

62 A.R. Battersby, E. Hunt, J.B. Paine and J. Saunders, J. Chem. Soc., Perkin Trans. 1 (1976) 1008.

63 G.M. Dubowchik and A.D. Hamilton, J. Chem. Soc., Chem. Commun., (1985) 904.

64 G.M. Dubowchik and A.D. Hamilton, J. Chem. Soc., Chem. Commun., (1986) 665.

65 G.M. Dubowchik and A.D. Hamilton, J. Chem. Soc., Chem. Commun., (1987) 293.

66 K.D. Karlin and Y. Gultneh, in J. Lippard (Ed.), Progress in Inorganic Chemistry, Vol. 35, Wiley, New York, 1987, p. 19.

67 R. Menif, A.E. Martell, P.J. Squattrito and A. Clearfield, Inorg. Chem., 27 (1990) 4723.

68 Y. Kobuke and Y. Satah, J. Am. Chem. Soc., 114 (1992) 789.

69 P.A. Vigato and D.E. Fenton, Inorg. Chim. Acta, 139 (1987) 39.

70 N.A. Bailey, M.M. Eddy, D.E. Fenton, S. Moss, A. Mukhopadhyay and J. Jones, J. Chem. Soc., Dalton Trans., (1984) 2281.

71 A. Aguiari, E. Bullita, U. Casellato, P. Guerriero, S. Sitran, S. Tamburini and P.A. Vigato, Inorg. Chim. Acta, 202 (1992) 157.

72 J. Jazwinsky, J.M. Lehn, R. Ziessel, J. Guilheim and C. Pascard, J. Chem. Soc., Chem. Commun., (1987) 1691.

73 A.M. Sargeson, Pure Appl. Chem., 58 (1986) 1511.

74 T.J. Meade and D.H. Bush, in S.J. Lippard (Ed.), Progress in Inorganic Chemistry, Vol. 33, Wiley, New York, 1985, p. 59.

75 D. MacDowell and J. Nelson, Tetrahedron Lett., 29 (1988) 385.

76 D. MacDowell, J. Nelson and V. McKee, Polyhedron, 8 (1989) 1143.

77 A. Atkinson, N.A. Bailey, D.E. Fenton, P.D. Hempstead and G.P. Westwood, personal communications.

78 J. de O. Cabral, M.F. Cabral, M.G.B. Drew, F.S. Esho, O. Haas and S.M. Nelson, J. Chem. Soc., Chem. Commun., (1982) 1066.

79 J. de O. Cabral, M.F. Cabral, G.B. Drew, S. Esho, and S.M. Nelson, J. Chem. Soc., Chem. Commun., (1982) 1068.

80 G. Bombieri, F. Benetollo, A. Polo, L. De Cola, D.L. Smailes and L.M. Vallarino, Inorg. Chem., 25 (1986) 1127.
F. Benetollo, G. Bombieri, L. De Cola, A. Polo, D.L. Smailes and L.M. Vallarino, Inorg. Chem., 28 (1989) 3447.

81 M.G.B. Drew, J. de O. Cabral, M.F. Esho and S.M. Nelson, J. Chem. Soc., Chem. Commun., (1979) 1033.

82 C.L. Honeybourne, Tetrahedron, 29 (1973) 1549.

83 L.F. Lindoy and D.H. Bush, in W.L. Jolly (Ed.), Preparative Inorganic Reactions, Vol. 6, Wiley–Interscience, New York, 1971, p. 1.

84 D.H. Cook and D.E. Fenton, J. Chem. Soc., Dalton Trans., (1979) 266.
D.H. Cook and D.E. Fenton, J. Chem. Soc., Dalton Trans., (1979) 810.
D.H. Cook, D.E. Fenton, M.G.B. Drew, A. Rodgers, M. McCann and S.M. Nelson, J. Chem. Soc., Dalton Trans., (1979) 414.

85 V.W. Day, T.J. Marks and W.A. Wachter, J. Am. Chem. Soc., 97 (1975) 4519.
T.J. Marks and D.R. Stojakovic, J. Am. Chem. Soc., 100 (1978) 1695.

86 S.M. Nelson, S.G. McFall, M.G.B. Drew and A.H. Othman, Proc. R. Ir. Acad., Sect. B, 77 (1977) 523.

87 S.M. Nelson, Pure Appl. Chem., 52 (1980) 2461.

88 D.E. Fenton, Pure Appl. Chem., 58 (1986) 1437.

89 N. Bailey, D.E. Fenton, P.C. Hellier, P.D. Hempstead, U. Casellato and P.A. Vigato, J. Chem. Soc., Dalton Trans., (1992) 2809.

90 A.M. Arif, J.D.J. Becker-Dirks, C.J. Gray, F.A. Hart and M.B. Hursthouse, J. Chem. Soc., Dalton Trans., (1987) 1665.

91 C.J. Gray and F.A. Hart, J. Chem. Soc., Dalton Trans., (1987) 2289.

92 K.K. Abib and D.E. Fenton, Inorg. Chim. Acta, 95 (1984) 119.

93 K.K. Abib and D.E. Fenton, Inorg. Chim. Acta, 82 (1984) 223.

94 J. Hunter, J. Nelson, C. Harding, M. McCann and V. McKee, J. Chem. Soc., Chem. Commun., (1990) 1148.

95 M.P. Mgwenya, A.E. Martell and J. Reilbenspies, J. Chem. Soc., Chem. Commun., (1990) 1207.

96 C. Harding, V. McKee and J. Nelson, J. Am. Chem. Soc., 113 (1991) 9684.

97 D.M. Rudkevich, W.P.R.V. Stauthamer, W. Verboom, J.F.J. Engbersen, S. Harkema and D.N. Reinhoudt, J. Am. Chem. Soc., 114 (1992) 9671.
C.J. van Staveren, J. van Eerden, F.C.J.M. van Veggel, S. Harkema and D.N. Reinhoudt, J. Am. Chem. Soc., 110 (1988) 5008.

98 M.G.B. Drew, J. Nelson and S.M. Nelson, J. Chem. Soc., Dalton Trans., (1981) 1678.

99 P. Guerriero, S. Tamburini, P.A. Vigato, R. Seraglia and P. Traldi, Org. Mass Spectrom., 27 (1992) 231.

100 P. Guerriero, U. Casellato, S. Tamburini, P.A. Vigato and R. Graziani, Inorg. Chim. Acta, 129 (1987) 127.
J.-C. Bunzli, E. Moret, U. Casellato, P. Guerriero and P.A. Vigato, Inorg. Chim. Acta, 150 (1988) 133.

101 S. Aime, M. Botta, S. Tamburini and P.A. Vigato, unpublished work.

102 N.A. Bailey, D.E. Fenton, I.T. Jackson, R. Moody and C.O. Rodriguez de Barbarin, J. Chem. Soc., Chem. Commun., (1983) 1463.

103 J.C. Dutton, G.D. Fallon and K.S. Murray, J. Chem. Soc., Chem. Commun., (1990) 65.

104 M.G.B. Drew, J. de O. Cabral and M.F. Cabral, J. Chem. Soc., Chem. Commun., (1979) 1033.

105 S.M. Nelson, F.S. Esho, M.G.B. Drew and P. Bird, J. Chem. Soc., Chem. Commun., (1979) 1035.

106 E. Bullita, P. Guerriero, S. Tamburini and P.A. Vigato, J. Less-Common Met., 153 (1989) 211.

107 P.A. Vigato, P. Guerriero, S. Tamburini, R. Seraglia and P. Traldi, Org. Mass Spectrom., 25 (1990) 420.

108 S. Tamburini, P.A. Vigato, U. Casellato and R. Guerriero, J. Chem. Soc., Dalton Trans., (1989) 1993.
S. Tamburini, P.A. Vigato, D. Chiarello and P. Traldi, Inorg. Chim. Acta, 156 (1989) 271.

109 H. Adams, N.A. Bailey, W.D. Carlisle, D.E. Fenton and G. Rossi, J. Chem. Soc., Dalton Trans., (1990) 1271.
H. Adams, N.A. Bailey, S.R. Collins, D.E. Fenton and S.J. Kitchen, Int. Symp. on Macrocyclic Chemistry, University of Twente, Enschede, 1993, A2.

110 N.A. Bailey, D.E. Fenton, S.J. Kitchen, T.H. Lilley, M.G. Williams, P.A. Tasker, A.J. Leong and L.P. Lindoy, J. Chem. Soc., Dalton Trans., (1991) 623.

111 N.A. Bailey, D.E. Fenton, S.J. Kitcher, T.H. Lilley, M.G. Williams, P.A. Tasken, A.J. Leong and L.F. Lindoy, J. Chem. Soc., Dalton Trans., (1991), 2989.
H. Adams, N.A. Bailey, R. Bastida, D.E. Fenton, Y.-S. Ho and P.D. Hempstead, J. Chem. Res. (S), (1992) 190; J. Chem. Res. (M), (1992) 1501.

112 L.G. Armstrong and L.F. Lindoy, Inorg. Chem., 14 (1975) 1322.
L.G. Armstrong, L.F. Lindoy, M. McPartlin, G.M. Mockler and P.A. Tasker, Inorg. Chem., 16 (1977) 1665.
D.E. Fenton, B.P. Murphy, A.J. Leong, L.F. Lindoy, A. Bashall and M. McPartlin, J. Chem. Soc., Dalton Trans., (1987) 2543.

113 P.G. Grimsley, L.F. Lindoy, H.C. Lip, R.J. Smith and J.T. Baker, Aust. J. Chem., 30 (1977) 2095.
L.G. Armstrong, P.G. Grimsley, L.F. Lindoy, H.C. Lip, V.A. Morris and R.J. Smith, Inorg. Chem., 17 (1978) 2350.
K.R. Adam, L.F. Lindoy, H.C. Lip, J.H. Rea, B.W. Skelton and A.H. White, J. Chem. Soc., Dalton Trans., (1981) 74.
K.R. Adam, A.J. Leong, L.F. Lindoy, H.C. Lip, B.W. Skelton and A.H. White, J. Chem. Soc., 105 (1983) 4645.
K.R. Adam, S. Donnelly, A.J. Leong, L.F. Lindoy, B.J. McCool, A. Bashall, M.R. Dent, B.P. Murphy, M. McPartlin, D.E. Fenton and P.A. Tasker, J. Chem. Soc., Dalton Trans., (1990) 1635.

114 K.R. Adam, G. Anderegg, L.F. Lindoy, H.C. Lip, M. McPartlin, J.M. Rea, R.J. Smith and P.A. Tasker, Inorg. Chem., 19 (1980) 2956.
K.R. Adam, L.F. Lindoy, R.S. Smith, G. Anderegg, K. Henrich, M. McPartlin and P.A. Tasker, J. Chem. Soc., Chem. Commun., (1979) 812.
A. Ekstrom, L.F. Lindoy, H.C. Lip, R.J. Smith, H.J. Goodwin, M. McPartlin and P.A. Tasker, J. Chem. Soc., Dalton Trans., (1979) 1029.
A. Ekstrom, L.F. Lindoy and R.J. Smith, J. Am. Chem. Soc., 101 (1979) 4014.
A. Ekstrom, L.F. Lindoy and R.J. Smith, J. Chem. Soc., Dalton Trans., 19 (1980) 724.
L.F. Lindoy, H.C. Lip, J.M. Rea, R.J. Smith, K. Henrich, M. McPartlin and P.A. Tasker, Inorg. Chem., 19 (1980) 3360.
K.R. Adam, K.P. Dancey, A.J. Leong, L.F. Lindoy, B.J. McCool, M. McPartlin and P.A. Tasker, J. Am. Chem. Soc., 110 (1988) 8471.
H. Adams, N.A. Bailey, D.E. Fenton, I.G. Ford, S.J. Kitcher, M.G. Williams, P.A. Tasker, A.J. Leong and L.F. Lindoy, J. Chem. Soc., Dalton Trans., (1991) 1665.

115 K.R. Adam, M. Antolovich, D.S. Baldwin, L.G. Bridgen, P.A. Duckworth, L.F. Lindoy, A. Barshall, M. McPartlin and P.A. Tasker, J. Chem. Soc., Dalton Trans., (1992) 1869.
K.R. Adam, M. Antolovich, D.S. Baldwin, P.A. Duckworth, A.J. Leong, L.F. Lindoy, M. McPartlin and P.A. Tasker, J. Chem. Soc., Dalton Trans., (1993) 1013.
K.R. Adam, D.S. Baldwin, P.A. Duckworth, A.J. Leong, L.F. Lindoy, M. McPartlin and P.A. Tasker, J. Chem. Soc., Chem. Commun., (1987) 1124.
U. Kallert and R. Mattes, Inorg. Chim. Acta, 180 (1991) 263.

116 N.A. Bailey, D.E. Fenton, M.G. Williams and D.J. Winter, J. Chem. Soc., Dalton Trans., (1989) 1727.

117 P.G. Owston, R. Peters, E. Ramsammy, P.A. Tasker and J. Trotter, J. Chem. Soc., Chem. Commun., (1980) 1218.
A.J. Greenwood, K. Henrick, P.G. Owston and P.A. Tasker, J. Chem. Soc., Chem. Commun., (1980) 88.
K. Henrick, P.M. Judd, P.G. Owston, P. Peters, P.A. Tasker and R.W. Turner, J. Chem. Soc., Chem. Commun., (1983) 1253.
C.W.G. Ansell, K.P. Dancey, M. McPartlin, P.A. Tasker and L.F. Lindoy, J. Chem. Soc., Dalton Trans., (1983) 1789.
K.R. Adam, B.J. McCool, A.J. Leong, L.F. Lindoy, C.W.G. Aspell, P.J. Baillie, K.P. Dancey, L.A. Drummond, K. Henrick, M. McPartlin, D.K. Uppal and P.A. Tasker, J. Chem. Soc., Dalton Trans., (1990) 3435.
A.F. Cameron, D.W. Taylor and R.H. Nuttal, J. Chem. Soc. A, (1971) 3402.
C.J. Brown and J.F.P. Lewis, Acta Crystallogr. C., 40 (1984) 368.

118 R. Menif and A.E. Martell, J. Chem. Soc., Chem. Commun., (1989) 1521.
R. Menif, J. Reibenspies and A.E. Martell, Inorg. Chem., 30 (1991) 3446.

119 D. McDowell and J. Nelson, Tetrahedron Lett., 29 (1988) 385.
J. Jazwinski, J.M. Lenh, R. Meric, J.P. Vigneron, M. Cesario, J. Guilhem and C. Pascal, Tetrahedron Lett., 28 (1987) 3489.

120 M.G.B. Drew, J. Hunter, D.J. Marrs, J. Nelson and C. Harding, J. Chem. Soc., Dalton Trans., (1992) 3235.

121 G.L. Rothermiel, Jr., L. Miao, A.L. Hill and S.C. Jackels, Inorg. Chem., 31 (1992) 4854.

122 J.D.J. Backer-Dirks, C.J. Gray, F.A. Hart, M.B. Hursthouse and B.C. Schoop, J. Chem. Soc., Chem. Commun., (1979) 774.
M. Arif, C.J. Gray, F.A. Hart and M.B. Hursthouse, Inorg. Chim. Acta, 109 (1985) 179.

123 W. Radecka-Paryzek, Inorg. Chim. Acta, 45 (1980) L147.

124 W. Radecka-Paryzek, Inorg. Chim. Acta, 52 (1981) 261.

125 K.K. Abib, D.E. Fenton, U. Casellato, P.A. Vigato and R. Graziani, J. Chem. Soc., Dalton Trans., (1984) 351.

126 P.H. Smith, J.R. Brainard, D.E. Morris, G.D. Jarvinen and R.R. Ryan, J. Am. Chem. Soc., 111 (1989) 7437.

127 F. Benetollo, A. Polo, G. Bombieri, K.K. Fonda and M.L. Vallarino, Polyhedron, 9 (1990) 1411.

128 G. Bombieri, F. Benetollo, A. Polo, L. De Cola, W.T. Hawkins and L.M. Vallarino, Polyhedron, 8 (1989) 2157.

129 L. De Cola, D.L. Smailes and L.M. Vallarino, Inorg. Chem., 25 (1986) 1729.

130 L. De Cola, D.L. Smailes and L.M. Vallarino, Inorg. Chim. Acta, 110 (1985) L1.

131 W.D. Carlisle, D.E. Fenton, P.B. Roberts, U. Casellato, P.A. Vigato and R. Graziani, Transition Met. Chem., 11 (1986) 292.
N.A. Bailey, C.O. Rodriguez de Barbarin, D.E. Fenton and S. Gou, Int. Symp. on Macroacyclic Chemistry, University of Twente, Enschede, 1993, A16.
Y. Ikawa, T. Nagata and K. Maruyama, Chem. Lett., (1993) 1049.

132 E. Bullita, P. Guerriero, S. Tamburini, P.A. Vigato, R. Bonora and L. Marchesini, in L. Cecille, M. Caserci and L. Pietrelli (Eds.), New Separation Chemistry Techniques for Radioactive Waste and Other Specific Applications, Elsevier, London, 1991, p. 189.
E. Bullita, P. Guerriero, S. Tamburini, P.A. Vigato, J.C. Dupuy, M. Prevost, R. Bonora and L. Marchesini, Mater. Chem. Phys., 31 (1992) 181.

133 T.S. Franczky, K.R. Czerwinski and K.N. Raymond, J. Am. Chem. Soc., 114 (1992) 8138.

134 J.L. Sessler, T.D. Mody and U. Lynch, Inorg. Chem., 31 (1992) 529.
J.L. Sessler, T.D. Mody and U. Lynch, J. Am. Chem. Soc., 115 (1993) 3346.
135 N.H. Pilkington and R. Robson, Aust. J. Chem., 23 (1970) 2225.
136 H. Okawa and S. Kida, Inorg. Nucl. Chem. Lett., 7 (1971) 751.
H. Okawa and S. Kida, Bull. Chem. Soc. Jpn., 45 (1972) 2225.
137 M. Tadokoro, H. Okawa, N. Matsumoto, M. Koikawa and M. Tadokoro, J. Chem. Soc., Dalton Trans., to be published.
138 S. Tamburini, P.A. Vigato and P. Traldi, Org. Mass Spectrom., 21 (1986) 183.
P. Zanello, A. Cinquantini, P. Guerriero, S. Tamburini and P.A. Vigato, Inorg. Chim. Acta, 117 (1986) 91.
139 S.K. Mandal and K. Nag, J. Chem. Soc., Dalton Trans., (1984) 2141.
R. Das, K.K. Nanda, A.K. Mukherjee, M. Mukheryee, M. Helliwell and K. Nag, J. Chem. Soc., Dalton Trans., (1993) 2241.
140 S.K. Mandal, L.K. Thompson, K. Nag, J.-P. Charland and E.J. Gabe, Inorg. Chem., 26 (1987) 1391.
S.K. Mandal, B. Adhikary and K. Nag, J. Chem. Soc., Dalton Trans., (1986) 1175.
S.K. Mandal, L.K. Thomson, K. Nag, J.-P. Charland and E.J. Gabe, Can. J. Chem., 65 (1987) 2815.
R. Das and K. Nag, Inorg. Chem., 30 (1991) 2831.
K.K. Nanda, R. Das, M.J. Newlands, R. Hynes, E.J. Gabe and K. Nag, J. Chem. Soc., Dalton Trans., (1992) 897.
K.K. Nanda, R. Das, K. Venkatsubramanian, P. Paul and K. Nag, J. Chem. Soc., Dalton Trans., (1993) 2515.
141 R. Graziani, M. Vidali, U. Casellato and P.A. Vigato, Acta Crystallogr. B,32 (1976) 1681.
142 N.A. Bailey, D.E. Fenton, C.A. Phillips. U. Casellato, S. Tamburini, P.A. Vigato and R. Graziani, Inorg. Chim. Acta, 109 (1985) 91.
143 R. Graziani, M. Vidali, G. Rizzardi, U. Casellato and P.A. Vigato, Inorg. Chim. Acta, 36 (1979) 145.
R. Graziani, M. Vidali, U. Casellato and P.A. Vigato, Transition Met. Chem., 3 (1978) 99.
R. Graziani, M. Vidali, U. Casellato and P.A. Vigato, Transition Met. Chem., 3 (1978) 239.
144 S. Chung, K. Lai and T.M. Swager, 205th ACS Natl. Meet., Division of Inorganic Chemistry, Denver, CO, 1993, 54.
145 P. Guerriero, U. Casellato, D. Ajò, S. Sitran, P.A. Vigato and R. Graziani, Inorg. Chim. Acta, 142 (1988) 305.
146 J.D. Crane, D.E. Fenton, J.M. Latour and A.J. Smith, J. Chem. Soc., Dalton Trans., (1991) 2979.
M. Andruch, E. Bakalbassis, O. Kahn, J.C. Trombe and P. Porcher, Inorg. Chem., 32 (1993) 1616.
M. Andruch, O. Kahn, J. Sainton, Y. Dromzee and S. Jeannin, Inorg. Chem., 32 (1993) 1623.
M. Mikuriya, T. Fujii, T. Tokii and A. Kawamori, Bull. Chem. Soc. Jpn., 66 (1993) 1675.
147 U. Casellato, P. Guerriero, S. Tamburini, P.A. Vigato and R. Graziani, Inorg. Chim. Acta, 134 (1987) 165.
148 I.A. Kahwa, J. Selbin, T.C.-Y. Hsieh and R.A. Laine, Inorg. Chim. Acta, 118 (1986) 179.
I.A. Kahwa, F.R. Fronczek and J. Selbin, Inorg. Chim. Acta, 126 (1987) 227.
149 P. Guerriero, P.A. Vigato, J.-C.G. Bunzli and E. Moret, J. Chem. Soc., Dalton Trans., (1990) 647.
150 I.A. Kahwa, S. Folkes, D.J. Williams, S.V. Ley, G.A. O'Mahoney and G.L. McPherson, J. Chem. Soc., Chem. Commun., (1989) 1531.

K.D. Matthews, R.A. Fairman, A. Johnson, K.V.M. Spence, I.A. Kahwa, G.L.McPherson and H. Robothem, J. Chem. Soc., Dalton Trans., (1993) 1719.
I.A. Kahwa, F.R. Fronczek and J. Selbin, Inorg. Chim. Acta, 148 (1988) 273.
151 U. Casellato, P. Guerriero, S. Sitran, P.A. Vigato, C. Marega, A. Marigo and R. Zannetti, Inorg. Chim. Acta, 171 (1990) 103.
152 U. Casellato, P. Guerriero, S. Tamburini, S. Sitran and P.A. Vigato, J. Chem. Soc., Dalton Trans., (1991) 2145.
153 C. Benelli, P. Guerriero, S. Tamburini and P.A. Vigato, Mater. Chem. Phys., 31 (1992) 137.
154 P. Guerriero, S. Tamburini, P.A. Vigato and C. Benelli, Inorg. Chim. Acta, 189 (1991) 19.
C. Benelli, P. Guerriero, S. Tamburini and P.A. Vigato, Basic and Applied Aspect of Rare Earths, 2nd Workshop, Venice, 1991, pp. 9, 41.
155 U. Casellato, P. Guerriero, S. Tamburini, P.A. Vigato and R. Graziani, J. Chem. Soc., Dalton Trans., (1990) 1533.
156 A. Aguiari, E. Buppita, V. Casellato, P. Guerriero, S. Tamburini and P.A. Vigato, Inorg. Chim. Acta, 219 (1994) 135.
D. Cunningham, J.F. Gallagher, T. Higgins, P. McArdle, J. McGiuley and M. O'Gara, J. Chem. Soc., Dalton Trans., (1993) 2183.
157 U. Casellato, D. Fregona, S. Sitran, S. Tamburini, P.A. Vigato and P. Zanello, Inorg. Chim. Acta, (1984) 309.
U. Castellato, D. Fregona, S. Sitran, S. Tamburini and P.A. Vigato, Inorg. Chim. Acta, 110 (1985) 161.
158 C.J. van Staveren, J. van Eerden, F.C.J.M. van Veggel, S. Harkema and D.N. Reinhoudt, J. Am. Chem. Soc., 110 (1988) 4994.
159 F.C.J.M. van Veggel, S. Harkema, M. Bos, W. Verboom, C.J. van Staveren, G.J. Gerritsma and D.N. Reinhoudt, Inorg. Chem., 28 (1989) 1133.
160 K.E. Koenig, G.M. Lein, P. Stuckler, T. Kaneda and D.J. Cram, J. Am. Chem. Soc., 101 (1979) 3553.
161 A.D. Hamilton, H.-D. Rubin and A.B. Bocarsly, J. Am. Chem. Soc., 108 (1984) 7255.
162 K. Maruyama, F. Kobayashi and A. Osuka, Chem. Lett., (1987) 821.
K. Maruyama, F. Kobayashi and A. Osuka, Bull. Chem. Soc. Jpn., 63 (190) 2672.
A. Hamilton, J.-M. Lehn and J.L. Sessler, J. Am. Chem. Soc., 108 (1986) 5158.
163 C. Fraser and B. Bosnic, 205th ACS Natl. Meet., Division of Inorganic Chemistry, Denver, CO, 1993, 554.
C. Fraser, L. Johnston, A.L. Rheingold, B.S. Haggerty and G.K. Williams, Inorg. Chem., 31 (1992) 1835.
C. Fraser, R. Ostrander, A.L. Rheingold, C. White and B. Bosnich, Inorg. Chem., 33 (1994) 324.
164 S. Liu, L. Gemini, S.J. Rettig, R.C. Thompson and C. Orvig, J. Am. Chem. Soc., 114 (1992) 6081.
165 L. Casella, M. Gullotti, G. Pallanza, A. Pintar and A. Marchesini, J. Biochem., 251 (1988) 441.
166 D.J. Spira-Solomon, M.D. Allendorf and E.L. Solomon, J. Am. Chem. Soc., 108 (1986) 5318.
167 S.S. Tandon, L.K. Thompson and J.N. Bridson, J. Chem. Soc., Chem. Commun., (1992) 911.
S.S. Tandon, L.K. Thompson, J.N. Bridson, V. McKee and A.J. Downard, Inorg. Chem., 31 (1992) 4635.
168 B. Reinhammar and B.G. Malmstrom, in T. Spiro (Ed.), Copper Proteins, Metal Ions in Biology, Vol. 3, Wiley, New York, 1981, p. 110.

169 K.D. Karlin and Y. Gultneh, Prog. Inorg. Chem., 35 (1987) 219.

170 R. Malkin and B.G. Malmstrom, Adv. Enzymol., 33 (1970) 170.

171 K.D. Karlin, Q.-F. Gan, A. Farooq, S. Liu and J. Zubieta, Inorg. Chim. Acta, 165 (1989) 37.

172 K.D. Karlin, Q.-F. Gan, A. Farooq, S. Liu and J. Zubieta, Inorg. Chem., 29 (1990) 2551.

173 H. Adams, N. Bailey, D.E. Fenton, C. Fukuhara, P.C. Hellier and P.D. Hempstead, J. Chem. Soc., Dalton Trans., (1992) 729.

174 H. Adams, N.A. Bailey, M.J.S. Dwyer, D.E. Fenton, P.C. Hellier, P.D. Hempstead and J.M. Latour, J. Chem. Soc., Dalton Trans., (1993) 1207.

175 F.C.J.M. van Veggel, M. Bos, S. Harkema, W. Verboon and D.N. Reinhoudt, Angew. Chem., Int. Edn. Engl., 28 (1989) 746.

176 F.C.J.M. van Veggel, M. Bos, S. Harkema, H. van de Bovenkamp, W. Verboon, J. Reedijk and D.N. Reinhoudt, J. Org. Chem., 56 (1991) 225.

177 M. Tadokoro, H. Okawa, N. Matsumoto, M. Koikawa and S. Kida, J. Chem. Soc., Dalton Trans., (1991) 1657.
M. Tadokoro, H. Sakiyama, N. Matsumoto, H. Okawa and S. Kida, Bull. Chem. Soc. Jpn., 63 (1990) 3337.

178 H. Okawa, J. Nishio, M. Ohba, M. Tadokoro, N. Matsumoto, M. Koikawa, S. Kida and D.E. Fenton, Inorg. Chem., 32 (1993) 2949.

179 M. Tadokoro, H. Okawa, N. Matsumoto, M. Kodera and S. Kida, Symp. on Coordination Chemistry in Japan, Kanazawa, 1990.

180 S. Brooker and P.D. Croucher, J. Chem. Soc., Chem. Commun., (1993) 1278.

181 U. Casellato, P.A. Vigato and M. Vidali, Coord. Chem. Rev., 23 (1977) 31.
M.D. Glick and R.L. Lintvedt, in J. Lippard (Ed.), Progress in Inorganic Chemistry, Vol. 21, Wiley, New York, 1977, p. 233.

182 R.L. Lintvedt, M.J. Heeg, M. Ahmad and M.D. Glick, Inorg. Chem., 21 (1982) 2350.

183 B. Andrelczyk, R.L. Lintvedt and M.D. Glick, J. Am. Chem. Soc., 94 (1972) 8633.

184 R.L. Lintvedt, B.A. Shoenfelner, C. Ceccarelli and M.D. Glick, Inorg. Chem., 21 (1982) 2113.

185 R.L. Lintvedt, B.A. Shoenfelner, C. Ceccarelli and M.D. Glick, Inorg. Chem., 23 (1984) 2867.

186 F. Teixidor, A. Llobet, L. Escriche and J. Casabò, Polyhedron, 4 (1985) 215.

187 F. Teixidor, A. Llobet, J. Casabò and S. Bordas, Thermochim. Acta, 79 (1984) 315.

188 F. Teixidor, A. Llobet, J. Casabò, X. Solans, M. Font-Altaba and M. Aguilò, Inorg. Chem., 24 (1985) 2315.

189 F. Teixidor, J. Colomer, A. Llobet, J. Casabò, X. Solans and M. Font-Altaba, Inorg. Chim. Acta, 128 (1987) 15.

190 F. Teixidor, J. Colomer, J. Casabò, J. Rius, E. Molins and C. Miravitlles, Inorg. Chem., 28 (1989) 678.

191 G.C. Dismukes, Photochem. Photobiol., 43 (1986) 99.
G.C. Dismukes, K. Ferris and P. Watnick, Photobiochem. Photobiophys., 3 (1982) 243.

192 J.A. Kirby, A.S. Robertson, J.P. Smith, A.C. Thompson, S.R. Cooper and M.P. Klein, J. Am. Chem. Soc., 103 (1981) 5529.

193 A.F. Kulikov, V.R. Bogatyrenko, G.I. Likhtenshtein, S.I. Allakhverdiyev, V.V. Klimov, V.A. Shulalov and A.A. Krasnoskii, Biophysics, 28 (1983) 381.

194 G.W. Brudvig and R.H. Crabtree, in S.J. Lippard (Ed.), Progress in Inorganic Chemistry, Vol. 37, Wiley, New York, 1989, p. 99.

195 E. Gojon, J.-M. Latour, S.J. Greaves, D.C. Povy, V. Ramdas and G.W. Smith, J. Chem. Soc., Dalton Trans., (1990) 2043.

196 B. Hoskins, R. Robson and D. Vince, J. Chem. Soc., Chem. Commun., (1973) 392.
M. Mikuriya, K. Nakadera and T. Kotera, Chem. Lett., (1993) 637.

197 D. Lunean, J.-M. Savariault and J.-P. Tuchagues, Inorg. Chem., 27 (1988) 3912.
198 P. Guerriero, D. Ajò, P.A. Vigato, U. Casellato, P. Zanello and R. Graziani, Inorg. Chim. Acta, 141 (1988) 103.
199 M. Sakamoto, S. Itose, T. Ishimori, N. Matsumoto, H. Okawa and S. Kida, J. Chem. Soc., Dalton Trans., (1989) 2083.
200 N.A. Bailey, D.E. Fenton, R. Moody and P.J. Scrimshire, Inorg. Chim. Acta, 124 (1986) L1.
N.A. Bailey, D.E. Fenton, R. Moody, P.J. Scrimshire, E. Beloritzky, P.H. Fries and J.-M. Latour, J. Chem. Soc., Dalton Trans., (1988) 2817.
201 B.F. Hoskins, R. Robson, G.A. Williams and J.C Wilson, Inorg. Chem., 30 (1991) 4160.
202 K. Shindo, Y. Mori, K. Motoda, H. Sakiyama, N. Matsumoto and H. Okawa, Inorg. Chem., 31 (1992) 4987.
203 M. Mikuriya, Y. Yamato and T. Tokii, Chem. Lett., (1991) 1429.
M. Mikuriya, Y. Yamato and T. Tokii, Bull. Chem. Soc. Jpn., 65 (1992) 1446.
J.A. Bonadies, M.L. Kirk, M.S. Lah, D.P. Kessissoglou, W.E. Hatfield and V.L. Pecoraro, Inorg. Chem., 28 (1989) 2037.
J.A. Bonadies, M.J. Maroney and L. Pecoraro, Inorg. Chem., 28 (1989) 2044.
K. Bertoncello, G.D. Fallon, K.S. Murray and E.R.T. Tieking, Inorg. Chem., 30 (1991) 3562.
M. Mikuriya, K. Majima and Y. Yamato, Chem. Lett., (1992) 1929.
M. Mikuriya, Y. Yamato and T. Tokii, Bull. Chem. Soc. Jpn., 65 (1992) 2624.
204 M. Suzuki, Y. Hayashi, K. Munezawa, M. Suenaga, H. Senda and A. Uehara, Chem. Lett., (1991) 1929.
M. Suzuky, H. Senda, Y. Kobayashi, H. Oshio and A. Vehara, Chem. Lett., (1988) 1763.
205 P.A. van der Schaaf, M.P. Hogerhlide, D.M. Grove, A.L. Spek and G. van Koten, J. Chem. Soc., Chem. Commun., (1992) 1703.
K.F. Tesh and T.P. Hamusa, J. Chem. Soc., Chem. Commun., (1991) 879.
M.K. Chan and W.H. Armstrong, J. Am. Chem. Soc., 111 (1989) 9121.
M.K. Chan and W.H. Armstrong, J. Am. Chem. Soc., 112 (1990) 4958.
M.K. Chan and W.H. Armstrong, J. Am. Chem. Soc., 113 (1991) 5055.
206 N.A. Bailey, D.E. Fenton, R. Moody, C.O. Rodriguez de Barbarin, I.N. Sciambarella, J.M. Latour, D. Limosin and V. McKee, J. Chem. Soc., Dalton Trans., (1987) 2519.
207 D.E. Fenton, S.J. Kitchen, C.M. Spencer, S. Tamburini and P.A. Vigato, J. Chem. Soc., Dalton Trans., (1988) 685.
M. Sakamoto, Bull. Chem. Soc. Jpn., 60 (1987) 1545.
H.C. Aspinall, J. Black, I. Dodd, M.M. Harding and S.J. Winkley, J. Chem. Soc., Dalton Trans., (1993) 709.
208 V. McKee and W.B. Shepard, J. Chem. Soc., Chem. Commun., (1985) 158.
S. Brooker and V.McKee, J. Chem. Soc., Chem. Commun., (1989) 619.
S. Brooker, V. McKee, V.B. Shepard and L.K. Pannell, J. Chem. Soc., Dalton Trans., (1987) 2555.
209 D. Luneau, J.-M. Savariault, P. Cassoux and J.-P. Tuchagues, J. Chem. Soc., Dalton Trans., (1988) 1225.
210 S.S. Tandon, L.K. Thompson and J.N. Bridson, Inorg. Chem., 32 (1993) 32.
N.A. Bailey, D.E. Fenton, P.B. Roberts and A.M. Walford, J. Chem. Soc., Dalton Trans., (1987) 1865.
211 S.S. Tandon and V. McKee, J. Chem. Soc., Dalton Trans., (1989) 19.
212 V. McKee and S.S. Tandon, J. Chem. Soc., Chem. Commun., (1988) 385.
213 V. McKee and S.S. Tandon, J. Chem. Soc., Dalton Trans., (1991) 221.

214 V. McKee and S.S. Tandon, J. Chem. Soc., Chem. Commun., (1988) 1334.
215 M. Bell, A.J. Edwards, B.F. Hoskins, E.H. Kachab and R. Robson, J. Am. Chem. Soc., 111 (1989) 3603.
A.J. Edwards, B.F. Hoskins, E.H. Kachab, A. Markiewicz, K.S. Murray and R. Robson, Inorg. Chem., 31 (1992) 3585.
216 M.J. Grannas, B.F. Hoskins and R. Robson, J. Chem. Soc., Chem. Commun., (1990) 1644.
217 B.F. Hoskins, R. Robson and P. Smith, J. Chem. Soc., Chem. Commun., (1990) 488.
218 V. McKee and S.S. Tandon, Inorg. Chem., 28 (1989) 2902.
S. Brooker, V. McKee and J. Nelson, XXVIII Int. Conf. Coord. Chem., Brisbane, 1989, M98.
C. Gedye, C. Harding, V. McKee, J. Nelson and J. Patterson, J. Chem. Soc., Chem. Commun., (1992) 392.
S.K. Chandra and A. Chakravorty, Inorg. Chem., 30 (1991) 3795.
S.K. Chandra, P. Chakravorty and A. Chakravorty, J. Chem. Soc., Dalton Trans., (1993) 863.
219 H. Sakiyama, K. Motoda, H. Okawa and S. Kida, Chem. Lett., (1991) 1133.
H. Sakiyama, K. Tokuyama, J. Nishio, N. Matsumoto and H. Okawa, Chem. Lett., (1992) 1021.
H. Sakiyama, K. Tokuyama and H. Okawa, 63rd Natl. Meet. of the Chemical Society of Japan, Osaka, 1992, Abstr. I27.
220 S.S. Tandon, L.K. Thompson and J.M. Bridson, Inorg. Chem., 32 (1993) 32.
221 S.M. Nelson, F. Esho, A. Lavery and M.G.B. Drew, J. Am. Chem. Soc., 105 (1983) 5693.
M.G.B. Drew, F.S. Esho and S.M. Nelson, J. Chem. Soc., Chem. Commun., (1982) 1347.
222 K.P. McKillop, S.M. Nelson and V. McKee, J. Chem. Soc., Chem. Commun., (1988) 387.
223 M.G.B. Drew, P.C. Yates, J. Trocha-Grimshaw, K.P. McKillop and S.M. Nelson, J. Chem. Soc., Chem. Commun., (1985) 262.
224 D.E. Fenton, C.M. Regan, U. Casellato, P.A. Vigato and M. Vidali, Inorg. Chim. Acta, 58 (1982) 83.
225 D.E. Fenton, J.R. Tate, U. Casellato, S. Tamburini, P.A. Vigato and M. Vidali, Inorg. Chim. Acta, 83 (1984) 23.
226 R.L. Lindvedt and J.K. Zehetmair, Inorg. Chem., 29 (1990) 2204.
227 S. Tamburini, P.A. Vigato, P. Guerriero, U. Casellato and A. Aguiari, Inorg. Chim. Acta, 183 (1991) 81.
228 A. Aguiari, E. Bullita, U. Casellato, P. Guerriero, S. Tamburini and P.A. Vigato, in U. Tonellato and P.A. Vigato (Eds.), Macrocyclic and Supramolecular Chemistry in Italy, a Photograph, Padua, 1990, p. 161.
U. Casellato, P. Guerriero, S. Tamburini, P.A. Vigato and R. Graziani, Inorg. Chim. Acta, 119 (1986) 215.
229 P.D. Beer, O. Kocian, R.J. Mortimer and P. Spencer, J. Chem. Soc., Chem. Commun., (1992) 602.
230 U. Casellato and P.A. Vigato, unpublished work.
231 A. Benito, J. Cano, R. Martínez-Máñez, J. Soto, J. Payá, F. Lloret, M. Julve, J. Fans and M.D. Marcos, Inorg. Chem., 32 (1993) 1197.
232 P.D. Beer, Adv. Inorg. Chem., 39 (1993) 79.
P.D. Beer, Chem. Soc. Rev., 18 (1989) 409.
P.D. Beer, Z. Chen, M.G.B. Drew, J. Kingston, M. Ogden and P. Spencer, J. Chem. Soc., Chem. Commun., (1993) 1046.
233 T.E. Edmonds, in T.E. Edmonds (Ed.), Chemical Sensors, Blackie, Glasgow, 1988, Chap. 8, p. 193.

234 P.D. Beer and H. Sikanyika, Polyhedron, 9 (1990) 1091.

235 P.D. Beer and K. Wild, Proc. 16th Int. Macrocyclic Conf., 1991, p. 106.

236 P.D. Beer, J. Chem. Soc., Chem. Commun., (1986) 1678.

237 P.D. Beer and C.G. Crane, Polyhedron, 7 (1988) 2649.

238 P.D. Beer, C.G. Crane and M.G.B. Drew, J. Chem. Soc., Dalton Trans., (1991) 3235.

239 R. Ziessel and J. Suffert, J. Chem. Soc., Chem. Commun., (1990) 1105.

240 M.-T. Youinou, J. Suffert and R. Ziessel, Angew. Chem., Int. Edn. Engl., 31 (1992) 775.

241 J.E. Parks, B.E. Wagner and R.H. Holm, J. Organomet. Chem., 56 (1973) 53.

242 C.J. Chandler, L.W. Deady and J.A. Reiss, J. Heterocycl. Chem., 18 (1981) 599.

243 B. Nicholls and M.C. Whiting, J. Chem. Soc., (1959) 551.

244 B. Rees and P. Coppens, Acta Crystallogr. B, 29 (1973) 2516.

245 U. Casellato, P. Guerriero, S. Tamburini, P.A. Vigato and C. Benelli, Inorg. Chim. Acta, 207 (1993) 39.
D. Coucouvanis, S.G. Jonasdottir, D. Christodoulou, C.G. Kim and J. Kampf, Inorg. Chem., 32 (1993) 2987.
S.G. Jonasdottir, C.G. Kim and D. Coucouvanis, Inorg. Chem., 32 (1993) 3591.

246 D.P. Kessissoglou, C.P. Raptopoulou, E.G. Bakalbassis, A. Terzis and J. Mrozinski, Inorg. Chem., 31 (1992) 4854.

247 P.E. Kruger, G.D. Fallon, B. Moubaraki and K.S. Murray, J. Chem. Soc., Chem. Commun., (1992) 1726.

248 A. Bencini, A. Bianchi, E. Garcia-Espana, M. Giusti, M. Micheloni and P. Paoletti, Inorg. Chem., 26 (1987) 681.
A. Bencini, A. Bianchi, E. Garcia-Espana, S. Mangani, M. Micheloni, P. Orioli and P. Paoletti, Inorg. Chem., 28 (1989) 1243.
A. Bencini, A. Bianchi, M. Castello, P. Dapporto, J. Faus, E. Garcia-Espana, M. Micheloni, P. Paoletti and P. Paoli, Inorg. Chem., 28 (1989) 1188.
A. Bencini, A. Bianchi, E. Garcia-Espana, S. Mangani, M. Micheloni, P. Orioli and P. Paoletti, Inorg. Chem., 27 (1988) 1104.
A. Bencini, A. Bianchi, P. Dapporto, E. Garcia-Espana, M. Micheloni and P. Paoletti, Inorg. Chem., 28 (1989) 1188.

249 A. Bencini, A. Bianchi, M. Micheloni, P. Paoletti, E. Garcia-Espana and M.A. Nino, J. Chem. Soc., Dalton Trans., (1991) 1171.

250 M.G. Basallote and A.E. Martell, Inorg. Chem., 29 (1990) 1467.
B. Szpoganicz, R.J. Motekaitis and A.E. Martell, Inorg. Chem., 29 (1990) 1467.

251 M.G. Basallote, D. Chen and A.E. Martell, Inorg. Chem., 28 (1989) 3494.

252 P.K. Coughlin, J.C. Dewan, S.J. Lippard, E.I. Watanabe and J.-M. Lehn, J. Am. Chem. Soc., 101 (1979) 265.

253 P.K. Coughlin, S.J. Lippard, A.E. Martin and J.E. Bulkowski, J. Am. Chem. Soc., 102 (1980) 7616.

254 P.K. Coughlin and S.J. Lippard, J. Am. Chem. Soc., 103 (1981) 3228.

255 A. Bencini, A. Bianchi, E. Garcia-Espana, M. Micheloni and P. Paoletti, Inorg. Chem., 27 (1988) 176.

256 J. Comarmond, B. Dietrich, J.-M. Lehn and R. Louis, J. Chem. Soc., Chem. Commun., (1985) 74.

257 T. Shimada, M. Kodera, H. Okawa and S. Kida, J. Chem. Soc., Dalton Trans., (1992) 1121.

258 Y. Okuno, K. Uoto, Y. Sasaki, O. Yonemitsu and T. Tomohiro, J. Chem. Soc., Chem. Commun., (1987) 874.

259 H.Y. Okuno, K. Uoto, O. Yonemitsu and T. Tomohiro, J. Chem. Soc., Chem. Commun., (1987) 1018.

260 K. Uoto, T. Tomohiro and H(Y). Okuno, Inorg. Chim. Acta, 170 (1990) 123.
261 T. Tomohiro, K. Uoto and H(Y). Okuno, J. Chem. Soc., Dalton Trans., (1990) 2459.
262 H(Y). Okuno, K. Uoto, T. Tomohiro and M.-T. Youinou, J. Chem. Soc., Dalton Trans., (1990) 3375.
263 M. Kodaka, T. Tomohiro and H(Y). Okuno, Chem. Express, 5 (1990) 97.
264 M. Kodaka, T. Tomohiro and H(Y). Okuno, Chem. Express, 5 (1990) 117.
265 M. Kodaka, T. Tomohiro and H(Y). Okuno, J. Phys. Chem., 95 (1991) 6741.
266 T. Tomohiro, K. Uoto and H(Y). Okuno, J. Heterocycl. Chem., 27 (1990) 1233.
267 K. Uoto, T. Tomohiro and H(Y). Okuno, J. Heterocycl. Chem., 27 (1990) 893.
268 H(Y). Okuno, K. Uoto and T. Tomohiro, Chem. Express, 5 (1990) 37.
269 T. Tomohiro and H(Y) Okuno, Inorg. Chim. Acta, 204 (1993) 147.